

Guidance book

Eurocodes 3 and 4

Application to steel-concrete composite road bridges



Liberté • Égalité • Fraternité

RÉPUBLIQUE FRANÇAISE

ministère de l'Écologie
du Développement
et de l'Aménagement
durables

The Technical Department for Transport, Roads and Bridges Engineering and Road Safety (Service d'études techniques des routes et autoroutes - Sétra) is a technical department within the Ministry of Transport and Infrastructure. Its field of activities is the road, the transportation and the engineering structures.

The Sétra supports the public owner

The Sétra supplies State agencies and local communities (counties, large cities and urban communities) with informations, methodologies and tools suited to the specificities of the networks in order to:

- improve the projects quality;
- help with the asset management;
- define, apply and evaluate the public policies;
- guarantee the coherence of the road network and state of the art;
- put forward the public interests, in particular within the framework of European standardization;
- bring an expertise on complex projects.

The Sétra, producer of the state of the art

Within a very large scale, beyond the road and engineering structures, in the field of transport, intermodality, sustainable development, the Sétra:

- takes into account the needs of project owners and prime contractors, managers and operators;
- fosters the exchanges of experience;
- evaluates technical progress and the scientific results;
- develops knowledge and good practices through technical guides, softwares;
- contributes to the training and information of the technical community.

The Sétra, a work in partnership

- The Sétra associates all the players of the French road community to its action: operational services; research organizations; Scientific and Technical Network (Réseau Scientifique et Technique de l'Equipement – RST), in particular the **Public Works Regional Engineering Offices (Centres d'études techniques de l'Equipement – CETE)**, companies and professional organizations; motorway concessionary operators; other organizations such as French Rail Network Company (Réseau Ferré de France – RFF) and French Waterways Network (Voies Navigables de France - VNF); Departments like the department for Ecology and Sustainable Development...
- The Sétra regularly exchanges its experience and projects with its foreign counterparts, through bilateral co-operations, presentations in conferences and congresses, by welcoming delegations, through missions and expertises in other countries. It takes part in the European standardization commissions and many authorities and international working groups. The Sétra is an organization for technical approval, as an EOTA member (European Organisation for Technical Approvals).

Guidance book

Eurocodes 3 and 4

Application to steel-concrete composite road bridges



This document is the translation of the work "Eurocodes 3
et 4 - Application aux ponts-routes mixtes acier-béton"
published in july 2007 under the reference 0720.

This guidance book has been written by Laurence DAVAINE, Florent IMBERTY and Joël RAOUL (SETRA/CTOA, TECHNICAL CENTRE FOR HIGHWAYS & MOTORWAYS, FRANCE) assisted by:

Eric CHASCO, SETRA/CTOA, then South West CETE (TECHNICAL ENGINEERING CENTRE FOR INFRASTRUCTURE)

Eric Gogny, CTICM (INDUSTRIAL TECHNICAL CENTRE FOR STEELWORK)

Bernard PREVOST, East CETE

Jacques RESPLENDINO, CETE of Lyon

Patrice SCHMITT, SETRA/ CTOA then SNCF (NATIONAL RAILWAYS ADMINISTRATION, FRANCE)

Ferry TAVAKOLI, CETE of Lyon

The figures have been created by Philippe JULLIEN, SETRA/CTOA.

Contents

Part I: Introduction

1 - Purpose of the guide	11
2 - Eurocodes used	11

Part II: Composite two-girder bridge

1 - Introduction	15
2 - General design data	15
2.1 - <i>Traffic related data</i>	15
2.2 - <i>Environmental data</i>	17
3 - Description of the deck - Construction	18
3.1 - <i>Longitudinal elevation</i>	18
3.2 - <i>Transverse cross-section</i>	18
3.3 - <i>Structural steel distribution (main girders and transverse cross bracing)</i>	18
3.4 - <i>Construction phases (slab concreting)</i>	21
3.5 - <i>Reinforced concrete slab</i>	24
4 - Materials	28
4.1 - <i>Material toughness and through-thickness properties</i>	28
4.2 - <i>Concrete</i>	30
4.3 - <i>Reinforcement</i>	31
4.4 - <i>Shear connectors</i>	31
4.5 - <i>Partial factors for materials</i>	31
5 - Actions	33
5.1 - <i>Permanent loads</i>	33
5.2 - <i>Concrete shrinkage</i>	34
5.3 - <i>Creep – Modular ratios</i>	37
5.4 - <i>Variable actions</i>	39
6 - Combinations of actions	45
6.1 - <i>Design situations</i>	45
6.2 - <i>Notations</i>	45
6.3 - <i>ULS combinations other than fatigue</i>	47
6.4 - <i>SLS combinations</i>	47
7 - Global analysis	49
7.1 - <i>Analysis methods: general</i>	49
7.2 - <i>Internal forces and moments – Stresses</i>	50
8 - Justification of the composite cross-sections at ULS other than fatigue	57
8.1 - <i>Classification of cross-sections</i>	57
8.2 - <i>Cross-section justification principles</i>	60
8.3 - <i>Verification of cross-section at internal support P1</i>	65
8.4 - <i>Verification of cross-section at mid-span P1-P2</i>	71
8.5 - <i>Verification of the frame post rigidity</i>	74
8.6 - <i>Lateral torsional buckling (LTB) of the lower flange in compression around internal support P1</i>	76
9 - Justification at fatigue ULS	86
9.1 - <i>Verification of the structural steel bridge part</i>	86
9.2 - <i>Verification of the longitudinal reinforcement</i>	100
10 - Justification of the cross-sections at SLS	106
10.1 - <i>General</i>	106
10.2 - <i>Stress limitations</i>	106
10.3 - <i>Web breathing</i>	112
10.4 - <i>Control of cracking</i>	113

11 - Shear connection	118
11.1 - General	118
11.2 - Design resistance of headed stud connectors	118
11.3 - Design for characteristic SLS combination of actions	119
11.4 - Design for ULS combination of actions other than fatigue	121
11.5 - Design for fatigue ULS combination of actions	125
11.6 - Shear connection detailing	128
11.7 - Synopsis for the design example	130
11.8 - Influence of shrinkage and thermal action on the studs design at both deck ends	131
12 - Local justifications in the concrete slab	133
12.1 - Transverse reinforcement verifications	133
12.2 - Longitudinal reinforcement verifications	141
12.3 - Punching shear (ULS)	143

Part III: Special features of composite box-girder bridge

1 - Description of the composite box section	149
1.1 - Main characteristics	149
1.2 - Structural steel distribution	150
2 - Actions and combinations of actions	153
2.1 - Permanent loads	153
2.2 - Concrete shrinkage	153
2.3 - Concrete creep – Modular ratio	153
2.4 - Variable actions	154
3 - Global analysis	155
3.1 - General	155
3.2 - Shear lag	156
3.3 - Internal forces and moments	156
4 - Section analysis	158
4.1 - Shear lag (SLS and fatigue ULS)	158
4.2 - Shear lag (ULS)	161
5 - Verification of the box section at support P1 for ULS combination of actions	162
5.1 - Mechanical properties of the gross cross-section	162
5.2 - Internal forces and moments	163
5.3 - Effective area of the bottom flange	163
5.4 - Effective area of the web	168
5.5 - Effective mechanical properties of the box section	169
5.6 - Bending resistance verification	170
5.7 - Shear resistance verification	170
5.8 - Interaction between moment and shear force	172
5.9 - Conclusion	173
6 - Verification of the box section at support P1 for SLS combination of actions	174

Appendices

Appendice I: References	177
Appendice II: Class 4 I-shaped cross-section	180

Notations

The following list is not exhaustive. Other notations may be introduced locally in the text.

Capital Latin letters

A_a	Cross-sectional area of the structural steel section
A_b	Cross-sectional area of concrete
A_c	Cross-sectional area of the compression zone of a section
$A_{c,eff}$	Effective cross-sectional area of the compression zone of a section
A_s	Cross-sectional area of reinforcement
A_v	Structural steel shear area
C_d	Rigidity of bracing transverse frame
E_{cm}	Secant modulus of elasticity of concrete
E_a	Modulus of elasticity of structural steel
E_s	Modulus of elasticity of reinforcement steel
F	Applied force
F_{wk}	Characteristic value of resultant wind force
G_k	Characteristic (nominal) value of the effect of permanent actions
I	Second moment of area
L_e	Equivalent span
L	Span; length
M_{Ed}	Design bending moment
$M_{a,Ed}$	Design bending moment applied to the structural steel section
$M_{c,Ed}$	Design bending moment acting on the composite section
$M_{el,Rd}$	Design value of the elastic resistance moment of the composite section
$M_{f,Rd}$	Design value of the plastic resistance moment of a cross-section consisting of the flanges only
$M_{pl,Rd}$	Design value of the plastic resistance moment
N_{Ed}	Design axial force
P_{Rk}	Characteristic value of the shear resistance of a single connector
Q_{k1}	Characteristic value of the leading variable action 1
$Q_{ki,2 \geq 2}$	Characteristic value of the accompanying variable action i
RH	Ambient relative humidity (in %)
S	Characteristic value of the action due to shrinkage
T_0	Initial temperature
T_{Ed}	Design value of the temperature
T_k	Characteristic value of the thermal action
$T_{e,min}$	Minimum uniform bridge temperature component
T_{min}	Minimum shade air temperature with an annual probability of being exceeded of 0.02 (equivalent to a mean return period of 50 years)
$T_{e,max}$	Maximum uniform bridge temperature component
T_{max}	Maximum shade air temperature with an annual probability of being exceeded of 0.02 (equivalent to a mean return period of 50 years)
$\Delta T_{N,con}$	Maximum contraction range of uniform bridge temperature component ($T_0 - T_{e,min}$)
$\Delta T_{N,exp}$	Maximum expansion range of uniform bridge temperature component ($T_{e,max} - T_0$)
ΔT_u	Uniform temperature component
ΔT_{My}	Linear thermal gradient following a transverse horizontal axis

ΔT_{Mz}	Linear thermal gradient following a vertical axis
ΔT_E	Non-linear part of the thermal gradient, giving rise to self-balancing stresses
$\Delta T_{M,heat}$	Linear temperature difference component (heating)
$\Delta T_{M,cool}$	Linear temperature difference component (cooling)
$V_{b,Rd}$	Design value of the shear resistance in case of shear plate buckling in the structural steel web
V_{Ed}	Design shear force
V_{Rd}	Design resistance for shear
$V_{pl,Rd}$	Plastic design shear resistance
$V_{pl,a,Rd}$	Plastic design shear resistance applied to the structural steel section

Small Latin letters

a	Length of a web plate between adjacent vertical stiffeners
b	Width of a structural steel element
b_{eff}	Effective width (concrete slab; steel bottom flange of a box girder)
b_0	Centre-to-centre distance between outside rows of shear connectors
c_{dir}	Directional factor (wind)
$c_{f,x}$	Force coefficient (wind) following the x axis
c_{season}	Seasonal factor (wind)
$c_0(z)$	Orography factor of a structure at height z with respect to the ground
$c_e(z)$	Exposure factor (at height z)
$c_r(z)$	Roughness factor (at height z)
c_s	Size factor (wind)
c_d	Dynamic factor (wind)
c_{nom}	Nominal concrete cover
c_{min}	Minimum concrete cover
Δc_{dev}	Allowable deviation for the concrete cover
d	Diameter of the shank of a stud connector; lever arm in reinforced concrete calculations
e	Thickness of the concrete slab; spacing of rows of connectors
f_{cd}	Design value of concrete compressive strength
f_{ck}	Characteristic compressive cylinder strength of concrete at 28 days
f_{cm}	Mean value of concrete cylinder compressive strength
f_{ctm}	Mean value of axial tensile strength of concrete
$f_{ctk,0,05}$	5% fractile of the characteristic axial tensile strength of concrete
$f_{ctk,0,95}$	95% fractile of the characteristic axial tensile strength of concrete
f_{sk}	Characteristic yield strength of reinforcement
f_y	Yield strength of the structural steel
f_u	Ultimate strength of the structural steel
f_{yk}	Characteristic value of the yield strength of the structural steel
h	Height; overall depth
h_0	Notional size of the concrete slab
k_σ	Plate buckling coefficient for normal stresses
k_τ	Plate buckling coefficient for shear stresses
n_0	Structural steel / concrete modular ratio for short-term loading
n_{ba}	Structural steel / reinforcement modular ratio
n_L	Structural steel / concrete modular ratio for long-term loading

p	Perimeter of the concrete slab section
q_{fk}	Characteristic value of the uniformly distributed load due to pedestrian and cycle traffic
q_{nom}	Nominal value of the lineic load due to bridge equipments (safety devices, pavement,...)
q_{min}	Minimum value of the lineic load due to bridge equipments
q_{max}	Maximum value of the lineic load due to bridge equipments
s	Spacing of reinforcing steel bars of a single layer
t	Plate thickness; date (following construction phases)
t_0	Mean age of the concrete at loading
v_b	Basic wind velocity (at 10 m height, on a flat area with negligeable vegetation and without obstacles)
$v_{b,0}$	Fundamental value of the basic wind velocity
V_{Ed}	Design value of the longitudinal shear per unit length
w	Carriageway width between safety devices
w_{max}	Limiting calculated crack width
y	Position of the centre of gravity of a section
z_e	Reference height for external wind action
z_0	Roughness length
$z_{0,II}$	Roughness length of a category II terrain (= 0.05 m)

Capital Greek letters

$\Delta\sigma_c$	Reference value of the fatigue strength at $N_c = 2.10^6$ cycles (direct stresses)
$\Delta\sigma_p$	Stress range from load p (fatigue in structural steel)
$\Delta\sigma_{E,2}$	Equivalent constant amplitude stress range related to 2 million cycles (direct stress)
$\Delta\sigma_{s,p}$	Stress range from load p (fatigue in reinforcing bars)
$\Delta\tau_c$	Reference value of the fatigue strength at $N_c = 2.10^6$ cycles (shear stresses)
$\Delta\tau_{E,2}$	Equivalent constant amplitude stress range related to 2 million cycles (shear stress)
ϕ	Damage equivalent impact factor (structural steel)
ϕ_s	Diameter of a steel reinforcing bar
ϕ^*	Modified diameter of a steel reinforcing bar
ϕ_{trans}	Diameter of a transverse steel reinforcing bar
ϕ_{long}	Diameter of a longitudinal steel reinforcing bar

Small Greek letters

α	Factor ; angle ; compressed height percentage
α_{cc}	Factor on the concrete compressive strength
α_{Qi}	Adjustment factors on concentrated load TS of LM1 on lanes i (i=1, 2, ...)
α_{qi}	Adjustment factors on uniformly distributed load UDL of LM1 on lanes i (i=1, 2,...)
α_{qr}	Adjustment factor on load model LM1 on the remaining area
α_{th}^a	Coefficient of linear thermal expansion for structural steel
α_{th}^c	Coefficient of linear thermal expansion for concrete
β	Weighting factor; reduction factor for shear lag effect
β_{as}	Function describing the development in time for autogenous shrinkage
β_{ds}	Function describing the development in time for drying shrinkage
β_Q	Adjustment factor on load model LM2
χ	Reduction factor (≤ 1) for instability (lower indices: c, p, w, LT, op)

ε	Strain; factor $\sqrt{\frac{235}{f_y}}$
ε_r	Shrinkage strain
ε_{ca}	Autogenous shrinkage strain
ε_{cd}	Drying shrinkage strain
ε_{th}	Thermal shrinkage strain
φ	Creep function
φ_{fat}	Damage equivalent impact factor (reinforcing steel)
γ_c	Partial factor for resistance of concrete
$\gamma_{c,fat}$	Partial factor for resistance of concrete for fatigue loading
$\gamma_{F,f}$ (or $\gamma_{F,fat}$)	Partial factor for equivalent constant amplitude range $\Delta\sigma_E$, $\Delta\tau_E$
γ_M	Partial factor for resistance of structural steel
$\gamma_{M,f}$	Partial factor for resistance of structural steel for fatigue loading
$\gamma_{Mf,s}$	Partial factor for resistance of a stud connector for fatigue loading
$\gamma_{M,ser}$	Partial factor for resistance of structural steel at Serviceability Limit State (SLS)
γ_s	Partial factor for resistance of reinforcing steel
$\gamma_{s,fat}$	Partial factor for resistance of reinforcing steel for fatigue loading
γ_v	Partial factor for resistance of a stud connector
η	Coefficient on the yield strength of structural steel
η_1 η_3	Ratio between applied stress and yield strength in a structural steel cross-section
$\bar{\eta}_1$ $\bar{\eta}_3$	Ratio between applied force and resistance in a structural steel cross-section
$\bar{\lambda}$	Reduced slenderness (possible lower indices: c, p, w, LT, op)
λ	Damage equivalent factor (structural steel)
λ_s	Damage equivalent factor (reinforcing steel)
λ_v	Damage equivalent factor (shear connectors)
μ	Moment of area
ν	Poisson's ratio
ρ	Reduction factor ($\leq 1,0$) for effective area of a structural steel cross-section
ρ_c	Reduction factor for efficace ^p width
ρ_s	Reinforcement ratio in a concrete cross-section
σ_{cr}	Elastic critical plate buckling stress
σ_E	Elastic critical Euler's stress
σ_{Ed}	Design value of a direct stress in a cross-section
τ_{cr}	Elastic critical shear buckling stress
τ_{Ed}	Design value of a shear stress in a cross-section
ψ	Stress ratio between opposite edges of a structural steel plate
ψ_L	Creep multiplier for modular ratio
ψ_0	Factor for the combination value of a variable action
ψ_1	Factor for the frequent value of a variable action
ψ_2	Factor for the quasi-permanent value of a variable action

Part I

Introduction



1 - Purpose of the guide

This document has been written to guide the designer in calculating a steel-concrete composite bridge under Eurocodes. It does not deal with the conceptual design (dealt with elsewhere in other documents in the SETRA collections), but with the verification part of the design. It does not attempt to be exhaustive and to cover every type of composite structure (filler beam decks for example, fall under Eurocode 4, but are not addressed in this guidance book). The designer has a duty to maintain an open critical mind to the structure he is designing.

Attention is drawn to the composite bridges subjected to normal force which are only partly covered by Eurocode 4. For example, composite decks in bow-string bridges are covered (EN1994-2, 5.4.2.8), but not composite decks for cable stay bridges (EN1994-2, 1.1.3(1)).

This guidance book does not aim to present the various actions on the bridges, nor how they are modelled. The most common actions have been adopted for calculation purposes. No attempt is made to address the effects of seismic action, an abnormal convoy or an accident action (shock, for example).

Following this general introduction, Part II is constructed on the basis of a design calculation note for a two-girder bridge. Part III repeats the same operating and environmental data, but for a box-girder bridge. Only the specific box-girder aspects are dealt with, like the shear lag in the stiffened steel bottom flange and the buckling of this plate, for example.

The design calculation note gives rise to comments:

- by additions in a right-hand margin separated from the main text, where reference is made to the Eurocodes clauses used for the calculation opposite,
- when the modelling or calculation choices have been made by the writers, the discarded options are however mentioned and the choice is justified.

This calculation note does not detail the verification of all the deck cross-sections. Only two noteworthy cross-sections are dealt with: on intermediate support and at central mid-span.

This guidance book will be further completed to give details, among other things, on the justification for the transverse elements, on the verifications in transient construction phases (launch of the structural steel part, slab sequence concreting, etc.), on the calculation of joints and so on.

2 - Eurocodes used

The final versions of EN standards (after ratification by the European Committee for Standardization (CEN)) and their National Annexes (peculiar to each European country) are used. A list of references can be found in appendix I. The calculation presented in this book has been performed with the French National Annexes. Where the French National Annexes have to be published after this guidance book, their most recent version has been used. As they could also be slightly modified before being published, and as the designer could have to use the National Annexes from another European country, any reference to these National Annexes is clearly indicated.

When designing a composite bridge, the guiding standard is Part 2 of Eurocode 4 (EN1994-2). Figure 1 shows the main standards used with EN1994-2 and the call priority of texts between each other. In theory, EN1994-2 only calls on the general Eurocodes (i.e. Eurocodes 0, 1, 7 and 8) and the Parts 2 of other "material" Eurocodes (i.e. Eurocodes 2, 3, 5, 6 and 9). Therefore, for a bridge, a part 1-1 (general rules) of a "material" Eurocode can only be called on via the Part 2 of this same Eurocode.

This practical rule has not always been respected due to a parallel drafting of Parts 2 of Eurocodes 2, 3 and 4. In fact, EN1994-2 should have been drafted after EN1992-2 and EN1993-2.

In addition, to limit the references in EN1994-2 (of necessity more numerous, given the composite nature of the cross-sections) and maintain a legible text for use by designers, it was decided that EN1994-2 should be independent of EN1994-1-1. The EN1994-1-1 clauses required to understand Part 2 are therefore repeated.

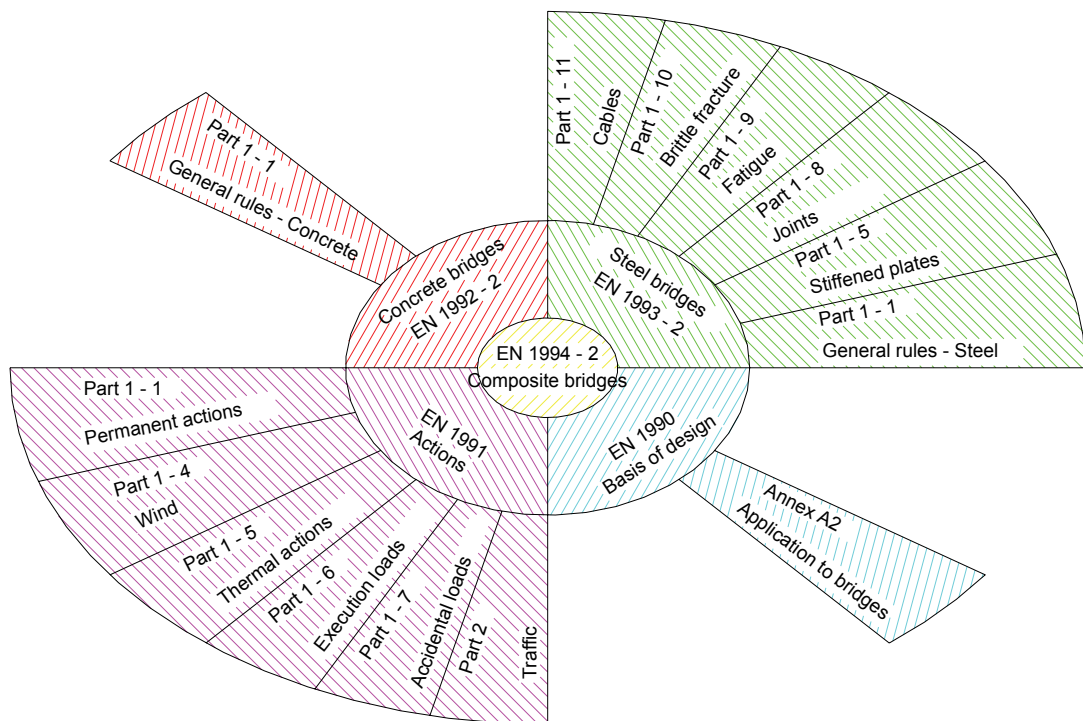


Figure 1: Main Eurocodes used to design a composite bridge deck

Part II

Composite two-girder bridge



1 - Introduction

The text is arranged as a standard design calculation note. Having defined the general design data of the bridge, the deck geometry, the construction phases and materials are described directly in detail.

The actions are then dealt with one by one together with how they are introduced into the longitudinal bending analysis model. The cracked global analysis is presented following a rapid reminder of combinations of actions at the Serviceability Limit State (SLS) and the Ultimate Limit State (ULS). The determination of the internal moments and forces (M, V and N) and of the longitudinal and shear stresses in each cross-section of the deck, are simultaneously presented.

The second part of this standard design calculation note for the composite two-girder bridge starts in Chapter 8 and is devoted to miscellaneous justifications:

- strength at ULS for a cross-section on intermediate support or at mid-span,
- lateral torsional buckling under traffic loads,
- fatigue,
- strength at SLS,
- control of cracking,
- connection at the steel/concrete interface,
- local justifications of the concrete slab.

Special features not dealt with under the example due to the retained hypotheses for the deck design are referred to in appendices. This mainly involves the justification at ULS of a class 4 I-shaped cross-section under bending.

2 - General design data

These data have been chosen to examine the most general calculation case as possible.

2.1 - Traffic related data

A two-lane traffic road 3.5 meter wide takes the bridge. Each lane is bordered by a 2.0 meter wide safety strip on the right-hand side and a normalised safety barrier. The total width of the pavement between safety devices (see Figure 2.1) is therefore 11 meter.

The LM1 load model, made up of the uniformly distributed load (UDL) and the concentrated loads of the tandem system (TS), is used. It is supplemented by the LM2 load model for local justifications of the concrete slab.

*EN1991-2, 4.3.2
EN1991-2, 4.3.3*

The definition of the LM1 model vertical loads gives rise to a series of adjustment coefficients α_{Qi} , α_{qi} and α_{qr} . The values given to these coefficients are defined by the National Annex of each country with the possibility of being based on traffic classes.

EN1991-2, 4.3.2 (3)

As the French National Annex to EN1991-2 was not available when this guidance book was drafted, the values defined by the National Application Document (DAN) to ENV1991-3, based on a class 2 traffic, have been adopted.

Lane no.	α_{Qi}	α_{gi}	α_{gr}
1	0.9	0.7	/
2 or more	0.8	1.0	/
Remaining area	/	/	1

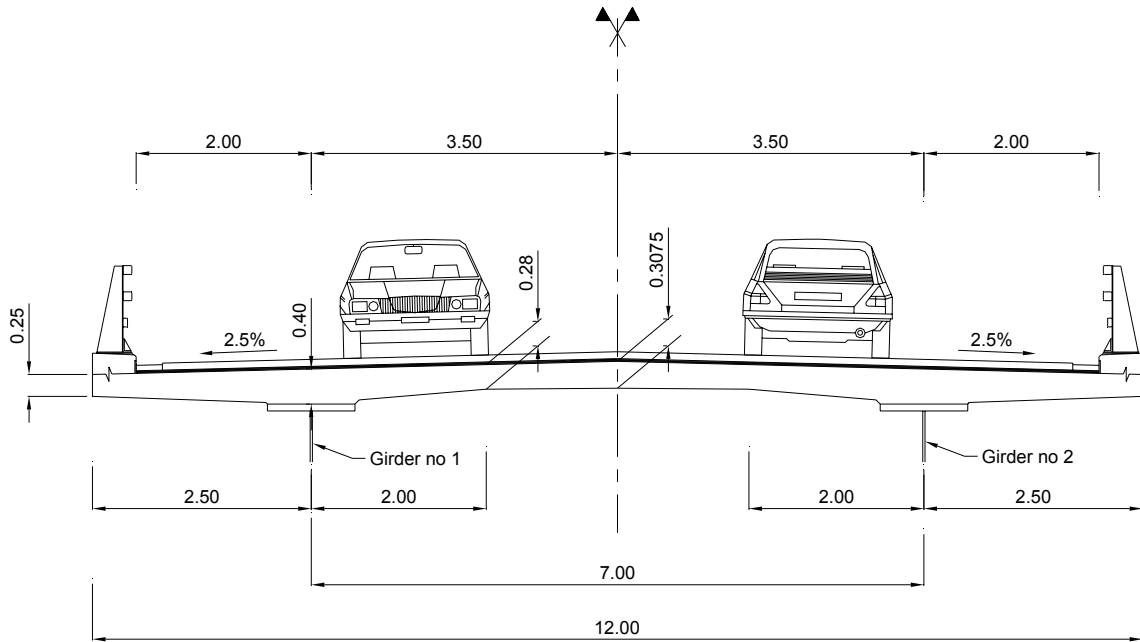


Figure 2. 1: Cross section with traffic data

The design life of the bridge is taken as equal to 100 years.

The Fatigue Load Model 3 (FLM3) is used for fatigue verifications, in connection with the simplified method of the equivalent stress range. EN1991-2, 4.6.4

2.2 - Environmental data

Freezing :

The bridge is located in a moderate freezing zone with very frequent de-icing agents. The environmental exposure classes chosen for the structure (XC and XD) useful for calculating the concrete cover, are given below :

- the exposure class under the waterproofing layer is XC3,
- it becomes XC4 for the bottom face of the concrete slab,
- for the longitudinal concrete support of the safety barrier and for the cornice (if in concrete), they become XC4 and XD3.

EN1992-1-1, Table 4.1

It is assumed that the slab and the longitudinal concrete support of the safety barrier were produced with the same concrete and that the longitudinal concrete support of the safety barrier is not protected by a waterproofing layer.

In application of the “Recommandations for the durability of hardened concretes subjected to freeze” (LCPC, 2003) and the standard EN 206, the concrete should be at least of class C35/45.

EN 206

The notion of exposure classes is explained in greater detail in the SETRA guidance book on concrete bridges under Eurocode 2.

Humidity :

The ambient relative humidity (RH) is assumed to be equal to 80% for this example.

Temperature :

EN1991-1-5

The minimum ambient air temperature (mean return period of 50 years) to which the structure is subjected is assumed to be equal to -20°C. This item of data is necessary to determine the structural steel toughness and its through-thickness properties.

The maximum temperature is also necessary to design the bearings on support and the expansion joints, but this is not addressed in this guidance book.

A thermal gradient is taken into account through the deck depth. It is detailed in Part II, paragraph 5.4.6 of this guide.

3 - Description of the deck - Construction

3.1 - Longitudinal elevation

The bridge has a symmetrical composite two-girder structure with three spans of 60 m, 80 m and 60 m (i.e. a total length between abutments of 200 m). This is a theoretical example for which a few geometrical simplifications have been made:

- the horizontal alignment is straight,
- the top face of the deck is flat,
- the bridge is straight,
- the structural steel main girders are of constant depth: 2800 mm.

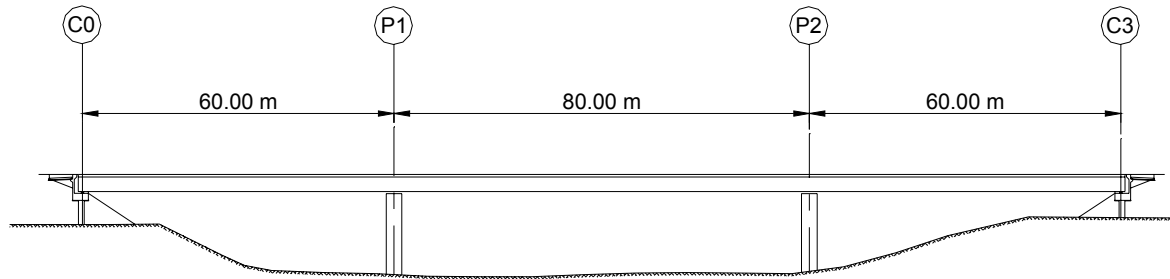


Figure 3. 1: Span distribution

3.2 - Transverse cross-section

The transverse cross-section of the slab and of the non-structural bridge equipments is symmetrical with respect to the axis of the bridge. The slab shows a 2.5% superelevation either side of the bridge axis (see Figure 2.1). The slab thickness varies from 0.4 m on main girders to 0.25 m at its free edges and 0.3075 m at its axis of symmetry.

The total slab width is 12 m. The centre-to-centre spacing between main girders is 7 m and the slab cantilever either side is 2.5 m long.

3.3 - Structural steel distribution (main girders and transverse cross bracing)

The structural steel distribution for a main girder, presented in Figure 3.2, has been designed based on experience acquired in building two-girder bridges in France. As the Eurocodes focus on the verification part of the design, this guide does not present the conceptual design process which has led to this steel distribution. It merely sets out to justify the adopted geometry.

Every main girder has a constant depth of 2800 mm and the variations in thickness of the upper and lower flanges are found towards the inside of the girder. The lower flange is 1200 mm wide whereas the upper flange is 1000 mm wide.

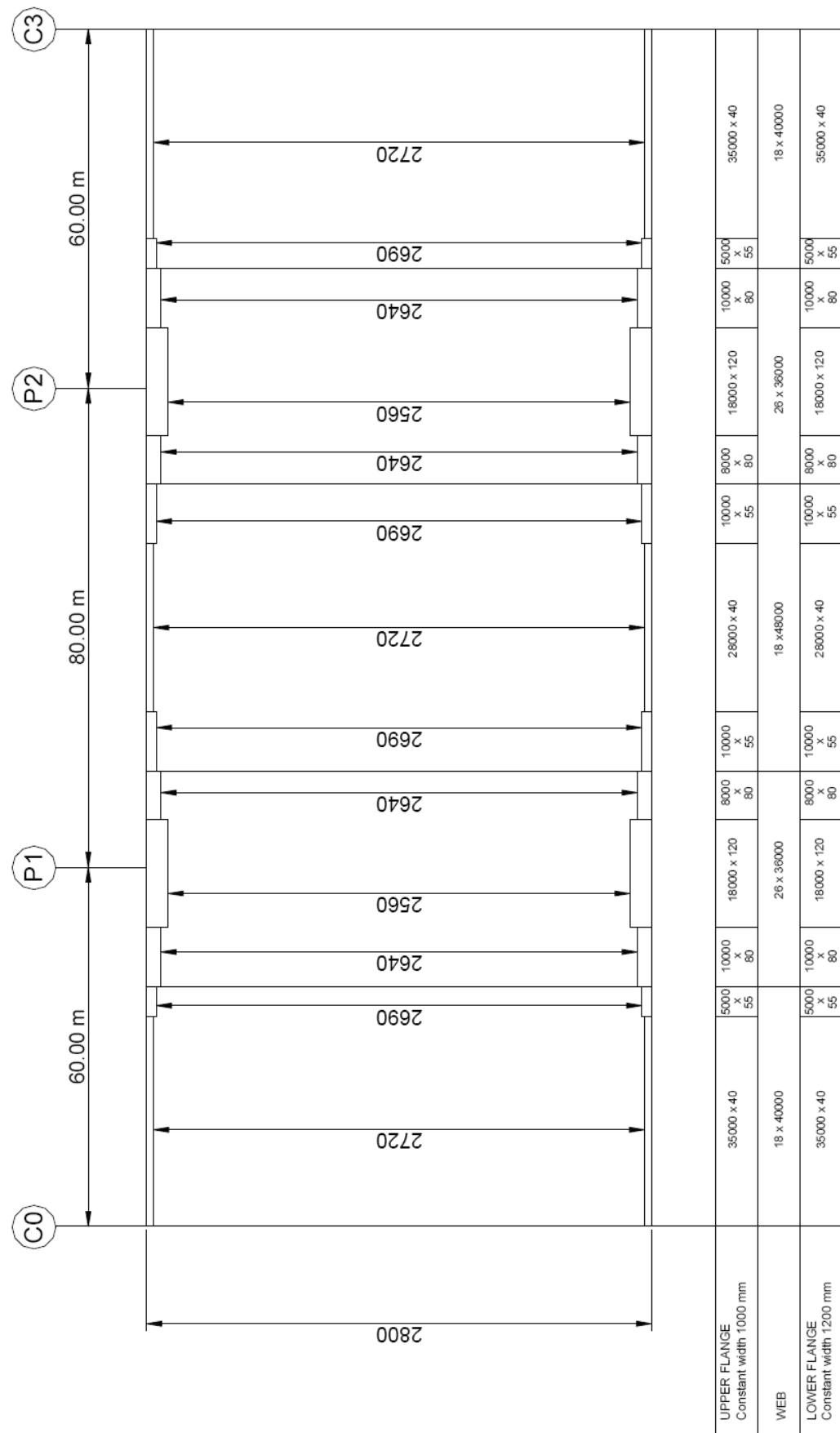


Figure 3.2: Structural steel distribution for a main girder

The two main girders have transverse bracing at abutments and at internal supports, as well as every 7.5 m in side spans (C0-P1 and P2-C3) and every 8 m in central span (P1-P2). Figures 3.3 and 3.4 illustrate the geometry and dimensions adopted for this transverse cross-bracing. The transverse girders in span are made of IPE600 rolled sections whereas the transverse girders at internal supports and abutments are built-up welded sections. The vertical T-shaped stiffeners are duplicated and welded on the lower flange at supports whereas the flange of the vertical T-shaped stiffeners in span has a V-shaped cutout for fatigue reasons.

Note: The transverse girder at support should be carefully justified for the bracing rigidity and the transmission of the transverse horizontal forces. Other designs can be found in other books.

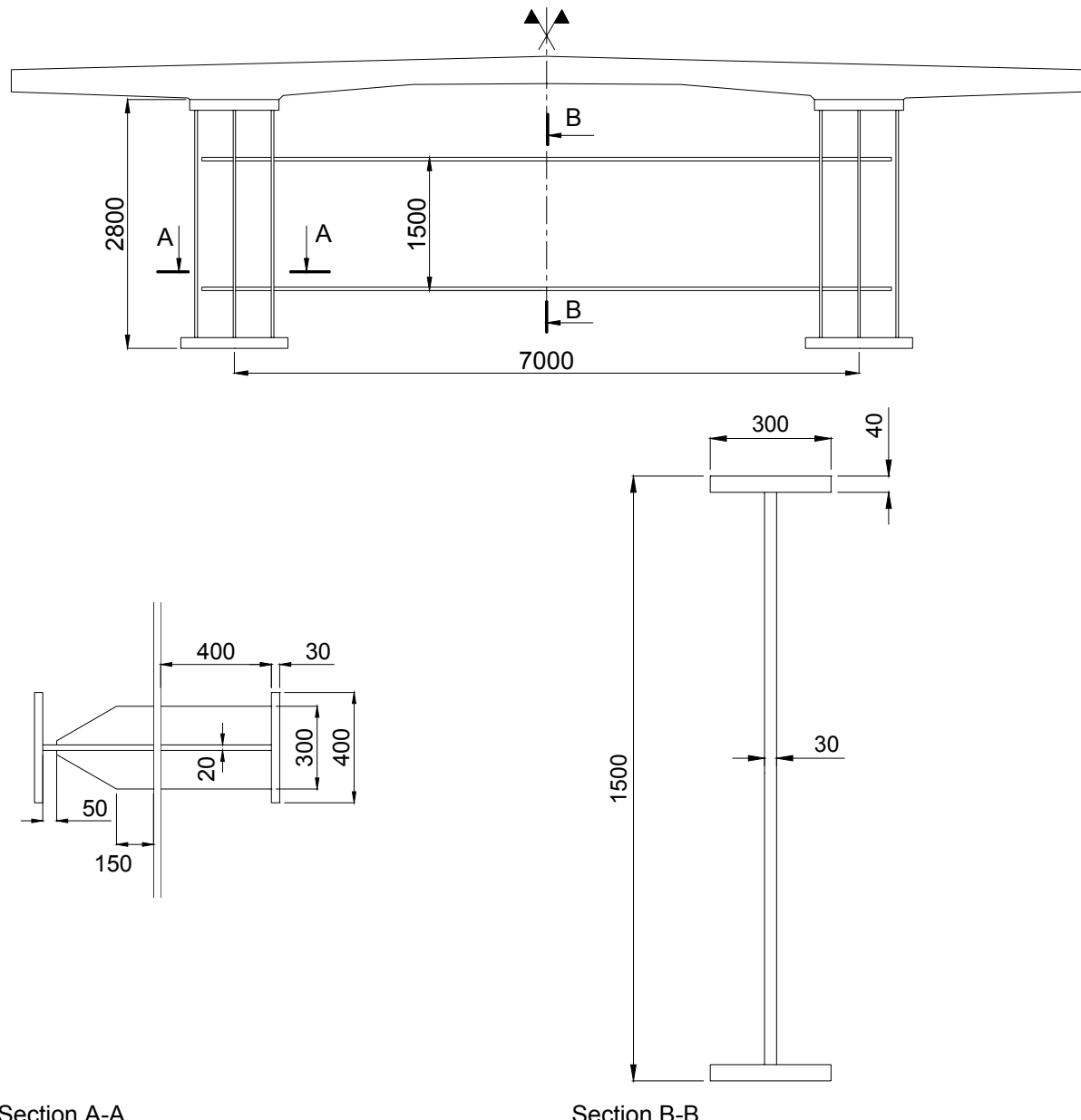


Figure 3.3: Detailing of transverse cross-bracing at supports

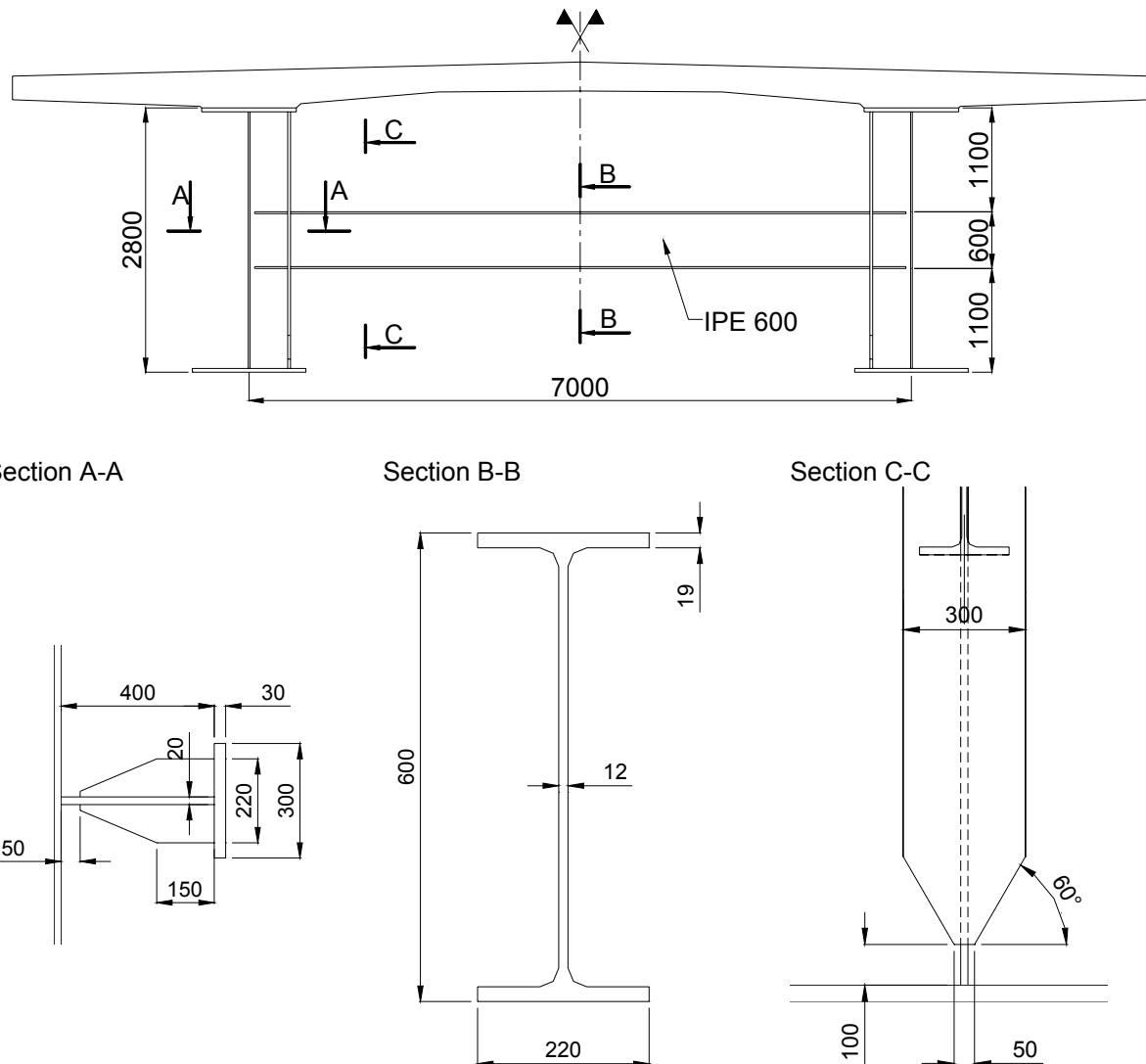


Figure 3.4: Detailing of transverse cross-bracing in span

3.4 - Construction phases (slab concreting)

The assumptions pertaining to the construction phases are important for all the verifications during installation of the structural steel structure of the deck and during concreting. They are also necessary to determine the values of steel/concrete modular ratios (see paragraph 5.3). Finally the calculation of internal moments and forces in the deck should take construction phases into account.

EN1994-2, 5.4.2.4

The following construction phases have been adopted:

- installation of the structural steel structure of the deck ;
- on-site pouring of the concrete slab segments by casting them in a selected order:

The total length of 200 m has been broken down into 16 identical 12.5-m-long concreting segments. They are poured in the order indicated in Figure 3.5. The selfweight of the mobile formwork is assessed in the calculations at 2 kN/m².

The start of pouring the first slab segment is the time origin ($t = 0$). Its definition is necessary to determine the respective ages of the concrete slab segments during the construction phases.

The time taken to pour each slab segment is assessed at 3 working days. The first day is devoted to the concreting, the second day to its hardening and the third to moving the mobile formwork. This sequence respects a minimum concrete strength of 20 MPa before removal of the formwork. This avoids damaging the partially hardened concrete, of which the composite properties will be required in the later concreting phases.

EN1994-2, 6.6.5.2(3)

The slab is thus completed within 66 days (including the non-working days over the weekend).

- installation of non-structural bridge equipments:

It is assumed that this installation is completed within 44 days, so that the deck is fully constructed at the date $t = 66 + 44 = 110$ days.

Given these choices Table 3.1 shows the ages of the various slab segments and the mean value of the age t_0 for all the concrete put in place at each construction phase.

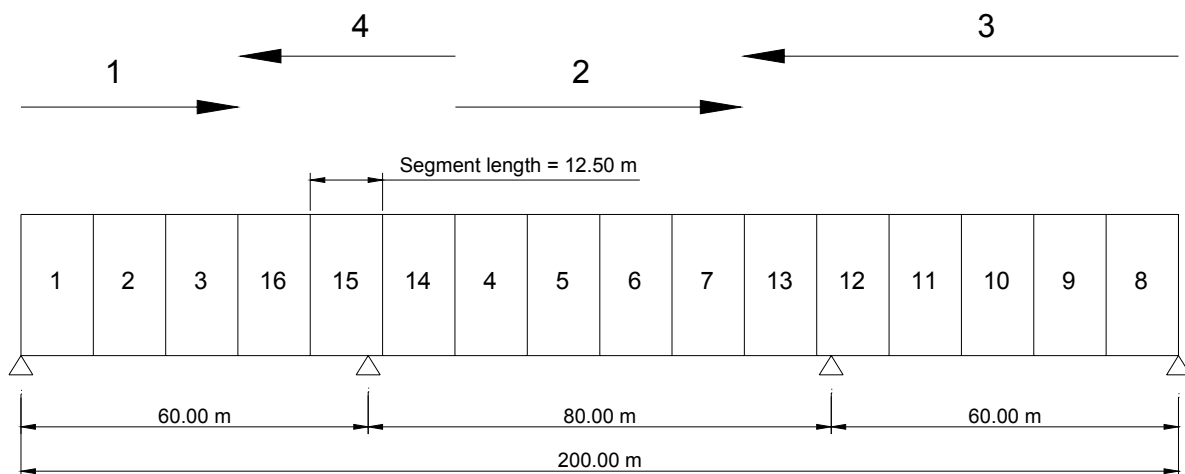


Figure 3.5: Order for concreting the slab segments

A deliberate decision has been made in this guidance book not to apply a difference in level at the internal supports (prestressing by imposed deformations). When differences in level are planned, a minimum period of 14 days should be respected in the construction sequence between the end of concreting (for the spans concerned by this imposed prestressing) and the start of prestressing operations. This condition allows the use of a single value for the modular ratio at any given stage of prestressing. This modular ratio is calculated with the mean value of the age t_0 of the already put in place concrete at the time of prestressing operations.

EN1994-2, 5.4.2.2(3)

Finally, it should be pointed out that a minor variation in the times adopted for the construction phases has little influence on the values of the modular ratio and even less on the values of internal forces and moments obtained from the global analysis.

Load case	Instant t when applying the load case	seg. 1	seg. 2	seg. 3	seg. 4	seg. 5	seg. 6	seg. 7	seg. 8	seg. 9	seg. 10	seg. 11	seg. 12	seg. 13	seg. 14	seg. 15	seg. 16	Mean value of the concrete age at the considered instant t
concreting segment 1	0	3	5	8	11	13	16	19	21	24	29	32	37	40	45	50	53	3.00
concreting segment 2	3	8	5	8	11	13	16	19	21	24	26	29	34	37	42	47	50	6.50
concreting segment 3	8	5	3	5	8	11	13	16	19	21	24	26	29	32	37	42	47	7.33
concreting segment 4	11	11	8	3	5	8	11	13	16	19	21	24	26	29	32	37	42	10.50
concreting segment 5	16	16	13	8	5	11	11	13	13	18	21	24	26	26	29	34	37	11.40
concreting segment 6	19	19	16	16	11	8	3	8	3	8	11	16	16	13	8	5	3	14.17
concreting segment 7	24	24	21	16	13	8	3	8	3	8	11	16	16	13	8	5	3	17.14
concreting segment 8	29	29	26	21	18	13	8	5	3	8	11	16	16	13	8	3	18.00	18.00
concreting segment 9	32	32	29	24	21	16	11	8	3	8	11	16	16	13	8	3	21.00	21.00
concreting segment 10	37	37	34	29	26	21	16	13	8	3	8	11	16	16	13	8	3	21.90
concreting segment 11	40	40	37	32	29	24	19	16	11	8	3	8	11	16	16	13	8	24.73
concreting segment 12	45	45	42	37	34	29	24	21	16	13	8	3	8	11	16	13	8	24.73
concreting segment 13	50	50	47	42	39	34	29	26	21	18	13	8	5	8	11	13	8	27.67
concreting segment 14	53	53	50	45	42	37	32	29	24	21	16	11	8	3	8	11	8	28.54
concreting segment 15	58	58	55	50	47	42	37	34	29	26	21	16	11	8	5	8	3	31.50
concreting segment 16	61	61	58	53	50	45	40	37	32	29	24	19	16	11	8	3	3	32.40
end of concrete hardening in the whole slab	66	66	63	58	55	50	45	42	37	34	29	24	21	16	13	8	3	35.25
superstructures	110	110	107	102	99	94	89	86	81	78	73	68	65	60	57	52	47	79.25
End of construction	110	110	107	102	99	94	89	86	81	78	73	68	65	60	57	52	47	79.25

Table 3.1: Age of concrete slab segments at the end of the construction phases

3.5 - Reinforced concrete slab

3.5.1 - Reinforcing bars concrete cover

The nominal concrete cover is the sum of a minimum concrete cover and an allowance in execution for deviation:

$$c_{\text{nom}} = c_{\text{min}} + \Delta c_{\text{dev}}$$

$\Delta c_{\text{dev}} = 5$ mm is adopted for the slab concreted in situ because of:

- quality control (usual in bridge engineering design in France where a Quality Insurance Plan is obligatory),
- choice of a simple geometry for the slab.

EN1992-1-1, 4.4.1

*EN1992-1-1, 4.4.1.3
+ National Annex*

This choice assumes nevertheless that the required measures on site are described in the Special Contract Documents.

The nominal concrete cover results from a compromise between a high value which is favorable to durability, and a lower value which is favorable to a good mechanical behaviour of the slab.

For the specific case dealt with here the following concrete covers have been adopted for the reinforcing bars (further details, in particular the definition of structural classes, can be found in the SETRA guidance book on concrete bridges under Eurocode 2) :

- for the upper reinforcement layer (XC3):

Structural class: $4 + 2 - 1 - 1 = 4$

(-1 for the concrete strength \geq C30/37 ; -1 for the type of cement)

hence $c_{\text{min}} = 25$ mm

hence $c_{\text{nom}} = 30$ mm

- for the lower reinforcement layer (XC4):

Structural class: $4 + 2 - 1 - 1 = 4$

(-1 for the concrete strength \geq C35/45 ; -1 for a compact concrete cover)

hence $c_{\text{min}} = 30$ mm

hence $c_{\text{nom}} = 35$ mm

3.5.2 - Maximum value of the crack width

The maximum values of the crack width w_{max} adopted in this guidance book are as recommended by the Eurocodes and their National Annexes. They depend on the exposure class (see paragraph 2.2 of this part II):

- for local bending of the slab:

$w_{\text{max}} = 0.3$ mm for the frequent SLS combination of actions

EN1992-2, 7.3.1, Table

7.101N

+ National Annex

- for the longitudinal global bending:

$w_{\text{max}} = 0.3$ mm for the frequent SLS combination of actions

$w_{\text{max}} = 0.3$ mm for the indirect non-calculated actions (restrained shrinkage), in the tensile zone for the characteristic SLS combination of actions

*EN1994-2, 7.4.1 (4),
note*

Note: For longitudinal global bending the « SETRA Recommendations on controlling cracking in slabs » [39] stipulate a 0.3 mm opening limit for rare SLS combination of actions and a 0.2 mm opening limit under indirect non-calculated actions. Given the increased traffic loads in EN1991-2 and the doubling of the term $\Delta\sigma_s$ taking the tension stiffening effect into account, these limits would have been excessively severe. The limit for frequent combination of actions which is stipulated in the French National Annex to EN1992-2 is more relevant. It has been used in this guidance book.

Two methods are usable to control cracking:

a) Method 1 (called direct method):

The crack opening is directly calculated in a conventional manner and is checked to be lower than a maximum limit imposed by the design specifications.

EN1994-2, 7.4.1(2)
which refers to EN1992-1-1, 7.3.4

b) Method 2 (called indirect method):

Specific detailing of the reinforcing bars should be respected according to the stress level in these bars (maximum bar diameters and/or maximum bar spacing). Compliance with these provisions ensures that the crack opening is limited to the maximum value imposed by the design specifications.

EN1994-2, 7.4.1(3)

Method 1 can be used for both transverse (reinforced concrete behaviour) and longitudinal (composite behaviour) bending. Method 2 can be used for the longitudinal bending (composite behaviour).

In this guidance book method 1 will be used for local transverse bending (reinforced concrete behaviour) and method 2 for the global longitudinal bending (composite behaviour). Method 1 is further detailed in the SETRA guidance book on concrete bridges under Eurocode 2.

3.5.3 - Description of the slab reinforcement

For both reinforcing steel layers, the transverse reinforcing bars are placed outside the longitudinal reinforcing bars, on the side of the slab free surface.

Transverse reinforcing steel

- at mid-span of the slab (between the main steel girders):

High bond bars with diameter $\varnothing = 20$ mm and spacing $s = 170$ mm in upper layer
High bond bars with diameter $\varnothing = 25$ mm and spacing $s = 170$ mm in lower layer

- in the slab sections supported by the main steel girders:

High bond bars with diameter $\varnothing = 20$ mm and spacing $s = 170$ mm in upper layer
High bond bars with diameter $\varnothing = 16$ mm and spacing $s = 170$ mm in lower layer

Longitudinal reinforcing steel

- in span:

High bond bars with diameter $\varnothing = 16$ mm and spacing $s = 130$ mm in upper and lower layers
(i.e. in total $\rho_s = 0,92\%$ of the concrete section)

- in intermediate support regions:

High bond bars with diameter $\varnothing = 20$ mm and spacing $s = 130$ mm in upper layer
High bond bars with diameter $\varnothing = 16$ mm and spacing $s = 130$ mm in lower layer
(i.e. in total $\rho_s = 1,19\%$ of the concrete section)

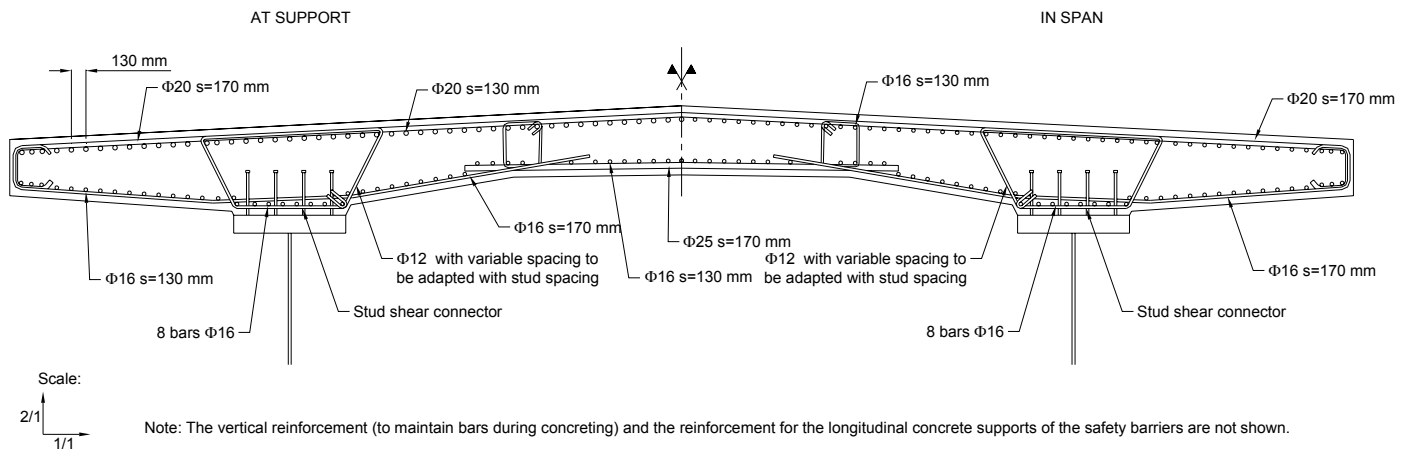


Figure 3.6: Steel reinforcement in a slab cross-section

For the example dealt with here the lengths in Figure 3.7 classify the cross-sections between span regions and intermediate support regions for calculation of the longitudinal reinforcing steel. These lengths are conventional and have not been optimized.

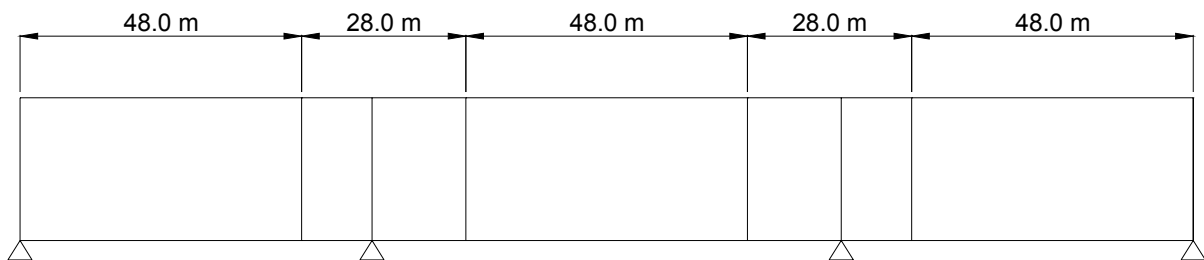


Figure 3.7: Location of mid-span and support sections for longitudinal reinforcement

3.5.4 - Modeling the slab to calculate the general longitudinal bending

For simplification reasons the actual slab cross-section of a half-deck (see Figure 3.8) is modeled by a main rectangular area to the actual width (i.e. 6 m) and a secondary rectangular area modelling a concrete haunch which has the same width as the upper structural steel flange (i.e. 1 m). The respective depths e_1 and e_2 of these rectangles are calculated so that the actual and modeled sections have the same mechanical properties (same area and same centre of gravity). This gives $e_1 = 30.7$ cm and $e_2 = 10.9$ cm.

The mechanical properties of the whole slab cross-section are:

- Area: $A_b = 3.9 \text{ m}^2$
- Second moment of area (around a horizontal axis Δ located at the steel/concrete interface): $I_\Delta = 0.283 \text{ m}^4$
- Perimeter : $p = 24.6 \text{ m}$

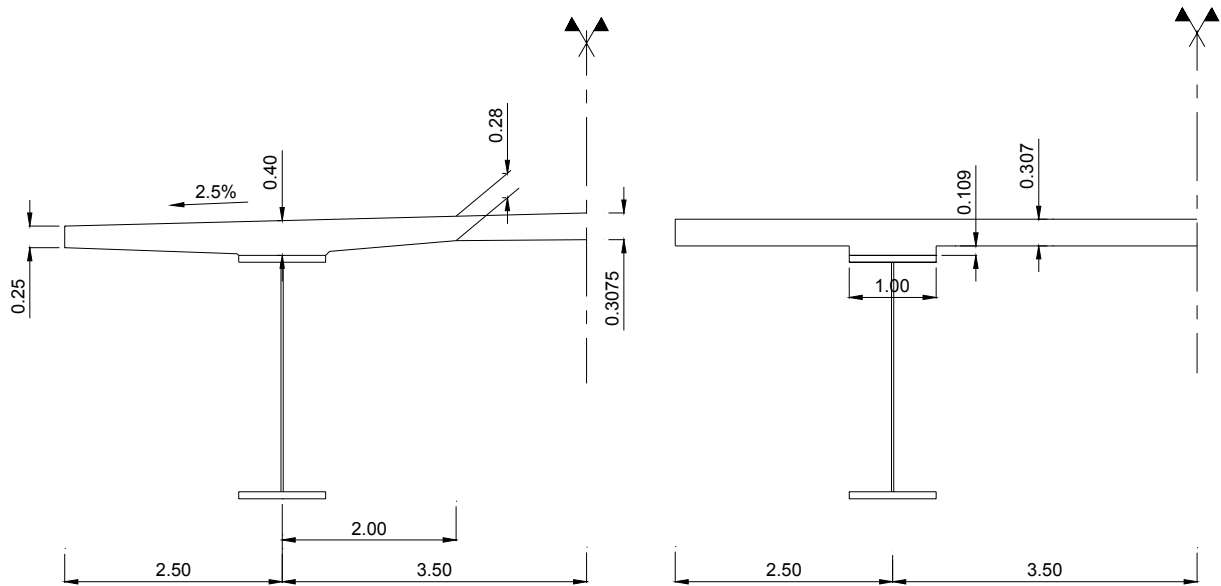


Figure 3.8: Modeling the concrete slab for the longitudinal global bending

Similarly, to model the reinforcement, each longitudinal bars layer is replaced by a single point-shaped bar with the same area and located in the web plane of the main steel girder. The reinforcement areas are introduced into the design model as percentages of the total area of the concrete slab:

		ρ_s (%)	y (mm)
Mid-span cross-sections	top layer	0,46	61 mm with respect to the upper face of the modelled slab main rectangle
	bottom layer	0,46	21 mm with respect to the lower face of the modelled slab main rectangle
Support cross-sections	top layer	0,73	63 mm with respect to the upper face of the modelled slab main rectangle
	bottom layer	0,46	21 mm with respect to the lower face of the modelled slab main rectangle

The vertical position y of the layer is a mean value calculated by taking account of the transverse superelevation of the actual slab and of the concrete cover assessed in paragraph 3.5.1 of this guidance book.

4 - Materials

EN1994-2 limits the scope of each material when they are used in a composite structure:

- concrete classes between C20/25 and C60/75 (or for lightweight concretes, between LC20/25 and LC60/75);
- structural steel grades between S235 and S460.

EN1994-2, 3.1(2)

EN1994-2, 3.3(2)

EN1992-1-1 also limits the use of its calculation rules (design and detailing) to reinforcing steels with yield strength between 400 and 600 MPa.

EN1992-1-1, 3.2.2(3)

EN1994-2 only deals with the stud shear connectors. Other types of shear connectors could be referred to in the National Annex of each European country (case of angle connectors in France).

EN1994-2, 1.1.3(3)

4.1 - Material toughness and through-thickness properties

4.1.1 - General

Steel grade S355 has been chosen for the example of this guidance book.

Under this grade the structural steels commonly used in bridge design are the non-alloy structural steels defined in EN10025-2 and the normalized rolled weldable fine grain structural steels defined in EN10025-3.

Note: Thermomechanical rolled weldable fine grain structural steels (EN 10025-4), structural steels with improved atmospheric corrosion resistance (EN 10025-5) and structural steels in the quenched and tempered condition (EN 10025-6) could also be used but no provision is made for them in this guidance book.

The following subgrades (also called steel quality) should be adopted to ensure a good weldability and a better toughness in the upper plateau of the toughness-temperature relationship (see Figure 1.1 of EN1993-1-10, for example):

thickness	Subgrade (or quality)
$t \leq 30 \text{ mm}$	S 355 K2 or S 355 N
$30 \text{ mm} < t \leq 80 \text{ mm}$	S 355 N
$80 \text{ mm} < t$	S 355 NL

Table 4.1: Subgrade choice as a function of plate thickness

EN1994-2, 3.3 (1) which refers to EN1993-2, 3.2.3(2) + National Annex

4.1.2 - Resistance to brittle fracture

In addition to Table 4.1, the steel subgrades should be chosen to avoid brittle fracture at low temperatures. This subgrade depends mainly on the plate thickness, on the the tensile stress level σ_{Ed} in the section and on the service temperature T_{Ed} .

EN1993-2, 3.2.3

Table 4.2 below gives the maximum permissible thicknesses as function of σ_{Ed} and T_{Ed} as well as the steel subgrades used for the example.

σ_{Ed}	0.75 f_y		0.5 f_y		0.25 f_y	
T_{Ed}	-30 °C	-20 °C	-30 °C	-20 °C	-30 °C	-20 °C
S355 K2 or N	50	60	80	95	130	150
S355 NL	75	90	110	135	175	200

Table 4.2: Maximum permissible thicknesses (in mm)

The combination of actions to be considered to calculate σ_{Ed} is the accidental one where the thermal action is the accidental load:

$$A [T_{Ed}] + \sum G_k + \gamma_1 Q_{k1} + \gamma_2 Q_{k2}$$

In practice, this comes down in common cases to calculate σ_{Ed} for the permanent loads and the frequent traffic loads $\gamma_1 Q_{k1}$.

The service temperature T_{Ed} can be taken as equal to the characteristic value of the minimum shade air temperature T_{min} defined in annex A of EN1991-1-5 (temperature with an annual probability of being exceeded of 0.02 or a mean return period of 50 years). A value of T_{min} equal to -20°C will be assumed in this guidance book, as stated in paragraph 2.2.

At the pre-design stage $\sigma_{Ed} = 0.5 f_y$ can be assumed but this point should be verified after finishing design to adjust the steel subgrade as appropriate. It will then be possible to interpolate between the σ_{Ed} values defined in Table 4.2.

In the negative bending moment regions and even if the flange remains in compression for the characteristic combination of actions, 0.25 f_y will be the lowest stress level used to determine the maximum permissible thickness.

EN1993-1-10, Table 2-1 (partial)

EN1993-1-10, 2.2(4)

EN1991-1-5, Annex A

4.1.3 - Synopsis of choices for grades and subgrades

Tables 4.1 and 4.2 give the following choices in the present case ($T_{Ed} = -20^\circ\text{C}$ and $\sigma_{Ed} = 0.5 f_y$).

Thickness	Subgrade
$t \leq 30 \text{ mm}$	S 355 K2
$30 \leq t \leq 80 \text{ mm}$	S 355 N
$80 \leq t \leq 135 \text{ mm}^{(*)}$	S 355 NL

(*) This value may be increased if the absolute value of tensile stress σ_{Ed} is lower than 0.5 f_y with a threshold at $\sigma_{Ed} = 0.25 f_y$ (up to $t_{max} = 200 \text{ mm}$ if $T_{Ed} = -20^\circ\text{C}$).

The permissible thicknesses assume also that fatigue criteria have been verified by using the equivalent stress range method at 2 million cycles with a partial factor $\gamma_{Mf} = 1.35$. They have been calibrated on the assumption that fatigue verifications govern the design. If this is not the case, they could eventually be increased but using a complex calculation based on fracture mechanics (see EN1993-1-10, 2.4).

4.1.4 - Structural steel mechanical properties

They are given in EN10025-2 for steel grade S355K2 and in EN10025-3 for steel grades S355N and S355NL.

t (mm)	≤ 16	>16	>40	>63	>80	>100
f_y	355	345	335	325	315 ^(*)	295 ^(*)
f_u	470	470	470	470	470	450

Table 4.3: Decrease of f_y and f_u according to the plate thickness t

(*) It will be noticed that the thermomechanical structural steel S355M has yield strengths f_y that are clearly higher for the thick plates ($f_y = 320$ MPa for $t = 120$ mm), but lower ultimate strengths f_u with maximum permissible thicknesses of 120/130 mm due to the manufacturing process of these structural steels.

The structural steel has a modulus of elasticity $E_a = 210\,000$ MPa.

Its coefficient of linear thermal expansion is normally $\alpha_{th}^a = 12 \cdot 10^{-6}$ per °C. To simplify the global analysis, it is taken here as equal to the concrete coefficient, i.e. $\alpha_{th}^a = \alpha_{th}^c = 10 \cdot 10^{-6}$ per °C.

EN1993-1-1, 3.2.6

EN1992-1-1, 3.1.3(5)

Note: To calculate the variation in length of the bridge, the same coefficient $12 \cdot 10^{-6}$ per °C is used for both materials.

EN1994-2, 5.4.2.5(3)

4.2 - Concrete

Normal concrete of class C35/45 is used for the reinforced slab. The main mechanical properties are as follows :

- characteristic compressive cylinder strength at 28 days: $f_{ck} = 35$ MPa
- mean value of axial tensile strength: $f_{ctm} = -3.2$ MPa
- 5% fractile of the characteristic axial tensile strength: $f_{ctk,0.05} = -2.2$ MPa
- 95% fractile of the characteristic axial tensile strength: $f_{ctk,0.95} = -4.2$ MPa
- mean value of concrete cylinder strength at 28 days: $f_{cm} = f_{ck} + 8 = 43$ MPa
- modulus of elasticity : $E_{cm} = 22\,000 (f_{cm} / 10)^{0.3} = 34\,077$ MPa

EN1992-1-1, 3.1.2
Table 3.1

The design value of the compressive strength f_{cd} is defined differently in EN1994-2 (for the composite behaviour in global longitudinal bending) and in EN1992-2 (for the reinforced concrete behaviour in transverse bending):

- composite behaviour: $f_{cd} = f_{ck} / \gamma_c$
- reinforced concrete behaviour: $f_{cd} = \alpha_{cc} f_{ck} / \gamma_c$

EN1994-2, 2.4.1.2(2)
EN1992-2, 3.1.6(101)
+ National Annex

The recommended value of α_{cc} (coefficient that takes account of the influence of the long-term effects on the compressive strength) in EN1992-2 is 0.85. The French National Annex modified it for the value of 1.0 used in this guidance book.

Note: The coefficient α_{cc} does not appear in EN1994-2. It must not be confused with another 0.85 coefficient which is applied to f_{ck} when the plastic stress distributions are defined for calculating the plastic resistance moment (EN1994-2, 6.2.1.2). This coefficient (fixed by calibrating) covers the hypothesis of using a rectangular distribution instead of a parabola-rectangle distribution.

4.3 - Reinforcement

The reinforcing bars used in this guidance book are class B high bond bars with a yield strength $f_{sk} = 500$ MPa.

EN1992-1-1, 3.2 + Annex C

In EN1992-1-1 the elasticity modulus of reinforcing steel is $E_s = 200\,000$ MPa. However, in order to simplify with respect to the modulus used for the structural steel, EN1994-2 allows the use of $E_s = E_a = 210\,000$ MPa which will be done in this book.

EN1994-2, 3.2(2)

More comprehensive information on the mechanical properties of these reinforcing bars can be found in the SETRA guidance book for concrete bridges under Eurocode 2.

Note: The reader's attention is drawn to the notations used for the yield strength of reinforcement. It is noted f_{yk} in Eurocode 2 whereas f_y is the yield strength of the structural steel in Eurocode 4.

In this book the notations used for reinforcement are those of Eurocode 4, i.e. f_{sk} for the reinforcing steel and f_{yk} for the structural steel, even when referring to Eurocode 2.

4.4 - Shear connectors

Stud shear connectors in S235J2G3 steel grade have been adopted for the example of this book. Their ultimate strength is $f_u = 450$ MPa.

EN 13918

See also Chapter 11 of this Part II for further details.

4.5 - Partial factors for materials

This guidance book does not deal with accidental and seismic design situations.

For Ultimate Limit State (ULS):

Design situation	γ_c (concrete)	γ_s (reinforcement)	γ_m (structural steel)		γ_v (studs)
Persistent Transient	1.5	1.15	$\gamma_{m0} = 1.0$ $\gamma_{m1} = 1.1$ $\gamma_{m2} = 1.25$	Yielding, local instability Resistance of members to instability Resistance of joints	1.25
Reference	EN1992-1-1, 2.4.2.4		EN1993-2, 6.1 and Table 6.2		EN1994-2, 2.4.1.2 + National Annex

For Fatigue Ultimate Limit State:

$\gamma_{C,fat}$ (concrete)	$\gamma_{S,fat}$ (reinforcement)	γ_{Mf} (structural steel)			$\gamma_{Mf,s}$ (studs)
1.5	1.15	Assessment method	Low consequence of failure	High consequence of failure	1.25
		Damage tolerant	1.0	1.15	
		Safe life	1.15	1.35	
EN1992-1-1, 2.4.2.4		EN1993-1-9, Table 3.1			EN1994-2, 6.8.2 + National Annex

In bridge design the French National Annexes have adopted the safe life concept (100 years). The use of this concept does not exclude regular inspections of bridges.

For Serviceability Limit State (SLS):

γ_C (concrete)	γ_S (reinforcement)	$\gamma_{M,ser}$ (structural steel)	γ_V (studs)	
1.0	1.0	1.0	1.25	
EN1992-1-1, 2.4.2.4		EN1993-2, 7.3 (1)	<p>Note: The stud resistance P_{RK} is modified between SLS and ULS, and not the value of γ_V.</p> <p>EN1994-2, 6.8.1 (3)</p>	

For concrete and reinforcement the values of γ_C and γ_S are not used in practice during design verifications.

5 - Actions

5.1 - Permanent loads

Distinction is made in the permanent loads between the selfweights of the structural steel girders, of reinforced concrete slab and of non-structural bridge equipments.

5.1.1 - Selfweight

The density of the structural steel is taken as equal to 77 kN/m³.

EN1991-1-1, Table A-4

To calculate the internal forces and moments and the stresses for the longitudinal bending global analysis, the selfweight of the in-span located transverse cross girders is modeled by a vertical uniformly distributed load of 1500 N/m applied to each main girder (about 10% of the weight of this main girder). This value has been evaluated on the basis of Figure 3.2.

The selfweight of the at-support located transverse cross girders has no influence on the internal forces and moments of the longitudinal global analysis. It only influences the vertical reaction at supports (piles and abutments) but this is not dealt with in this book.

The modeled concrete slab cross-section is presented in paragraph 3.5.4 of this Part II.

The density of the reinforced concrete is taken as equal to 25 kN/m³.

EN1991-1-1, Table A-1

5.1.2 - Non-structural bridge equipments

Item	Characteristics	Maximum multiplier	Minimum multiplier
Concrete support of the safety barrier	area 0.5 x 0.2 m	1.0	1.0
Safety barrier	65 kg/ml	1.0	1.0
Cornice	25 kg/ml	1.0	1.0
Waterproofing layer	3 cm thick	1.2	0.8
Asphalt layer	8 cm thick	1.4	0.8

The density of the waterproofing material and of the asphalt is taken as equal to 25 kN/m³.

EN1991-1-1, Table A-6

The dimensions from the table above correspond to the nominal selfweight loads for which no minimum or maximum multiplier is necessary. The nominal value of the waterproofing layer is multiplied by +/-20% and the nominal value of the asphalt layer by +40% / -20% in order to take a new pavement surfacing into account (during asphalt repairs, for example). Table 5.1 gives the load intensities per unit length (for one of the main steel girder, with an additional 0.1 m long waterproofing layer on the vertical side of both concrete supports of the safety barriers).

EN1991-1-1, 5.2.3

Item	q_{nom} (kN/ml)	q_{max} (kN/ml)	q_{min} (kN/ml)
Concrete support of the safety barrier	2.5	2.5	2.5
Safety barrier	0.638	0.638	0.638
Cornice	0.245	0.245	0.245
Waterproofing layer	4.2	5.04	3.36
Asphalt layer	11	15.4	8.8
Total	18.58 kN/ml	23.82 kN/ml	15.54 kN/ml

Table 5. 1: Non-structural bridge equipments loads

Figure 5.1 details the non-structural bridge equipments used for the example of the guide.

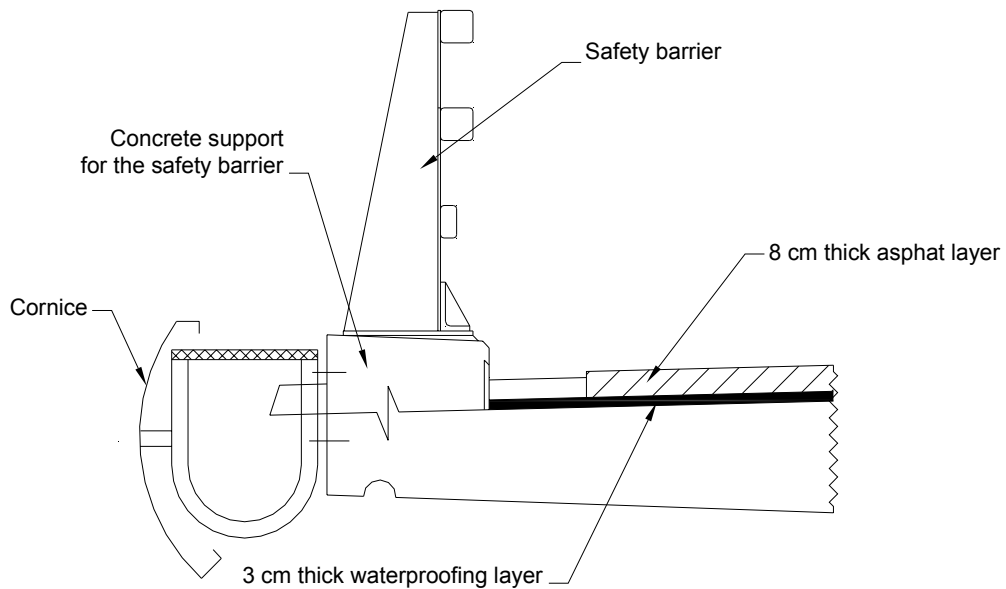


Figure 5.1: Non-structural bridge equipments details

Note: The detailing and the adopted dimensions in this book for the non-structural bridge equipments are definitely not recommendations when designing a bridge. The reader should look up other specialized publications on these topics which have been published elsewhere in the SETRA collections.

5.2 - Concrete shrinkage

The concrete shrinkage is an imposed deformation ε_r applied to the concrete area in compression. It has three possible physical origins:

Thermal shrinkage ε_{th} :

It is a short term loading which conveys the difference in temperature between the concrete and the structural steel at the time of concrete hardening.

Autogenous shrinkage ε_{ca} :

It is a short term loading which begins just after the concrete is poured and corresponds to the continuing hydration of the cement after the hardening. This reduces the volume of concrete initially poured.

Drying shrinkage ε_{cd} :

It is a long term loading which corresponds to a progressive evaporation of the water contained in the concrete. It applies gradually during the bridge life.

Although it takes place over the bridge life, drying shrinkage starts as soon as the concrete is poured. EN1992-1-1 (to which EN1994-2 refers) therefore deals with ε_{ca} and ε_{cd} simultaneously. A total shrinkage $\varepsilon_{cs} = \varepsilon_{ca} + \varepsilon_{cd}$ will then be calculated for the first time when the bridge will be open to traffic loads (i.e. persistent design situation at the date $t_{ini} = 110$ days) and at infinite time (i.e. persistent design situation at the date $t_{fin} = 100$ years $\approx \infty$).

EN1992-1-1, 3.1.4(6)

Thermal shrinkage is dealt with in EN1994-2 as it is a peculiarity of a composite structure.

5.2.1 - Shrinkage deformation for persistent design situation at traffic opening (date t_{ini})

The calculation of ε_{cs} requires the age t of the concrete at the considered date t_{ini} . At this date every slab segment has a different age. To simplify, the mean value of the ages of all slab segments is considered taking account of the construction phases: $t = 79.25$ days (see Table 3.1).

Autogenous shrinkage

$$\varepsilon_{\text{ca}}(t) = \beta_{\text{as}}(t) \cdot \varepsilon_{\text{ca}}(\infty)$$

$$\varepsilon_{\text{ca}}(\infty) = 2.5 (f_{\text{ck}} - 10) \cdot 10^{-6} = 6.25 \cdot 10^{-5}$$

$$\beta_{\text{as}}(t) = 1 - \exp(-0.2 \sqrt{t}) = 0.8314 \text{ for } t = 79.25$$

$$\text{Hence } \varepsilon_{\text{ca}}(t) = 5.2 \cdot 10^{-5}.$$

EN 1992-1-1, 3.1.4(6)

Drying shrinkage

$$\varepsilon_{\text{cd}}(t) = \beta_{\text{ds}}(t, t_s) \cdot k_h \cdot \varepsilon_{\text{cd},0}$$

$\varepsilon_{\text{cd},0}$ is the nominal unrestrained drying shrinkage value and is calculated by:

$$\varepsilon_{\text{cd},0} = 0.85 \cdot \left[(220 + 110 \cdot \alpha_{\text{ds}1}) \cdot \exp\left(-\alpha_{\text{ds}2} \frac{f_{\text{cm}}}{f_{\text{cm}0}}\right) \right] \cdot 10^{-6} \cdot \beta_{\text{RH}}$$

The relative humidity adopted for the design is 80%, from which the coefficient

$$\beta_{\text{RH}} = 1.55 \cdot \left[1 - \left(\frac{\text{RH}}{100} \right)^3 \right] = 0.7564 \text{ is deduced. } f_{\text{cm}0} \text{ is a reference value of the}$$

mean compressive strength taken as equal to 10 MPa. The coefficients $\alpha_{\text{ds}1}$ and $\alpha_{\text{ds}2}$ represent the hardening speed of the cement. For a normal type of cement (class N) $\alpha_{\text{ds}1} = 4$ and $\alpha_{\text{ds}2} = 0.12$.

$$\text{Hence } \varepsilon_{\text{cd},0} = 2.53 \cdot 10^{-4}.$$

The coefficient k_h depends on the notional size $h_0 = \frac{2A_c}{u}$ where $A_c = 3.9 \text{ m}^2$ is

the concrete area (see 3.5.4) and u is the slab perimeter exposed to drying effects. u is obtained by subtracting from the actual perimeter $p = 24.6 \text{ m}$ the lengths which are not in direct contact with the atmosphere (i.e. the width of the upper steel flanges and the width of the waterproofing layer):

$$u = p - 11 - 2 \times 1.0 = 11.6 \text{ m}$$

$$\text{Hence } h_0 = 672 \text{ mm, then } k_h = 0.7.$$

EN 1992-1-1, Annex B2

By hypothesis the concrete age t_s when drying shrinkage begins is taken as equal to 1 day. This therefore gives:

$$\beta_{\text{ds}}(t, t_s) \frac{t - t_s}{t - t_s + 0.04 \cdot \sqrt{h_0^3}} = 0.10 \text{ for } t = 79.25 \text{ days}$$

$$\text{Hence } \varepsilon_{\text{cd}}(t) = 1.8 \cdot 10^{-5}$$

EN 1992-1-1, Table 3.3

Shrinkage for the persistent design situation at traffic opening

$$\varepsilon_{\text{cs}}(t) = \varepsilon_{\text{ca}}(t) + \varepsilon_{\text{cd}}(t)$$

Finally $\varepsilon_{\text{cs}} = 7 \cdot 10^{-5}$ is applied to each slab segment as soon as the corresponding concrete is put in place. 26% of this strain are produced by autogenous shrinkage and 74% by drying shrinkage.

A possible simplified hypothesis consists of applying this early age shrinkage deformation in a single phase at the end of the slab concreting. It is incorporated (phase by phase or all at once) for the structure justifications at traffic opening in the load combinations for the persistent design situation.

5.2.2 - Shrinkage deformation for persistent design situation at infinite time

The age of the concrete is then infinite. Making t tend towards the infinite in the equations from the previous paragraph gives $\beta_{as}(\infty) = 1$ and $\beta_{ds}(\infty, t_s) = 1$.

Subsequently $\varepsilon_{cs}(\infty) = \varepsilon_{cd}(\infty) + \varepsilon_{ca}(\infty)$ with $\varepsilon_{ca}(\infty) = 6.25 \cdot 10^{-5}$ and $\varepsilon_{cd}(\infty) = k_h \varepsilon_{cd,0} = 1.77 \cdot 10^{-4}$.

Finally $\varepsilon_{cs}(\infty) = 2.4 \cdot 10^{-4}$ is applied to the complete concrete slab (in a single phase). 74% of this strain are produced by drying shrinkage and 26% by autogenous shrinkage.

This action is incorporated for the bridge verifications in the load combinations for the persistent design situation at infinite time.

5.2.3 - Thermal shrinkage deformation

EN1994-2 allows take account of the thermal shrinkage produced by the difference in temperature ΔT between structural steel and concrete when concreting.

The recommended value of ΔT is 20°C but it could be modified by the National Annex of each European country. The strict application of EN1994-2 thus gives a strain $\varepsilon_{th} = \alpha_{th}^c \Delta T = 2 \cdot 10^{-4}$ which is relatively high.

EN1994-2, 7.4.1(6)

In fact, on-site measurements show that this temperature difference is correct but a part of the corresponding thermal shrinkage applies to a structure which has not yet a composite behaviour. For this reason the French National Annex proposes to use the value of thermal shrinkage which is given in "SETRA Recommendations on controlling cracking in slabs" [39]:

$$\varepsilon_{th} = \alpha_{th}^c \cdot \frac{\Delta T}{2} = 1 \cdot 10^{-4}$$

EN1994-2, 7.4.1(6)
+ National Annex

The thermal shrinkage applies to the structure at the same time as the early age shrinkage $\varepsilon_{cs} = 7 \cdot 10^{-5}$. It is normally only used to determine the cracked zones of the global analysis (see paragraph 7.2.3 of this Part II) and to control the crack width in the concrete slab. To simplify (and to limit the calculations) the choice has been made to deal with it in the same way as with the shrinkage at traffic opening.

5.2.4 - Synopsis of shrinkage strain

For calculating the internal forces and moments for the persistent design situation at traffic opening, a shrinkage strain of $7 \cdot 10^{-5} + 1 \cdot 10^{-4} = 1.7 \cdot 10^{-4}$ is applied to each slab segment following the concreting order. For the persistent design situation at infinite time, a shrinkage strain of $2.4 \cdot 10^{-4}$ is applied to the complete slab after finishing all concreting phases.

For transient design situations corresponding to the different concreting phases, the calculations would be similar to those made for the persistent design situation at traffic opening, but with different dates and mean concrete ages for each transient situation. The corresponding calculation detail is not dealt with in this guide.

5.3 - Creep – Modular ratios

5.3.1 - General

When a constant compressive load is applied to a concrete specimen, the specimen is immediately deformed and then continues to deform gradually over time when the load is maintained. At infinite time the final observed strain is around 3 times higher than the initial one. The effect of this gradual deformation for constant applied load is called concrete creep.

The short-term actions inducing a global longitudinal bending of the composite structure (for example, the variable traffic actions on a bridge) are resisted by a composite area, cracked or not. To obtain the value of this composite area (in case of uncracked section), the concrete area is divided by a modular ratio $n_0 = E_a / E_{cm}$ (around 6) before adding the structural steel area.

The creep effect which, by its own definition, only influences the long-term loading is taken into account by a reduction of the concrete area, i.e. an increase in the modular ratio. In a very simple way as proposed in the current French rules for composite bridges, this increase should be a factor of 3 (consistent with the test on concrete specimens in compression).

EN1994-2 replaces this factor of 3 by a more refined equation, $1 + \psi_L \varphi(t, t_0)$, depending on the nature of the permanent applied load and on the creep coefficient defined in EN1992-1-1.

Notes:

Although far more sophisticated than a simple factor of 3, this method of taking creep into account is still a simplified method. It is only valid provided that only one of the two flanges of the main girder is composite. It does not therefore apply to decks with double composite action.

It is still possible to calculate the creep effect scientifically for all types of structure.

The modular ratio n_{ba} between reinforcing steel and structural steel is taken as equal to 1 (EN1994-2, 3.2(2)).

5.3.2 - Practical calculation of the modular ratio for long-term loading

The modular ratio is noted n_L for the long-term calculations of the bridge. It depends on the type of loading on the girder (through the coefficient ψ_L) and on the creep level at the time considered (through the creep coefficient $\varphi(t, t_0)$):

$$n_L = n_0 \cdot [1 + \psi_L \cdot \varphi(t, t_0)]$$

EN1994-2, 5.4.2.2 (2)

Coefficient n_0

$$n_0 = \frac{E_a}{E_{cm}} = \frac{210000}{22000 \left(\frac{f_{cm}}{10} \right)^{0.3}} = 6.1625$$

Creep multiplier ψ_L

ψ_L conveys the dependence of the modular ratio on the type of applied loading :

- permanent load (selfweight of the slab segments, non-structural bridge equipments): $\psi_L = 1.1$
- concrete shrinkage: $\psi_L = 0.55$

Creep coefficient

$$\varphi(t, t_0) = \varphi_0 \cdot \beta_c(t, t_0) = \varphi_0 \cdot \left(\frac{t - t_0}{\beta_H + t - t_0} \right)^{0.3} = \varphi_0 \text{ when } t \text{ tends towards the infinite.}$$

EN1992-1-1, annex B

β_H is a coefficient which only depends on the relative humidity and the notional size $h_0 = 672$ mm already calculated in the previous paragraph on shrinkage.

$$\varphi_0 = \varphi_{RH} \cdot \beta(f_{cm}) \cdot \beta(t_0) = \left[1 + \frac{1 - \frac{RH}{100}}{0.10 \cdot \sqrt[3]{h_0}} \cdot \alpha_1 \right] \cdot \alpha_2 \cdot \left[\frac{16.8}{\sqrt{f_{cm}}} \right] \cdot \left[\frac{1}{0.1 + t_0^{0.2}} \right]$$

The coefficients α_1 and α_2 take account of the influence of the concrete strength when $f_{cm} \geq 35$ MPa (otherwise $\alpha_1 = \alpha_2 = 1$). In this example, $f_{cm} = 43$ MPa resulting in the following deduction:

$$\alpha_1 = \left(\frac{35}{f_{cm}} \right)^{0.7} = 0.866$$

$$\alpha_2 = \left(\frac{35}{f_{cm}} \right)^{0.2} = 0.960$$

t_0 is the mean value of the concrete age (in days) when the considered load case is applied to the structure:

- Permanent load (selfweight of a slab segment):

When the slab segment j ($2 \leq j \leq 16$) is concreted, the first $j-1$ already concreted slab segments all have different ages. The mean value of these $j-1$ ages gives the mean age t_{0j} of all the concrete for the load case which corresponds to the concreting phase of the slab segment j . As many values of n_L as the number of concreting phases should then be calculated (i.e. 15 because the effects of concreting the first slab segment are taken up by the structural steel alone).

To simplify, EN1994-2 allows the use of just one mean value of t_0 to be considered in calculating all the slab concreting phases. This value would logically be the mean value of the ages t_{0j} for each concreting phase. The final column in Table 3.1 gives the 15 values of t_{0j} and their mean value gives $t_0 = 18.4$ days.

Failing specification in EN1994-2 to calculate this mean value, given the very low influence of this choice in t_0 on the final distribution of internal forces and moments in the bridge, and to simplify the calculations, the mean value of the concrete age for all the concreting phases has been considered in this guidance book as equal to half the concreting time of the entire slab, i.e. $t_0 = 66/2 = 33$ days.

- Permanent load (non-structural bridge equipments):

The non-structural bridge equipments loading is applied to the bridge 44 days after the end of the concreting phases. Table 3.1 gives the mean value of the concrete ages of the various slab segments at this time: $t_0 = 79.25$ days.

- Concrete shrinkage:

It is assumed that shrinkage begins as soon as the concrete is poured and extends through its lifetime. EN1994-2 imposes a value of $t_0 = 1$ day for evaluating the corresponding modular ratio.

EN1994-2, 5.4.2.2 (3)

EN1994-2, 5.4.2.2 (4)

Calculation of n_L

The following table summarizes the intermediate values for the calculation of the creep factor and the modular ratio values used in the design of the bridge in this guide.

Load case	ψ_L	t_0 (days)	$\varphi(\infty, t_0)$	n_L
Concreting	1.10	33	1.394	15.61
Shrinkage	0.55	1	2.677	15.24
Bridge equipments	1.10	79.25	1.179	14.15

Note:

A special load case has not been dealt with in the example. This involves prestressing by imposed deformations (for example, a difference in level at an internal support or prestressing tendons in the concrete slab). In this case several hypothesis are imposed by EN1994-2:

- do not apply the prestressing effect before 14 days have lapsed since the last concreting
- take a creep multiplier ψ_L equal to 1.5
- use a mean value of t_0 (as for the concreting phases) when the structure is prestressed step by successive stages

EN1994-2, 5.4.2.2 (2) and (3)

5.4 - Variable actions

5.4.1 - General

The most common variable actions have been used for the global longitudinal bending analysis:

- traffic load model 1 (LM1) made up of the tandem system TS and the uniformly distributed load UDL;
- thermal actions: only the gradient is modeled;
- thermal expansion of the deck should also be taken into account, but for the studied two-girder bridge (where the longitudinal displacements are free on supports) it only has an influence on the design of bearings at supports and on the expansion joints at both deck ends, which are not dealt with in this book.

Other traffic load models are used selectively:

- wind related actions on the bridge, with or without traffic load, to write the combinations of actions in Chapter 6 below;
- traffic load model 2 (LM2) with a single axle for local verifications of the concrete slab;
- fatigue load models 3 and 4 (FLM3 and FLM4) for the fatigue verifications.

Note that every military (or exceptional) traffic loading specific to the studied design should be defined in the Special Contract Documents for both the characteristic values of actions and the related combination rules.

This guide does not give any definition or rules for using the traffic load models in EN1991-2, but only the special features of the load models adopted for the studied design: transverse influence line, traffic lanes positioning, representative values of the traffic load, etc.

5.4.2 - Transverse positioning of the traffic lanes (for global bending analysis)

UDL and TS from load model LM1 are positioned longitudinally and transversally on the deck so as to achieve the most unfavorable effect for the studied main girder (girder no. 1 in Figure 5.2).

A straight transverse influence line is used (see Figure 5.3) with the assumption that a vertical load introduced in the web plane of a main girder goes entirely in this girder. This hypothesis is safe-sided in common cases as the torsional stiffness of the cross-section is neglected. A more accurate calculation taking account of the warping of cross-sections is still possible.

Every longitudinal influence line of the girder no. 1 is commonly defined by the position of the cross-section studied along the deck and the type of internal forces or moments calculated. The unfavourable parts of each longitudinal influence line are then loaded according to the transverse distribution of the traffic vertical loads UDL and TS between the two main girders.

The pavement width between internal vertical faces of the concrete longitudinal supports of the safety barriers (which should be higher than 10 cm) reaches $w = 11$ m, centered on the deck axis. Three traffic lanes each 3 m wide and a 2 m wide remaining area can be placed within this width.

EN 1991-2, 4.2.3.

Given the transverse symmetry of the deck, only girder no. 1 is studied. The traffic lanes are thus arranged in the most unfavorable way according to Figure 5.2.

EN 1991-2, 4.2.4.



Figure 5.2: Positionning the traffic lanes for calculating the girder no 1 in longitudinal global bending

5.4.3 - Tandem System TS

For simplifying the longitudinal global bending calculations, EN1991-2 allows that each axle of the tandem TS may be centered in its traffic lane. The vertical load magnitudes per axle are given in EN1991-2 Table 4.2.

EN1991-2, 4.3.2(1) (a)

Note: Whilst waiting for the French National Annex to EN1991-2, not available when this guidance book was written, the adjustment factors α_Q of the French National Application Document (NAD) to ENV1991-3 are used.

Figure 5.3 indicates the transverse position of the three tandems considered with respect to the main structural steel girders.

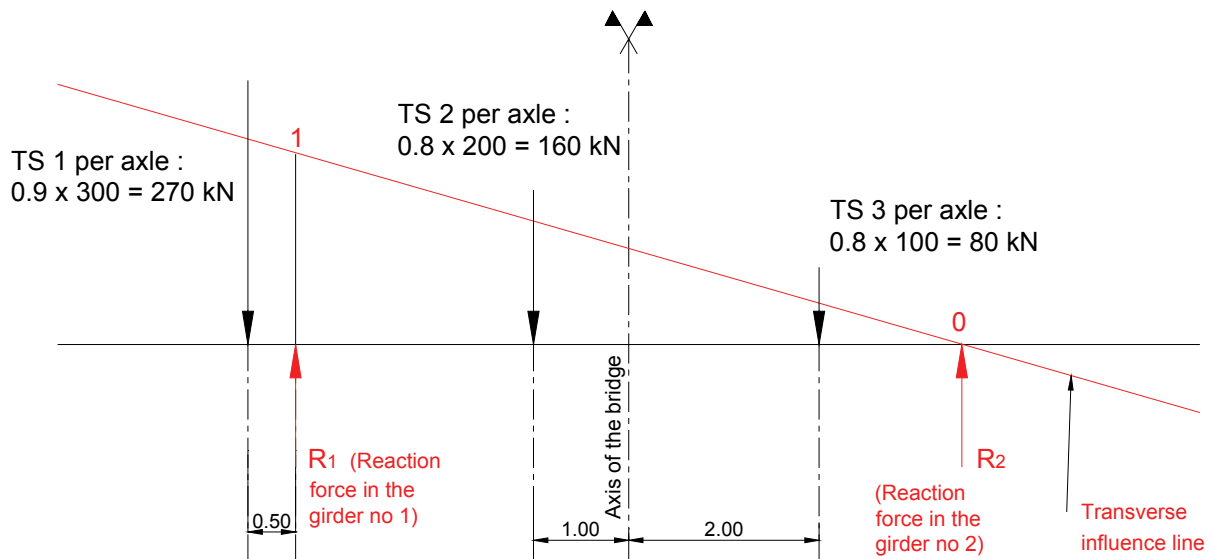


Figure 5.3: Tandem TS loading on the deck

The structural system in Figure 5.3 is isostatic and the reaction forces on each main girder are therefore:

$$R_1 = 409.3 \text{ kN} \text{ for an axle (two per tandem)}$$

$$R_2 = 100.7 \text{ kN}$$

Each traffic lane can only support a single tandem TS in the longitudinal direction. The three used tandem TS (one per lane) could not be necessarily located in the same transverse cross-section.

5.4.4 - Uniformly Distributed Load UDL

Given the used transverse influence line, the traffic lanes are loaded with UDL up to the axis of girder no. 2 (see Figure 5.4) i.e. the positive part of the influence line. The vertical load magnitudes of UDL are given in EN1991-2 Table 4.2.

EN1991-2, 4.3.2(1) (b)

In the longitudinal direction, each traffic lane is loaded over a length corresponding to the unfavorable parts of the longitudinal influence line defined by the studied internal forces or moments and the studied cross-section.

Note: Whilst waiting for the French National Annex to EN1991-2, the adjustment factors α_Q of the French National Application Document (NAD) to ENV1991-3 are used.

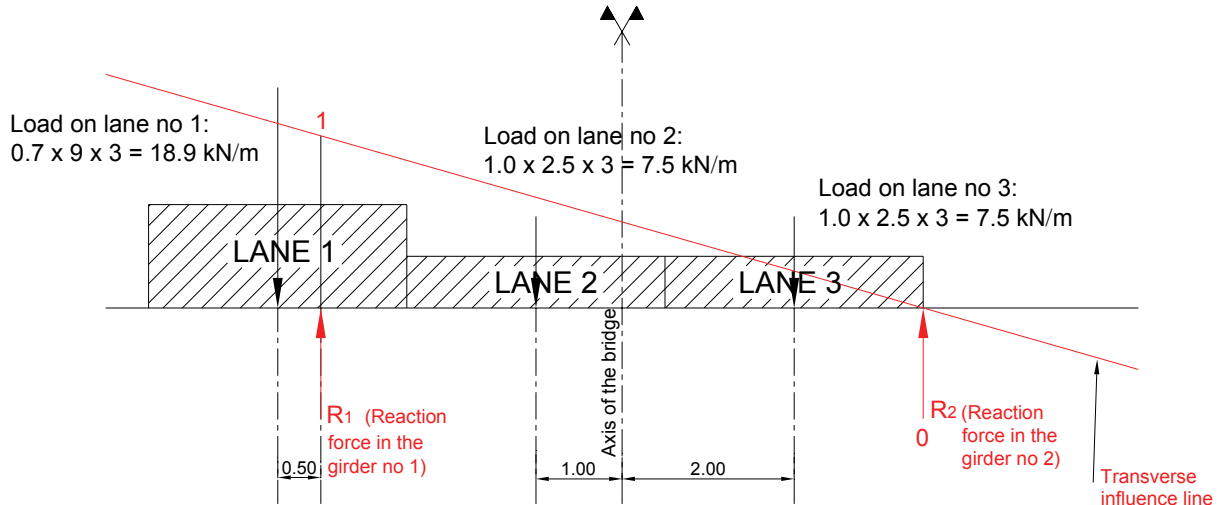


Figure 5.4: UDL transverse distribution on the bridge deck

As for TS loading, the structural system in Figure 5.4 is isostatic and the reaction forces per unit length on each main girder are therefore:

$$R_1 = 26.7 \text{ kN/m}$$

$$R_2 = 7.2 \text{ kN/m}$$

Note that if lane no. 3 extended beyond the axis of main girder no. 2 it would only be partly loaded in the positive zone of the transverse influence line.

5.4.5 - Synopsis of traffic load model LM1

The two-dimensional bar model corresponding to a half-deck is therefore loaded with an uniformly distributed load of 26.7 kN/m and a system of two concentrated loads of 409.3 kN (per load) which are longitudinally 1.2 m spaced. The curves for internal forces and moments are calculated by loading systematically all the longitudinal influence lines and two envelopes are finally obtained for the two traffic load types (see Figure 7.5).

5.4.6 - Thermal actions

The characteristic value of thermal action is noted T_k and is broken down into four constituent components according to Figure 5.5:

- an uniform component: ΔT_u
- a linear thermal gradient following the transverse horizontal axis of the deck: ΔT_{My}
- a linear thermal gradient following the vertical axis of the deck: ΔT_{Mz}
- a non-linear part of the thermal gradient: ΔT_E

This guidance book does not consider the horizontal component ΔT_{My} of the linear thermal gradient. The component ΔT_E gives rise to a self-balancing stress distribution in the considered cross-section of the deck i.e. that these stresses do not give rise to any internal force or moment. The sum $\Delta T_{Mz} + \Delta T_E$ is taken into account in bridge design by using a specific temperature difference following the vertical axis of the deck.

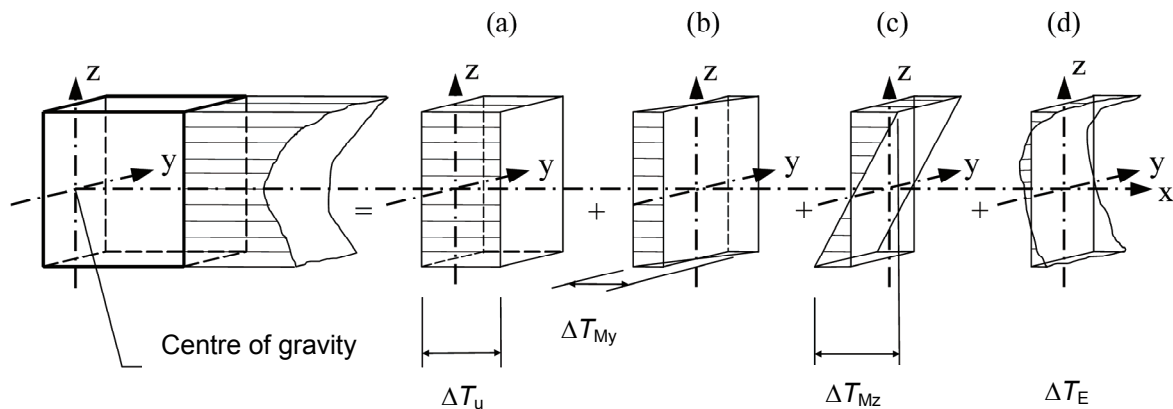


Figure 5.5: Constituent components of a temperature profile

a) Uniform temperature component

This component induces a variation in length of the bridge (when the longitudinal displacements are free on supports) which is not studied for the design example of this guide. See paragraph 4.1.4 for the values of linear thermal expansion coefficients.

Three values are required to calculate the temperature range:

- an initial temperature which is assumed as equal to $T_0 = +10^\circ\text{C}$ in this guide. This value is given by the Special Contract Documents and is specific to the construction site;
- the minimum shade air temperature T_{\min} (defined on a map of France of effective readings): $T_{\min} = -20^\circ\text{C}$. This item of data is also used to select the steel subgrades (see paragraph 4.1);
- the maximum shade air temperature T_{\max} (defined on a map of France of effective readings).

The uniform bridge temperature components $T_{e,\min}$ and $T_{e,\max}$ are deduced from T_{\min} and T_{\max} by reading charts of Figure 6.1 in EN1991-1-5. The ranges of the uniform bridge temperature component are therefore:

- maximum contraction range: $\Delta T_{N,con} = T_0 - T_{e,\min}$
- maximum expansion range: $\Delta T_{N,exp} = T_{e,\max} - T_0$

EN1991-1-5, Fig. 6.1

Note: Specific rules are planned for designing the expansion joints and the bearings at support (French National Annex to EN1991-1-5).

EN1991-1-5, 6.1.3.3 (3),
note 2
+ National Annex

b) Temperature difference component following the vertical axis of the deck

The National Annex of EN1991-1-5 should choose to one of the two following definitions for this thermal component in a bridge:

- a linear thermal gradient over the entire depth of the bridge deck (not adopted in the French National Annex);
- a non-linear thermal gradient which can be defined by two methods, continuous or discontinuous (see Figure 5.6). The values ΔT_1 and ΔT_2 are defined according to the type of deck surfacing in annex B to EN1991-1-5.

EN1991-1-5, 6.1.4.1

EN1991-1-5, 6.1.4.2 +
annex B

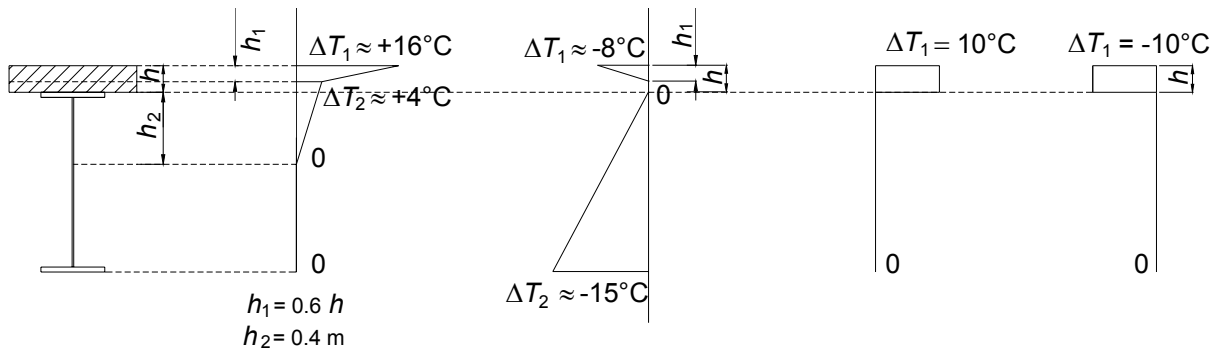


Figure 5.6: Possible definitions for the non-linear thermal gradient in a composite bridge

In accordance with the French National Annex to EN1991-1-5, this guidance book adopted the non-linear discontinuous thermal gradient with a temperature difference of +/- 10°C between the slab concrete and the structural steel. The linear temperature difference components are noted $\Delta T_{M,heat}$ (heating) and $\Delta T_{M,cool}$ (cooling).

This thermal gradient is classified as a variable action (like traffic load) and is applied to composite cross-sections which are described with the short-term modular ratio.

c) Simultaneity of uniform and temperature difference components

The characteristic value of thermal action T_k is defined as an envelope of eight combinations of actions written with the two fundamental thermal actions described above (points a and b):

EN1991-1-5, 6.1.5

$$0.35 \Delta T_{N,con} \text{ (or } \Delta T_{N,exp}) + \Delta T_{M,heat} \text{ (or } \Delta T_{M,cool})$$

$$\Delta T_{N,con} \text{ (or } \Delta T_{N,exp}) + 0.75 \Delta T_{M,heat} \text{ (or } \Delta T_{M,cool})$$

These combinations are not used for the design example in this guide where the uniform temperature component is not considered.

5.4.7 - Wind actions

The wind actions are not detailed in this guide as they have no impact on the longitudinal global bending analysis of the bridge because of the retained span lengths (a dynamic response calculation is not necessary).

6 - Combinations of actions

6.1 - Design situations

The bridge should be verified for the following design situations:

- Transient design situations:
 - for the structural steel alone under its selfweight (with various construction phases according to the chosen assembly steps),
 - at the end of concreting phases for each slab segment (16 situations, for the example of this guide),
 - for applying any differences in level on internal supports (or prestressing by imposed deformations);
- Permanent design situations:
 - at traffic opening (state of the bridge at the end of its construction),
 - at the end of the bridge lifetime, i.e. 100 years (considered as the infinite time in the calculations);
- Accidental design situations:
 - earthquake,
 - shocks,
 - other

This guide does not deal with load cases related to differences in level at internal supports, nor the verifications related to accidental or transient design situations. The Serviceability Limit State (SLS) and the Ultimate Limit State (ULS) combinations of actions are defined for every permanent design situation.

6.2 - Notations

Notations

The most commonly-used loads are designated by:

- $G_{k,sup}$: characteristic value of an *unfavourable* permanent action (nominal value of selfweight and maximum value of bridge equipments) taking account of construction phases
- $G_{k,inf}$: characteristic value of a *favourable* permanent action (nominal value of selfweight and minimum value of bridge equipments) taking account of construction phases
- S : envelope of characteristic values of internal forces and moments (or strains) due to concrete shrinkage
- T_k : envelope of characteristic values of internal forces and moments (or strains) due to thermal action
- F_{wk} : envelope of characteristic values of internal forces and moments (or strains) due to wind actions on the bridge only (mean return period of 50 years)
- $F_{wk,T}$: envelope of characteristic values of internal forces and moments (or strains) due to wind actions on the bridge and on the traffic vehicles (mean return period of 50 years)
- F_w^* : envelope of characteristic values of internal forces and moments (or strains) due to wind actions compatible with the traffic Load Model no. 1 of EN1991-2. According to the French National Annex of EN1991-1-4, $F_w^* = F_{wk,T}$.
- UDL_k : envelope of characteristic values of internal forces and moments (or strains) due to the vertical uniformly distributed loads from Load Model no. 1 in EN1991-2
- TS_k : envelope of characteristic values of internal forces and moments (or strains) due to the vertical concentrated loads from Load Model no. 1 in EN1991-2
- q_{fk} : envelope of characteristic values of internal forces and moments (or strains) due to the vertical uniformly distributed loads on the footways and cycle tracks

General

An envelope calculation with $G_{k,sup}$ and $G_{k,inf}$ is necessary for the permanent loads, only because of the variability of the deck surfacing load. The nominal value of the selfweight is considered. The variability of an eventual prestressing in the concrete slab should always be considered by a maximum and minimum value of the load magnitude.

EN1990, 4.1.2

When the footways or cycle tracks loading should be considered for the design, two characteristic load magnitudes should be considered successively:

- $UDL_k + TS_k + q_{fk,comb}$ with $q_{fk,comb} = 3 \text{ kN/m}^2$ (recommended value, may be modified by the Design Specifications) which forms the multi-component action called **gr1a group**,
- $q_{fk} = 5 \text{ kN/m}^2$ (recommended value, may be modified by the Design Specifications) which forms the action called **gr3 group**.

EN1991-2, 4.5.1

*EN1991-2, Table 4.4a
(note)*

If the Design Specifications provide for a possible dense crowd over the entire deck surface (including on the footways, the cycle tracks and any central reserve), then the **gr3 group** is replaced by the **gr4 group** with a characteristic load value imposed at $q_{fk} = 5 \text{ kN/m}^2$.

The load model no. 2 (single axle LM_2) will be defined and used later for local justifications of the concrete slab. It is always used alone, never with another traffic load, and forms the **gr1b group**.

EN1991-2, 4.3.5

The braking and acceleration forces (called **gr2 group**) are not considered in the design example of this guide. They are horizontal loads and mainly used in designing the bearings at support and the expansion joints which are not covered by the guide.

EN1991-2, 4.4.1

If a specific vehicle is defined in the Design Specifications (for example, an abnormal convoy), its characteristic vertical load and its traffic conditions (alone or within the normal traffic) should be specified in the Special Contract Documents. This specific vehicle (with or without accompanying traffic load) is called **gr5 group**.

EN1991-2, 4.3.4

The combinations of actions indicated below have been established using EN1990 and its normative annex A2 "application for bridges" in the most general way as possible i.e. by considering systematically all the multi-component actions and the environmental wind and thermal actions (except snow action, defined by EN1991-1-3). Given the loads actually used in the design bridge example of this guide, the whole of these combinations is not applied in later design examples.

6.3 - ULS combinations other than fatigue

In the **permanent** design situation for **design justifications of structural elements** (except piled foundations, spread foundations, abutment walls or other elements submitted to geotechnical actions), the following fundamental ULS combinations of actions should be considered:

$$\begin{aligned}
 & + 1.35 \{ UDL_k + TS_k + q_{fk,comb} \} + 1.5 \min \{ F_w^* ; 0.6 \cdot F_{Wk,T} \} \\
 & + 1.35 \{ UDL_k + TS_k + q_{fk,comb} \} + 1.5 \{ 0.6 \cdot T_k \} \\
 & + 1.35 \mathbf{gr1b} \\
 1.35 G_{k,sup} \text{ (or } 1.0 G_{k,inf}) \\
 & + (1.0 \text{ or } 0.0) S \quad + 1.35 \mathbf{gr2} + 1.5 \{ 0.6 \cdot T_k \} \\
 & + 1.35 \mathbf{gr3} + 1.5 \{ 0.6 \cdot T_k \} \quad [\text{or } + 1.35 \mathbf{gr4} + 1.5 \{ 0.6 \cdot T_k \}] \\
 & + 1.35 \mathbf{gr5} \\
 & + 1.5 F_{Wk} \\
 & + 1.5 T_k + 1.35 \{ 0.4 \cdot UDL_k + 0.75 \cdot TS_k + 0.4 \cdot q_{fk,comb} \}
 \end{aligned}$$

Notes:

- $gr5$ may be combined with the wind action (i.e. add the term $1.5 \min \{ F_w^* ; 0.6 \cdot F_{Wk,T} \} = 1.5 \cdot 0.6 F_{Wk,T}$) or with thermal action (i.e. add the term $1.5 \{ 0.6 \cdot T_k \}$) according to the Design Specifications.
- The French National Annex of EN1990 could change the ULS combination coefficient 0.6 to 0 for the thermal action T_k .
- The coefficient $\gamma_{SH} = 1$ for the shrinkage S action is imposed by EN1992-1-1, 2.4.2.1. Moreover concrete shrinkage is taken into account in the calculation only if its effect is unfavourable.

The above-mentioned combinations of actions correspond to Equation (6.10) in EN1990, 6.4.3.2. Equations (6.10 a) and (6.10 b) have not been retained. The γ values for actions other than shrinkage have been drawn from Table A.2.4(B) of Annex A2 to EN1990. The γ_0 factors used for defining the combination value of a variable action have been drawn from Table A.2.1 of Annex A2 to EN1990.

6.4 - SLS combinations

6.4.1 - Characteristic SLS combinations

For justifying the serviceability of the bridge (permanent design situation) the following characteristic SLS combinations of actions should be considered (A2.4.1 of Annex A2 to EN1990):

$$\begin{aligned}
 & + \{ UDL_k + TS_k + q_{fk,comb} \} + \min \{ F_w^* ; 0.6 \cdot F_{Wk,T} \} \\
 & + \{ UDL_k + TS_k + q_{fk,comb} \} + \{ 0.6 \cdot T_k \} \\
 & + \mathbf{gr1b} \\
 G_{k,sup} \text{ (or } G_{k,inf}) + (1.0 \text{ or } 0.0) S \\
 & + \mathbf{gr2} + \{ 0.6 \cdot T_k \} \\
 & + \mathbf{gr3} + \{ 0.6 \cdot T_k \} \quad [\text{or } + \mathbf{gr4} + \{ 0.6 \cdot T_k \}] \\
 & + \mathbf{gr5} \\
 & + F_{Wk} \\
 & + T_k + \{ 0.4 \cdot UDL_k + 0.75 \cdot TS_k + 0.4 \cdot q_{fk,comb} \}
 \end{aligned}$$

Note: $gr5$ may be combined with the wind action (i.e. add the term $\min \{ F_w^* ; 0.6 \cdot F_{Wk,T} \} = 0.6 F_{Wk,T}$) or with thermal action (i.e. add the term $\{ 0.6 \cdot T_k \}$) according to the Design Specifications.

6.4.2 - Frequent SLS combinations

For justifying the serviceability of the bridge (permanent design situation) the following frequent SLS combinations of actions should be considered (A2.4.1 of Annex A2 to EN1990):

$$\begin{aligned} & + 0.4. UDL_k + 0.75. TS_k + \{ 0.5. T_k \} \\ & + 0.4. \mathbf{gr3} + \{ 0.5. T_k \} \\ & + 0.75. \mathbf{gr1b} \\ G_{k,sup} \text{ (or } G_{k,inf}) + (1.0 \text{ or } 0.0) S & + 0.75. \mathbf{gr4} + \{ 0.5. T_k \} \\ & + 0.2. F_{Wk} \\ & + 0.6. T_k \end{aligned}$$

No simultaneousness of the traffic load $UDL_k + TS_k$ with the reduced value $q_{fk,comb}$ for loading on footways has to be considered for calculating the frequent value of $gr1a$ group (see EN1991-2, 4.5.2). A specific combination is then used for each frequent value of the components of $gr1a$ group (defined in Table A2.1 of Annex A2 to EN1990).

6.4.3 - Quasi-permanent SLS combinations

For justifying the serviceability of the bridge (permanent design situation) the only quasi-permanent SLS combination of actions to consider is as follows (A2.4.1 of Annex A2 to EN1990):

$$G_{k,sup} \text{ (or } G_{k,inf}) + (1.0 \text{ or } 0.0) S + 0.5. T_k$$

7 - Global analysis

The global analysis is the calculation of the whole bridge for determining the internal forces and moments and the corresponding stresses in all its cross-sections. This is calculated by respecting the construction phases and by considering two peculiar dates in the bridge life – at traffic opening (short term situation) and at infinite time (long term situation or 100 years old).

7.1 - Analysis methods: general

Taking deformed geometry into account

The deformed geometry has no influence on the internal forces and moments in case of a girder bridge. The analysis is therefore a **first order analysis**. EN1994-2, 5.2.1

The lateral torsional buckling is justified by using specific verification formulae (see paragraph 8.6). It could also be justified by defining a deformed initial geometry of the structure, followed by a second order analysis. EN1994-2, 5.3.2(1)

Influence of the material non-linearities

The composite cross-section resistance in sagging bending moment region is generally a plastic resistance calculation which takes into account the material non-linearities. The internal forces and moments (and then the stress distribution) are nevertheless calculated with a **linear elastic analysis**. EN1994-2, 5.4.1.1(1)

This analysis should take the cracking of concrete, its shrinkage and its creep into account as well as the construction phases. EN1994-2, 5.4.2.1(1)

Taking the concrete cracking into account

This is normally achieved by two successive global analysis : EN 1994-2, 5.4.2.3(2)

- In a first global analysis - called « **uncracked analysis** » - the concrete strength is considered for calculating the mechanical properties of all the cross-sections in the modeled main girder;
- In a given cross-section if the longitudinal upper fibre tensile stress σ_c in the concrete slab is lower than $-2.f_{ctm}$ ($= -6.4$ MPa in the example) for characteristic SLS combination of actions, then the concrete of this cross-section should be considered as cracked in the second global analysis. This criterion thus defines **cracked zones** on both sides of the intermediate supports;
- In a second global analysis - called « **cracked analysis** » - the concrete slab stiffness in the cracked zones is reduced to the stiffness of its reinforcing steel. The internal forces and moments - as well as the corresponding stress distributions - of this cracked analysis are used in the following chapters to justify all the transverse cross-sections of the deck.

On condition that: EN 1994-2, 5.4.2.3 (3)

- the ratio between two adjacent span lengths is always higher than 0.6 and,
- no differences in level are used at internal supports,

the cracked analysis may be performed directly by using cracked zones which are defined by considering 15% of the span lengths on both sides at each internal support.

Note: A major part of the tensile stress σ_c in the concrete slab returned by the so-called un-cracked analysis is provided by the shrinkage. This shrinkage is far less important in a pre-cast slab and the use of the $-2.f_{ctm}$ criterion thus logically reduces the length of the cracked zones at internal supports. The simplified method (15%) thus gives very different results and its use is not recommended for pre-cast slabs.

Taking shear lag into account in the concrete slab

The shear lag in the concrete slab is taken into account by reducing the actual slab width to an “effective” width. It thus influences the mechanical properties of the cross-sections which are used in the calculations of the global analysis. For a two-girder bridge the shear lag has really an influence for small span lengths (less than about 40 m) or for very wide bridges.

EN1994-2, 5.4.1.2

See also paragraph 7.2.2 below for a practical example of effective widths calculations.

7.2 - Internal forces and moments – Stresses

7.2.1 - Design model

To analyse the global longitudinal bending, the deck is modeled as a continuous line of bar elements which corresponds to the neutral fibre of the modeled main girder and which is simply supported at piles and abutments. With respect to a fixed reference (which can be attached, for example, to the final longitudinal profile of the pavement) this neutral fibre changes throughout the calculation according to the mechanical properties (areas and second moments of area) allocated to the bar elements in the model. This is due to the different modular ratios to be considered and to the fact that a given cross-section could be composite or not, with a cracked concrete or not, following the phases of the global analysis.

In addition to the cross-sections at internal and end supports and at mid-spans, some peculiar cross-sections are worthy of being at the bar element ends:

- at the quarter and three-quarters of each span (to define the effective widths of the slab to calculate the stress distribution, see paragraph 7.2.2),
- at the ends of every slab concreting segment,
- at the thickness changes in the structural steel distribution.

Every load case is introduced into the design model with the corresponding mechanical properties of the cross-sections. The internal forces and moments are calculated load case by load case following the indications in paragraph 7.1.

7.2.2 - Effective width of the concrete slab

In a given cross-section of one of the main girder, the effective width of the concrete slab is the sum of 3 terms (see Figure 7.1):

$$b_{\text{eff}} = b_0 + \beta_1 b_{e1} + \beta_2 b_{e2}$$

with:

- b_0 (= 750 mm for the example), the centre-to-centre distance between the outside stud rows;
- $b_{ei} = \min \{L_e/8 ; b_i\}$ where L_e is the equivalent span length in the considered cross-section and where b_i is the actual geometric width of the slab associated to the main girder;
- $\beta_1 = \beta_2 = 1$ except for the cross-sections at end supports C0 and C3 where $\beta_i = 0,55 + 0,025 \cdot L_e/b_{ei} < 1,0$ with b_{ei} taken as equal to the effective width at mid-end span.

EN1994-2, 5.4.1.2 (5)

EN1994-2, 5.4.1.2 (6)

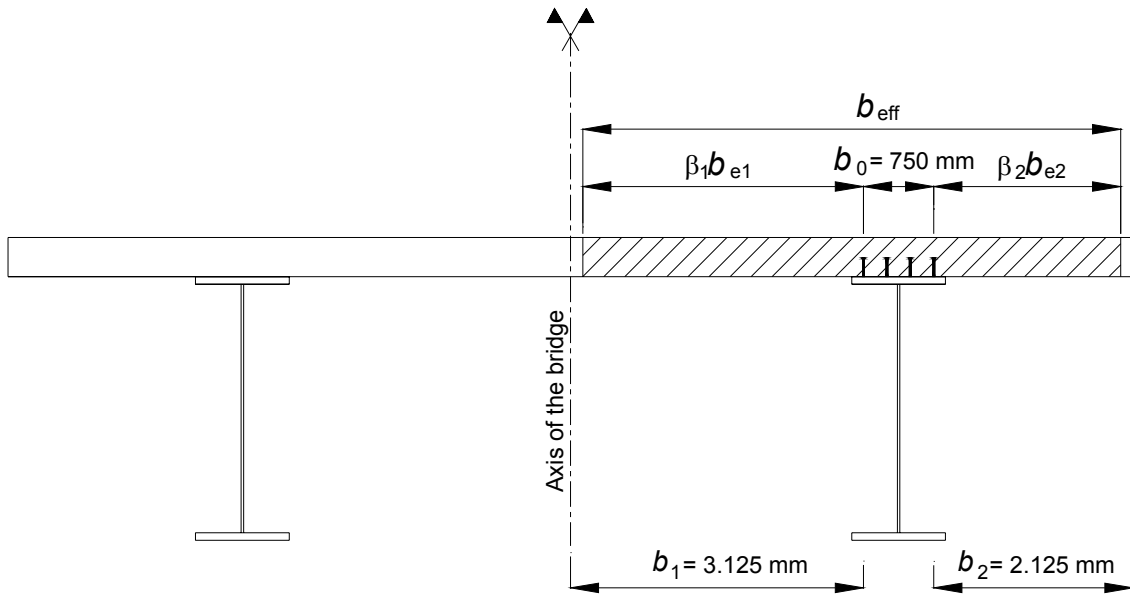


Figure 7.1: Effective slab width for a main girder in a given cross-section

The equivalent spans are:

- $L_{e1} = 0.85 \cdot L_1 = 0.85 \cdot 60 = 51$ m for the cross-sections located in the end spans C0-P1 and P2-C3 and for the cross-sections located at end supports C0 and C3;
- $L_{e2} = 0.7 \cdot L_2 = 0.7 \cdot 80 = 56$ m for the cross-sections located in the central span P1-P2;
- $L_{e3} = 0.25 \cdot (L_1 + L_2) = 0.25 \cdot (60 + 80) = 35$ m for the cross-sections located at internal supports P1 and P2.

EN1994-2, Figure 5.1

As $L_{ei}/8$ is always greater than b_i for the example it is deduced that the effective width is equal to the actual width except for the cross-sections at end supports C0 and C3 where the factor β_i has an impact:

- $\beta_1 = 0.55 + 0.025 \cdot L_{e1}/b_{e1} = 0.55 + 0.025 \cdot 51/3.125 = 0.958 < 1.0$,
- $\beta_2 = 0.55 + 0.025 \cdot L_{e2}/b_{e2} = 0.55 + 0.025 \cdot 51/2.125 = 1.15$ but as $\beta_2 < 1$ $\beta_2 = 1$ is retained.

EN1994-2, Figure 5.1

The slab width will therefore vary linearly from 5.869 m at end support C0 to 6.0 m for the abscissa $0.25 \cdot L_1 = 15$ m in the span C0-P1. Afterwards it will be constant and equal to 6.0 m up to the abscissa $2 \cdot L_1 + L_2 - 0.25 \cdot L_1 = 185$ m and then it will vary linearly from 6.0 m to 5.869 m at end support C3.

This variable effective width is always taken into account to calculate the longitudinal stress distribution.

To calculate the internal forces and moments with a linear elastic global analysis, constant widths may be used for each span by considering the values at mid-span. For the example this means that the calculation can be performed with the actual slab width over the entire bridge length, i.e. the shear lag in the concrete slab has no influence on the internal forces and moments. This is logical with regards to the chosen span lengths for the example which are relatively high for a two-girder bridge.

EN1994-2, 5.4.1.2(4)

7.2.3 - Determining cracked zones at internal supports

A global un-cracked analysis is first performed for the example. The internal forces and moments as well as the longitudinal stresses σ_c in the concrete slab are calculated by considering the concrete participation in the bending stiffness of all the cross-sections. Figure 7.2 shows the stresses thus obtained for SLS characteristic combination of actions as well as the zones where this stress exceeds $-2.f_{ctm}$ in the upper fibre of the concrete slab.

The observed discontinuities in these envelope curves correspond to the end cross-sections of the concreting slab segments and to the cross-sections in which the thicknesses of the structural steel change. Although the bending moment is equal to zero in the cross-sections at the deck ends, the corresponding drawn stresses are not because their values include the self-balancing stresses due to the shrinkage and the thermal action (called “primary effects” or “isostatic effects” in EN1994-2).

Figure 7.2 also shows that the cracked zone associated to a given internal support is not necessarily continuous (this is especially true for P2 in central span). A single cracked zone, continuous and as long as possible, has been taken into account for each internal support in the subsequent cracked global analysis.

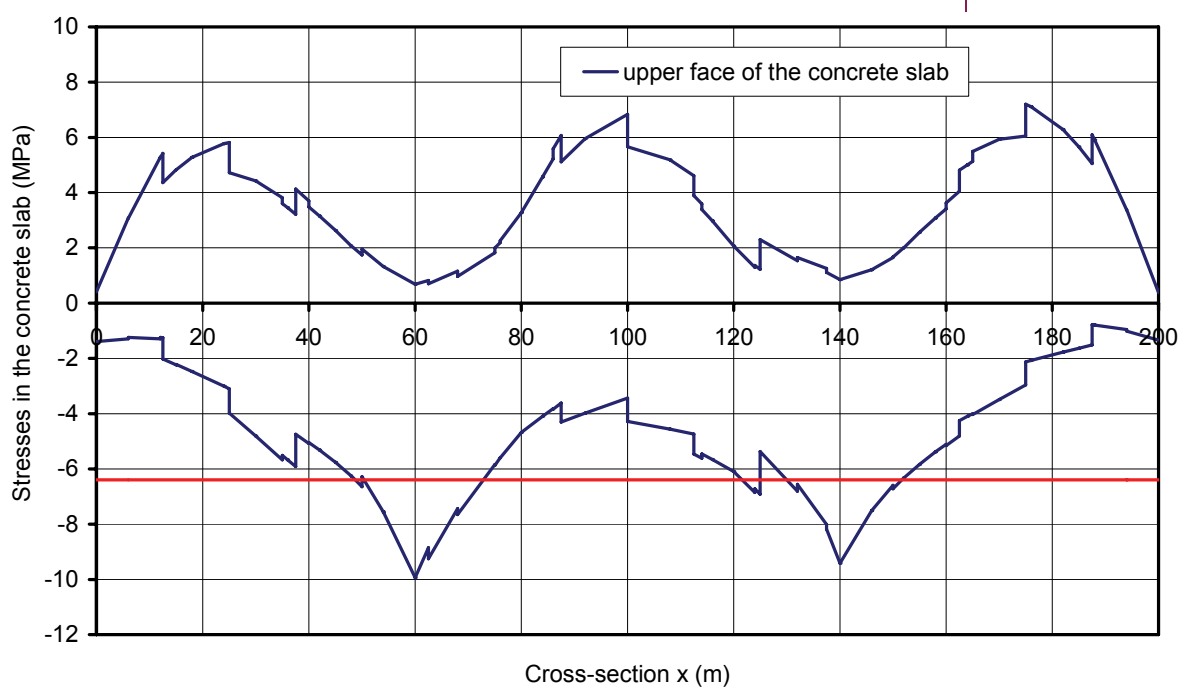


Figure 7.2: Cracked zones used in the global analysis

In practical terms, this gives:

- a cracked zone around P1 which starts at the abscissa $x = 49$ m (i.e. 18.3% for the cracked length in the left end span) and which ends at the abscissa $x = 72.8$ m (i.e. 16.0% for the cracked length in the central span);
- a cracked zone around P2 which starts at the abscissa $x = 121.6$ m (i.e. 23.0% for the cracked length in the central span) and which ends at the abscissa $x = 151.6$ m (i.e. 19.3% for the cracked length in the right end span).

To reduce the cracked zones or to give them a better symmetry, the order for concreting slab segments could be modify (see Figure 3.5). It should also be noticed that the calculation accuracy is linked to the adopted meshing for the bar

elements of the design model.

For the example, the simplified 15% method could also have been used to perform directly the cracked global analysis. The cracked zones would have been slightly reduced.

7.2.4 - Actions and cracked zones

During the second global analysis, the cracked zones modify the introduction of some actions in the design model.

Concrete shrinkage

The shrinkage action is modeled in the bar elements by introducing a normal force $N_b = E_{cm} \cdot \varepsilon_{cs} \cdot A_b$ which is applied to the centre of gravity of the concrete slab. This force results in a normal force N_b and a bending moment $M_b = N_b z_b$ applied to the centre of gravity of the composite cross-section (neutral fibre of the model) where z_b is the distance between the centre of gravity of the concrete slab and of the composite cross-section.

To determine the cracked zones these force and moment (which are called "isostatic" or "primary" effects of shrinkage by EN1994-2) are applied in all cross-sections of the design model. In EN1994-2 « hyperstatic » or « secondary » effect of shrinkage is the difference between the internal forces and moments calculated in the continuous girder by the elastic linear Strength of Materials for the action of the isostatic effects of shrinkage, and the isostatic effects themselves (see Figure 7.4).

For the cracked global analysis the isostatic effects of shrinkage (N_b and M_b) are no longer applied in the cross-sections located in the cracked zones around internal supports. The early age and the thermal shrinkages $\varepsilon_{cs} + \varepsilon_{th} = 1.7 \cdot 10^{-5}$ are still applied, slab segment by slab segment, except in the cracked zones, by using the short-term modular ratio ($n_0 = 6.1625$). The long term shrinkage (for the persistent design situation at infinite time) $\varepsilon_{cs} = 2.4 \cdot 10^{-4}$ is applied in a single phase for the entire concrete slab, except in the cracked zones, by using the long term modular ratio $n_L = 15.24$.

EN1994-2, 5.4.2.2 (8)

Thermal gradient

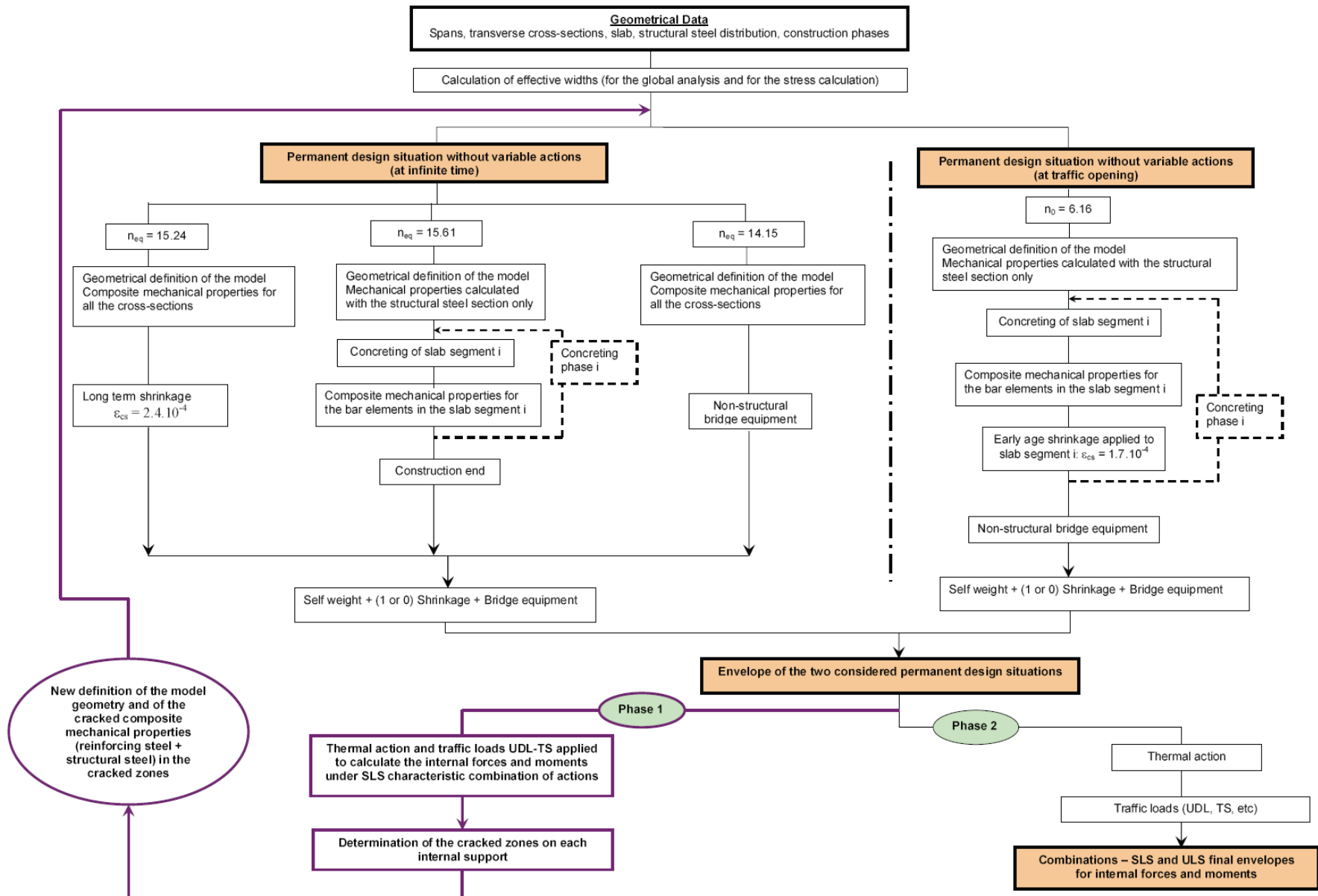
The thermal gradient is a variable action applied to the bridge in which the mechanical properties of the composite cross-sections have been calculated by using the short-term modular ratio ($n_0 = 6.1625$). In the cracked zones it is dealt with in the same way to the shrinkage. This is why the stress block (+/-10°C) definition has been chosen for the thermal gradient in the French National Annex to EN1991-1-5.

EN1994-2, 7.4.1 (6)

7.2.5 - Organizing the global analysis calculations

Figure 7.3 shows the sequence of the longitudinal bending calculations in the design model. This especially includes the changes in the mechanical properties of the cross-sections following the successive introduction of the load cases into the model with respect to the adopted construction phases.

Figure 7.3: Global analysis organisation chart



7.2.6 - Results

Figures 7.4 to 7.7 illustrate a few results of internal forces and moments coming from the global analysis of the deck in the design example of this guide.

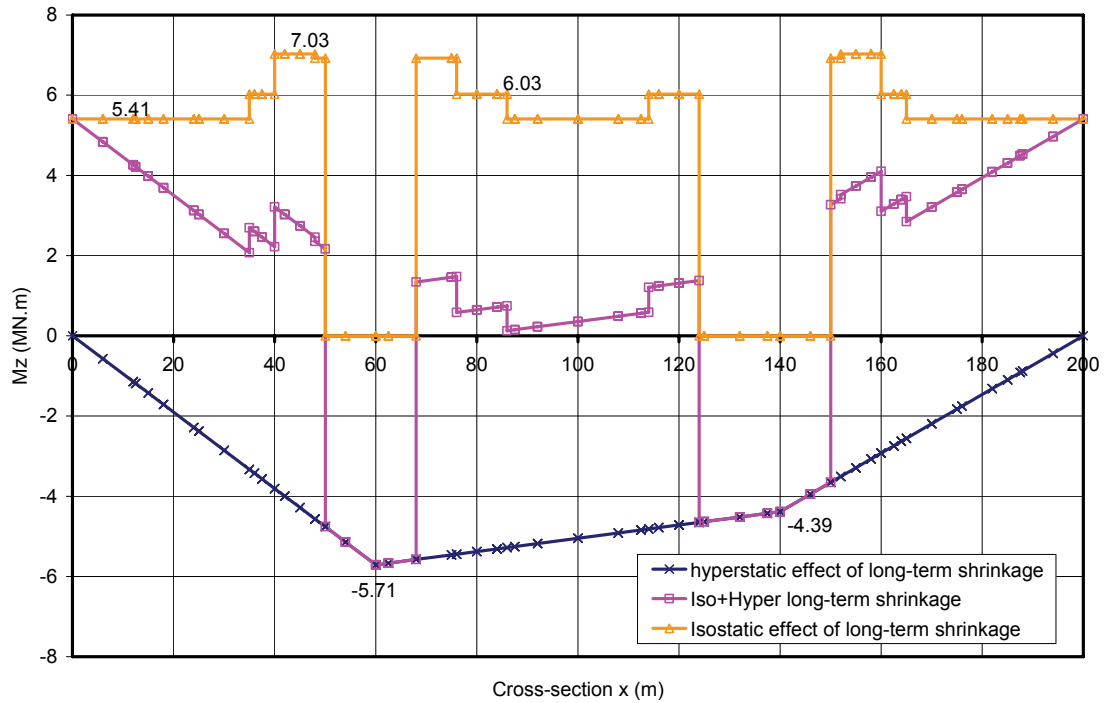


Figure 7.4: Isostatic and hyperstatic moments due to the long-term concrete shrinkage

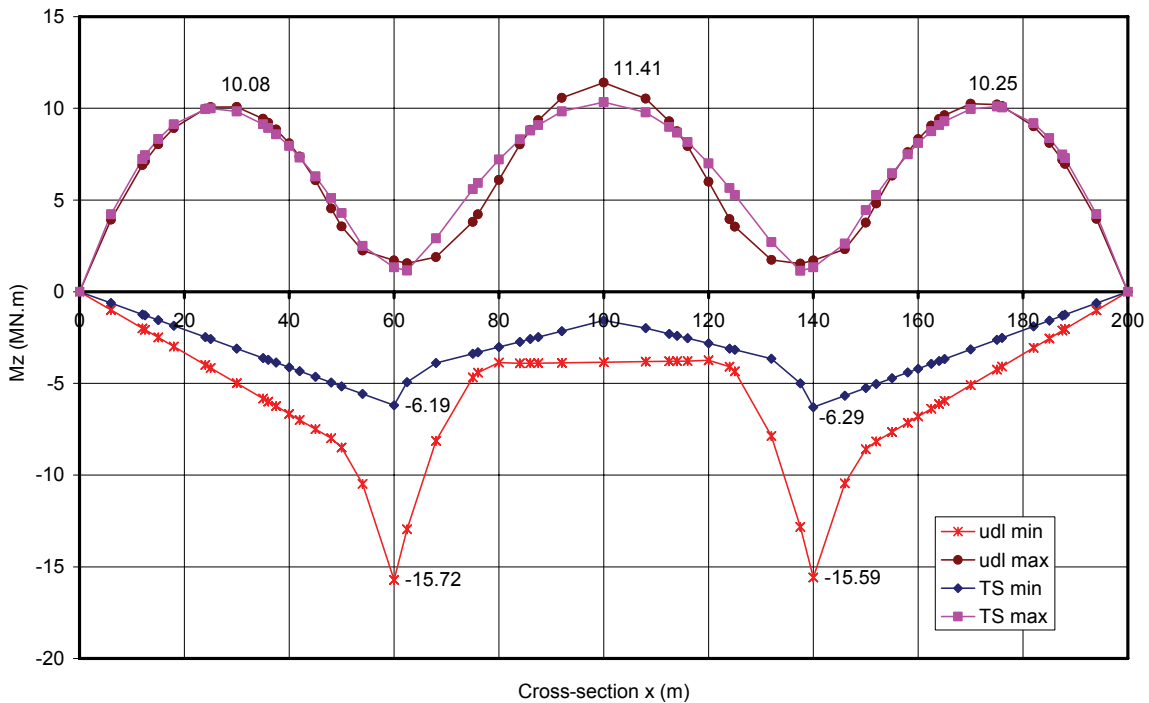


Figure 7.5: Moments for the uniformly distributed and tandem system traffic loads (UDL and TS)

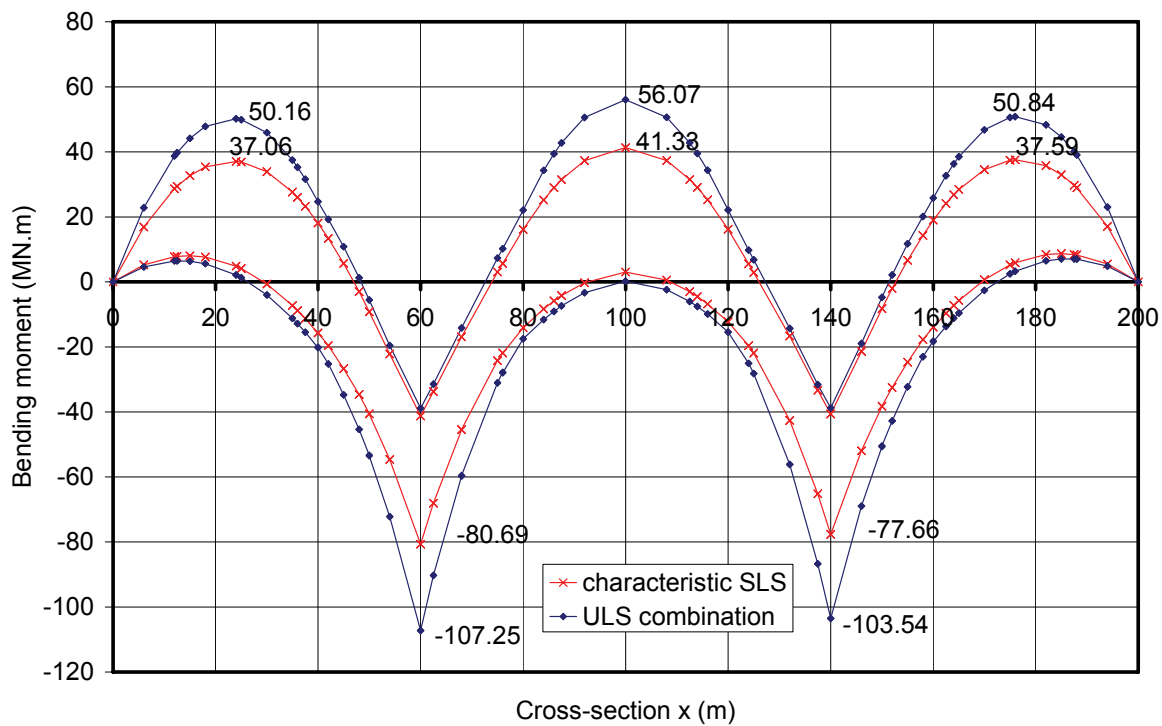


Figure 7.6: Moments for the final ULS and characteristic SLS combinations of actions

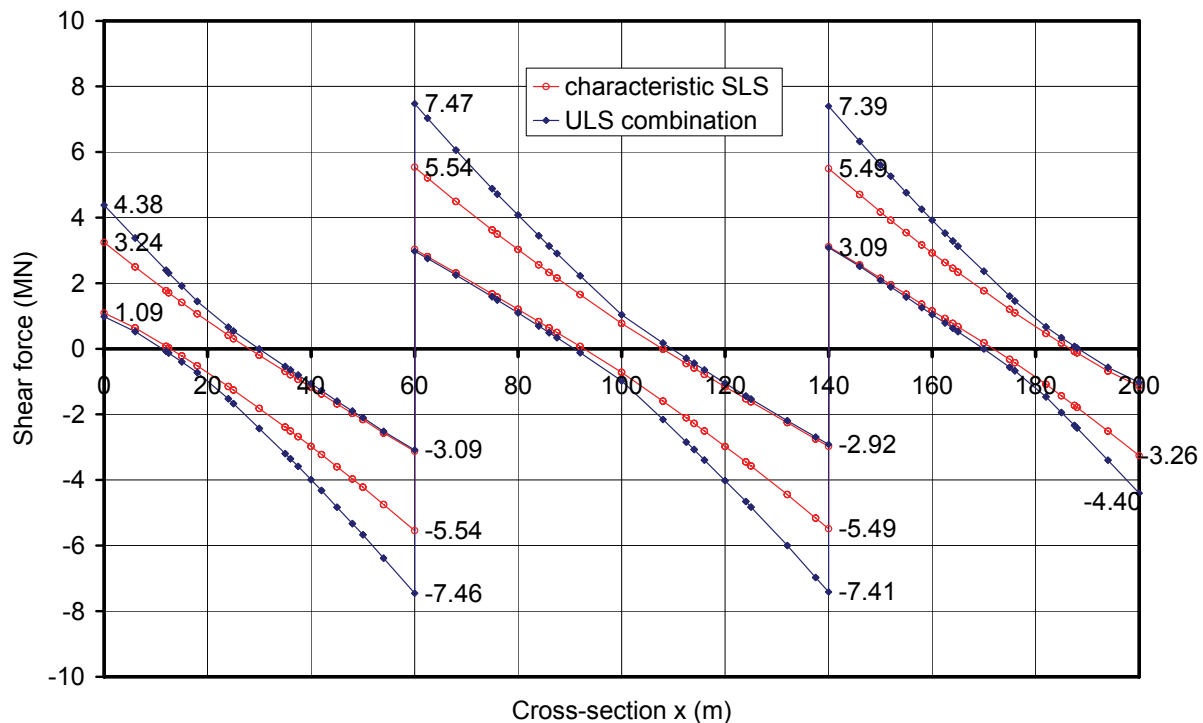


Figure 7.7: Shear forces for the final ULS and characteristic SLS combinations of actions

8 - Justification of the composite cross-sections at ULS other than fatigue

According to EN1994-2, 6.1.1, a composite cross-section should be checked at ULS in terms of:

- **resistance of cross-section**: EN1994-2, 6.2.1 and 6.2.2 ;
- resistance to **shear buckling**: EN1994-2, 6.2.2 ;
- resistance to **transverse load** during launching: EN1994-2, 6.5 (not dealt with as this guide does not address the construction phase justification) ;
- resistance to **slip** between concrete and steel (connection): EN1994-2, 6.6 (see chapter 11 of this part II) ;
- **fatigue** resistance: EN1994-2, 6.8 (see chapter 9 of this part II).

The resistance to **lateral torsional buckling** (EN1994-2, 6.4) is dealt with in this chapter 8 despite involving global instability of the lower compressed steel flange.

8.1 - Classification of cross-sections

8.1.1 - General definition of the Classes

EN1993-1-1, 5.5 introduces the concept of "classes of cross-section" which is used to prejudge the ultimate bending resistance and compression resistance of structural steel sections with regards to the risk of local buckling. Cross sections are classified on a scale of 1 to 4 based on the slenderness (width/thickness noted c / t) of the different compressed panels making them up, on their yield strength and their stress distribution at ULS:

- **Class 1**: Solid cross-section which can reach its plastic strength without buckling and which has a sufficient plastic behaviour to form a plastic hinge with the rotation capacity required to perform a global plastic analysis of the structure.
- **Class 2**: Solid cross-section which can reach its plastic moment resistance without buckling and which can form a plastic hinge with a limited rotation capacity, so that this plastic hinge can not be introduced in a global plastic analysis of the structure.
- **Class 3**: Cross-section which can reach its elastic resistance (stresses in the extreme fibre could be equal to the yield strength) but not its plastic moment resistance due to buckling.
- **Class 4**: Cross-section with slender compression elements which cannot reach its elastic resistance due to buckling.

Table 8.1 summarizes the attributes of each Class for a cross section under pure bending.

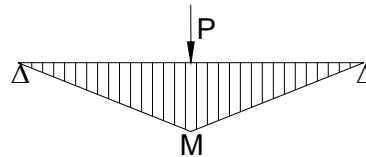
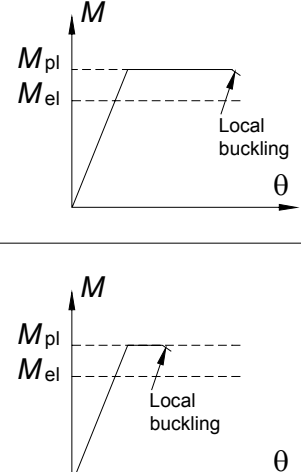
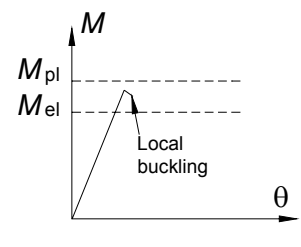
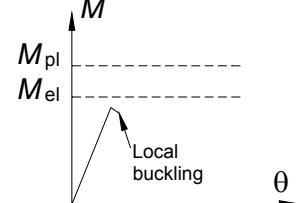
CLASS	BEHAVIOUR MODEL	DESIGN STRENGTH	PLASTIC ROTATION CAPACITY
			Significant
1	 <p>Diagram showing a beam under pure bending with a triangular deflection curve. A vertical force P is applied at the center, and a moment M is applied at the supports. The deflection curve is a triangle with a maximum deflection Δ at the center.</p>	PLASTIC BEHAVIOUR of the gross cross-section	Limited
2	 <p>Diagram showing a beam under pure bending with a triangular deflection curve. A vertical force P is applied at the center, and a moment M is applied at the supports. The deflection curve is a triangle with a maximum deflection Δ at the center. A local buckling indicator is shown near the center of the deflection curve.</p>	PLASTIC BEHAVIOUR of the gross cross-section	None
3	 <p>Diagram showing a beam under pure bending with a triangular deflection curve. A vertical force P is applied at the center, and a moment M is applied at the supports. The deflection curve is a triangle with a maximum deflection Δ at the center. A local buckling indicator is shown near the center of the deflection curve.</p>	ELASTIC BEHAVIOUR of the gross cross-section	None
4	 <p>Diagram showing a beam under pure bending with a triangular deflection curve. A vertical force P is applied at the center, and a moment M is applied at the supports. The deflection curve is a triangle with a maximum deflection Δ at the center. A local buckling indicator is shown near the center of the deflection curve.</p>	ELASTIC BEHAVIOUR of the effective cross-section	None

Table 8.1: Classification principle for cross-section under pure bending

8.1.2 - Determining a composite cross-section Class in practise

The classification system established for steel beams also applies to composite beams. The Class of a composite cross-section is the highest Class of the compressed elements making it up.

*EN1994-2, 5.5.1(1)
EN1994-2, 5.5.1(2)*

Three preliminary comments are possible:

- Local buckling can only be induced by compressive stresses. Any element subjected only to tensile stress must be classified in Class 1, irrespective of its slenderness;
- If an element is a Class n element under uniform compression then it always is in Class $m \leq n$ under any other stress distribution which can only reduce the compressive stresses;
- If the shear connectors fulfil the spacing required in EN 1994-2, 6.6.5.5, (see chapter 11 of this Part II) then a steel flange in compression connected to a concrete slab is in Class 1.

EN1994-2, 5.5.2(1)

To classify an **internal compression element** (i.e. an element bordered to opposite edges by two other perpendicular elements) as an I-girder web or a sub-panel in the bottom flange of a box-girder steel bridge, Table 5.2 sheet 1 of 3 in EN1993-1-1 should be used.

EN1993-1-1, Table 5.2

To classify an **outstand compression element** (i.e. an element bordered to only one edge) as the cantilever part of an I-girder flange, Table 5.2 sheet 2 of 3 in EN1993-1-1 should be used.

These tables provide the limit slenderness between Classes. To determine the Class of an element in a given cross-section this element is first assumed to be in Class 1 or 2 and then calculated with its plastic resistance. The Plastic Neutral Axis (PNA) location in the section is used to determine the limit slenderness of this element (between Class 2 and Class 3) and to justify the plastic assumption. If not, the elastic stress distribution at ULS (coming from the global cracked analysis and taking the construction phases of the structure into account) is used to determine the limit slenderness between Class 3 and Class 4. If the actual slenderness of the element exceeds this limit, this element is in Class 4.

EN1994-2 allows that a cross-section with Class 3 web and Class 1 or 2 flanges may be treated as an effective Class 2 cross-section. The cross-section is then justified according to its plastic resistance. The plastic resistance moment is calculated by assuming that the effective compressive parts of the web are limited to $20\epsilon t_w$ (see Figure 8.1), i.e. by suppressing the web zone likely to buckle.

EN1994-2, 5.5.2(3)

In a composite bridge the in-span cross-sections under sagging (positive) bending moment are usually in Class 1 or 2 (the compressive part of the web is very small due to a very high location of the PNA and the upper steel flange connected to a compressed concrete slab is in Class 1). On the other side the cross-section located in internal support regions under hogging (negative) bending moment are usually in Class 3 or 4 (fairly important part of the web in compression).

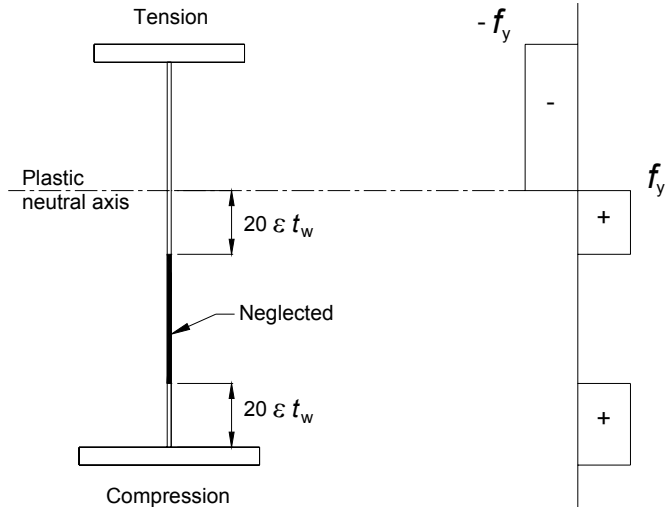


Figure 8.1: Effective cross-section in Class 2

8.2 - Cross-section justification principles

8.2.1 - Bending resistance

Class 1 or 2 cross-sections can be checked by using the plastic or elastic bending resistance. Class 3 cross-sections are checked with the elastic bending resistance, or possibly reclassified as effective Class 2 cross-section and then checked with the plastic bending resistance. Class 4 cross-sections are also checked with the elastic bending resistance but by using the effective cross-section, reduced to take account of buckling.

Note lastly that a section can always be checked by a very general non linear analysis, irrespective of its Class.

a) Plastic verification

The location of the Plastic Neutral Axis (PNA) as well as the plastic resistance moment $M_{pl,Rd}$ are calculated by using the following design yield strengths for the materials: EN1994-2, 6.2.1.2(1)

- structural steel (tension or compression): $f_{yd} = f_{yk} / \gamma_{M0}$
- reinforcing steel (tension) : $f_{sd} = f_{sk} / \gamma_s$
- concrete (compression) : $0.85.f_{cd} = 0.85.f_{ck} / \gamma_c$

The strength of the concrete in tension and of the reinforcing steel bars in compression is neglected in the cross-section resistance.

Figures 8.2 (resp. 8.3) illustrate very generally the plastic stress distribution used for an I-girder under sagging bending moment $M_{Ed} \geq 0$ (resp. under hogging bending moment $M_{Ed} < 0$).

For a High Strength Steel (S420 or S460) the concrete could be cracked because of too much compression. The subsequent reduced cross-section resistance is modeled by a reduction factor β which depends on the location of the PNA and is directly applied to $M_{pl,Rd}$. EN1994-2, 6.2.1.2(2)

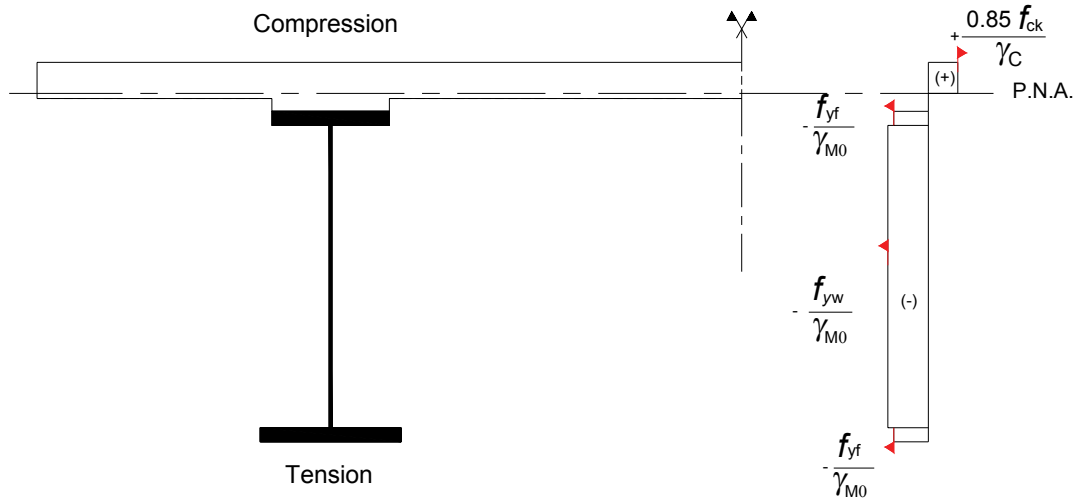


Figure 8.2: Calculation of the design value of the positive plastic resistance moment $M_{pl,Rd}^+$

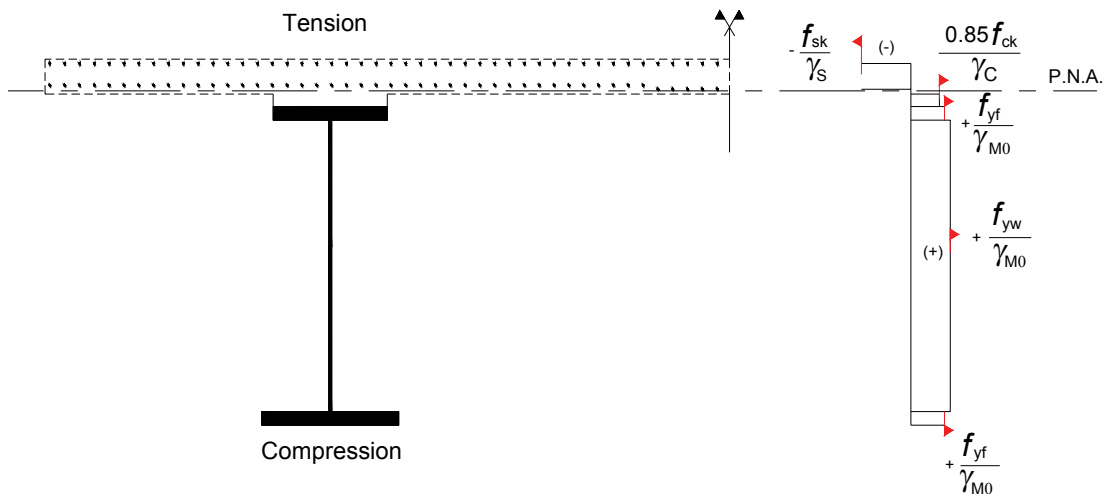


Figure 8.3: Calculation of the design value of the negative plastic resistance moment $M_{pl,Rd}^-$

For Class 1 or 2 cross-sections, i.e. generally under sagging bending moment in the mid-span region, the ULS bending moment should be checked against the plastic resistance moment: $M_{Ed} \leq M_{pl,Rd}$.

EN1994-2, 6.2.1.2(1)

In addition, M_{Ed} is calculated by a cracked elastic global analysis (see chapter 7 of this Part II) which takes no account of the influence of a possible Class 1 or 2 cross-section yielding in the mid-span region on the longitudinal M_{Ed} distribution. If the cross-section located at or near the adjacent internal support is in Class 3 or 4, and if the ratio of lengths of the spans adjacent to that support (shorter/longer) is less than 0.6, the loading case leading to the maximum bending moment in span is close to that leading to the minimum bending moment at support. EN 1994-2 limits M_{Ed} to $0.9 \cdot M_{pl,Rd}$ in the Class 1 or 2 cross-section in span to avoid any moment redistribution which could be harmful.

EN1994-2, 6.2.1.3(2)

b) Elastic verification

The limiting stresses at ULS are given per material:

EN1994-2, 6.2.1.5(2)

- f_{yd} for structural steel,
- f_{sd} for reinforcing steel bars,
- f_{cd} for concrete in compression.

The strength of concrete in tension is neglected.

Note also that the elastic check could be performed with the stresses calculated in the mid-plane of the steel flanges instead of in the extreme fibres.

EN1993-1-1, 6.2.1(9)

c) Effective cross-section for Class 4 section

For a Class 4 cross-section the stresses at ULS coming from the global analysis (and calculated with the gross area possibly reduced due to shear lag effect) are used to calculate the initial area A_c of the compressed part of the structural steel cross-section, and then the effective area $A_{c,eff} = \rho A_c$ of this compressed part (with a reduction factor $\rho < 1$).

EN1994-2, 6.2.1.5(7)

The area A_c can be made up of several Class 4 elements (flanges and webs) and the calculation of $A_{c,eff}$ is thus iterative. Based on the initial stresses at ULS, a first calculation gives the reduction factor and the effective area for the first element. The ULS stresses are recalculated with the mechanical properties from this first effective cross-section and then used to determine the reduction factor and the effective area of the second element. And so on.

EN1993-1-5, 4.4(4)

note 1

The flange element areas are always reduced before the web element areas. This order only normally has an impact on a box-girder cross-section where the bottom flange may easily be in Class 4 (see Part III of this guidance book). Conversely the flanges of an I-girder are rarely in Class 4. The effective flange area is calculated with the stresses in its mid-plane.

EN1993-1-5, 4.4(3)

For a given Class 4 element ρ is calculated according to EN1993-1-5, section 4.4, when the element has no longitudinal stiffeners (for example a flange of an I-girder, or an unstiffened web of an I-girder). Otherwise ρ is calculated according to EN1993-1-5, section 4.5 (for example the stiffened bottom flange of a box-girder cross-section, or the stiffened web of an I-girder).

EN1993-1-5, 4.4

EN1993-1-5, 4.5

The calculation of reduction factors ρ for each element in practise (i.e. the use of Sections 4.4 and 4.5 of EN1993-1-5) is presented as design examples in the remainder of this guidance book:

- an I-shaped cross-section in Annex II;
- a box-girder cross-section with a longitudinally stiffened bottom flange in Part III.

EN1993-1-5, 4.6(1)

Following the iterative procedure the stresses at ULS are recalculated with the effective area of the cross-section and then compared to the limiting stresses for an elastic check (like a Class 3 cross-section).

The recalculation of the stresses at ULS with the composite effective area (at each step of the iterative calculation) should take account of:

- any shift e_N in the position of the neutral axis of the effective area compared to the initial one, which induces an additional bending moment $N_{Ed}e_N$ if a normal force N_{Ed} is applied;
- the construction phases, i.e. distinguish the internal forces and moments resisted by the effective structural steel area only from the ones resisted by the effective composite area (calculated with a modular ratio dependent on the applied load case).

EN1993-1-5, 4.3(4) note

EN1993-1-5, 4.4(3) note

Figure 8.4 suggests a method for an unstiffened I-girder cross-section (where only the web is in Class 4) under the bending moment $M_{Ed} < 0$ alone (most common situation). M_a is the part of the bending moment M_{Ed} resisted by the structural steel area alone and M_c is the part of M_{Ed} resisted by the composite area ($M_{Ed} = M_a + M_c$). The effective stresses to be checked are recalculated with the effective mechanical properties and the moments M_a and M_c .

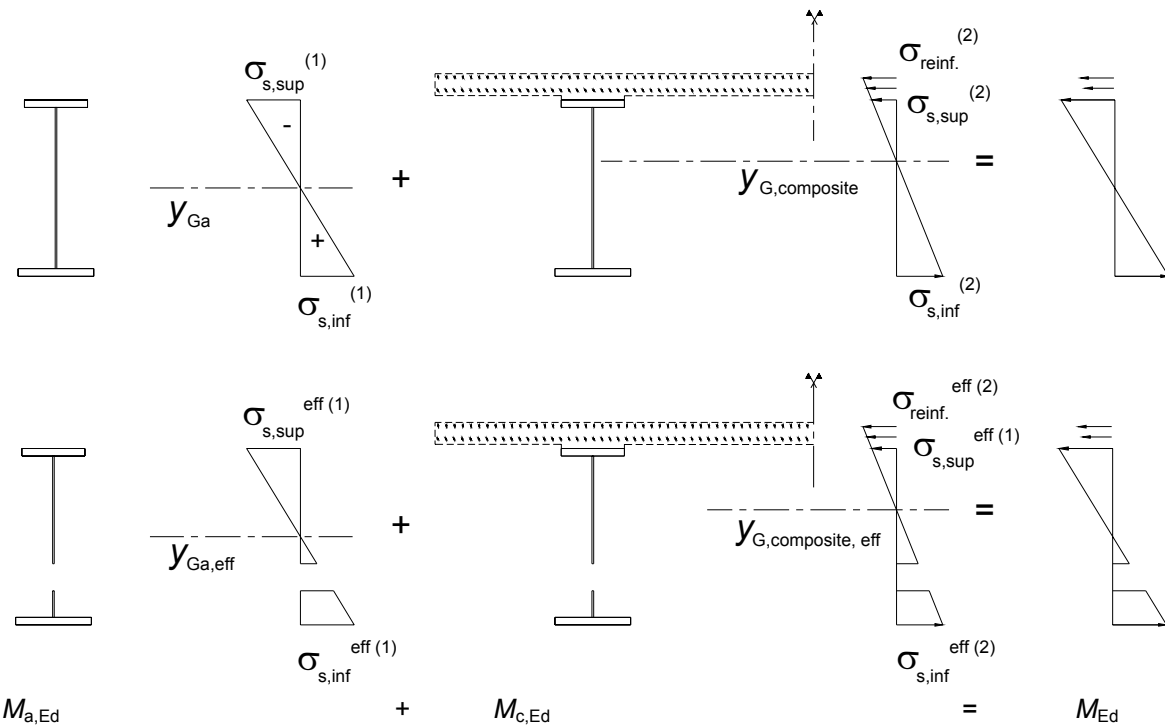


Figure 8.4: Principle for recalculating the stresses in an effective cross-section

8.2.2 - Shear resistance

Whatever the Class of the composite cross-section the criterion $V_{Ed} \leq V_{pl,a,Rd}$ should be checked where $V_{pl,a,Rd}$ is the plastic design shear resistance of the structural steel. If no torsion is applied to the cross-section, $V_{pl,a,Rd}$ is given by:

$$V_{pl,a,Rd} = A_v \frac{f_y}{\gamma_{M0} \sqrt{3}} \quad \text{where } A_v \text{ is the structural steel shear area under } V_{Ed}$$

(normally the girder web area multiplied by a factor η which depends on the steel grade).

When the web becomes too slender it could buckle under V_{Ed} . Then the following criterion should be also checked:

$$V_{Ed} \leq V_{b,Rd}$$

where $V_{b,Rd}$ is the design resistance for shear buckling:

$$V_{b,Rd} = V_{bw,Rd} + V_{bf,Rd} \leq \frac{\eta f_y}{\gamma_{M1} \sqrt{3}} h_w t_w$$

η should be defined in the National Annex of EN1993-1-5. In this guidance book the recommended values have been used:

- $\eta = 1.2$ for structural steel up to and including S460,
- $\eta = 1.0$ for higher steel grades.

$V_{bf,Rd}$ corresponds to the contribution from the flanges in the design shear buckling resistance. Although EN1993-1-5 suggests a method for calculating this contribution it is negligible compared to the contribution from the web in case of traditional bridge girders, as shown in the following design examples. In addition, if it is taken into account, it is also to be checked that the welds between web and flanges could transfer the shear force.

$V_{bw,Rd}$ corresponds to the contribution from the web in the design shear buckling resistance. Its calculation is shown directly in the following design

EN1994-2, 6.2.2

EN1993-1-1, 6.2.6(2) and (3)

EN1993-1-5, 5.1(2)

EN1993-1-5, 5.5(1)

EN1993-1-5, 5.2(1)

EN1993-1-5, 5.1(2)

EN1993-1-5, 5.2(2) and 9.3.5(1)

EN1993-1-5, 5.3

examples.

Lastly note that the contribution from the reinforced concrete slab is neglected in the design plastic and design buckling shear resistances of a composite cross-section.

*EN1994-2, 6.2.2.2(1)
and 6.2.2.3(2)*

8.2.3 - Bending and shear interaction

When V_{Ed} is greater than half of $V_{Rd} = \min(V_{b,Rd}; V_{pl,a,Rd})$, V_{Ed} reduces the bending resistance of the cross-section. The reduction to be taken into account depends on the cross-section Class.

EN1994-2, 6.2.2.4(1)

- **For Class 1 or 2 cross-sections of an I-girder**, the yield strength of the structural steel shear area A_V is reduced before calculating the design value of the plastic bending resistance $M_{pl,Rd}$.

EN1994-2, Figure 6.7

When calculating $M_{pl,Rd}$ the shift in the position of the Plastic Neutral Axis (which is due to the change in the yield strength of the shear area A_V) is not taken into account.

EN1994-2, 6.2.2.4(4)

- **For Class 3 or 4 cross-sections of an I-girder**, EN1993-1-5 defines an interaction criterion:

$$\bar{\eta}_1 + \left[1 - \frac{M_{f,Rd}}{M_{pl,Rd}} \right] \left[2\bar{\eta}_3 - 1 \right]^2 \leq 1,0$$

$$\text{with } \bar{\eta}_1 = \frac{M_{Ed}}{M_{pl,Rd}} \geq \frac{M_{f,Rd}}{M_{pl,Rd}} \text{ and } \bar{\eta}_3 = \frac{V_{Ed}}{V_{bw,Rd}}.$$

EN1993-1-5, 7.1(1)

The calculation of $M_{pl,Rd}$ for a cross-section with Class 4 elements only takes account of the effective area of the composite and/or steel flanges (due to shear lag effect as well as local buckling if the flange is in Class 4). Even if the web is in Class 4, its gross area is considered for evaluating $M_{pl,Rd}$.

$M_{f,Rd}$ is calculated with the same assumptions as $M_{pl,Rd}$ but neglecting the web area totally.

EN1994-2, 6.2.2.5(2)

The interaction criterion needs not to be checked for the cross-sections located less than $h_w/2$ from a support with a vertical stiffener.

EN1993-1-5, 7.1(2)

Reduction factors for $M_{pl,Rd}$ and $M_{f,Rd}$ are also to be used if a normal force N_{Ed} is applied. The previous interaction criteria are still valid with the reduced values of $M_{pl,Rd}$ and $M_{f,Rd}$.

EN1993-1-5, 7.1(4)

Of course the bending and shear interaction can be checked under concomitant internal forces and moments.

Two design examples are dealt with in the remainder of Chapter 8 for different cross-sections of the two-girder bridge: at internal support P1 (Class 3 cross-section) and at mid-span P1-P2 (Class 1 cross-section).

8.3 - Check of cross-section at internal support P1

8.3.1 - Geometry and stresses

At internal support P1 at ULS the concrete slab is in tension over its whole height. Its contribution is therefore neglected in the cross-section resistance. The stresses in Figure 8.5 are subsequently calculated and obtained by summing the various steps whilst respecting the construction phases.

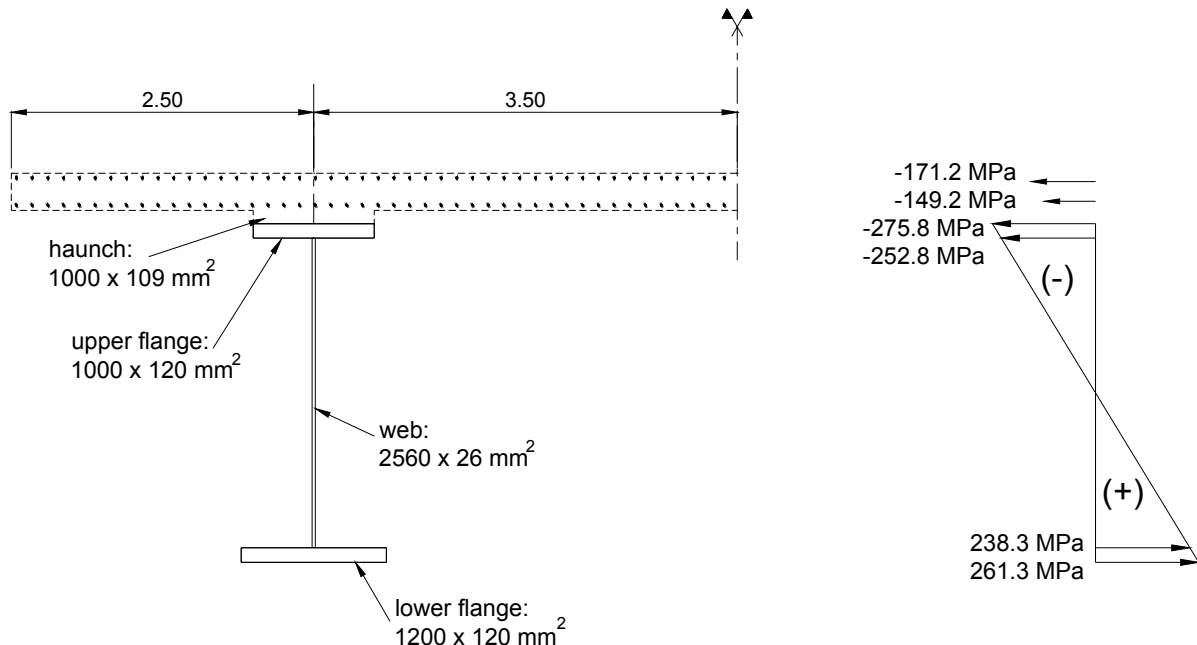


Figure 8.5: Stresses at ULS in cross-section at internal support P1

The internal forces and moments in this cross-section are (see Chapter 7 of this Part II):

$$M_{Ed} = 107.25 \text{ MN.m}$$

$$V_{Ed} = 7.47 \text{ MN}$$

8.3.2 - Determining the cross-section Class

Upper flange in tension therefore in Class 1

Lower flange in compression:

$$\frac{b_{fi} - t_w}{2t_{fi}} = \frac{5.48\varepsilon}{2t_{fi}} \leq 9\varepsilon \text{ therefore in Class 1.}$$

EN 1993-1-1, Table 5.2
(sheet 2 of 3)

The web is in tension in its upper part and in compression in its lower part. The position of the Plastic Neutral Axis (PNA) is determined as follows:

- Design plastic resistance of reinforcing steel bars:
 $F_{ap} = A_s f_{sk} / \gamma_s = 10.08 \text{ MN}$
- Design plastic resistance of the upper steel flange:
 $F_{fs} = A_{fs} f_{yf} / \gamma_{M0} = 35.40 \text{ MN}$
- Design plastic resistance of the lower steel flange:
 $F_{fl} = A_{fl} f_{yf} / \gamma_{M0} = 42.48 \text{ MN}$
- Design plastic resistance of the steel web assumed to be entirely in compression:
 $F_w = A_w f_{yw} / \gamma_{M0} = 22.96 \text{ MN}$

From $F_{ap} + F_{fs} \leq F_w + F_{fi}$ and $F_{ap} + F_{fs} + F_w \geq F_{fi}$ the PNA is deduced to be located in the steel web at a distance x from the web to upper flange weld. Writing the forces equilibrium around the PNA deduces:

$$x = \frac{F_w + F_{fi} - (F_{ap} + F_{fs})}{2t_w f_{yw}} = 1113 \text{ mm}$$

Over half the web height is in compression:

$$\alpha = \frac{h_w - x}{h_w} = 0.565 > 0.5$$

Therefore the limiting slenderness between Class 2 and Class 3 is given by:

$$\frac{h_w}{t_w} = 98.46 \gg \frac{456\epsilon}{13\alpha - 1} = 59.31$$

The steel web is at least in Class 3 and reasoning is now based on the elastic stress distribution at ULS given in Figure 8.5:

$$\psi = -252.8 / 238.3 = -1.061 \leq -1$$

therefore the limiting slenderness between Class 3 and Class 4 is given by:

$$\frac{h_w}{t_w} = 98.46 \leq 62\epsilon(1 - \psi)\sqrt{-\psi} = 108.6$$

It is deduced that the steel web is in Class 3.

Conclusion: The cross-section at support P1 is in Class 3 and is checked by an elastics section analysis.

EN 1993-1-1, Table 5.2
(sheet 1 of 3)

EN 1993-1-1, Table 5.2
(sheet 1 of 3)

8.3.3 - Bending resistance check

Are verified in succession:

$$261.3 \text{ MPa} \leq f_{yf} / \gamma_{M0} = 295 \text{ MPa},$$

$$\sigma_{s,sup} = -275.8 \text{ MPa} \geq -f_{yf} / \gamma_{M0} = -295 \text{ MPa},$$

$$\text{and } \sigma_{reinf,max}^{eff(2)} = -171.2 \text{ MPa} \geq -f_{sk} / \gamma_s = -434.8 \text{ MPa}.$$

The cross-section at P1 is therefore checked for bending at ULS.

The verifications are here performed with the stresses in the extreme fibres of the structural steel flanges. Remember that the use of the stresses in the mid-plan of the flanges is also allowable.

EN1993-1-1, 6.2.1(9)

8.3.4 - Shear resistance check

As $\frac{h_w}{t_w} = 98.46 \geq \frac{31\epsilon}{\eta} \sqrt{k_r} = 51.13$ (see the calculation of k_r below) the web (stiffened by the vertical stiffeners) should be checked in terms of shear buckling.

EN1993-1-5, 5.1(2)

The maximum design shear resistance is given by $V_{Rd} = \min(V_{b,Rd}; V_{pl,a,Rd})$ where $V_{b,Rd} = V_{bw,Rd} + V_{bf,Rd} \leq \frac{\eta f_{yw}}{\gamma_{M1}\sqrt{3}} h_w t_w = 14.46 \text{ MN}.$

EN1994-2, 6.2.2

$$V_{pl,a,Rd} = \frac{\eta f_{yw}}{\gamma_{M0}\sqrt{3}} h_w t_w = 15.91 \text{ MN}$$

EN1993-1-1, 6.2.6

Calculation of $V_{bw,Rd}$ (web contribution to the design shear buckling resistance)

EN1993-1-5, 5.2 (1)

$$V_{bw,Rd} = \frac{\chi_w f_{yw}}{\gamma_{M1} \sqrt{3}} h_w t_w$$

The vertical stiffeners at the bracing transverse frames which border the web panel adjacent to the support P1 and located in span P1-P2, are assumed to be rigid (to be checked by using Section 9 of EN1993-1-5). They are equally spaced by $a = 8$ m.

$$k_r = 5.34 + 4 \left(\frac{h_w}{a} \right)^2 = 5.75$$

$$\sigma_E = \frac{\pi^2 E t_w^2}{12(1-\nu^2) h_w^2} = 19.58 \text{ MPa}$$

$$\tau_{cr} = k_r \sigma_E = 112.56 \text{ MPa}$$

$$\bar{\lambda}_w = \sqrt{\frac{f_{yw}}{\tau_{cr} \sqrt{3}}} = 1.33 \geq 1.08$$

$$\chi_w = \frac{1.37}{0.7 + \bar{\lambda}_w} = 0.675$$

Therefore $V_{bw,Rd} = 8.14$ MN.

EN1993-1-5, Annex A3

EN1993-1-5, 5.3 (3)

EN1993-1-5, Table 5.1

Calculation of $V_{bf,Rd}$ (flange contribution to the design shear buckling resistance)

EN1994-2, 6.2.2.5(1)

The lower flange of the cross-section is a structural steel section whereas its upper flange is a composite section (structural steel + reinforcing steel). The formulae for calculating $V_{bf,Rd}$ should be used with the lower steel flange properties.

The design plastic bending resistance $M_{f,Rd}$ of the cross-section consisting of the flanges only should be first calculated (see Figure 8.6). $M_{f,Rd}$ is calculated as $M_{pl,Rd}$ but neglecting the web contribution.

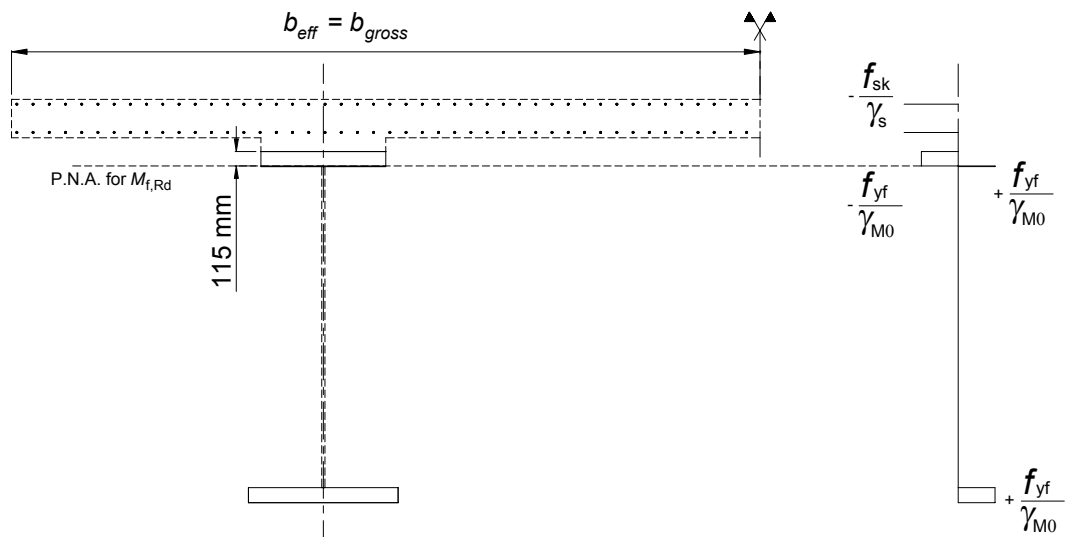


Figure 8.6: Design plastic resistance moment of the flanges only

From $F_{ap} + F_{fs} = 10.08 + 35.40 = 45.48 \text{ MN} \geq F_{fi} = 42.48 \text{ MN}$ the PNA is located in the upper flange at a distance x from its upper extreme fibre:

$$F_{ap} + b_{fs}x \frac{f_{yf}}{\gamma_{M0}} = b_{fs}(t_{fs} - x) \frac{f_{yf}}{\gamma_{M0}} + F_{fi}$$

Therefore $x = 115 \text{ mm}$ and then $M_{f,Rd} = 117.31 \text{ MN.m}$.

$$c = a \left(0.25 + \frac{1.6b_{fi}t_{fi}^2f_{yf}}{t_w h_w^2 f_{yw}} \right) = 3110 \text{ mm}$$

$$V_{bf,Rd} = \frac{b_{fi}t_{fi}^2f_{yf}}{c\gamma_{M1}} \left(1 - \left(\frac{M_{Ed}}{M_{f,Rd}} \right)^2 \right) = 0.245 \text{ MN}$$

EN1993-1-5, 5.4(1)

In the example, the flange contribution represents 3% of the design shear buckling resistance which is negligible. It is generally recommended not take this contribution into account. Otherwise the following checks should also be performed:

- the web to flange weld should be designed for the shear stress per unit length of $\frac{\eta f_{yw} t_w}{\gamma_{M1} \sqrt{3}}$;
- the transverse stiffeners along the web panel edges (and possibly the longitudinal stiffeners) should act as rigid end post (see paragraph 8.5);
- the flanges are not completely used for resisting to bending moment (i.e. $M_{Ed} \leq M_{f,Rd}$ which is verified in the example: $M_{Ed} = 107.25 \leq 117.31 \text{ MN.m}$).

EN1993-1-5, 9.3.5

EN1993-1-5, 9.3

Cross-section verification

EN1993-1-5, 5.5

The criterion $\eta_3 = \frac{V_{Ed}}{V_{Rd}} = 7.47/8.14 = 0.92 \leq 1.0$ is verified.

Therefore the cross-section at support P1 is checked under shear force.

8.3.5 - M, V interaction check

$$V_{Ed} = 7.47 \text{ MN} \geq 0.5 V_{Rd} = 4.07 \text{ MN}$$

EN1994-2, 6.2.2.4(1)

Therefore the M, V interaction should be checked. The cross-section at P1 is in Class 3 and the interaction criterion is then given by EN1993-1-5, 7.1:

$$\bar{\eta}_1 + \left[1 - \frac{M_{f,Rd}}{M_{pl,Rd}} \right] \left[2\bar{\eta}_3 - 1 \right]^2 \leq 1.0$$

EN1994-2, 6.2.2.4(3)

According to EN1993-1-5, 7.1, the criterion should be verified at all sections other than those located at a distance less than $h_w/2$ from the support P1. The internal forces and moments to consider are thus slightly reduced to $V_{Ed} = 7.25 \text{ MN}$ and $M_{Ed} = 98.55 \text{ MN.m}$.

EN1993-1-5, 7.1(2)

$M_{f,Rd} = 117.31 \text{ MN.m}$ has already been calculated. The design plastic resistance moment of the cross-section at P1 is calculated bearing in mind that the PNA is located 1113 mm from the web to upper flange joint (see Figure 8.7). This gives $M_{pl,Rd} = 135.6 \text{ MN.m}$.

$$\bar{\eta}_3 = \frac{V_{Ed}(\text{at } h_w/2)}{V_{bw,Rd}} = 0.89$$

$$\bar{\eta}_1 = \frac{M_{Ed}(\text{at } h_w/2)}{M_{pl,Rd}} = 0.727$$

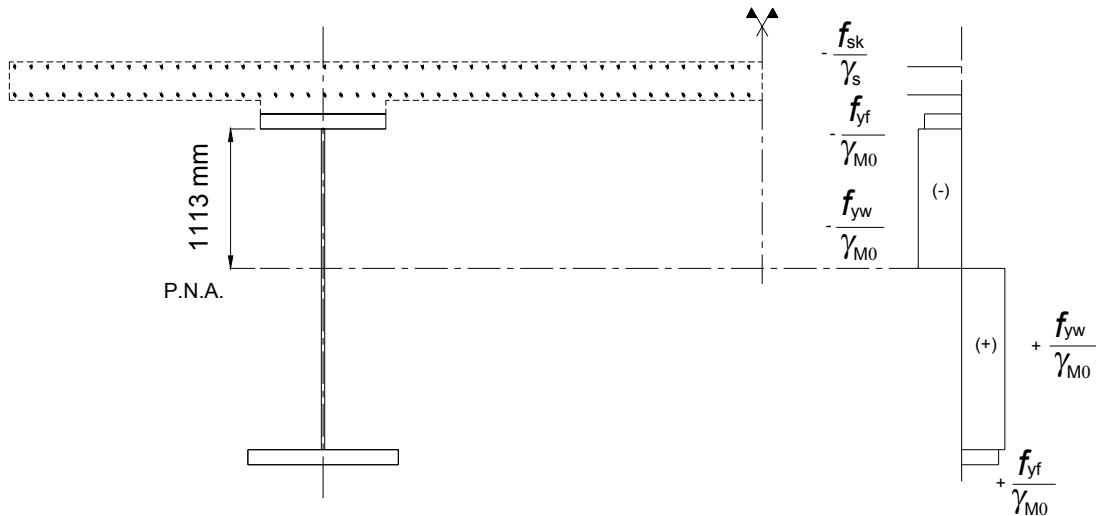


Figure 8.7: PNA and design plastic resistance moment $M_{pl,Rd}$

As $\bar{\eta}_1 \leq \frac{M_{f,Rd}}{M_{pl,Rd}} = 0.865$, $\bar{\eta}_1 = 0.865$ is adopted and the interaction criterion thus gives:

$$\bar{\eta}_1 + \left[1 - \frac{M_{f,Rd}}{M_{pl,Rd}} \right] \left[2\bar{\eta}_3 - 1 \right]^2 = 0.947 \leq 1.0$$

The cross-section is thus checked for the M, V interaction.

Note: M_{Ed} (at $h_w/2$) is lower than $M_{f,Rd}$ and can therefore be completely resisted by the flanges only, so that all the web strength can be used for the shear resistance. The criterion $(\bar{\eta}_1; \bar{\eta}_3)$ needs not to be checked and the cross-section is directly verified for the M, V interaction.

8.3.6 - Alternative: Effective Class 2 cross-section

As the cross-section at P1 is in Class 3, an alternative with elastic bending verification (performed in the previous paragraph 8.3.3) is possible by using the effective Class 2 cross-section (see Figure 8.8).

EN1994-2, 5.5.2(3)

The position of the PNA of this effective cross-section is determined by writing the equilibrium of the forces which are resisted by each cross-section element (flanges, webs and reinforcing steel bars). The web part to be neglected is deduced following the definition of an effective Class 2 cross-section.

The design plastic resistance moment of the effective cross-section in Figure 8.8 is $M_{pl,Rd} = 127.5$ MN.m.

The bending resistance verification for the cross-section at P1 is therefore simply written as $M_{Ed} = 107.25$ MN.m $\leq M_{pl,Rd}$.

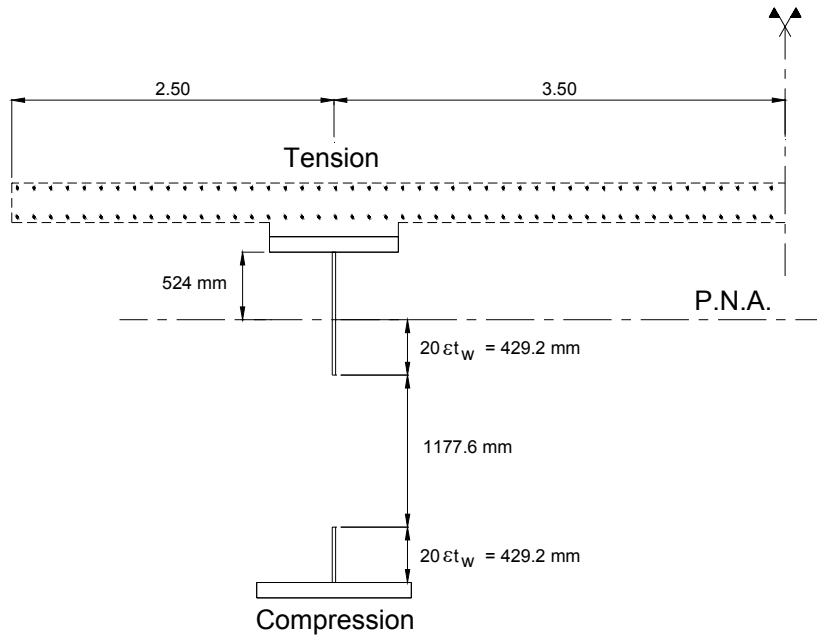


Figure 8.8: Effective Class 2 cross-section at support P1

Note that this verification gives more « resistance margin » in the cross-section than the elastic verification. Here $\eta_1 = \frac{M_{Ed}}{M_{pl,Rd}} = 0.841$ to be compared to

$\eta_1 = \frac{\sigma_{max}}{f_y} = 275.8/295 = 0.935$ for the elastic verification (see paragraph 8.3.3).

This margin could be even larger if the web slenderness ($h_w/t_w = 98.46$) was closer to the limit between Class 2 and Class 3 (59.31) than to the limit between Class 3 and Class 4 (108.6).

The shear resistance check in paragraph 8.3.4 is still valid. $\eta_3 = \frac{V_{Ed}}{V_{Rd}} > 0.5$ still exists and the M, V interaction should be considered.

For the interaction, the cross-section is considered to be in Class 2. The yield strength of the shear resistance area is multiplied by a reduction factor $1-\rho$ with:

$$\rho = \left[2 \frac{V_{Ed}}{V_{Rd}} - 1 \right]^2 = \left[2 \cdot \frac{7.47}{8.14} - 1 \right]^2 = 0.698$$

$M_{pl,Rd}$ is then recalculated with the plastic stress distribution in Figure 8.9 without modifying the position of the PNA: $M_{pl,Rd} = 120.3$ MN.m.

And the cross-section is verified for the M, V interaction by making sure that $M_{Ed} = 107.25$ MN.m $\leq M_{pl,Rd}$.

EN1994-2, 6.2.2.4(2)

EN1994-2, 6.2.2.4(4)

Note: As referral to EN1993-1-5, 7.1, is not made for the interaction, the calculations use the shear design force V_{Ed} at the support and not the shear design force at a distance $h_w/2$ from the support. This gives a lower value of $M_{pl,Rd}$ which is thus safer-sided for the check.

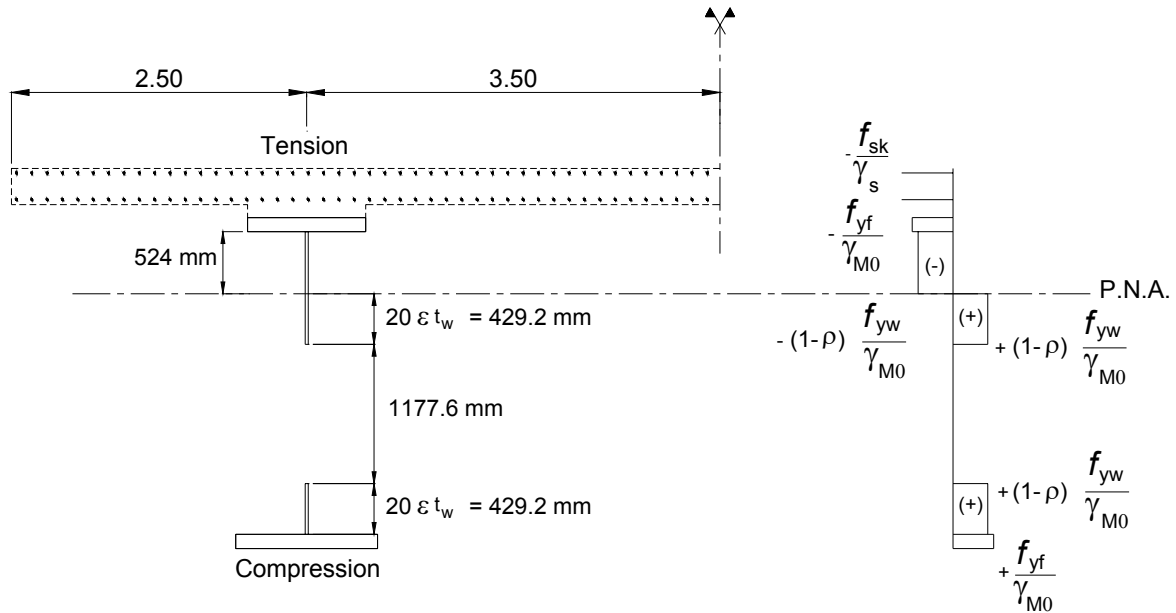


Figure 8.9: M, V interaction

8.4 - Verification of cross-section at mid-span P1-P2

8.4.1 - Geometry and stresses

At mid-span P1-P2 at ULS the concrete slab is in compression over its whole height. Its contribution is therefore taken into account in the cross-section resistance. The stresses in Figure 8.10 are subsequently calculated with the composite mechanical properties and obtained by summing the various steps whilst respecting the construction phases.

The internal forces and moments in this cross-section are:

$$M_{Ed} = 56.07 \text{ MN.m}$$

$$V_{Ed} = 1.04 \text{ MN}$$

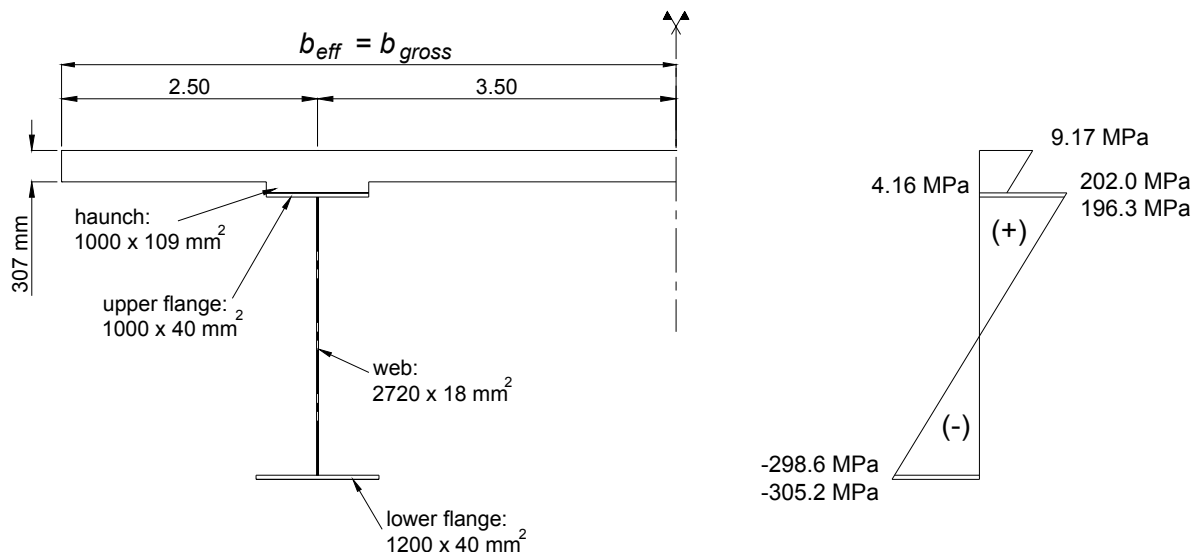


Figure 8.10: Stresses at ULS in cross-section at mid-span P1-P2

8.4.2 - Determining the cross-section Class

Lower flange in tension therefore in Class 1

The upper flange is composite and connected following the recommendations of EN1994-2, 6.6, therefore in Class 1.

To classify the steel web, the position of the Plastic Neutral Axis (PNA) is determined as follows:

- Design plastic resistance of the concrete in compression:

$$F_c = A_c \frac{0.85f_{ck}}{\gamma_c} = 38.675 \text{ MN}$$

The reinforcing steel bars in compression are neglected.

- Design plastic resistance of the structural steel upper flange:

$$F_{fs} = A_{fs} \frac{f_{yf}}{\gamma_{M0}} = 13.8 \text{ MN}$$

- Design plastic resistance of the structural steel web:

$$F_w = h_w t_w \frac{f_{yw}}{\gamma_{M0}} = 16.89 \text{ MN}$$

- Design plastic resistance of the structural steel lower flange:

$$F_{fi} = A_{fi} \frac{f_{yf}}{\gamma_{M0}} = 16.56 \text{ MN}$$

From $F_c \leq F_{fs} + F_w + F_{fi}$ and $F_c + F_{fs} \geq F_w + F_{fi}$ the PNA is deduced to be located in the structural steel upper flange at a distance x from the extreme upper fibre of this flange. Writing the forces equilibrium around the PNA deduces:

$$x = \frac{F_{fs} + F_w + F_{fi} - F_c}{2b_{fs}f_{yf}} = 12.5 \text{ mm}$$

As the PNA is located in the upper flange the whole web is in tension and therefore in Class 1.

Conclusion: The cross-section at mid-span P1-P2 is in Class 1 and is checked by a plastic section analysis.

EN1994-2, 5.5.2(1)

8.4.3 - Plastic section analysis

Bending resistance check

The design plastic resistance moment is calculated from the position of the PNA (see Figure 8.11): $M_{pl,Rd} = 79.59 \text{ MN.m}$

EN1994-2, 6.2.1.2(1)

$M_{Ed} = 56.07 \text{ MN.m} \leq M_{pl,Rd}$ is then verified.

The cross-section at adjacent support P1 is in Class 3 but there is no need to reduce $M_{pl,Rd}$ by a factor 0.9 because the ratio of lengths of the spans adjacent to P1 is 0.75 which is not less than 0.6.

EN1994-2, 6.2.1.2(1)

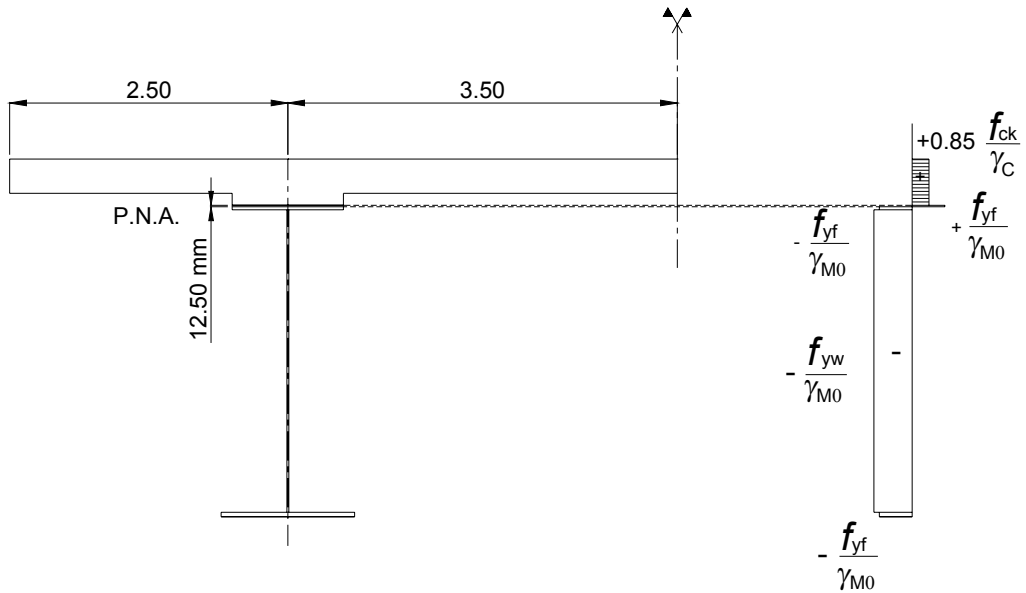


Figure 8.11: Design plastic resistance moment at mid-span P1-P2

Shear resistance check

As $\frac{h_w}{t_w} = 151.1 \geq \frac{31\epsilon}{\eta} \sqrt{k_t} = 51.36$, the web (stiffened by the vertical stiffeners) should be checked in terms of shear buckling. EN1993-1-5, 5.1(2)

The maximum design shear resistance is given by $V_{Rd} = \min(V_{bw,Rd}; V_{pl,a,Rd})$ en négligeant la contribution des semelles à la résistance au voilement sous cisaillement (voir paragraphe 8.3.4). EN1994-2, 6.2.2

$$V_{pl,a,Rd} = \frac{\eta f_yw}{\gamma_{M0} \sqrt{3}} h_w t_w = 11.7 \text{ MN} \quad \text{EN1993-1-1, 6.2.6}$$

Given the distribution of the bracing transverse frames in the span P1-P2 (spacing $a = 8 \text{ m}$), a vertical frame post is located in the studied cross-section (as for the cross-section at support P1). The shear buckling check is therefore performed in the adjacent web panel with the highest shear force. The maximum shear force observed in this panel is $V_{Ed} = 2.21 \text{ MN}$.

The vertical frame posts are assumed to be rigid (which is checked in paragraph 8.5 below). This gives: EN1993-1-5, Annex A3

$$k_t = 5.34 + 4 \left(\frac{h_w}{a} \right)^2 = 5.802$$

$$\sigma_E = \frac{\pi^2 E t_w^2}{12(1-\nu^2) h_w^2} = 8.312 \text{ MPa}$$

$$\tau_{cr} = k_t \sigma_E = 48.2 \text{ MPa}$$

$$\bar{\lambda}_w = \sqrt{\frac{f_yw}{\tau_{cr} \sqrt{3}}} = 2.032 \geq 1.08 \quad \text{EN1993-1-5, 5.5.3(3)}$$

$$\chi_w = \frac{1.37}{0.7 + \bar{\lambda}_w} = 0.501 \quad \text{EN1993-1-5, Table 5.1}$$

$$V_{bw,Rd} = \min \left(\frac{\chi_w f_{yw} h_w t_w}{\gamma_{M1} \sqrt{3}}, \frac{\eta f_{yw} h_w t_w}{\gamma_{M1} \sqrt{3}} \right) = \min (4.44; 10.64) = 4.44 \text{ MN}$$

The following criterion is then verified: $V_{Ed} = 2.21 \text{ MN} \leq V_{Rd} = \min (4.44; 11.7) = 4.44 \text{ MN}$.

M, V interaction check

As $V_{Ed} \leq 0.5 V_{Rd}$ there is no need to check the M, V interaction.

8.4.4 - Alternative: elastic section analysis

Whatever the Class a cross-section has, it can be justified by an elastic section analysis. Compared with the previous plastic section analysis, only the bending resistance check has to be performed again.

EN1994-2, 6.2.1.1(2)

This gives successively:

EN1994-2, 6.2.1.5(2)

$$\sigma_{s,inf} = -305.2 \text{ MPa} \geq -f_{yf} / \gamma_{M0} = -345 \text{ MPa} \text{ (lower flange),}$$

$$\sigma_{s,sup} = 202.0 \text{ MPa} \leq f_{yf} / \gamma_{M0} = 345 \text{ MPa} \text{ (upper flange),}$$

$$\text{and } \sigma_{c,max} = 9.2 \text{ MPa} \leq f_{cd} = f_{ck} / \gamma_c = 23.3 \text{ MPa} \text{ (concrete in compression).}$$

The reinforcing steel bars in compression may not be justified. In the example this check would give in the most compressed reinforcing steel bars from the upper layer:

$$\sigma_{reinf,max} = 92.2 \text{ MPa} \leq f_{sd} = f_{sk} / \gamma_s = 434.8 \text{ MPa,}$$

which is very easy verified.

8.5 - Verification of the frame post rigidity

The cross-section check under shear force carried out in paragraphs 8.3 and 8.4 requires to make sure that the vertical frame posts (acting as stiffeners and supports for web panels) are enough rigid to enable the truss behaviour of the structural steel web. Their design is presented in paragraph 3.3 of this Part II.

Note: When the shear force V_{Ed} in a given panel exceeds the critical shear resistance V_{cr} the vertical stiffener bordering this panel should be verified under the normal compression force $V_{Ed} - V_{cr}$ (EN1993-1-5, section 9). This is not dealt with in this guidance book but in a later supplement.

8.5.1 - Minimum rigidity under shear force

The minimum second moment of area for a standard vertical intermediate stiffener is given by:

EN1993-1-5, 9.3.3(3)

$$I_{st} \geq 0.75 h_w t_w^3 \text{ if } \frac{a}{h_w} \geq \sqrt{2}$$

$$I_{st} \geq 1.5 \frac{h_w^3 t_w^3}{a^2} \text{ if } \frac{a}{h_w} < \sqrt{2}$$

The second moment of area of the stiffener is calculated with a web part acting together (see Figure 8.12). In the unfavourable case of a small web thickness

EN1993-1-5, 9.1(2)

$(t_w = 18 \text{ mm})$ and a maximum web height $(h_w = 2720 \text{ mm})$ this gives $I_{st} = 888.4 \cdot 10^6 \text{ mm}^4$.

As $\frac{a}{h_w} = 2.94 \geq \sqrt{2}$ it should be verified that:

$$I_{st} = 888.4 \cdot 10^6 \text{ mm}^4 \geq 0.75 h_w t_w^3 = 11.9 \cdot 10^6 \text{ mm}^4.$$

The vertical frame posts of the design example thus clearly act as rigid edges and supports for the web panels under shear force as already assumed in paragraphs 8.3 and 8.4.

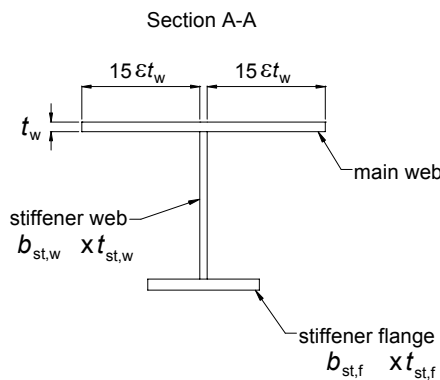
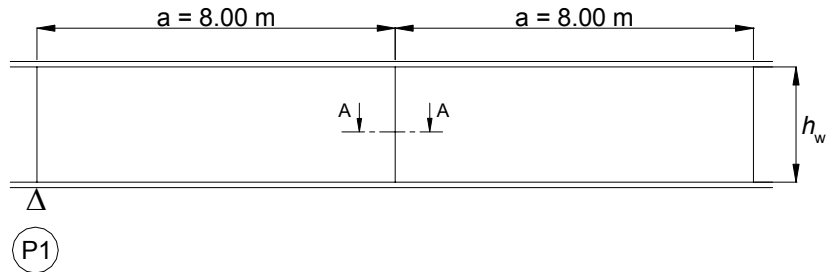


Figure 8.12: Defining the vertical post of a web panel

8.5.2 - Torsional buckling

It should be checked that the vertical web stiffeners do not buckle under torsion (which can occur for vertical T-shaped open stiffeners). The following criterion applies:

$$\frac{I_T}{I_P} \geq 5.3 \frac{f_y}{E_a}$$

where $I_T = 3766.7 \cdot 10^3 \text{ mm}^4$ is the St. Venant torsional constant for the stiffener alone (acting without the web part) and $I_P = 2045.14 \cdot 10^6 \text{ mm}^4$ is the polar second moment of area of the stiffener alone around its edge welded to the web plate.

Remember that $I_P = I_{Gy} + I_{Gz} + Az^2$ where I_{Gy} and I_{Gz} are the principal second moment of area, A is the stiffener area and z is the distance between the pole and the neutral axis of the cross-section.

$$\text{Therefore } \frac{I_T}{I_P} = 1.84 \cdot 10^{-3} \leq 5.3 \frac{f_y}{E_a} = 8.71 \cdot 10^{-3}.$$

As the criterion has not been verified, the more precise method in 9.2.1(9) of EN1993-1-5 is used. By considering that the vertical stiffener is hinged at both ends and warping is not prevented the torsional buckling critical stress is as follows:

EN1993-1-5, 9.2.1(8)

EN1993-1-5, 9.2.1(9)

$$\sigma_{cr,T} = G \frac{I_T}{I_p} + \frac{\pi^2 E_a}{h_w^2} \frac{I_\omega}{I_p}$$

with $I_\omega = 1.16 \cdot 10^{13} \text{ mm}^6$ calculated with the same pole P as the polar second moment of area, i.e. the welded joint of the stiffener to the web.

The torsional buckling of the stiffener is still not verified:

$$\sigma_{cr,T} = 148.6 + 1589.0 = 1737.6 \text{ MPa} \geq 6 f_y = 2070 \text{ MPa}$$

EN1993-1-5, 9.2.1(9)
+ National Annex

The factor 6 could be modified by the National Annex of EN1993-1-5. A additional term could also be considered in $\sigma_{cr,T}$ for modeling the out-of-plane bending stiffness of the web to which the stiffener is welded.

8.6 - Lateral torsional buckling (LTB) of the lower flange in compression around internal support P1

The LTB verification of the lower flange in a two-girder composite bridge under traffic loads is studied as the lateral column buckling of the isolated lower flange which is in compression around the internal supports (P1 for the design example). This lower flange is then assumed to be laterally simply supported at piles and abutments (which means the design of a very rigid bracing transverse frame at any support, as it is usually provided due to the wind action transmission from the deck to the supports). The lower flange is also assumed to be laterally elastically supported at the bracing frames. The lateral stability of the flange is thus linked to the frame rigidity which is first calculated.

Secondly the critical load for lateral column buckling should be calculated. EN1993-2 proposes two approaches:

- a simplified method which uses the Engesser's formula (as in the common practise in France) but which assumes an uniform cross-section and an uniform load over the whole length of the deck as well as an uniformly distributed lateral spring support in span;
- a general method by performing the critical load calculations as exactly as possible.

EN1993-2, 6.3.4.2 +
Annex D 2.4

EN1993-2, 6.3.4.1

8.6.1 - Rigidity C_d of bracing transverse frames

The common practise in France uses the formulae established in a paper by ROCHE and FOUCRIAT published in 1985 by OTUA, the French Technical Office for the Use of Steel [41]. It is intended to use these calculations taking account of the following modifications:

- use the same width as in Eurocodes for the web part acting together with the vertical frame post, i.e. replacing $21\varepsilon t_w$ by $15\varepsilon t_w$ (see Figure 8.12);
- not neglect the shear deformation in the displacement calculations δ_1 and δ_2 at the frame lower section for the two used load cases (see Figures 8.13 and 8.14), which represents an unfavourable reduction of around 15% in the stiffness C_d compared to the formulae in [41];
- simplify the two stages of the modeled transverse frame (see Figure 8.13) by suppressing the bar element representing the concrete slab (i.e. neglect the slab extensibility in the calculations).

As in [41] it is safe-sided assumed that no bending transmission occurs from the vertical frame posts to the concrete slab. The slab flexibility is therefore always neglected. In addition the joints between the transverse brace girder and the vertical frame posts are assumed to be fully rigid and the frame posts extensibility is also neglected.

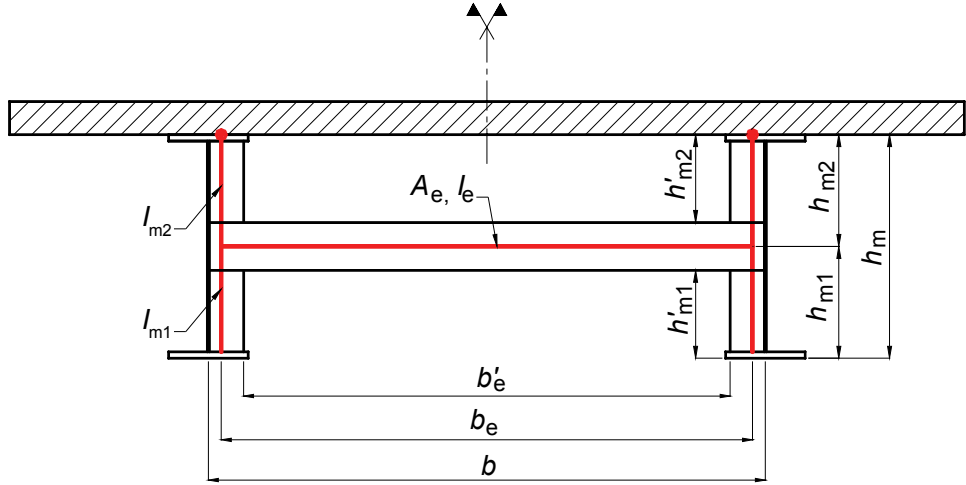
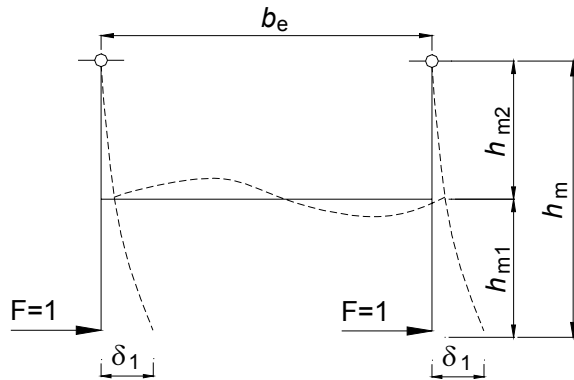


Figure 8.13: Notations defining the modeled transverse frame

Same direction forces (load case 1)



Opposite direction forces (load case 2)

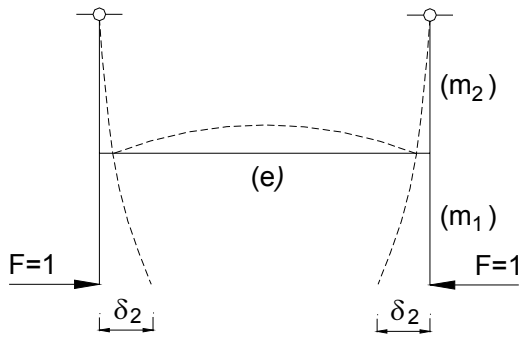


Figure 8.14: Load cases for the rigidity C_d calculation

Three new flexibility terms linked to the shear resistant areas of the transverse brace girder Σ_e and of the vertical frame posts Σ_m are introduced in the formulae for lateral displacements δ_1 and δ_2 :

$$A_t = \frac{h'_{m1}}{G\Sigma_m} \quad B_t = \frac{2b'_e}{G\Sigma_e} \quad D_t = \frac{h'_{m2}}{G\Sigma_m}$$

Remember also the terms from [41] and here re-used:

- for the flexibility of the lower part of a vertical frame post: $A = \frac{h'_{m1}^3}{3EI_{m1}}$

- for the flexibility of the transverse brace girder:

$$B_1 = \frac{b'_e h_{m1}^2}{2 EI_e}$$

$$B_2 = \frac{b'_e h_{m2}^2}{2 EI_e}$$

$$B_3 = \frac{b'_e h_m^2}{2 EI_e}$$

- for the extensibility of the transverse brace girder: $C = \frac{b'_e}{2EA_e}$

- for the flexibility of the upper part of a vertical frame post (neglecting the extensibility of the concrete slab):

$$D = \frac{h_{m2}^3}{3EI_{m2}}$$

The calculation of the hyperstatic frame in Figure 8.13 gives the literal formulae below for the lateral displacements δ_1 and δ_2 :

- for the same direction forces: $\delta_1 = [A + A_t] + \frac{1}{3}B_3 + \left[\frac{h_m}{b_e} \right]^2 B_t + [D + D_t]$
- for the opposite direction forces: $\delta_2 = [A + A_t] + B_t + C - \frac{\left[C - \frac{h_{m1}}{h_{m2}} B_2 \right]^2}{B_2 + C + [D + D_t]}$

The stiffness C_d of the bracing frame is then given by $C_d = \min \left[\frac{1}{\delta_1}; \frac{1}{\delta_2} \right]$.

With the proposed design in paragraph 3.3 for the in-span bracing frame, the above formulae give $\delta_1 = 4.9 \cdot 10^{-5} \text{ N}^{-1} \cdot \text{mm}$ and $\delta_2 = 9.3 \cdot 10^{-6} \text{ N}^{-1} \cdot \text{mm}$ and then a stiffness $C_d = 20.3 \text{ MN/m}$.

8.6.2 - ULS internal moment distribution for LTB

To verify the bridge for LTB around the internal support P1, only the combination of actions which gives the maximum bending moment at support P1 is considered:

- The global longitudinal bending analysis (see chapter 7 of this Part II) gives the envelope of the bending moment in the bridge deck before applying variable loads, but taking account of the construction phases and the concrete cracking. The lower limit of the envelope is adopted which corresponds to an ULS bending moment (without variable loads) of -73.26 MN.m at P1;
- UDL traffic load is placed on the deck in both longitudinal and transversal directions to get the most unfavourable effect. Thus only the two spans adjacent to the support P1 are loaded with an uniformly distributed load of 26.7 kN/m (see paragraph 5.4.4 of this Part II). This gives a maximum bending moment of -15.72 MN.m at P1;
- The Tandem System (TS) is placed symmetrically to the mid-plane of the central span with a vertical load of 409.3 kN per axle (see paragraph 5.4.5 of this Part II). This location does not give exactly the maximum bending moment at P1 but the committed error in the total bending moment is very small. This gives a maximum bending moment of -5.74 MN.m at P1.

To simplify, the effects of the thermal gradient are neglected and the maximum bending moment is then $M_{\max} = -102.23 \text{ MN.m}$ at P1. As the transverse traffic load distribution has been taken into account, the two main girders of the bridge are not loaded in the same way (see Figure 8.15). At support the relatively low deviation observed between the two girders is due to the fact that permanent loads are symmetric in the transverse direction and represent the most important part of the bending moment (72%) than the traffic loads (28%). This is also the reason why the observed deviations in a given girder are small between the supports P1 and P2 although the traffic loads were arranged to maximize the bending moment at P1.

This deviation between the two girders will no longer be considered and only one girder will be modeled with the maximum loads. This means that the second girder is submitted to the same loads, which is a safe-sided assumption. A more accurate calculation would have to be based on a more complicated 3D modeling.

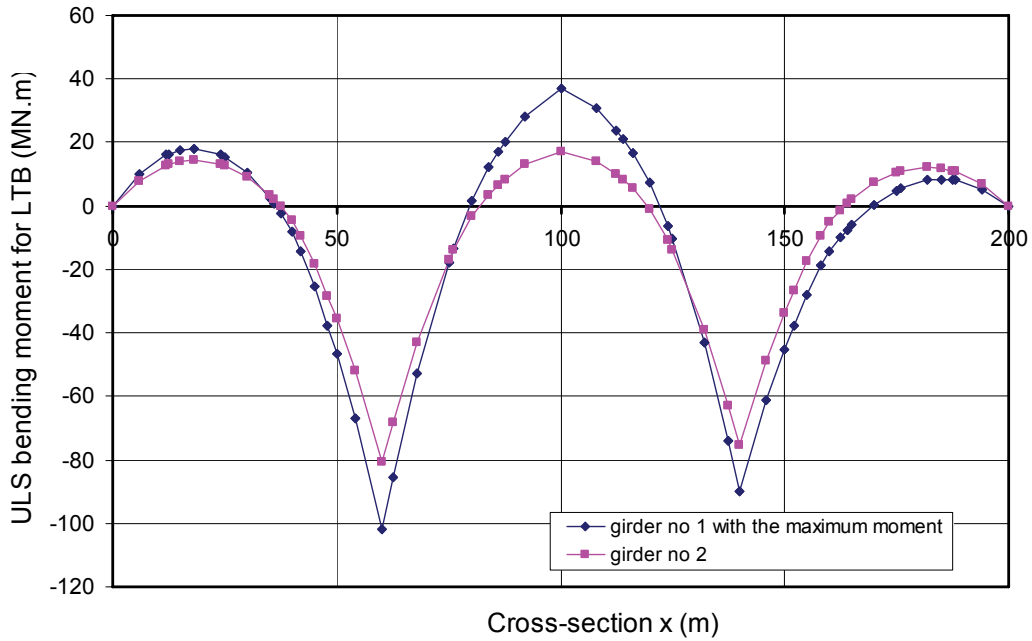


Figure 8.15: ULS bending moment in the two main girders for LTB verification

At P1 the concrete is cracked over the whole height of the slab and is not taken into account in the cross-section resistance. The bending moment M_{Ed} in Figure 8.15 gives thus a maximum compressive stress of 249 MPa in the mid-plane of the lower steel flange at support (by considering the construction phases in the stress calculation).

To study the lateral buckling of the lower flange in the modeled girder the bending moment in Figure 8.15 should be translated into a normal force distribution along this lower flange. This normal force is obtained by dividing the ULS bending moment M_{Ed} by the distance h between the two neutral axes of the girder flanges (steel for the lower and composite for the upper). h and M_{Ed} are variable along the girder and then the normal force N_{Ed} is also variable from a compressive force at internal support to a tensile force at mid-span. The obtained curve is shown in Figure 8.16. The maximum value at P1 reaches $N_{max} = 38.4$ MN.

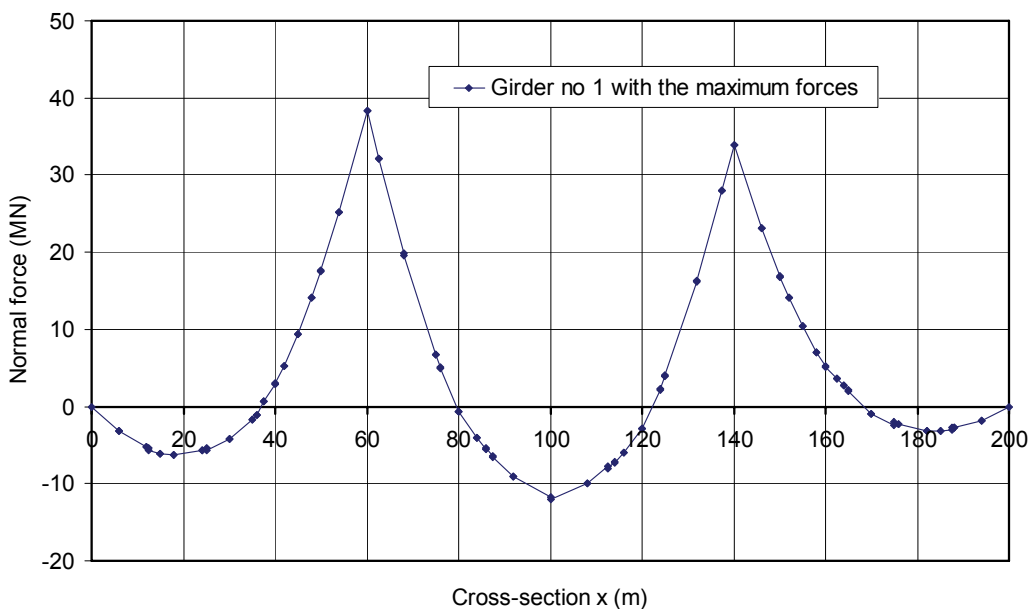


Figure 8.16: Variable normal force in the lower flange of the modeled girder

For the lateral column buckling model used here the variable normal force is resisted by a cross-section Ω made up of the lower steel flange acting with a web part of the main girder. In case of a bissymmetric I-girder under pure bending, writing the stress in the mid-plan of the lower flange as $M_{Ed}v/I$ and N_{Ed}/Ω , it can be easily prove that Ω is the sum of the flange area and a sixth of the web area: $\Omega = b_f t_f + h_w t_w / 6$.

8.6.3 - Simplified check method

The introduction to LTB verification has stated that the simplified method is normally not applicable because:

- the flange cross-section is variable;
- the bending moment gradient leads to a variation of the stresses, so a non uniform load is applied (it should be noticed that the maximum compressive stress value can be sometimes reached in the first in-span cross-section where the flange thickness changes instead of at internal support)

In case of a constant flange width the simplified method could be applied by calculating the critical stress with the maximum flange thickness and the maximum applied stress (at support or in the first in-span cross-section where the thickness changes). These assumptions minimize the critical load and are thus safe-sided. The calculation below is performed for the central span ($L = 80$ m).

$$c = \frac{C_d}{a} = 2.539 \cdot 10^6 \text{ N/m}^2 \text{ with } a = 8 \text{ m between adjacent transverse bracing}$$

$$I = \frac{t_f b_f^3}{12} = 17.28 \cdot 10^{-3} \text{ m}^4$$

$$\gamma = \frac{cL^4}{EI} = 28663.14$$

$$m = \frac{2}{\pi^2} \sqrt{\gamma} = 34.308 > 1$$

$$N_E = \frac{\pi^2 EI}{L^2} = 5.596 \cdot 10^6 \text{ N}$$

$$N_{\text{crit}} = mN_E = 192 \text{ MN}$$

EN1993-2, 6.3.4.2(6)

The reduced slenderness is calculated from the critical load:

$$\bar{\lambda}_{LT} = \sqrt{\frac{A_{\text{eff}} f_y}{N_{\text{crit}}}}$$

$$\text{with } A_{\text{eff}} = b_f t_f + \frac{h_{w,c} t_w}{3}$$

EN1993-2, 6.3.4.2(4)

$h_{w,c} = 1450$ mm determined from the stresses in the maximum thickness cross-section at P1.

$$A_{\text{eff}} = 156.567 \text{ mm}^2$$

$$f_y = 295 \text{ MPa for } t_f = 120 \text{ mm}$$

$$\text{Hence } \bar{\lambda}_{LT} = 0.4905$$

EN1993-2, 6.3.4.2(7)

The buckling curve d is used: $\alpha_{LT} = 0.76$.

$$\Phi_{LT} = \frac{1}{2} \left[1 + \alpha_{LT} \left(\bar{\lambda}_{LT} - 0.2 \right) + \bar{\lambda}_{LT}^2 \right] = 0.73$$

$$\chi_{LT} = \frac{1}{\Phi_{LT} + \sqrt{\Phi_{LT}^2 - \bar{\lambda}_{LT}^2}} = 0.787 \leq 1$$

EN1993-1-1, Table 6.3 and 6.4

The LTB criterion is therefore not verified:

$$\sigma_{\text{max}} = 249.25 \text{ MPa} \geq \frac{f_y}{\gamma_{M1}} \chi_{LT} = 211 \text{ MPa}$$

This simplified method remains safe compared to the general method. Given the deviation with which the criterion has not been verified, it nevertheless shows that the bracing frames initially designed in Chapter 3 of this Part II may be too flexible and/or too spaced out to justify the two-girder bridge for LTB under traffic loads, even with less safe methods. The remained of this chapter 8.6 is devoted to the general method.

8.6.4 - LTB critical load

No literal formulae exist in the scientific literature for calculating the buckling critical load of a continuous non-uniform girder under a variable normal force, simply supported and with discrete in-span spring supports of stiffness C_d . A model of the continuous girder for ULS combination of actions is built with bar elements by using a software which performs critical load calculations.

Description of the design model

An area and a second moment of area around the vertical axis for representing the lower flange (in compression around P1) are defined for each bar element in the model. These mechanical properties change along the model following the structural steel distribution along the bridge. The web part acting with the flange has no influence on the stiffness matrix used for calculating the critical amplification factor. It is not necessary to take account of this web part in the model. This increase in the cross-section area is only used when calculating the critical stresses (which can be performed without the software). EN1993-2, 6.3.4.2(7)

To get a critical load corresponding to a lateral buckling, the second moments of area around longitudinal and transversal axes are modeled to be very high and the vertical displacements are blocked for all the nodes in the model. In addition, the lateral displacements and the rotations around the longitudinal axis are blocked at piles and abutments, the discrete lateral spring supports with a stiffness C_d are imposed at the in-span transverse bracing frames positions.

This design model is then loaded with the variable normal force in Figure 8.16.

Results

Table 8.2 illustrates the lateral displacements corresponding to the first three buckling modes of the design model. The factor $\alpha_{cr,op}$ is the factor by which the ULS applied load should be multiplied to get the critical load for a given buckling mode. The observed buckling lengths, around 20 m, include several transverse bracing frames (at 8 m intervals in the central span).

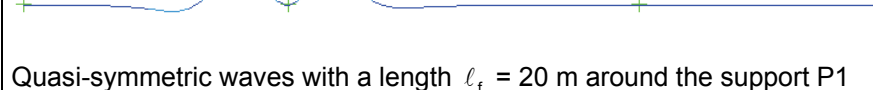
Mode	$\alpha_{cr,op}$	Description of the observed transverse displacement
1	8.8576	 Anti-symmetric waves with a length $\ell_f = 20$ m around the support P1
2	10.258	 Anti-symmetric waves with a length $\ell_f = 20$ m around the support P2
3	17.489	 Quasi-symmetric waves with a length $\ell_f = 20$ m around the support P1

Table 8.2: Transverse displacement of the first three critical modes

8.6.5 - General check method

The criterion to be verified is:

$$\frac{\chi_{op} \alpha_{ult,k}}{\gamma_{M1}} \geq 1.0$$

EN1993-1-1, 6.3.4(2)

where:

- $\alpha_{ult,k}$ is the minimum amplification factor to be applied to the ULS internal forces and moments to get the characteristic value of the resistance in the most loaded cross-section of the deck,
- χ_{op} is the reduction factor calculated with the reduced slenderness

$$\bar{\lambda}_{op} = \sqrt{\frac{\alpha_{ult,k}}{\alpha_{cr,op}}},$$

- $\alpha_{cr,op}$ is the minimum amplification factor to be applied to the ULS internal forces and moments to get the critical resistance to LTB.

The studied phenomena is a lateral torsional buckling (χ_{LT}) reduced to a lateral buckling (χ). To be safe the reduction factor to be used is $\chi_{op} = \min[\chi; \chi_{LT}]$.

$$\chi = \frac{1}{\Phi + \sqrt{\Phi^2 - \bar{\lambda}_{op}^2}} \leq 1.0 \text{ and } \Phi = \frac{1}{2} \left[1 + \alpha \left(\bar{\lambda}_{op} - 0.2 \right) + \bar{\lambda}_{op}^2 \right]$$

EN1993-1-1, 6.3.1.2

α should be chosen in Tables 6.1 and 6.2 of EN1993-1-1 following the nature of the deck cross-section. For a two-girder bridge in the support area the main girder is a welded section with $t_f > 40$ mm and therefore the buckling curve d with $\alpha = 0.76$ is normally used.

$$\chi_{LT} = \frac{1}{\Phi_{LT} + \sqrt{\Phi_{LT}^2 - \bar{\lambda}_{op}^2}} \leq 1.0 \text{ and } \Phi_{LT} = \frac{1}{2} \left[1 + \alpha_{LT} \left(\bar{\lambda}_{op} - 0.2 \right) + \bar{\lambda}_{op}^2 \right]$$

EN1993-1-1, 6.3.2.2

α_{LT} should be chosen in Tables 6.3 and 6.4 of EN1993-1-1 following the nature of the deck cross-section. For a two-girder bridge in the support area the main girder is a welded section with $h_w/b_{fi} > 2$ and therefore the buckling curve d with $\alpha_{LT} = 0.76$ is normally used.

For a two-girder bridge it is then deduced that $\chi_{op} = \chi = \chi_{LT}$.

8.6.6 - LTB verification around internal support P1

Design load amplification factor $\alpha_{ult,k}$

$\alpha_{ult,k} = \min(f_{yf}/\sigma_f)$ where σ_f is the longitudinal stress at ULS in the mid-plane of the girder no 1 lower flange. Figure 8.17 shows that this minimum value is obtained at support P1. Note that it is not always the case necessarily (the first flange thickness change that occurs in span could also often be the cross-section to study). Therefore $\alpha_{ult,k} = 295/249.5 = 1.184$.

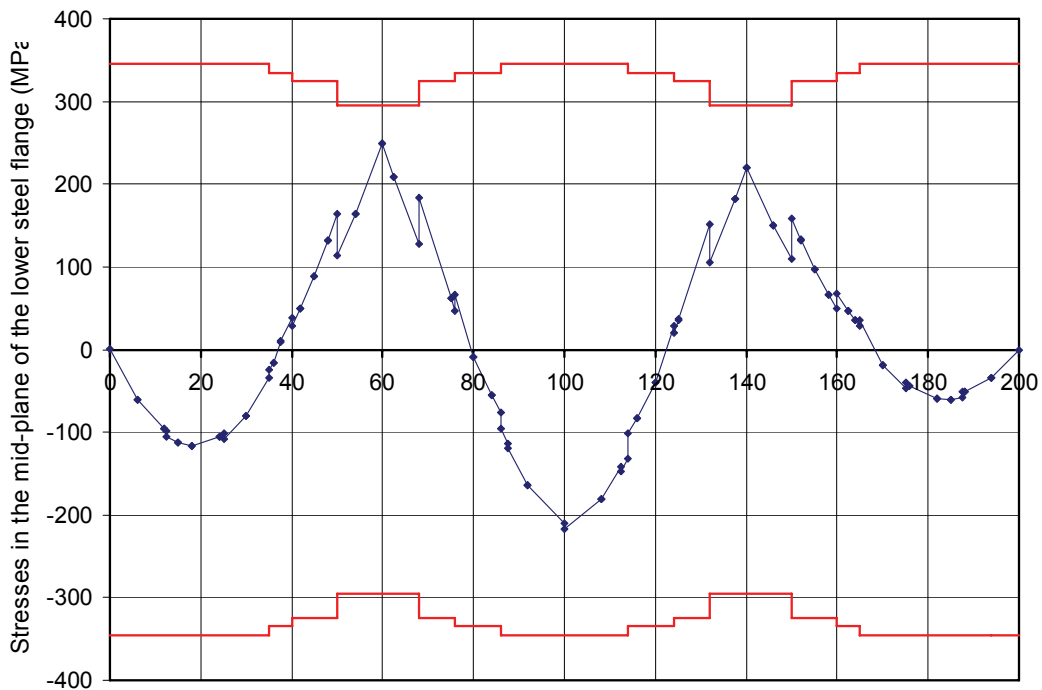


Figure 8.17: Stresses in the mid-plane of the lower flange in the girder no 1 at ULS

Reduction factor χ_{op} and check

The reduced slenderness is obtained from the two amplification factors $\alpha_{ult,k}$ and $\alpha_{cr,op}$:

$$\bar{\lambda}_{op} = \sqrt{\frac{\alpha_{ult,k}}{\alpha_{cr,op}}} = \sqrt{\frac{1.184}{8.858}} = 0.37 \geq 0.2$$

EN1993-1-1, 6.3.4(3)

$$\Phi_{LT} = \frac{1}{2} \left[1 + \alpha_{LT} (\bar{\lambda}_{op} - 0.2) + \bar{\lambda}_{op}^2 \right] = 0.63$$

EN1993-1-1, 6.3.2.2

$$\chi_{op} = \frac{1}{\Phi_{LT} + \sqrt{\Phi_{LT}^2 - \bar{\lambda}_{op}^2}} = 0.875 \leq 1.0$$

EN1993-1-1, 6.3.4(2)

The LTB criterion is then not verified:

$$\chi_{op} \frac{\alpha_{ult,k}}{\gamma_{M1}} = \frac{1.036}{1.1} = 0.94 < 1.0$$

The design of the transverse bracing frames in span should be revised to give them a better stiffness C_d in the zones surrounding the internal supports and/or to reduce their spacing.

8.6.7 - Modifying the bracing frame design

Minimum rigidity

Firstly without looking for a peculiar design of the bracing frame nor modify the initial spacing, several stiffnesses C_d are tested in order to define the minimum value necessary to justify the LTB criterion. For each tested value the factor $\alpha_{cr,op}$ is calculated by using the design model which is described in paragraph 8.6.4. The criterion $\chi_{op} \frac{\alpha_{ult,k}}{\gamma_{M1}}$ is then calculated to draw the curve in Figure 8.18.

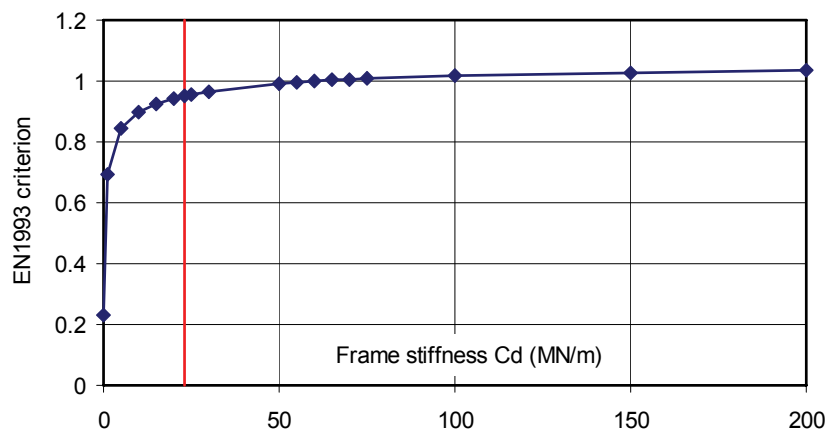


Figure 8.18: General criterion versus stiffness C_d of the in-span bracing frames

Note that the stiffness of the bracing frame should be approximately tripled ($C_d > 60$ MN/m) compared with the initial design if the wish is to barely verify the LTB criterion with keeping the initial spacing. In addition, the curve is « very flat » around the limit value 1.0 of the criterion, i.e. that a major increase in C_d does not have a very important influence on the general criterion.

A calculation where all the bracing frames behave as the supports on piles and abutments produces a value $\chi_{op} \frac{\alpha_{ult,k}}{\gamma_{M1}} = 1.049$ for the general criterion which is barely greater than 1 (horizontal asymptote in Figure 8.18).

Design of a new transverse bracing frame

It is still possible to suggest a design ensuring the required stiffness by nevertheless keeping the initial longitudinal spacing. To limit the transverse displacements of the lower part of the vertical frame posts the transverse brace girder IPE600 is lowered to 600 mm above the mid-plane of the lower flanges. The upper part of the bracing frame is then maintained by diagonals with a cross-section designed to prevent column buckling (see further on). Figure 8.19 illustrates this new bracing frame.

The stiffness of the new bracing frame is $C_d = 1/9.7 \times 10^{-3} = 103.1$ MN/m which is clearly three times greater than the stiffness of the base design.

Buckling of the frame diagonals

The frame elements are designed under transverse forces applied to the mid-planes of the lower flanges and equal to 1% of the longitudinal compressive normal force in the flange (extrapolation of EN1993-2, 6.3.4.2(5) written for the case of uniform girders).

EN1993-2, 6.3.4.2(5)

At the first bracing frame in the central span the normal force in the flange reaches $N_{Ed} = 19.58$ MN. By applying 1% of N_{Ed} in the same transverse

direction for both flanges (the least favorable case, see Figure 8.14), a normal force $F = 0.228 \text{ MN}$ is calculated in the diagonals of the first bracing frame.

Note: If the transverse forces are in opposite direction to each other, the calculated normal force is reduced to 0.03 MN in the diagonals.

$$I = 720.3 \text{ cm}^4$$

$$A = 3310 \text{ mm}^2$$

$L = 3.5 \text{ m}$ (diagonal length between joints)

$$\sigma_{\text{cr}} = \frac{\pi^2 EI}{AL^2} = 368.2 \text{ MPa}$$

$$\bar{\lambda} = \sqrt{\frac{f_y}{\sigma_{\text{cr}}}} = 0.982$$

The buckling curve a is used (hot finished circular hollow sections): $\alpha = 0.21$. Hence $\chi = 0.678$.

The following is clearly verified: $F = 0.228 \text{ MN} < F_{b,\text{Rd}} = \frac{\chi Af_y}{\gamma_{M1}} = 0.725 \text{ MN}$.

EN1993-1-1, Table 6.2

EN1993-1-1, 6.3.1.1(1)

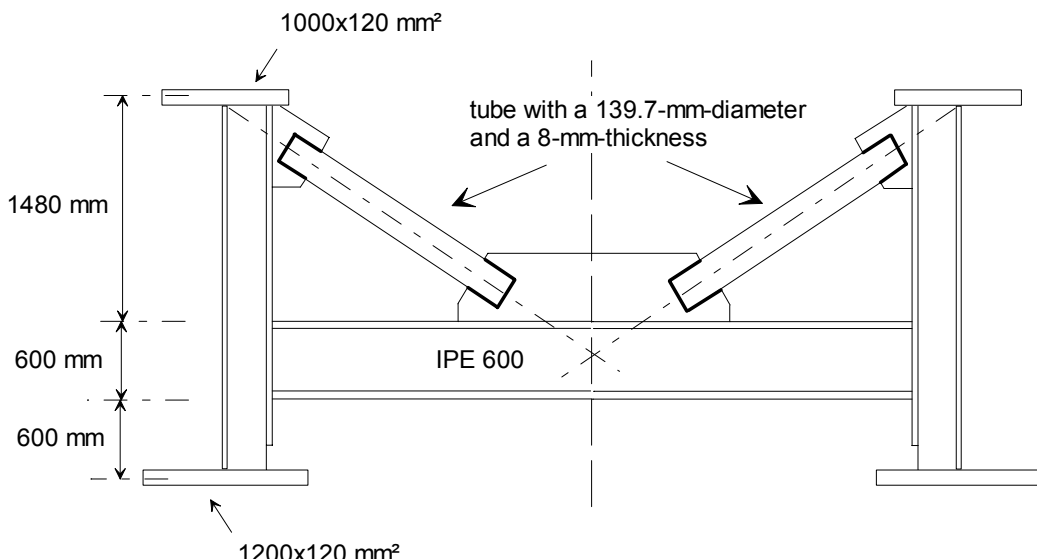


Figure 8.19: Suggestion for the in-span bracing frame design

LTB check around P1

If all the in-span bracing frames are replaced by the one in Figure 8.19, the lateral torsional buckling is justified by using the general criterion:

$\alpha_{\text{cr,op}} = 16.289$ for the first buckling mode with a similar deformation to the one in Table 8.2, but with a shorter wavelength ($\ell_f = 13 \text{ m}$ instead of 20 m).

$$\bar{\lambda}_{\text{op}} = 0.269 \geq 0.2$$

$$\Phi_{\text{LT}} = 0.563$$

$$\chi_{\text{op}} = 0.946 \leq 1.0$$

$$\chi_{\text{op}} \frac{\alpha_{\text{ult,k}}}{\gamma_{M1}} = \frac{1.12}{1.1} = 1.02 > 1.0$$

This replacement is not however necessary for all the bracing frames. If only the two frames surrounding each internal support (piles) are strengthened, then the lateral torsional buckling remains justified:

$$\alpha_{\text{cr,op}} = 15.706$$

$$\chi_{op} \frac{\alpha_{ult,k}}{\gamma_{M1}} = 1.014 > 1.0$$

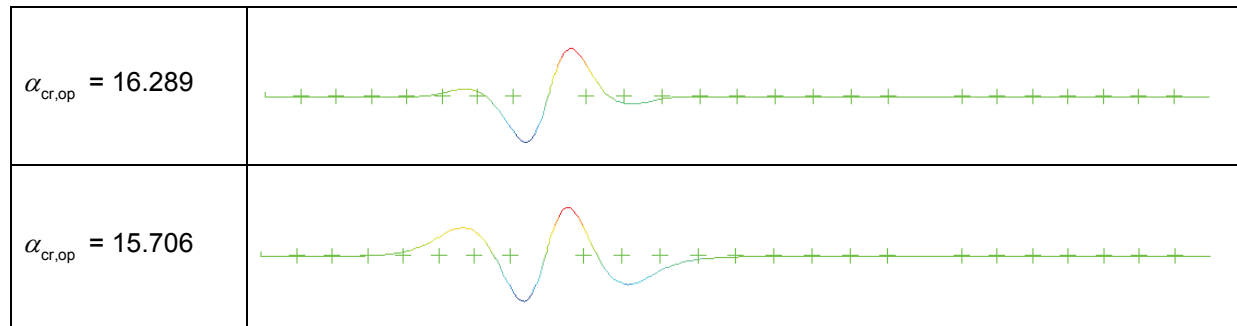


Table 8.3: Transverse displacements of the first critical modes by using tubes

9 - Justification at fatigue ULS

The fatigue verification consists of ensuring that the probability of a bridge collapse by crack propagation inside a deck component subjected to repeated stress variations remains low. In France, the safe life assessment method from EN1993-1-9 should be used.

EN 1993-1-9

The components to be checked under fatigue load in a composite bridge are:

EN1994-2, 6.8

- the structural steel part and its shear connectors,
- the reinforcing steel bars in the concrete slab,
- the concrete of the slab.

EN1994-2, 6.8 defines the provisions for fatigue verifications.

The fatigue verification of the concrete as well as of the transverse slab reinforcements are not dealt with in this guidance book (reference is made to the SETRA guidance book on concrete bridges designed under Eurocode 2). The shear connectors are checked under fatigue in chapter 11 of this part II.

9.1 - Verification of the structural steel bridge part

For the fatigue calculations in the structural steel bridge part EN1994-2 allows the use of the equivalent stress ranges simplified method. The stress variations in a given structural detail is thus obtained by the single crossing of the bridge by a lorry calibrated to have the same impact as the actual traffic. The simplified method is used with the fatigue load model no 3 defined in EN1991-2. This load model is called FLM3 in the remainder of this guide.

EN1994-2, 6.8.4(4)

EN1991-2 defines 5 different fatigue load models. They can be used for special justifications and following the verification format adopted by the main Eurocode used for the structural design (EN1994-2 for this guide).

EN1991-2, 4.6

All in all the verification format of the equivalent stress ranges simplified method is as follows:

$$\gamma_{Ff} \Delta \sigma_{E,2} \leq \frac{\Delta \sigma_c}{\gamma_{Mf}}$$

EN1993-2, 9.5, Eq. (8.1)

where:

- γ_{Ff} is the partial factor applied to the load models;

- $\Delta\sigma_{E,2}$ is the equivalent constant amplitude stress range related to 2 millions cycles;
- $\Delta\sigma_c$ is the reference value of the fatigue strength at 2 millions cycles (detail category);
- γ_{Mf} is the partial factor for the fatigue strength.

A similar format is found for the shear verifications under fatigue as well as for the shear and direct stresses interactions. This guide is limited to the direct stresses verifications. It is of course essential to consider all verifications for an actual design.

The stress range $\Delta\sigma_{E,2}$ under FLM3 is given by:

EN1994-2, 6.8.6(2)

$$\Delta\sigma_{E,2} = \lambda\Phi\Delta\sigma_p = \lambda\Phi[\sigma_{\max,f} - \sigma_{\min,f}]$$

where λ is the damage equivalent factor,
and Φ is the damage equivalent impact factor.

EN1993-2, 9.5.2
EN1994-2, 6.8.6

Remark that EN1994-2 notes $\Delta\sigma_E$ for the stress range whereas EN1993-2 notes it $\Delta\sigma_{E,2}$. The second notation is adopted in this guidance book.

9.1.1 - Partial factors

The partial factor for the fatigue loads is taken as equal to $\gamma_{Ff} = 1.0$.

EN1993-2, 9.3

The partial factor for the fatigue strength in the structural steel bridge part is taken as equal to $\gamma_{Mf} = 1.35$.

*EN1993-1-9,
Table 3.1*

It corresponds to a fatigue verification following the safe life assessment method with high consequences of the detail failure for the bridge (see table in the paragraph 4.5 of this Part II).

9.1.2 - The fatigue load model

Feature of FLM3

The fatigue load model FLM3 is used to calculate the longitudinal internal forces and moments in the bridge. This is a single-vehicle model made up of 4 axles (120 kN per axle). It moves in the middle of the slow lanes defined in the design. The contact surface of each wheel is a square with sides of 0.40 m (see Figure 9.1).

EN1991-2, 4.6.4

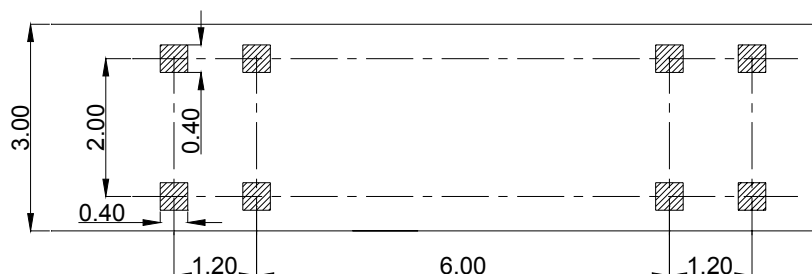


Figure 9.1: Vehicle of the fatigue load model FLM3

EN1991-2 provides for a possible second vehicle to better model the fatigue effects in the zones surrounding the internal supports (same geometry but with 36 kN per axle, and located at a distance which is not less than 40 m from the first vehicle). However the calibration of the equivalent stress ranges simplified method was performed with a single vehicle for each guiding Eurocode of a given design (EN1994-2 for the composite bridge in this book). Moreover the use of the second vehicle is subjected to the choice made in the National Annex of each European country.

EN1991-2, 4.6.4(3)

Number and location of the slow traffic lanes

Theoretically the design specifications should settle the number and the location of the slow traffic lanes on the bridge deck. As the deck has two traffic lanes in opposite directions for the example in this guide, two slow lanes are therefore considered for the calculations.

The location of these lanes has been chosen (for the design example) as corresponding to the actual painting marks on the pavement. This means here a transverse load distribution factor of 0.75 for the calculated main girder. This hypothesis should be individually considered for each bridge by foreseeing future traffic which could be different from the traffic retained in the design and which could induce a modification in the transverse distribution of the traffic lanes within the working life of the bridge.

As (safe-sided) alternative it could be envisaged to use Clause 4.6.1(4) in EN1991-2 as represented in Figure 9.2. The traffic lanes no 1 and 3 would then be the slow lanes.

EN1991-2, 4.6.1(4)

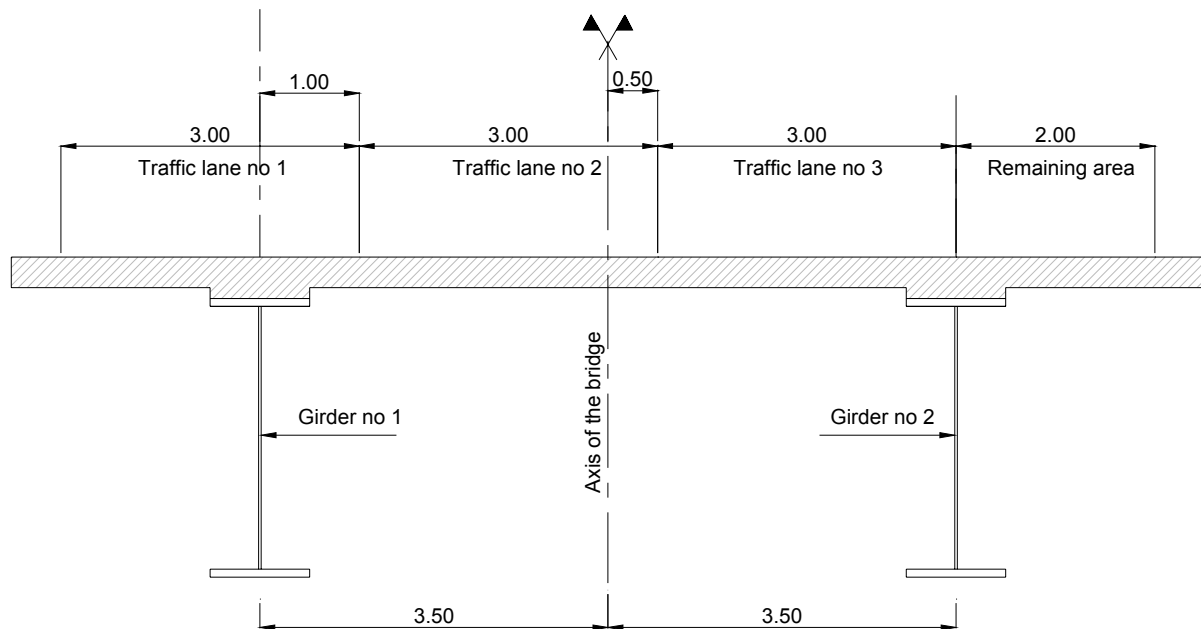


Figure 9.2: Possible location of the slow traffic lanes (no 1 and 3)

9.1.3 - Damage equivalent factor λ

The damage equivalent factor is given by:

$$\lambda = \prod_{i=1}^4 \lambda_i \leq \lambda_{\max}$$

EN1993-2, 9.5.2

a) Factor λ_1

The factor λ_1 takes into account the damage effects induced by the traffic volume following the length L of the influence line of the considered longitudinal internal force or moment in the deck. It also includes a « transit factor » from N_0 cycles per year to 2.10^6 cycles within 100 years.

Depending on the location of the studied cross-section and on the type of the internal force or moment, charts coming from EN1993-2 gives the corresponding value of λ_1 .

EN1993-2, Fig. 9.7

The following is obtained for the bending moment:

Location of the cross-section	Length of the influence line	Value of λ_1
In end-span	$L = 60 \text{ m}$	$2.55 - 0.7.(60-10)/70 = 2.05$
At internal support	$L = (60 + 80)/2 = 70 \text{ m}$	$1.70 + 0.5.(70-30)/50 = 2.10$
In central span	$L = 80 \text{ m}$	1.85

The following is obtained for the shear force:

Location of the cross-section	Length of the influence line	Value of λ_1
In end-span	$L = 0.4 \times 60 \text{ m}$	$2.55 - 0.7.(24-10)/70 = 2.41$
At internal support	$L = 80 \text{ m}$	2.20
In central span	$L = 0.4 \times 80 \text{ m}$	$2.55 - 0.7.(32-10)/70 = 2.33$

b) Factor λ_2

λ_2 accounts for the traffic composition:

$$\lambda_2 = \frac{Q_{m1}}{Q_0} \left(\frac{N_{obs}}{N_0} \right)^{\frac{1}{5}}$$

An indication of the number of heavy vehicles planned per year and per slow lane should be given in the Design Specifications. As this design example has no specifications, the guide is adopting the following hypothesis:

- A class 2 traffic (“roads and motorways with medium flow rates of lorries”). The indicative number of heavy vehicles for each slow lane is thus $N_{obs} = 0.5.10^6$;
- A long distance traffic composition defined for the Fatigue Load Model no. 4 (FLM4). The average gross weight Q_{m1} of the lorries per slow lane is therefore $Q_{m1} = 445 \text{ kN}$.

EN1991-2, 4.6
Table 4.5

EN1991-2, 4.6
Table 4.7

Remember that the bridge has two slow lanes here.

The reference values for Q_0 and N_0 are:

$Q_0 = 480 \text{ kN}$ (weight of FLM3) and $N_0 = 0.5.10^6$.

EN1993-2, 9.5.2(3)

This gives finally $\lambda_2 = 0.927$.

c) Factor λ_3

EN1993-2, 9.5.2(5)

The value of λ_3 follows the required design life of the structure. For a bridge this is generally 100 years and thus $\lambda_3 = 1.00$.

d) Factor λ_4

λ_4 takes into account the effects of the heavy traffic on the other additional slow lanes defined in the design. In the case of a single slow lane, $\lambda_4 = 1.0$. In the present case, the factor depends on the transverse influence of each slow lane on the internal forces and moments in the main girders:

$$\lambda_4 = \left[1 + \frac{N_2}{N_1} \left(\frac{\eta_2 Q_{m2}}{\eta_1 Q_{m1}} \right)^5 \right]^{\frac{1}{5}}$$

EN1993-2, 9.5.2(6)

$$\eta = \frac{1}{2} - \frac{e}{b} \text{ with:}$$

- e : eccentricity of the FLM3 load with respect to the bridge deck axis (in the example ± 1.75 m);
- b : distance between the main girders (in the example 7.0 m).

$$\eta_1 = \frac{1}{2} + \frac{1.75}{7.0} = 0.75 \text{ and } \eta_2 = \frac{1}{2} - \frac{1.75}{7.0} = 0.25 \text{ are deduced. The factor } \eta_1$$

represents the maximum influence of the transverse location of the traffic slow lanes on the fatigue-verified main girder. $N_1 = N_2$ (so many heavy vehicles in each slow lane) and $Q_{m1} = Q_{m2}$ (same type of lorry in each slow lane) will be considered here.

This gives finally $\lambda_4 = 1.0$.

e) Factor λ_{\max}

EN1993-2, 9.5.2(7)

For the bending moment, the product $\lambda = \prod_{i=1}^4 \lambda_i$ should remain lower than the maximum value λ_{\max} given by the table below (and obtained by reading charts from EN 1993-2).

Location of the cross-section	Length of the influence line	Value of λ_{\max}
In end-span	$L = 60$ m	2.0
At internal support	$L = (60 + 80)/2 = 70$ m	$1.80 + 0.90 \cdot (70-30)/50 = 2.52$
In central span	$L = 80$ m	2.0

For the shear force, EN1993-2 does not define a limit value.

For the guide example, this λ_{\max} has no influence and the damage equivalent factor is given by the following values for a detail located:

- in end-span (between 0 and $0.85 \cdot L_1 = 51$ m or between 149 m and 200 m): $\lambda = 1.9$
- at internal support (between $0.85 \cdot L_1 = 51$ m and $L_1 + 0.15 \cdot L_2 = 72$ m or between 128 m and 149 m): $\lambda = 1.947$
- in central span (between 72 m and 128 m): $\lambda = 1.715$

EN1993-2, Fig. 9.7

9.1.4 - Damage equivalent impact factor Φ

A factor $\Phi = 1$ is adopted for road bridges. The dynamic effects are directly included in the calibration of the FLM3 axle loads. EN1994-2, 6.8.6.1(7)

However Φ is increased when crossing an expansion joint: EN1991-2, 4.6.1(6)

$$\Phi = 1.3 \left[1 - \frac{D}{26} \right] \geq 1.0$$

where D (in m) is the distance between the detail verified for fatigue and the expansion joint (with $D \leq 6$ m).

9.1.5 - Stress range $\Delta\sigma_p$

a) Calculation of the internal forces and moments

The internal forces and moments are calculated by an elastic global analysis. The analysis is performed under the same conditions as the ones used to verify the bridge design under basic traffic loads, by considering the cracked zones around internal supports (see chapter 7 of this Part II of the guide). The calculation of the internal forces and moments is performed using the basic SLS combination of the non-cyclic loads to which the fatigue load is added. EN1994-2, 5.4.1 and 5.4.2

EN1992-1-1, 6.8.3

The basic traffic loads (LM1) are classified as cyclic loads and should not therefore be considered in this basic combination. The only non-cyclic variable load to take into account is the thermal action with a coefficient $\gamma_{1,1}$ then worth 0.6: EN1990, Annex A.2

$G_{k,sup}$ (or $G_{k,inf}$) + (1 or 0) $S + 0.6 T_k$
(see paragraph 6.2 for the notations).

Figure 9.3 illustrates the bending moment envelope corresponding to this basic combination of non-cyclic loads. EN1990, Annex A.2

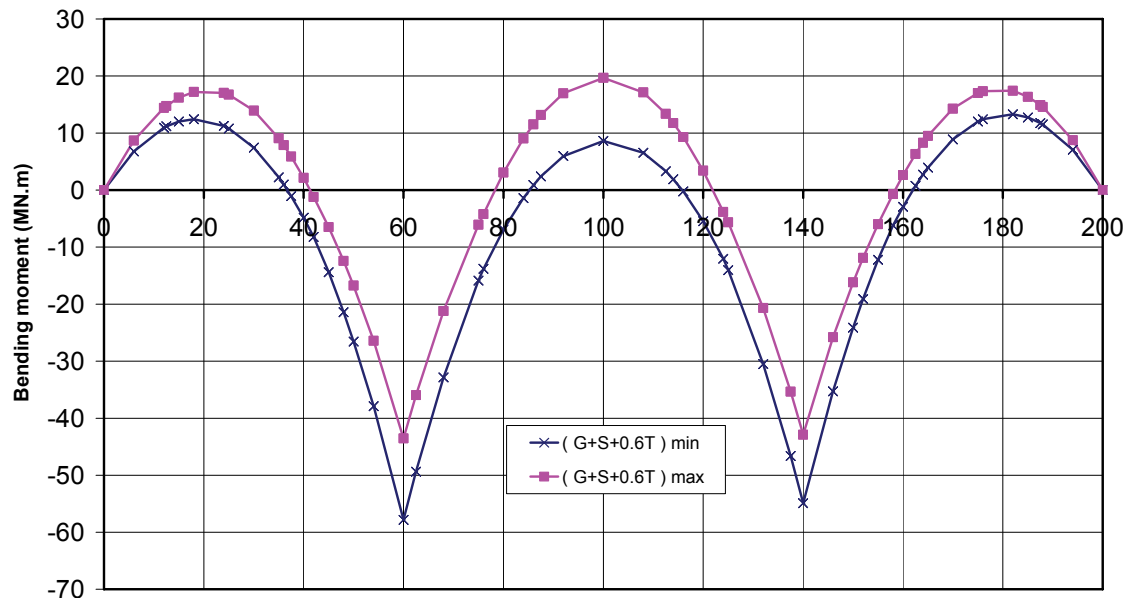


Figure 9.3 : Bending moments for the basic combination of non-cyclic loads

A variation of the internal forces and moments in the bridge under the fatigue load model crossing is added to this basic combination of self-weight and possibly thermal action:

$$[G_{k,sup} \text{ (or } G_{k,inf}) + (1 \text{ or } 0) S + 0.6 T_k] + \text{FLM3}$$

The basic combination of non-cyclic loads should therefore not be considered as an envelope, but as a given state of internal forces and moments in the bridge deck under permanent loads.

Figure 9.4 (resp. 9.5) below illustrates the bending curves $M_{Ed,min,f}$ and $M_{Ed,max,f}$ obtained by the fatigue load model FLM3 crossing. The FLM3 effect is added to the maximum (resp. minimum) bound of the envelope given in Figure 9.3.

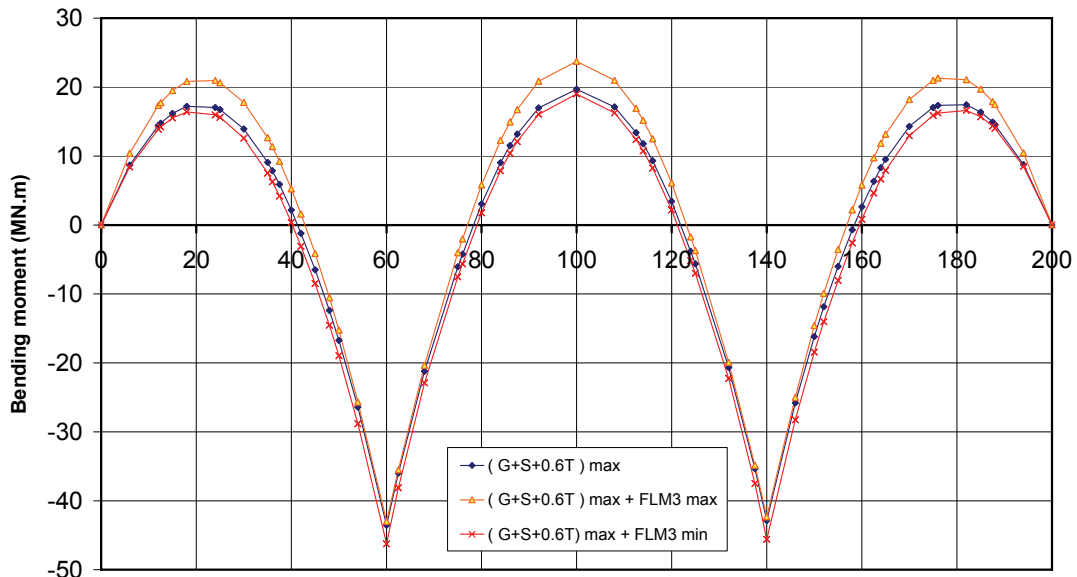


Figure 9.4: Bending moments for the basic combination (maximum value) and FLM3

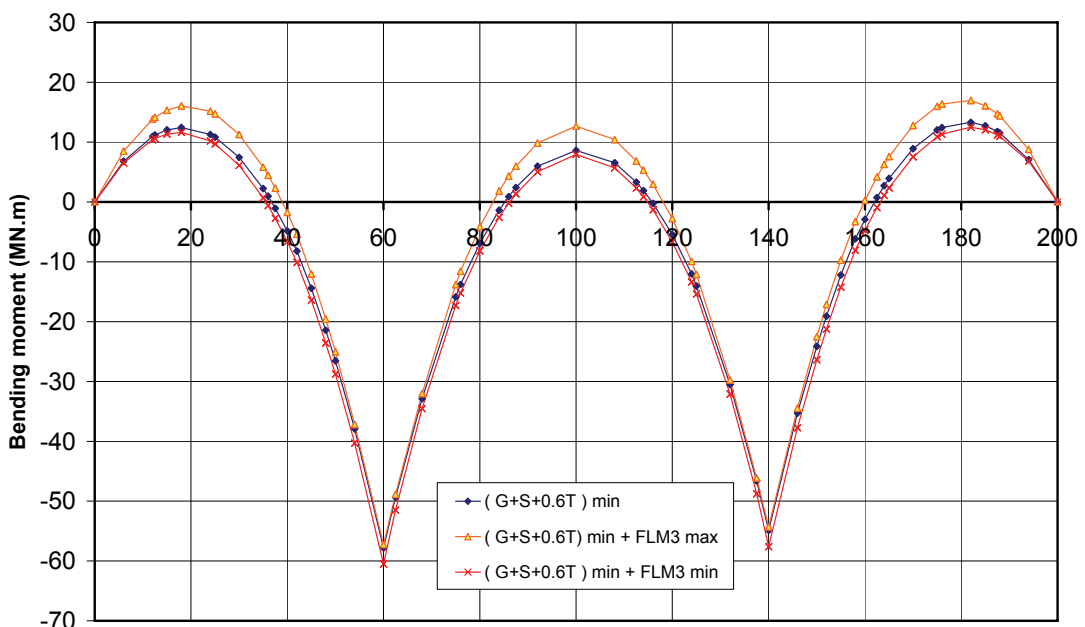


Figure 9.5: Bending moments for the basic combination (minimum value) and FLM3

b) Calculation of stresses

The stress range $\Delta\sigma_p$ is obtained by $\Delta\sigma_p = |\sigma_{\max,f} - \sigma_{\min,f}|$ where the stresses $\sigma_{\max,f}$ and $\sigma_{\min,f}$ are calculated from $M_{Ed,max,f}$ and $M_{Ed,min,f}$ with the short-term modular ratio $n_0 = 6.16$. To simplify the calculations, the self-equilibrated stresses (primary or isostatic effects) due to shrinkage and thermal action are neglected.

Respecting the sign conventions adopted in EN1994-2, 6.8, the bending moment $M_{Ed,max,f}$ is defined as the one which generates the maximum tensile force in the slab.

Three different situations are considered for the stresses calculations:

- 1st case

EN1994-2, 6.8.5.3

$M_{Ed,min,f}$ and $M_{Ed,max,f}$ cause tensile stresses in the concrete slab. The stresses are then written:

$$\sigma_{\max,f} = M_{a,Ed} \frac{V_a}{I_a} + M_{c,Ed} \frac{V_2}{I_2} + M_{FLM3,max} \frac{V_2}{I_2}$$

$$\sigma_{\min,f} = M_{a,Ed} \frac{V_a}{I_a} + M_{c,Ed} \frac{V_2}{I_2} + M_{FLM3,min} \frac{V_2}{I_2}$$

by breaking down $M_{Ed,max,f}$ (resp. $M_{Ed,min,f}$) into $M_{a,Ed} + M_{c,Ed} + M_{FLM3,max}$ (resp. $M_{FLM3,min}$). $M_{a,Ed}$ is resisted by the structural steel cross-section only; $M_{a,Ed} + M_{c,Ed}$ gives the bending moment for the basic combination of non-cyclic loads and $M_{c,Ed}$ is resisted by the composite cracked cross-section; and lastly $M_{FLM3,max}$ (resp. $M_{FLM3,min}$) is due to the FLM3 crossing and is resisted by the composite cracked cross-section.

Finally the stress range is given by:

$$\Delta\sigma_p = \Delta M_{FLM3} \cdot \frac{V_2}{I_2}$$

In this first case the stress range is independent of the stress distribution for the basic combination of non-cyclic loads.

- 2nd case

$M_{Ed,min,f}$ and $M_{Ed,max,f}$ cause compression in the concrete slab. The stresses are then written:

$$\sigma_{\max,f} = M_{a,Ed} \frac{V_a}{I_a} + M_{c,Ed} \frac{V_1}{I_1} + M_{FLM3,max} \frac{V_1}{I_1}$$

$$\sigma_{\min,f} = M_{a,Ed} \frac{V_a}{I_a} + M_{c,Ed} \frac{V_1}{I_1} + M_{FLM3,min} \frac{V_1}{I_1}$$

Finally the stress range is given by:

$$\Delta\sigma_p = \Delta M_{FLM3} \cdot \frac{V_1}{I_1}$$

In this second case the stress range is also independent of the stress distribution for the basic combination of non-cyclic loads.

- 3rd case

$M_{Ed,max,f}$ causes tensile stresses in the concrete slab and $M_{Ed,min,f}$ causes compression in the concrete slab. The stresses are then written:

$$\sigma_{\max,f} = M_{a,Ed} \frac{V_a}{I_a} + M_{c,Ed} \frac{V_2}{I_2} + M_{FLM3,max} \frac{V_2}{I_2}$$

$$\sigma_{\min,f} = M_{a,Ed} \frac{V_a}{I_a} + M_{c,Ed} \frac{V_1}{I_1} + M_{FLM3,min} \frac{V_1}{I_1}$$

Finally the stress range is given by:

$$\Delta\sigma_p = M_{c,Ed} \left[\frac{V_2}{I_2} - \frac{V_1}{I_1} \right] + M_{FLM3,max} \frac{V_2}{I_2} - M_{FLM3,min} \frac{V_1}{I_1}$$

In this third case the stress range depends on the stress distribution for the basic combination of non-cyclic loads.

The stress range should therefore be calculated for each envelope bound of the basic non-cyclic loads combination. It should also be noticed that the calculation of $M_{Ed,min,f}$ and $M_{Ed,max,f}$ has to be performed by only taking into account the hyperstatic (or secondary) effect of shrinkage.

Notes:

I_a / V_a is the elastic section modulus of the structural steel cross-section only.

I_1 / V_1 is the elastic section modulus of the uncracked composite cross-section (with $n_{eq} = n_0$).

I_2 / V_2 is the elastic section modulus of the cracked composite cross-section.

In this guide it is assumed that $M_{Ed,max,f}$ causes tensile stresses (resp. compression) in the concrete slab when the share of $M_{Ed,max,f}$ which is resisted by the slab (i.e. $M_{c,Ed,max,f} = M_{c,Ed} + M_{FLM3,max}$) is negative (resp. positive). Ditto for $M_{Ed,min,f}$.

Figures 9.6 to 9.9 illustrate the normal stress range $\Delta\sigma_p$ along the bridge, for the upper and lower faces of both structural steel flanges. In these figures the index 1 (resp. 2) indicates that the calculation has been performed with the minimum (resp. maximum) value of the bending moment for the basic non-cyclic loads combination. The curves $\Delta\sigma_0$ corresponding to a calculation performed with a fully cracked cross-section (envelope case) have also been drawn in these figures (see 1st case above).

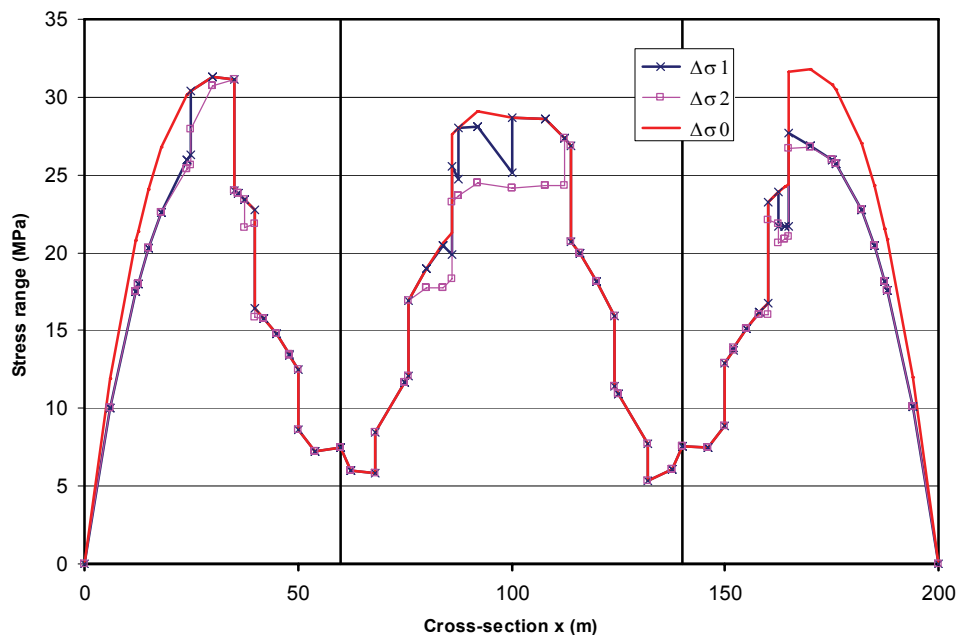


Figure 9.6: Stress range for the upper face of the lower flange

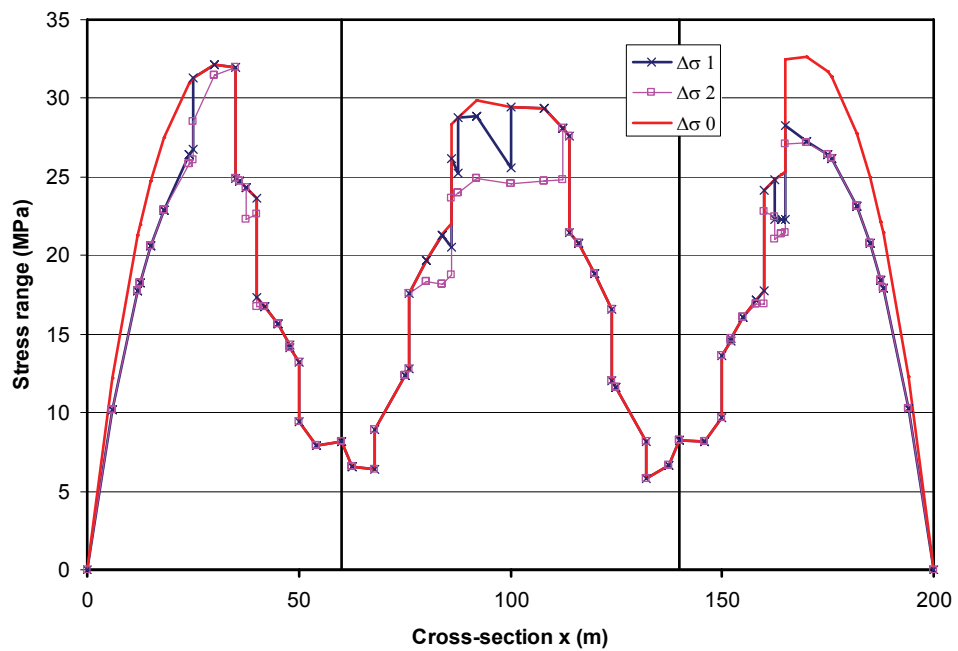


Figure 9.7: Stress range for the lower face of the lower flange

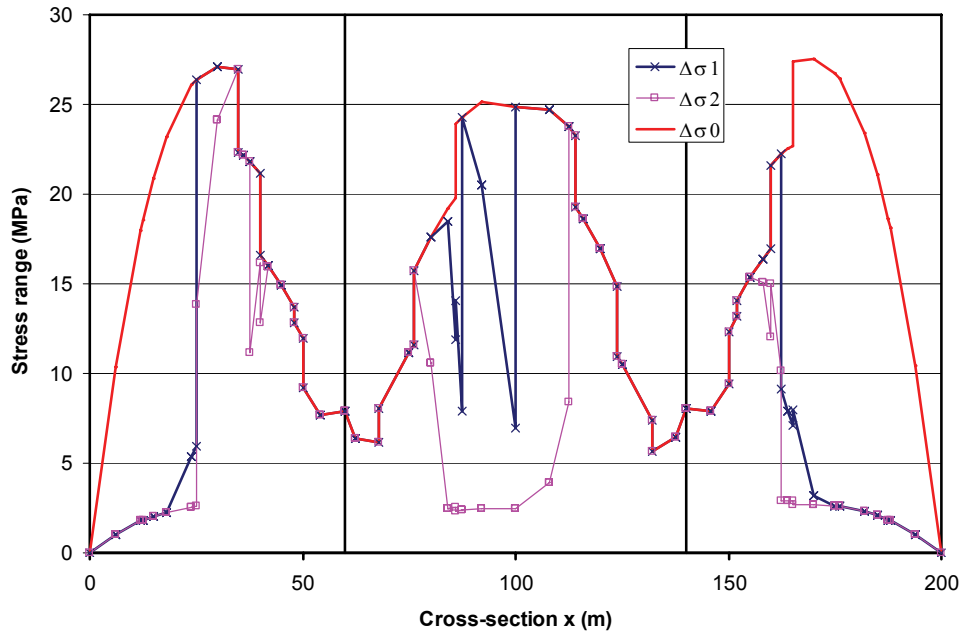


Figure 9.8: Stress range for the upper face of the upper flange

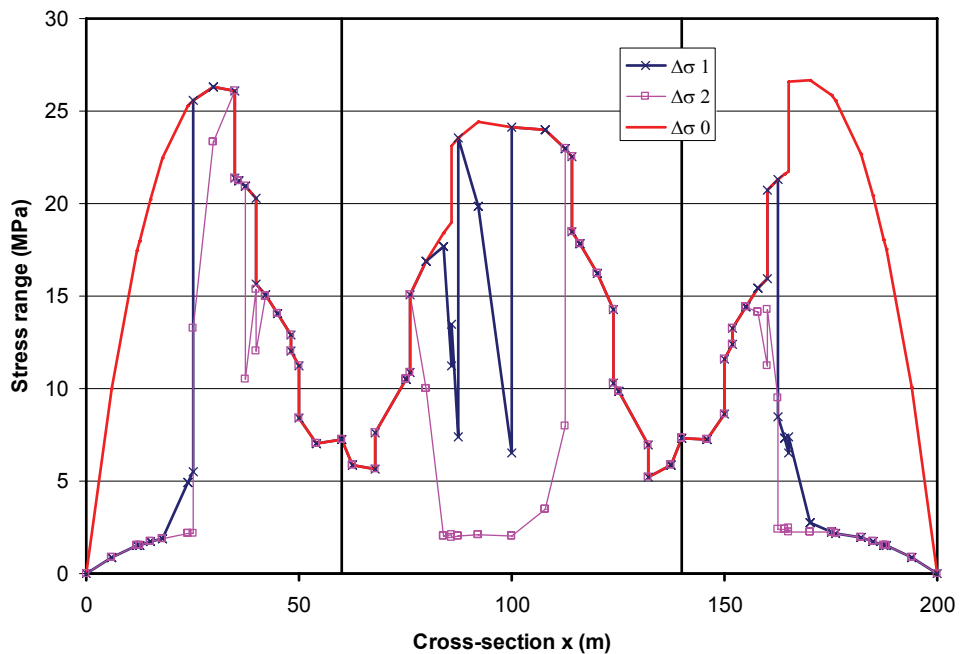


Figure 9.9: Stress range for the lower face of the upper flange

c) Taking account of the tension stiffening in the concrete slab

The previous calculations have been performed by neglecting the effect of the tension stiffening for the determination of stresses in the structural steel, as allowed in EN1994-2. However it can be interesting to take this favorable effect into account, chiefly for the fatigue verification of the upper steel flange at mid-span.

EN1994-2, 6.8.5.1(4)

By using the same principles as for the reinforcing steel verification (see paragraphs 9.2.2 and 10.4.3 of this Part II), it is possible to prove that taking the tension stiffening effect into account gives the following stresses in the structural steel:

$$\sigma_y = \sigma_{y,0} + \beta \frac{f_{ctm}}{\rho_s} \left[\frac{A_s y_s y}{I} + \frac{A_s}{A} \right]$$

In this equation $\sigma_{y,0}$ is the normal stress in the structural steel at a vertical distance y from the centre of gravity of the cracked composite cross-section, and calculated by neglecting the tension stiffening effect. Figure 10.10 will be referred to for the other notations. The sign conventions are here $\sigma > 0$ in case of compression.

By noting $\alpha_{st} = \frac{A/I}{A_a I_a}$ and $\Delta\sigma_s = \beta \frac{f_{ctm}}{\rho_s \alpha_{st}}$ (see also paragraph 9.2.2) the previous equation can also be rewritten as:

$$\sigma_y = \sigma_{y,0} + \Delta\sigma_s \left[\frac{A_s}{A_a} + \frac{A_s a}{I_a} y_a \right]$$

where y_a indicates the vertical position of the studied fibre with respect to the centre of gravity of the structural steel cross-section, and a is the distance between the baric centre of the reinforcing steel bars and the centre of gravity of the structural steel cross-section.

EN1994-2, 6.8.5.4(1)

The value $\beta = 0.2$ should be adopted for fatigue calculations.

Let us detail this calculation for the upper face of the upper steel flange at the abscissa $x = 30$ m within the 3rd slab segment in the end-span. This involves a cross-section where $M_{Ed,min,f}$ and $M_{Ed,max,f}$ cause tensile stresses in the concrete slab (1st case).

Calculation without tension stiffening

$$M_{c,Ed} = -7.27 \text{ MN.m}$$

$$M_{FLM3,min} = -1.33 \text{ MN.m} \text{ and } M_{c,Ed,min,f} = -7.27 - 1.33 = -8.60 \text{ MN.m}$$

$$M_{FLM3,max} = +3.83 \text{ MN.m} \text{ and } M_{c,Ed,max,f} = -7.27 + 3.83 = -3.44 \text{ MN.m}$$

$$\sigma_{y,min,f,0} = M_{c,Ed,min,f} \frac{V_2}{I_2} = -45 \text{ MPa, stress caused by } M_{c,Ed,min,f}$$

$$\sigma_{y,max,f,0} = M_{c,Ed,max,f} \frac{V_2}{I_2} = -18 \text{ MPa, stress caused by } M_{c,Ed,max,f}$$

$$\Delta\sigma_p = -18 + 45 = 27 \text{ MPa (see curve } \Delta\sigma_1 \text{ in Figure 9.8)}$$

Calculation with tension stiffening

All calculations done (see Figure 9.12), $\Delta\sigma_s = 49.6$ MPa and then:

$$\Delta\sigma_s \left[\frac{A_s}{A_a} + \frac{A_s a}{I_a} y_a \right] = 18 \text{ MPa}$$

This gives:

$$\sigma_{y,min,f} = \sigma_{y,min,f,0} + 18 = -45 + 18 = -27 \text{ MPa}$$

$$\sigma_{y,max,f} = \sigma_{y,min,f} \frac{M_{c,Ed,max,f}}{M_{c,Ed,min,f}} = -27 \frac{(-3.44)}{(-8.60)} = -11 \text{ MPa}$$

$$\Delta\sigma_p = -11 + 27 = 16 \text{ MPa}$$

The stress range has therefore moved from 27 MPa to 16 MPa thanks to the tension stiffening effect. The cross-section at the abscissa $x = 30$ m is then verified for fatigue.

Taking the favorable effect of the tension stiffening into account is only valid when the slab is cracked for both bending moments $M_{c,Ed,max,f}$ and $M_{c,Ed,min,f}$.

9.1.6 - Reference values of the fatigue strength

To each detail category corresponds a fatigue strength curve S-N. The curves are characterised by the value $\Delta\sigma_c$ which corresponds to the fatigue strength after 2 millions cycles for a specific detail.

Each construction detail figures in Tables 8.1 to 8.9 of EN1993-1-9. There is a description of the detail and the related requirements (particularly the size effects). Some detail categories take account of size effects via a reduction factor

$$k_s = \sqrt[5]{\frac{25}{t}} \text{ for the plate thicknesses } t \geq 25 \text{ mm.}$$

EN1993-1-9, Tables 8.1 to 8.9

This stress reduction applies to the details with transverse butt welds perpendicular to the direction of normal stresses (see Figure 9.10). The detail is then verified against the reduced category $\Delta\sigma_{c,red} = k_s \Delta\sigma_c$.

The main details encountered along a two-girder composite bridge are summarized in Figure 9.10.

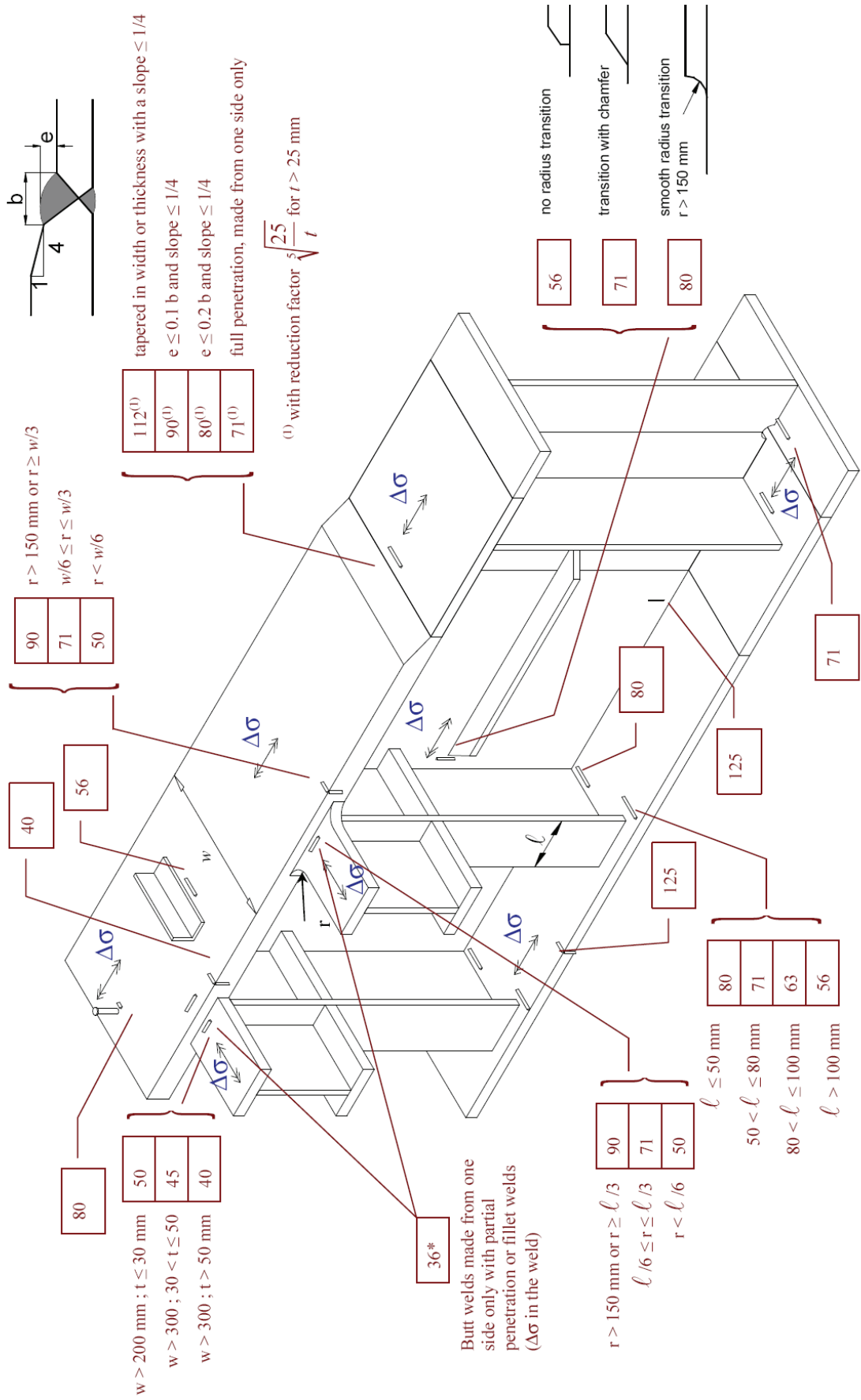


Figure 9.10: Usual detail categories in a two-girder composite bridge (in MPa)

9.1.7 - Verification of the structural steel bridge part under fatigue

At every singular point (joint) in the structural steel structure is associated a given detail category $\Delta\sigma_c$ for which should be verified:

$$\gamma_{Ff} \Delta\sigma_{E,2} \leq \frac{\Delta\sigma_c}{\gamma_{Mf}} \text{ where } \Delta\sigma_{E,2} = \lambda \varphi \Delta\sigma_p \text{ with } \Delta\sigma_p \text{ given by Figures 9.6 to 9.9.}$$

EN1993-2, 9.5.1(1)

For example:

- Studs welded on the upper steel flange:

The maximum stress range on the upper face of the upper steel flange is given by $\Delta\sigma_{E,2} = 1.9 \times 1 \times 27.1 = 51.5 \text{ MPa}$ at the abscissa $x = 30 \text{ m}$ which is still less than $\frac{\Delta\sigma_c}{\gamma_{Mf}} = 80/1.35 = 59.3 \text{ MPa}$.

- Transverse weld of the vertical T-shaped stiffener web on the lower steel flange:

The maximum stress range is given by $\Delta\sigma_{E,2} = 1.9 \times 1 \times 31.3 = 59.5 \text{ MPa}$ (achieved on the upper face of the lower flange at the abscissa $x = 30 \text{ m}$ for the 4th cross girder in the end-span) which is just equal to $\frac{\Delta\sigma_c}{\gamma_{Mf}} = 80/1.35 = 59.3 \text{ MPa}$.

- Butt weld in the lower flange for the change in thickness from 55 mm to 80 mm at the abscissa $x = 40 \text{ m}$:

The stress range is then given by $\Delta\sigma_{E,2} = 1.9 \times 1 \times 23.6 = 44.8 \text{ MPa}$ which is still less than:

$$\frac{\Delta\sigma_{c,red}}{\gamma_{Mf}} = \frac{\Delta\sigma_c}{\gamma_{Mf}} \left(\frac{25}{t} \right)^{0.2} = \frac{90}{1.35} \left(\frac{25}{55} \right)^{0.2} = 56.9 \text{ MPa}$$

This kind of verification under normal stresses should be performed for all the details encountered in the structure. The designer is also reminded that similar verifications also exist for the shear stresses.

9.2 - Verification of the longitudinal reinforcement

The fatigue verification of the longitudinal reinforcement involves justifying a similar criterion as used for the structural steel structure (and therefore assuming the use of the fatigue load model FLM3):

$$\gamma_{F,fat} \Delta \sigma_{S,eq} (N^*) \leq \frac{\Delta \sigma_{Rsk} (N^*)}{\gamma_{S,fat}}$$

where:

- $N^* = 10^6$ cycles;
- $\Delta \sigma_{Rsk} (N^*) = 162.5$ MPa, stress range for N^* cycles (straight and bent bars);
- $\gamma_{F,fat} = 1.0$ is the partial factor applied to the load model FLM3;
- $\gamma_{S,fat} = 1.15$ is the partial factor for the material;
- $\Delta \sigma_{S,eq} (N^*) = \lambda_s |\sigma_{s,max,f} - \sigma_{s,min,f}|$ is the equivalent constant amplitude normal stress range in reinforcement.

λ_s is the damage equivalent factor for the reinforcement. EN1994-2, 6.8.6.1(5) refers to Annex NN in EN1992-2 to calculate it. In this annex, the calibration of λ_s has been performed assuming a long-distance traffic type with static loads corresponding to a given traffic. This traffic can be modeled by the axles of the fatigue load model 3 multiplied by 1.75 in the support zones and by 1.40 in span.

To be coherent with the calculation of λ_s , the stresses $\sigma_{s,max,f}$ and $\sigma_{s,min,f}$ are calculated following EN1994-2, 6.8.5.4, by using the bending moments $M_{Ed,min,f}$ and $M_{Ed,max,f}$. These moments have been obtained from the bounds (maximum or minimum) of the envelope representing the basic combination of non-cyclic loads to which the crossing of FLM3 (multiplied by 1.75 or 1.40 following the zones) is added.

9.2.1 - Damage equivalent factor λ_s

The damage equivalent factor is given by:

$$\lambda_s = \varphi_{fat} \prod_{i=1}^4 \lambda_{s,i}$$

The calibration of the factor $\lambda_{s,1}$ is performed by using the static loads. So the global equation for λ_s takes into account the dynamic effect of the loads by using φ_{fat} . According to the annex B in EN1991-2, φ_{fat} is equal to 1.2 or 1.4 following the roughness quality of the pavement layer.

This approach differs from that of EN1993-2 where the dynamic effect ϕ is assumed to be included in the axle load of FLM3 used to calibrate the factor λ_1 . For the design example, a good roughness and a value $\varphi_{fat} = 1.2$ are adopted.

a) Factor $\lambda_{s,1}$

Just as λ_1 , $\lambda_{s,1}$ takes into account the damage effects due to the traffic volume according to the length L of the influence line for the longitudinal bending moment.

Reading the Figures NN.1 and NN.2 gives:

EN1994-2, 6.8.3(2)
which refers to
EN1992-1-1, 6.8.5

EN1992-1-1, 6.8.4,
Table 6.3N

EN1992-1-1, 6.8.4(1)
EN1992-1-1,
2.4.2.4(1)

EN1992-1-1, Annex
NN2.1 (101)

EN1992-2, Annex
NN.2 (103)

EN1992-2,
NN.2 (108)

EN1992-2, Figures
NN.1 and NN.2

Location of the cross-section	Length of the influence line	Value of $\lambda_{s,1}$
In end-span	$L = 60 \text{ m}$	1.21
At internal support	$L = (60 + 80)/2 = 70 \text{ m}$	1.19
In central span	$L = 80 \text{ m}$	1.25

Despite an identical traffic volume and spans, very different values are obtained for λ_1 and $\lambda_{s,1}$. As indicated in the introduction to this paragraph 9.2, this is explained by the use of various loads to calibrate the charts. The weight factors 1.75 and 1.4 of EN1992 are found elsewhere in our results:

EN1992-2,
NN.2 (101)

In central span: $\lambda_1 / \lambda_{s,1} = 1.85 / 1.25 = 1.48$

At support: $\lambda_1 / \lambda_{s,1} = 2.1 / 1.19 = 1.76$

b) Factor $\lambda_{s,2}$

Just as λ_2 , $\lambda_{s,2}$ accounts for the traffic composition:

EN1992-2,
NN.2 (105)

$$\lambda_{s,2} = \bar{Q} \cdot \sqrt[k_2]{\frac{N_{\text{obs}}}{2 \cdot 10^6}}$$

k_2 is the slope of the S-N curve beyond N^* cycles: $k_2 = 9$

EN1992-1-1,
Table 6.3N

N_{obs} and \bar{Q} represent the traffic volume. The traffic hypotheses from the design specifications, already used for the structural steel verification, are reapplied:

- $N_{\text{obs}} = 0.5 \cdot 10^6$ heavy vehicles per year and per slow lane,
- $\bar{Q} = 1$ (long-distance traffic).

EN1992-2,
Table NN.1

Ultimately, the following is obtained: $\lambda_{s,2} = 0.857$.

c) Factor $\lambda_{s,3}$

EN1992-2,
NN.2 (106)

$\lambda_{s,3} = 1.0$ for a required design life of 100 years (bridge case).

d) Factor $\lambda_{s,4}$

EN1992-2,
NN.2 (107)

Just as λ_4 , $\lambda_{s,4}$ takes into account the effects of the heavy traffic on the other slow lanes defined in the design:

$$\lambda_{s,4} = \sqrt[k_2]{\frac{\sum N_i}{N_1}} = \sqrt[9]{1 + \frac{N_2}{N_1}} = 1.08$$

for two slow lanes with the same traffic.

Remark that $\lambda_{s,4} \geq \lambda_4$ because the favorable effect of the transverse load distribution is no longer considered.

e) Synopsis

For the example in the guide, the damage equivalent factor λ_s is given by the following values for a detail located:

- in end span (between 0 and 51 m or between 149 m and 200 m): $\lambda_s = 1.344$;
- at internal support (between 51 m and 72 m or between 128 m and 149 m): $\lambda_s = 1.322$;
- in central span (between 72 m and 128 m): $\lambda_s = 1.388$.

9.2.2 - Stress range $\Delta\sigma_{s,p}$

The stress range is given by $\Delta\sigma_{s,p} = |\sigma_{s,max,f} - \sigma_{s,min,f}|$ where the stresses $\sigma_{s,max,f}$ and

*EN1992-2,
NN2.1 (101)*

$\sigma_{s,min,f}$ are calculated with the short-term modular ratio $n_0 = 6.16$ and from the bending moments $M_{Ed,min,f}$ and $M_{Ed,max,f}$. These moments have been obtained from the bounds (maximum or minimum) of the envelope representing the basic combination of non-cyclic loads (see Figure 9.3) to which the crossing of the FLM3 load model (multiplied by 1.75 in the support zones and by 1.40 elsewhere) is added.

Remember that the maximum moment $M_{Ed,max,f}$ is the one that generates the maximum tensile force in the slab.

As for the structural steel verification, three scenarios should be considered:

- 1st case

$M_{Ed,max,f}$ and $M_{Ed,min,f}$ cause tensile stress in the slab (cracked concrete). The stresses in the reinforcement are then written:

$$\sigma_{s,max,f} = \sigma_{s,max,f,0} + \Delta\sigma_{s,f}$$

EN1994-2, 6.8.5.4(1)

$$\text{with } \Delta\sigma_{s,f} = 0.2 \frac{f_{ctm}}{\alpha_{st}\rho_s} \text{ and } \alpha_{st} = \frac{A}{A_a I_a}$$

$\sigma_{s,max,f,0}$ is the stress in reinforcement that has been calculated from $M_{Ed,max,f} = M_{a,Ed,max,f} + M_{c,Ed,max,f}$ by neglecting the tension stiffening effect in the

$$\text{cross-section resistance: } \sigma_{s,max,f,0} = M_{c,Ed,max,f} \frac{V_2}{I_2}.$$

$\Delta\sigma_{s,f}$ represents the tension stiffening effect of the tensile concrete between the cracks. This term is the equivalent (for the fatigue verification) of the term explained for the SLS verifications of a composite cross-section (see chapter 10 of this Part II). A and I (resp. A_a and I_a) are the area and the second moment of area of the effective cracked composite cross-section (resp. of the structural steel cross-section only). ρ_s is the ratio (in %) of the longitudinal reinforcement area divided by the effective concrete slab area.

EN1994-2, 6.8.5.4(2)

Figure 9.12 shows the values taken by the term $\Delta\sigma_{s,f}$ along the bridge.

The stress $\sigma_{s,min,f}$ is obtained from Figure 9.11 by considering the tension stiffening effect of the concrete slab between the cracks which is proportional to $\Delta\sigma_{s,f}$ calculated for $\sigma_{s,max,f}$.

$$\sigma_{s,min,f} = \sigma_{s,min,f,0} + \frac{M_{c,Ed,min,f}}{M_{c,Ed,max,f}} \Delta\sigma_{s,f}$$

or:

$$\sigma_{s,min,f} = \sigma_{s,max,f} \frac{M_{c,Ed,min,f}}{M_{c,Ed,max,f}}$$

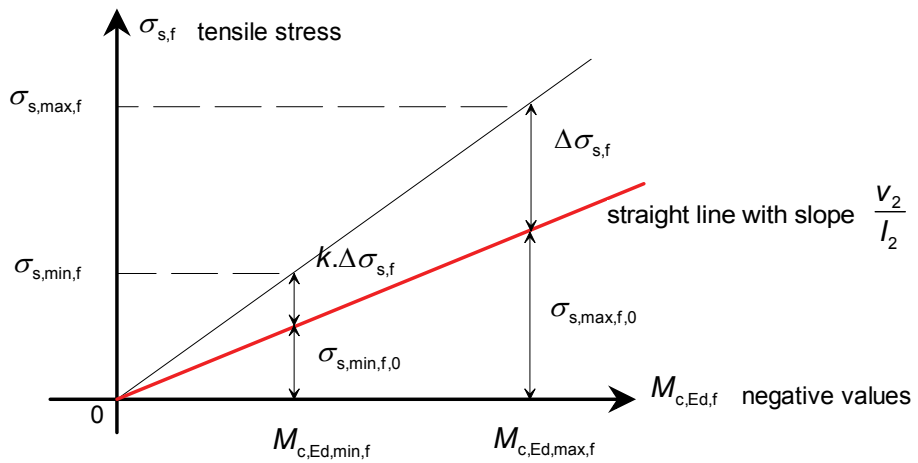


Figure 9.11: Calculation of the stress $\sigma_{s,min,f}$

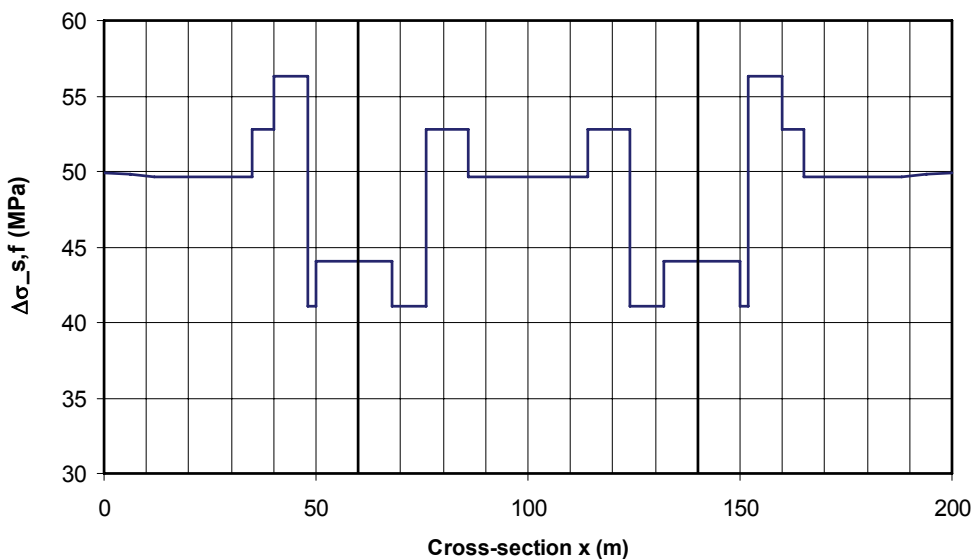


Figure 9.12: Variation of $\Delta\sigma_{s,f}$ along the two-girder bridge

- 2nd case

$M_{Ed,max,f}$ and $M_{Ed,min,f}$ cause compression in the slab. The stresses in the reinforcement are then written:

$$\sigma_{s,max,f} = M_{c,Ed,max,f} \frac{V_1}{I_1}$$

$$\sigma_{s,min,f} = M_{c,Ed,min,f} \frac{V_1}{I_1}$$

EN1994-2, 6.8.5.4(3)

Through difference $\sigma_{s,max,f} - \sigma_{s,min,f}$, the influence of the non-cyclic loads basic combination disappears and all that remains is the term due to the FLM3 load model calculated with $n_{eq} = 6.16$:

$$\Delta\sigma_{s,p} = \Delta M_{FLM3} \frac{V_1}{I_1}$$

- 3rd case

$M_{Ed,max,f}$ causes tensile stress in the slab and $M_{Ed,min,f}$ causes compression in the slab. The stresses in the reinforcement are then written:

$$\sigma_{s,max,f} = \sigma_{s,max,f,0} + \Delta\sigma_{s,f} \text{ as in the 1st case,}$$

$$\sigma_{s,min,f} = M_{c,Ed,min,f} \frac{V_1}{I_1} \text{ as in the 2nd case.}$$

The term $\Delta\sigma_{s,f}$ is therefore far less favorable than in the first case as its value is applied in full in the stress range $\Delta\sigma_{s,p}$.

9.2.3 - Verification of the reinforcing steel bars under fatigue

As for the cross-section analysis in chapter 8 of this guide, the check of reinforcements under fatigue (upper layer only in the context of this guide) is dealt with for two cross-sections, at internal support P1 and at mid-central span.

a) Cross-section at internal support P1

This cross-section is located in the cracked zone from the global analysis, inside the second-to-last slab concreting segment. For the non-cyclic loads basic combination, the reinforcing steel bars are subjected in the extreme cases to $M_{c,min} = -9.14 \text{ MN.m}$ or $M_{c,max} = 23.61 \text{ MN.m}$.

From these moments, the crossing of the fatigue load model FLM3 (multiplied by $0.75 \times 1.75 = 1.3125$ to take account of the transverse location of the slow lane compared with the main girder axis and the use conditions of charts in EN1992-2, Annex NN) adds $M_{FLM3,max} = -4.67 \text{ MN.m}$ or $M_{FLM3,min} = 0.99 \text{ MN.m}$. Thus the following bending moments in the reinforcing steel bars are ultimately obtained:

- case A:

$$M_{c,Ed,max,f} = -23.61 - 4.67 = -28.28 \text{ MN.m}$$

$$M_{c,Ed,min,f} = -23.61 + 0.99 = -22.62 \text{ MN.m}$$

- case B:

$$M_{c,Ed,max,f} = -9.14 - 4.67 = -13.81 \text{ MN.m}$$

$$M_{c,Ed,min,f} = -9.14 + 0.99 = -8.15 \text{ MN.m}$$

All these moments are negative and the stress calculations in the reinforcing steel bars are therefore performed with the cracked composite mechanical properties. In the remainder of the guide, the used values are those of case A. A similar calculation can be performed with the bending moments from case B.

$$\sigma_{s,max,f,0} = M_{c,Ed,max,f} \frac{V_2}{I_2} = -28.28 \times \frac{V_2}{I_2} = -86.9 \text{ MPa}$$

The tension stiffening effect is given by $\Delta\sigma_{s,f} = 44.0 \text{ MPa}$ in this cross-section at P1 (see Figure 9.12).

$$\sigma_{s,max,f} = \sigma_{s,max,f,0} + \Delta\sigma_{s,f} = -86.9 - 44.0 = -130.9 \text{ MPa}$$

$$\sigma_{s,min,f,0} = M_{c,Ed,min,f} \frac{V_2}{I_2} = -22.62 \times \frac{V_2}{I_2} = -69.5 \text{ MPa}$$

Using Figure 9.11 it is deduced:

$$\sigma_{s,min,f} = \sigma_{s,min,f,0} + \frac{M_{c,Ed,min,f}}{M_{c,Ed,max,f}} \Delta\sigma_{s,f} = -69.5 + (-22.62/-28.28).(-44.0) = -104.7 \text{ MPa}$$

The same value is obtained by $\sigma_{s,min,f} = \sigma_{s,max,f} \frac{M_{c,Ed,min,f}}{M_{c,Ed,max,f}} = (-22.62/-28.28)(-130.9) = -104.7 \text{ MPa}$.

The stress range is ultimately $\Delta\sigma_{s,p} = 130.9 - 104.7 = 26.2$ MPa. It should be multiplied by the damage equivalent factor $\lambda_s = 1.322$ at internal support (see paragraph 9.2.1) to obtain the maximum stress range.

The fatigue justification in the reinforcement (upper layer) at support P1 is therefore ensured:

$$\gamma_{F,fat} \Delta\sigma_{S,eq} (N^*) \leq \frac{\Delta\sigma_{Rsk} (N^*)}{\gamma_{S,fat}}$$

i.e. $1.0 \times 1.322 \times 26.2 = 34.7$ MPa << $162.5 / 1.15 = 141.3$ MPa.

b) Cross-section at mid-central span

This cross-section is located at the end of the 5th slab concreting segment (at the junction with the 6th), in the uncracked zone of the global analysis. For the non-cyclic loads basic combination, the reinforcing steel bars are subjected to $M_{c,min} = 10.96$ MN.m or $M_{c,max} = -0.14$ MN.m in the extreme cases.

From these moments, the crossing of fatigue load model FLM3 (multiplied by $0.75 \times 1.4 = 1.05$ to take account of the transverse location of the slow lane compared with the main girder axis and the use conditions of charts in EN1992-2, Annex NN) adds $M_{FLM3,max} = -0.94$ MN.m or $M_{FLM3,min} = 5.69$ MN.m.

Thus the following bending moments in the reinforcing steel bars are ultimately obtained:

- case A:

$$M_{c,Ed,max,f} = -0.14 - 0.94 = -1.08 \text{ MN.m}$$

$$M_{c,Ed,min,f} = -0.14 + 5.69 = 5.55 \text{ MN.m}$$

- case B:

$$M_{c,Ed,max,f} = 10.96 - 0.94 = 10.02 \text{ MN.m}$$

$$M_{c,Ed,min,f} = 10.96 + 5.69 = 16.65 \text{ MN.m}$$

Check with the bending moment from case A

$M_{c,Ed,max,f}$ is negative thus the maximum stress is calculated by using the cracked composite mechanical properties:

$$\sigma_{s,max,f,0} = M_{c,Ed,max,f} \frac{V_2}{I_2} = -1.08 \times \frac{V_2}{I_2} = -22.1 \text{ MPa}$$

The tension stiffening effect is given by $\Delta\sigma_{s,f} = 49.6$ MPa in this cross-section at mid-central span (see Figure 9.12).

$$\sigma_{s,max,f} = \sigma_{s,max,f,0} + \Delta\sigma_{s,f} = -22.1 + 49.6 = 27.5 \text{ MPa}$$

$M_{c,Ed,min,f}$ is positive thus the minimum stress is calculated by using the uncracked composite mechanical properties. The equation $\sigma_{s,min,f,0} = M_{c,Ed,min,f} \frac{V_1}{I_1}$ is not as simple as it appears because the

ratio $\frac{V_1}{I_1}$ takes various values during the construction. To simplify it is assumed here that $\sigma_{s,min,f,0}$

should be linked to the FLM3 crossing and is calculated with $n_{eq} = 6.16$:

$$\sigma_{s,min,f,0} = M_{c,Ed,min,f} \frac{V_1}{I_1} = 5.55 \times \left[\frac{V_1}{I_1} \right]_{n_{eq}=6.16} = 6.86 \text{ MPa}$$

Note: $\sigma_{s,min,f,0} = 6.75$ MPa would have been obtained if the construction phases were exactly followed. This result is very close to the one obtained by simplifying the calculation because the largest part of $M_{c,Ed,min,f}$ is brought by the fatigue load model FLM3 (5.69 MN.m to be added to -0.14 MN.m after the different phases of the construction).

Finally, the stress range is given by $\Delta\sigma_{s,p} = |-71.7 - 6.86| = 78.6$ MPa.

In the mid-span cross-section the damage equivalent factor is given by $\lambda_s = 1.388$ (see paragraph 9.2.1). Then the equivalent stress range is given by $1.388 \times 78.6 = 109.1$ MPa which remains less than 141.3 MPa.

Check with the bending moment from case B

Both bending moments $M_{c,Ed,min,f}$ and $M_{c,Ed,max,f}$ are positive. Then the maximum and minimum stresses in the reinforcing steel bars are calculated with the uncracked composite mechanical properties with $n_{eq} = 6.16$:

$$\Delta\sigma_{s,p} = \Delta M_{FLM3} \frac{V_1}{I_1} = (16.65 - 10.02) \times \left[\frac{V_1}{I_1} \right]_{n_{eq}=6.16} = 8.22 \text{ MPa}$$

In the mid-span cross-section the damage equivalent factor is given by $\lambda_s = 1.388$. Thus the equivalent stress range is given by $1.388 \times 8.22 = 11.41 \text{ MPa}$ which is far less than 141.3 MPa.

10 - Justification of the cross-sections at SLS

The justifications of a bridge at the Serviceability Limit States are used to (EN1990, 3.4):

- ensure its functioning under normal use,
- ensure the comfort of users,
- limit the deformations affecting the appearance,
- limit its vibrations,
- control the damage affecting its appearance, its durability or its functionning.

This guide does not deal with the deflections and the vibrations. The justifications for reinforcing steel dealt with in this chapter only relate to the global longitudinal bending analysis. Checking the local longitudinal bending in the concrete slab and the transverse reinforcing steel is dealt with in chapter 12 of this Part II.

10.1 - General

At SLS under global longitudinal bending the following should be verified:

- stress limitations in the structural steel, the reinforcing steel and the concrete for characteristic SLS combination of actions,
- cracking control in the concrete of the slab,
- web breathing.

For checking the crack width the actions are classified according to their origin:

- direct loading,
- indirect loading (for example, the shrinkage imposed deformations).

Remember that the maximum values of the crack width in global longitudinal bending are (see 3.5.2 of this Part II):

- 0.3 mm for the direct actions combined for frequent SLS combination of actions (according to the French National Annex of EN1992-2),
- 0.3 mm for the non-calculated indirect actions, in the tensile slab zones for the characteristic SLS combination of actions.

These two types of actions – direct and indirect – can not be added and the corresponding verifications are independent. The direct actions normally govern the design in the support zones whereas the indirect actions rather govern the design in the in-span zones.

10.2 - Stress limitations

The stresses calculated under elastic assumptions are limited in the structural steel at characteristic SLS, as in the slab concrete and in the reinforcing steel bars. Given the ULS verifications these stress limitations do not normally govern the design.

10.2.1 - In the structural steel

For the characteristic SLS combination of actions the following criteria for the normal and shear stresses in the structural steel should be verified (with notations from EN1993-2):

*EN1994-2, 7.2.2 (5)
which refers to
EN1993-2, 7.3*

$$\sigma_{Ed,ser} \leq \frac{f_y}{\gamma_{M,ser}}$$
$$\tau_{Ed,ser} \leq \frac{f_y}{\sqrt{3} \cdot \gamma_{M,ser}}$$
$$\sqrt{\sigma_{Ed,ser}^2 + 3\tau_{Ed,ser}^2} \leq \frac{f_y}{\gamma_{M,ser}}$$

The partial factor $\gamma_{M,ser} = 1.0$ is given by the National Annex of EN1993-2. Strictly speaking the Von Mises criterion only makes sense if it is calculated with concomitant stress values.

Unlike ULS where the simplification could be adopted, the stresses should be considered on the external faces of the steel flanges, not in the flange mid-plane.

EN1993-1-1, 6.2.1 (9)

Figures 10.1 to 10.5 illustrate the criteria verification for the design example of this guide. As these criteria are widely verified, two sets of curves are directly shown in each figure depending on whether the stresses have been calculated with or without taking the concrete strength into account. Of course the composite cross-section is justified using only one of these two calculations according to the sign of the bending moment $M_{c,Ed}$ applied to it.

Figures 10.1 and 10.2 make it clear that the normal stresses calculated in the steel flanges without taking the concrete strength into account are logically equal to zero at both deck ends. However this is not true for the stresses calculated by taking the concrete strength into account as the self-balancing stresses from shrinkage (still called isostatic effects or primary effects of shrinkage in EN1994-2) were then taken into account.

To be safe without increasing the number of stress calculations (and because this criterion is widely verified for the example), the Von Mises criterion has been assessed for each steel flange by considering the maximum normal stress in this flange and the maximum shear stress in the web (i.e. non-concomitant stresses).

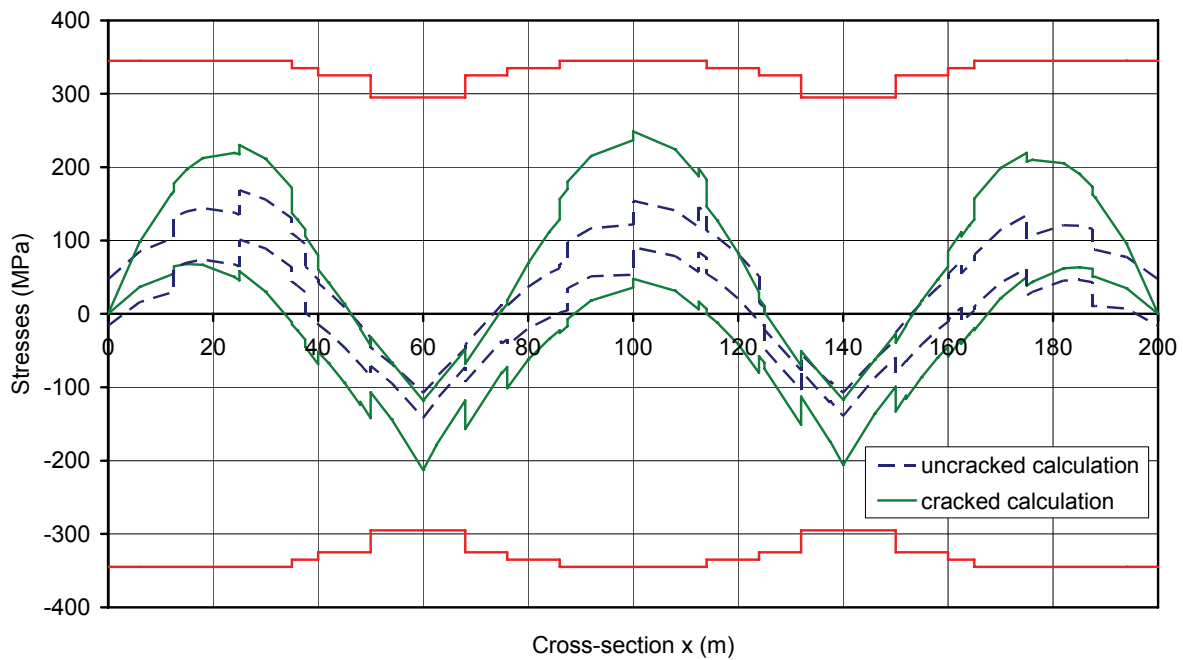


Figure 10.1: Checking the steel upper flange (SLS characteristic combination of actions)

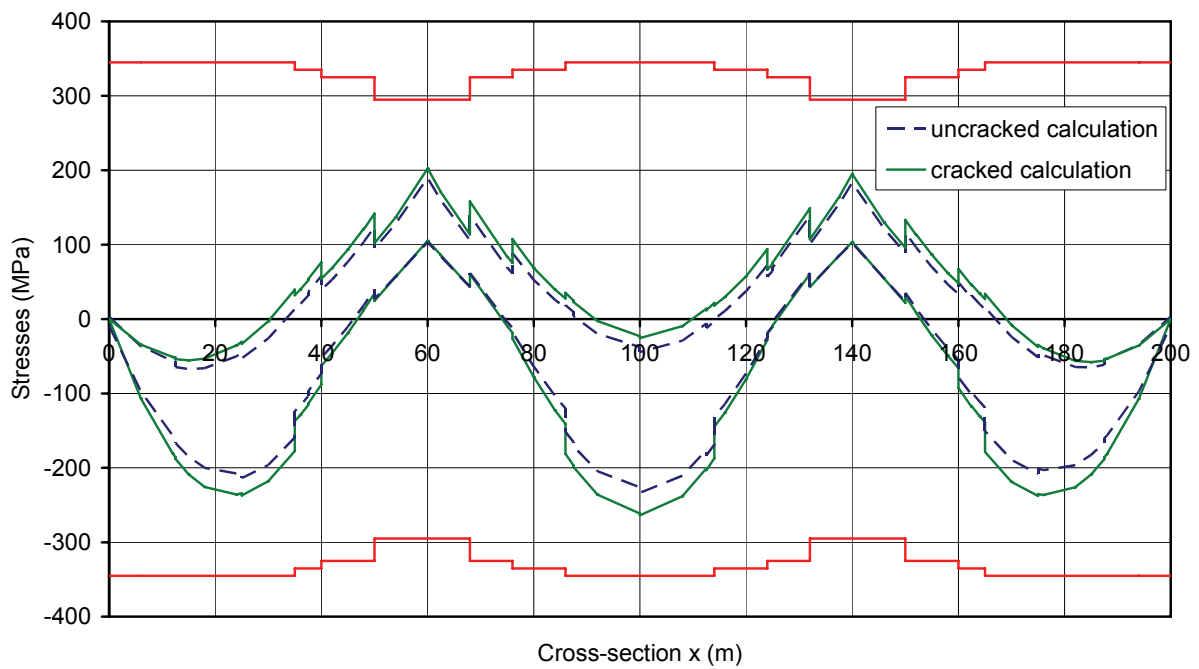


Figure 10.2: Checking the steel lower flange (SLS characteristic combination of actions)

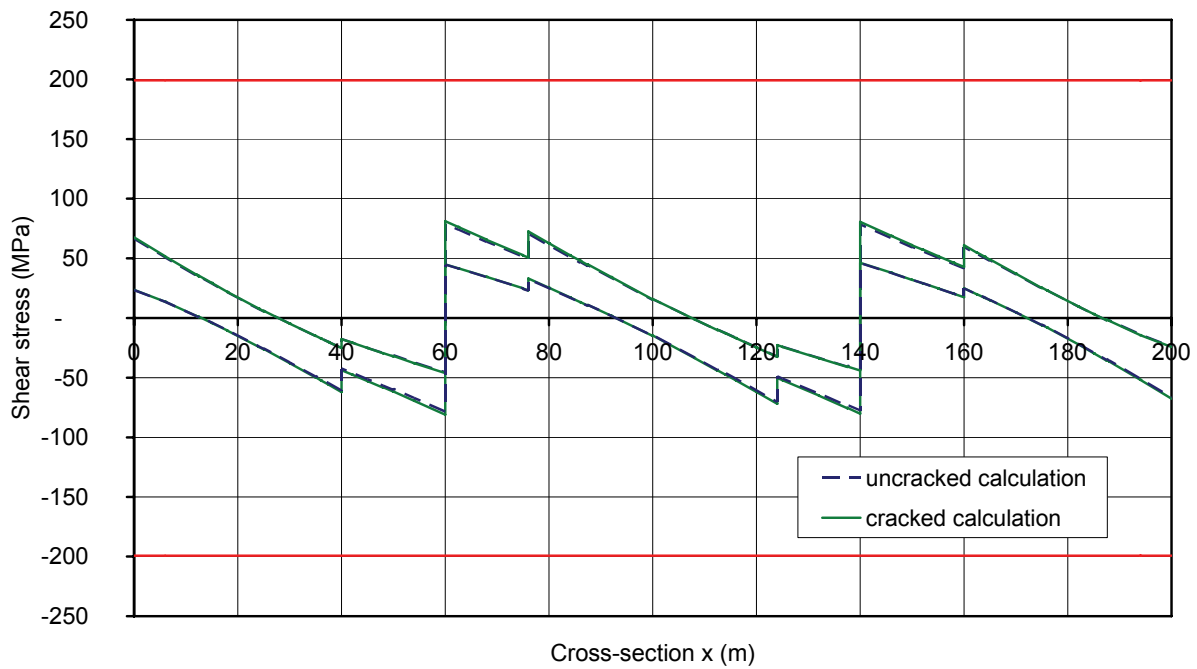


Figure 10.3: Checking the shear stress defined for the centre of gravity of the cross-section

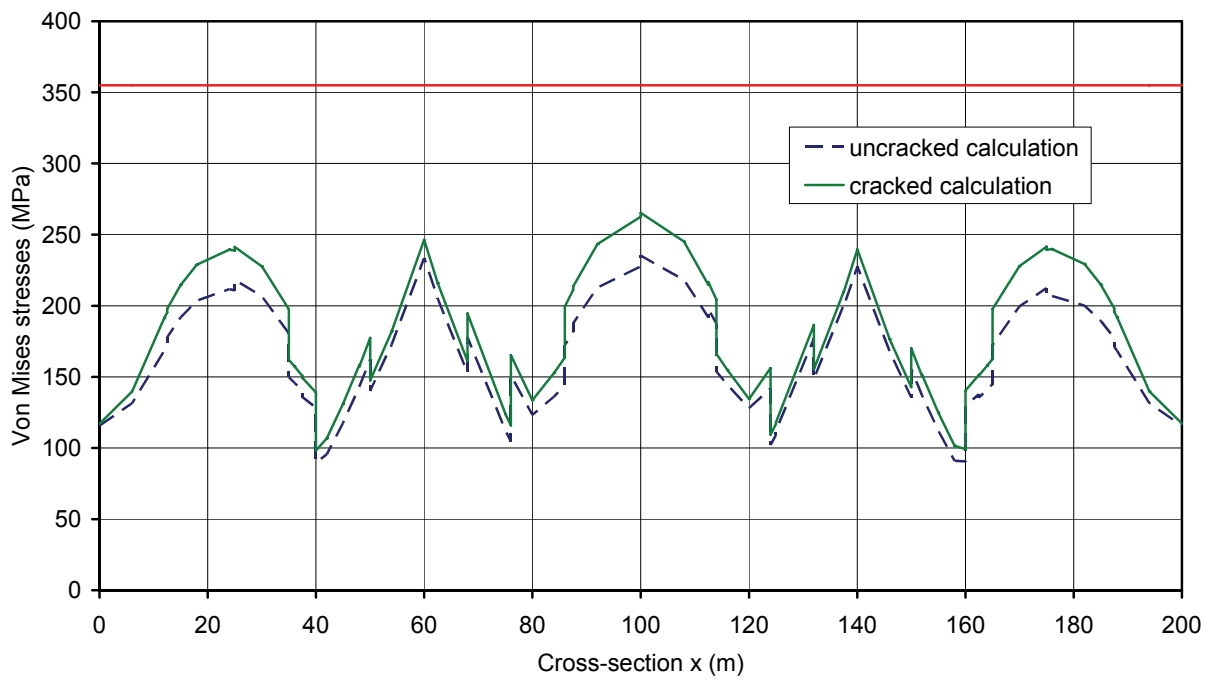


Figure 10.4: Checking the Von Mises criterion in the lower flange

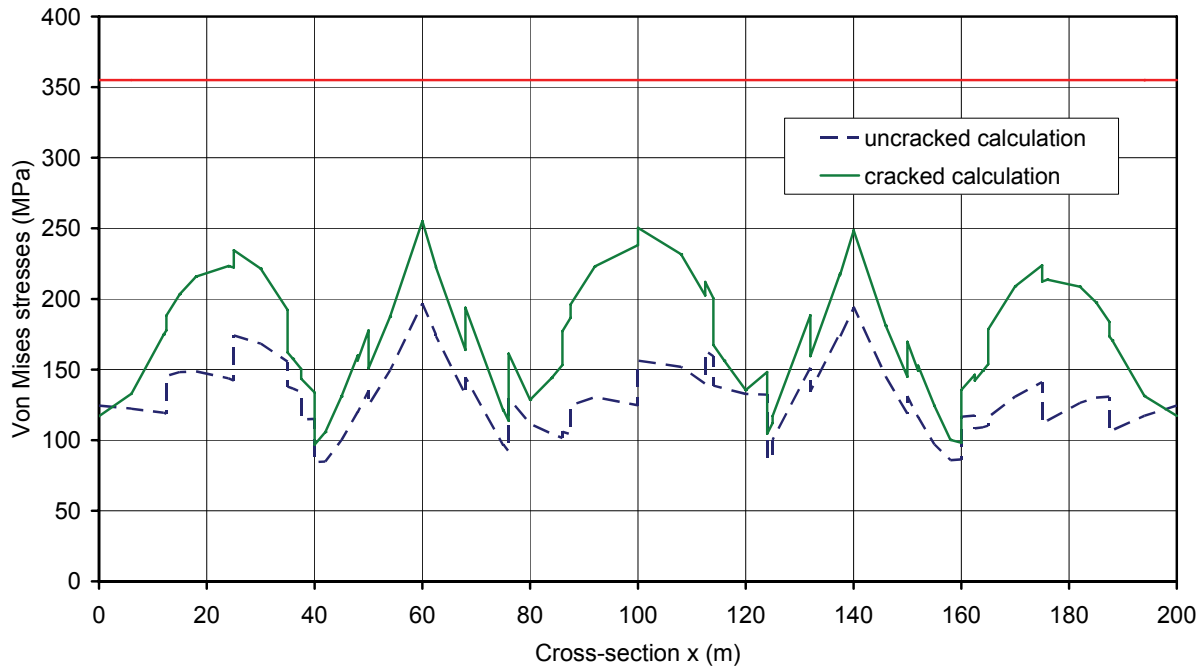


Figure 10.5: Checking the Von Mises criterion in the upper flange

Additional verification (fatigue under a low number of cycles):

It should be assessed that the stress variation in the structural steel framework due to variable loadings combined for the frequent SLS combination of actions is limited to:

$$\Delta\sigma_{\text{fre}} \leq \frac{1.5 f_y}{\gamma_{M,\text{ser}}}$$

This criterion is used to ensure that the "frequent" variations remain confined in the strictly linear part ($\pm 0.75 f_y$) of the structural steel stress-strain relationship. This thus overcomes any fatigue problems for a low number of cycles.

EN1993-2, 7.3 (2)

10.2.2 - In the concrete of the slab

The compression in the concrete should be limited to:

- $\sigma_c \leq 0.6 f_{ck}$ for the characteristic SLS combination of actions to limit the longitudinal global bending cracking.

EN1994-2, 7.2.2 (2)
which refers to
EN1992-1-1, 7.2

Note: This criterion is only indicated for concrete faces of exposure class XD, XF and XS. A slab in a composite bridge will normally be classified as XC. It has nevertheless been decided to apply this criterion as it especially affords overcome any fatigue problem in the concrete of the slab.

- $\sigma_c \leq 0.45 f_{ck}$ for the quasi-permanent SLS combination of actions to avoid having to perform a non-linear creep calculation (creep effects are taken into account in a simplified way by modular ratios assuming linear creep).

The factors $k_1 = 0.6$ and $k_2 = 0.45$ (recommended values) are subjected to a choice in the National Annex of EN1992-1-1.

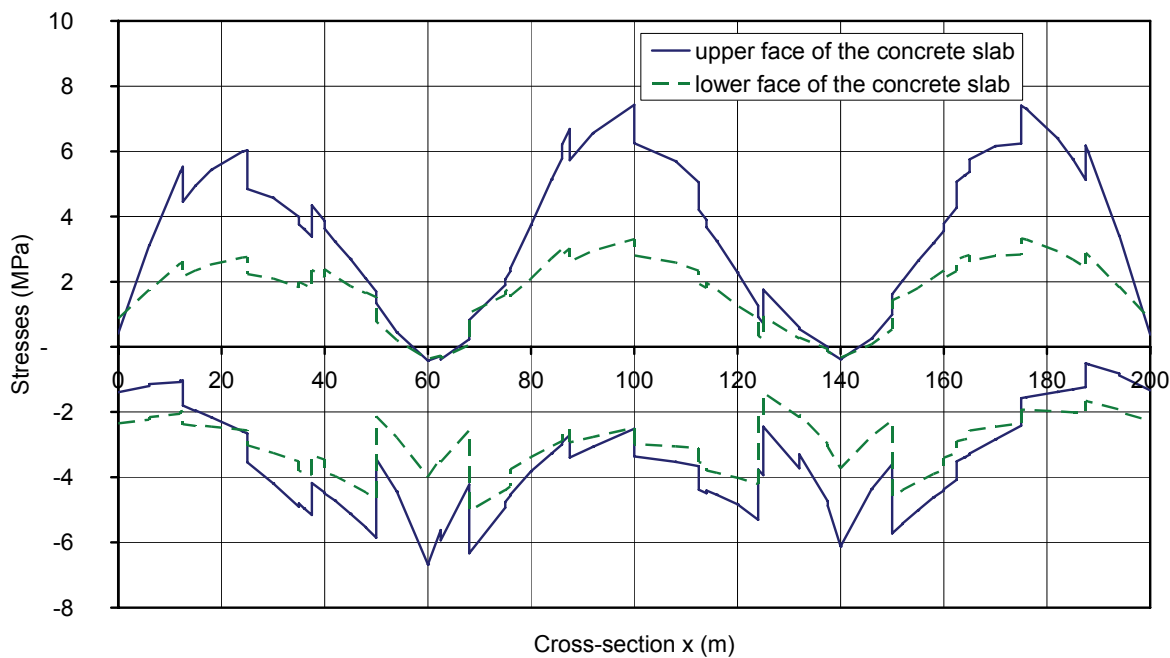


Figure 10.6: Stresses in the concrete slab for SLS characteristic combination of actions

Figure 10.6 illustrates the stress curves in both slab faces calculated by systematically taking into account the concrete strength even in the cross-sections where $M_{c,Ed}$ is negative and causes tensile stress in the slab. The verification is not performed, of course, in these latter sections. Note in the example that the stresses are far less than $0.6 f_{ck} = 21$ MPa.

The maximum compressive stress in the concrete slab for quasi-permanent SLS combination of actions only reaches 2.88 MPa for the design example which is far less than $0.45 f_{ck} = 15.7$ MPa.

10.2.3 - In the reinforcement

The tensile stress in the reinforcement should be limited to:

- $\sigma_s \leq 0.8 f_{sk}$ for characteristic SLS combination of actions to limit the longitudinal global bending cracking;
- $\sigma_s \leq 1.0 f_{sk}$ for characteristic SLS combination of actions if the tensile force is created by imposed deformations.

*EN1994-2, 7.2.2 (4)
which refers to
EN1992-1-1, 7.2 (5)*

The factors $k_3 = 0.8$ and $k_4 = 1.0$ (recommended values) are subjected to a choice in the National Annex of EN1992-1-1.

As for the Figures 10.1 to 10.5, Figure 10.7 systematically illustrates the calculations with and without the concrete strength contribution to the cross-section resistance. According to the sign of the bending moment $M_{c,Ed}$ applied to the composite cross-section, one or other of the values should be chosen for the verification. The stresses calculated with a contributing concrete strength are not equal to zero at the deck ends because of the shrinkage self-balancing stresses (isostatic or primary effects of shrinkage).

When $M_{c,Ed}$ is negative, the tension stiffening term $\Delta\sigma_s$ should be added to the stress values in Figure 10.7 calculated without taking the concrete strength into account. This term $\Delta\sigma_s$ is in the order of 100 MPa (see paragraph 10.4.3 of this same chapter).

The criterion $\sigma_s \leq 0.8 f_{sk} = 400$ MPa remains widely verified for the example.

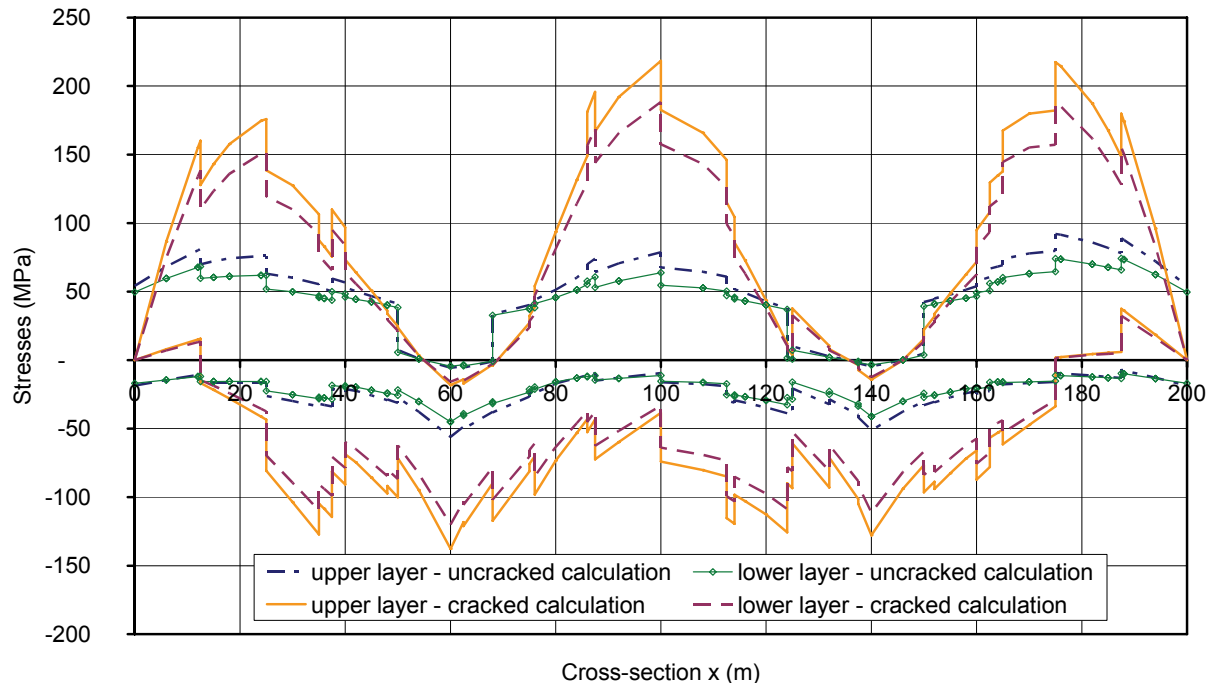


Figure 10.7: Stresses in the reinforcement for SLS characteristic combination of actions

10.3 - Web breathing

Every time a vehicle crosses the bridge, the web slightly deforms out of its plane according to the deformed shape of the first buckling mode and then returns to its initial shape. This repeated deformation called web breathing is likely to generate fatigue cracks at the weld joint between web and flange or between web and vertical stiffener.

For webs without longitudinal stiffeners (or for a sub-panel in a stiffened web), the web breathing occurrence can be avoided if:

$$\frac{h_w}{t_w} \leq \min[30 + 4L ; 300]$$

where L is the span length in meter ($L \geq 20$ m).

*EN1994-2, 7.2.3 (1)
which refers to
EN1993-2, 7.4*

For the design example this gives:

- in end-span: $h_w/t_w = 151.1 \leq 270$
- in central span: $h_w/t_w = 151.1 \leq 300$

Generally speaking this criterion is widely verified for road bridges. Otherwise EN1993-2 defines a more accurate criterion based on:

- the critical plate buckling stresses of the unstiffened web (or of the sub-panel): $\sigma_{cr} = k_\sigma \sigma_E$ and $\tau_{cr} = k_\tau \sigma_E$,
- the stresses $\sigma_{x,Ed,ser}$ and $\tau_{x,Ed,ser}$ for frequent SLS combination of actions (calculated at a peculiar point where a fatigue crack initiation could occur):

$$\sqrt{\left(\frac{\sigma_{x,Ed,ser}}{\sigma_{cr}}\right)^2 + \left(\frac{1.1 \tau_{x,Ed,ser}}{\tau_{cr}}\right)^2} \leq 1.1$$

10.4 - Control of cracking

10.4.1 - Minimum reinforcement area

The required minimum reinforcement area is given by:

$$A_{s,\min} = k_s k_c k_{ct,eff} \frac{A_{ct}}{f_{sk}}$$

EN1994-2, 7.4.2 (1)

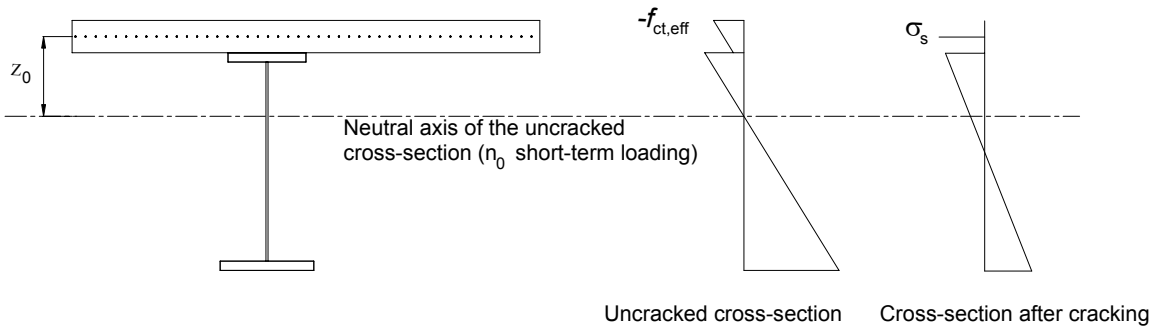


Figure 10.8: Stress distribution before and just after the concrete cracking

The term $k_c f_{ct,eff} A_{ct}$ is an approximate way to estimate the force in the tensile concrete under the bending moment that causes the concrete cracking:

- The stress in the mid-plane of the tensile concrete slab under this cracking bending moment which causes the stress $f_{ct,eff}$ in the upper fibre of the uncracked slab cross-section) is given by (see Figure 10.8):

$$\sigma_c = f_{ct,eff} \frac{z_0}{z_0 + \frac{h_c}{2}} = f_{ct,eff} \frac{1}{1 + \frac{h_c}{2z_0}}$$

$$\text{Hence } k_c = \frac{1}{1 + \frac{h_c}{2z_0}}$$

The tensile stress related to the indirect shrinkage should be added. It is not calculated and then assumed to be taken into account by adding 0.3 to the previous k_c formula.

- k_c should not be greater than 1.0 which corresponds to a uniform tensile force equal to $f_{ct,eff}$ over the whole slab.

Note: This gives frequently $k_c = 1.0$.

This tensile force is then globally reduced to take account different phenomena:

- the stress non-uniformity in the slab by the factor $k = 0.8$;
- the force transfer from the slab to the structural steel framework at the cracking instant by the factor $k_s = 0.9$.

The reinforcement is assumed to work at the yield strength f_{sk} and then the minimum reinforcement area is defined by equalizing the tensile force in the reinforcement and in the concrete slab at the cracking instant. This minimum reinforcement area should be put in place in all cross-sections.

EN1994-2, 7.4.2(5)

It will be seen in paragraphs 10.4.2 and 10.4.3 below that it can be necessary to reduce the value of f_{sk} for other justifications.

Design example for the two-girder bridge

To simplify, the calculation is performed taking into account the slab with a constant thickness e_1 .

- The elastic neutral axis of all the cross-sections is located in the steel web, so that the whole slab is in tension. Therefore A_{ct} is equal to the slab area: $A_{ct} = 1.95 \text{ m}^2$;
- $f_{ct,eff} = f_{ctm} = 3.2 \text{ MPa}$ (it can not be assumed that the cracking will always occur at concrete early age);
- $h_c = e_1 = 0.307 \text{ m}$ (slab thickness excluding the concrete haunch);
- $z_0 = 0.515 \text{ m}$ (calculated with a short-term modular ratio n_0);
- $k_c = \min \left[\frac{1}{1 + \frac{h_c}{2z_0}} + 0.3 ; 1.0 \right] = \min (1.07 ; 1.0) = 1.0 ;$
- $f_{sk} = 500 \text{ Mpa.}$

Hence $A_{s,min} = 89.86 \text{ cm}^2$ (i.e. $\rho = 0.46 \%$ of the concrete area as minimum reinforcement area).

At least half of this required reinforcement should be placed in the upper layer of reinforcing steel bars.

EN1994-2, 7.4.2 (3)

Note that this minimum reinforcement is widely put in place in the example of this guide. Then there is no need to refine the calculation by taking into account the transverse variation of the slab thickness as required by EN1994-2.

EN1994-2, 7.4.2 (4)

10.4.2 - Control of crack width under indirect loadings

This involves verifying that the crack widths remain less than 0.3 mm using the indirect method (see paragraph 3.5.2 of this Part II) in the tensile zones of the slab for characteristic SLS combination of actions. This assumes that the stress in the reinforcement is known. But that is not true under the effect of shrinkages (drying, endogenous and thermal shrinkage). The following conventional calculation is then suggested:

$$\sigma_s = k_s k_c k f_{ct,eff} \frac{A_{ct}}{A_s}$$

EN1994-2, 7.4.2(1)

Note that it is in fact the minimum reinforcement formula read back to front. Therefore this gives the stress which develops in the reinforcement due to shrinkage at the cracking instant.

With the reinforcement area chosen in in-span cross-section ($\rho_s = 0.92 \%$), this gives $\sigma_s = 0.9 \times 1.0 \times 0.8 \times 3.2 \times 1.95 / (0.92 \times 1.95 / 100) = 250.4 \text{ MPa}$.

High bond bars with diameter $\phi = 16 \text{ mm}$ have been chosen in the slab. This gives $\phi^* = \phi \cdot 2.9 / 3.2 = 14.5 \text{ mm}$. The maximum reinforcement stress is obtained by linear interpolation in Table 7.1 in EN1994-2:

EN1994-2, 7.4.2(2)

$\sigma_{s,max} = 255 \text{ MPa} > 250.4 \text{ MPa}$
The section is thus verified.

Note:

By assuming $k_c = 1.0$ the following relationship can generally be written:

$$A_{s,min} = 0.9 \cdot 1.0 \cdot 0.8 \cdot f_{ct,eff} \cdot A_{ct} / \sigma_{s,max}(\Phi)$$

$$\text{or } \rho_{min} = 0.9 \cdot 1.0 \cdot 0.8 \cdot f_{ct,eff} / \sigma_{s,max}(\Phi)$$

This equation can be presented as Table 10.1 below.

Φ (mm)	$f_{ct,eff} = 2.9$ MPa	$f_{ct,eff} = 3.0$ MPa	$f_{ct,eff} = 3.2$ MPa	$f_{ct,eff} = 3.5$ MPa
12	0.75 %	0.75 %	0.76 %	0.78 %
16	0.87 %	0.88 %	0.90 %	0.94 %
20	0.94 %	0.96 %	1.00 %	1.06 %
25	1.04 %	1.06 %	1.09 %	1.15 %

Table 10.1: Minimum reinforcement ratio for controlling the crack widths

Notes:

If high bond bars with diameter of 20 mm had been chosen, the minimum longitudinal reinforcement ratio would have been 1.0% instead of 0.9%. This condition is verified at support where high bond bars with diameter of 16 mm and of 20 mm give a reinforcement ratio of 1.2%.

Compressive zones can exist in the slab for characteristic SLS combination of actions (in an isostatic span for example). In this case it is advisable to put in place only the minimum reinforcement ratio with bars working to their yield strength f_{sk} , without trying to limit the crack width to a calculated value.

In the design example all the slab can be in tension for the characteristic SLS combination of actions, as shown in Figure 10.6. The previously calculated minimum reinforcement ratio should then be put in place everywhere.

10.4.3 - Control of crack width under direct loadings

The longitudinal bending global analysis gives the stresses in the upper reinforcement layer for the frequent SLS combination of actions, assuming a cracked behaviour of the cross-sections (see Figure 10.9).

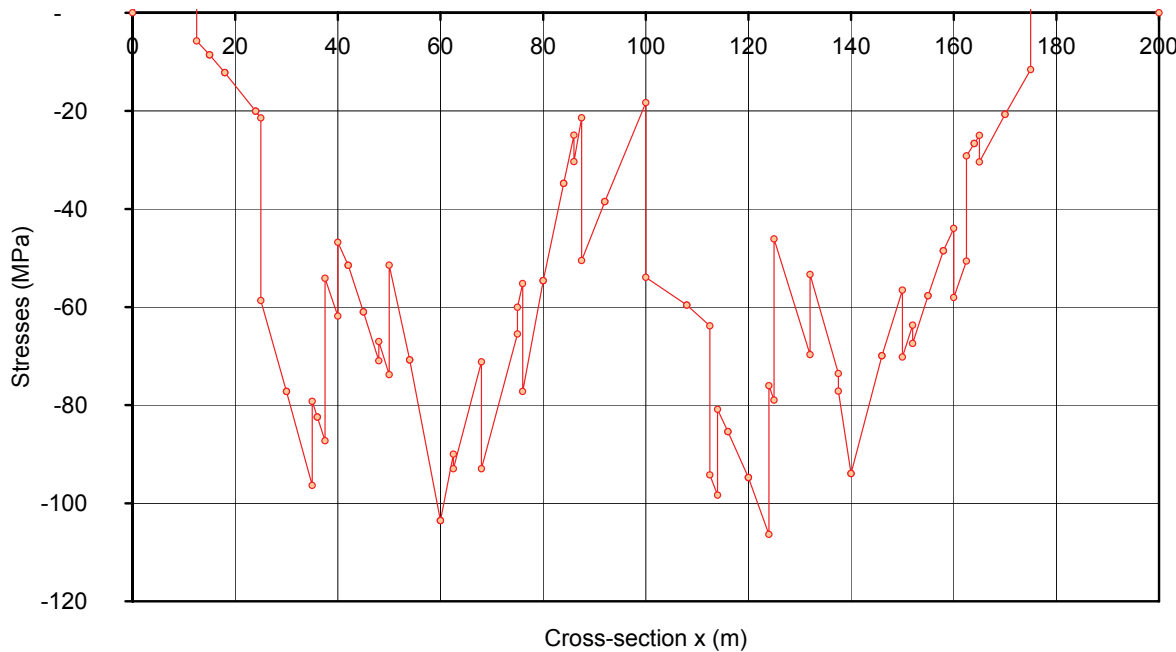


Figure 10.9: Maximum tensile stresses in the upper reinforcement layer for SLS frequent combination

The maximum tensile stresses obtained are as follows:

- 104 MPa at internal support P1,
- 94 MPa at internal support P2,
- 106 MPa (maximum) at the end of the concreting slab segment no. 7.

The observed differences are due to the dissymmetry of the concreting phases (slab segment order in Figure 3.5). It is worth noting that the maximum value is not obtained at support.

These values should be increased to take account of the the fact that the slab is connected to a structural steel framework:

EN1994-2, 7.4.3 (3)

$$\sigma_s = \sigma_{s,0} + \Delta\sigma_s$$

where $\sigma_{s,0}$ corresponds to the values in Figure 10.9.

The analytic equation of the term $\Delta\sigma_s$ can be proved from the forces equilibrium in the two modeled behaviours in Figure 10.10.

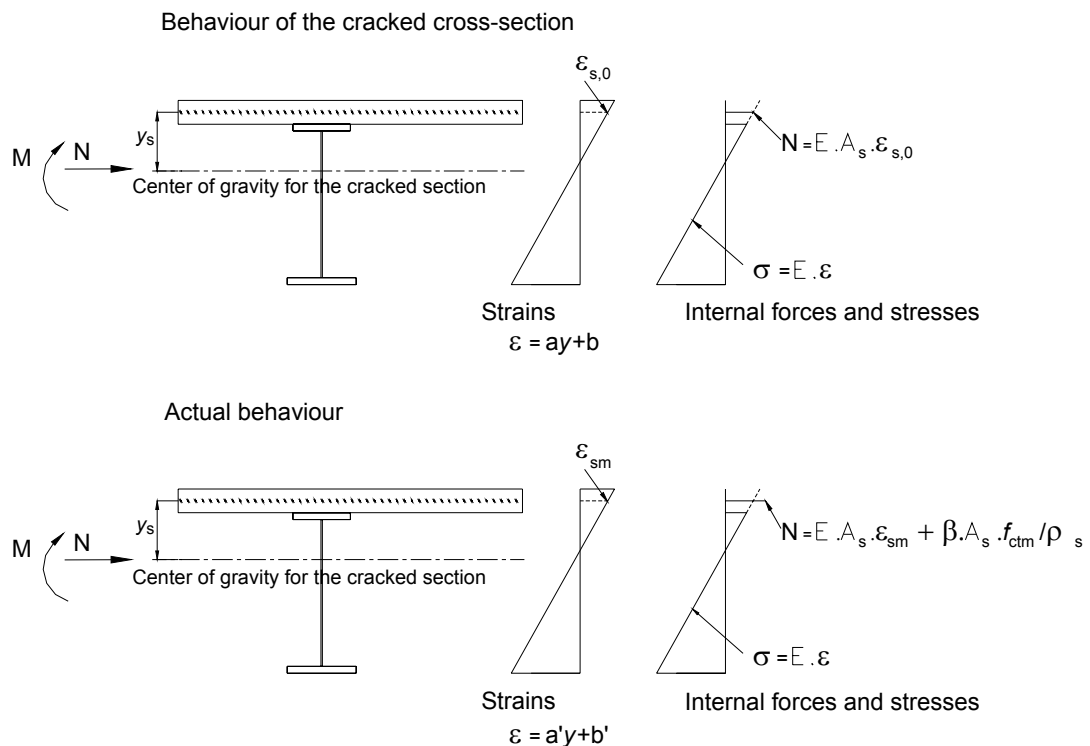


Figure 10.10: Origin of the stress term linked to the tension stiffening effect

Design example for the two-girder bridge

In the most loaded cross-section (end of the concreting slab segment no. 7) the stresses are given by:

$$\sigma_{s,0} = 106 \text{ MPa}$$

$$\alpha_{st} = \frac{A/I}{A_a/I_a} = 1.31 \text{ where } A \text{ and } I \text{ (resp. } A_a \text{ and } I_a\text{) are the area and the second moment of area of the effective cracked composite cross-section (resp. of the structural steel cross-section).}$$

$$\rho_s = 0.92 \% \text{ (longitudinal reinforcement ratio for an in-span cross-section)}$$

$$\Delta\sigma_s = 0.4 \cdot \frac{f_{ctm}}{\rho_s \alpha_{st}} = 0.4 \times 3.2 / (1.31 \times 0.0092) = 106.2 \text{ MPa}$$

$$\sigma_s = \sigma_{s,0} + \Delta\sigma_s = 212 \text{ MPa}$$

The maximum reinforcement bar diameter is obtained by linear interpolation in Table 7.1 of EN1994-2 (with a maximum crack width of 0.3 mm):

EN1994-2, Table 7.1

$$\phi_{\max}^* = 22.3 \text{ mm}$$

$$\text{Hence } \phi_{\max} = \phi_{\max}^* \frac{f_{ct,eff}}{f_{ct,0}} = 24.6 \text{ mm}$$

The maximum reinforcement bar spacing is obtained by linear interpolation in Table 7.2 of EN1994-2 (with a maximum crack width of 0.3 mm): $s = 235 \text{ mm}$.

EN1994-2, Table 7.2

The slab cracking is controlled:

- if the minimum reinforcement area is put in place (verified in paragraph 10.4.1) with steel bar diameters lower than 24.6 mm, which is the case as the longitudinal high bond bars have a maximum diameter of 20 mm (around the internal support);

or :

- if the minimum reinforcement area is put in place (verified in paragraph 10.4.1) with steel bar spacing lower than 235 mm, which is the case as the used spacing is equal to 130 mm.

It is deduced that the cracking in the most loaded cross-section is controlled.

Determining the border between support and in-span zones for the reinforcement design

To verify the border choice between support and in-span zones (see Figure 3.7 of this Part II), we look for the cross-sections where the stress level $\sigma_{s,0}$ is so high that the in-span reinforcement design is no longer sufficient to control the crack width for frequent SLS combination of actions.

In case of high bond bars with diameter of 16 mm in the in-span zone, this stress is calculated as follows:

$$\phi^* = \phi \frac{f_{ct,0}}{f_{ct,eff}} = 14.5 \text{ mm}$$

$\sigma_s = 255 \text{ MPa}$ (linear interpolation in Table 7.1 of EN1994-2)

$$\sigma_{s,0} = \sigma_s - \Delta\sigma_s = 255 - 0.4 \times 3.2 / (0.0092 \times 1.22) = 141 \text{ MPa}$$

(in fact α_{st} varies from 1.22 to 1.40 along the bridge according to the adopted thickness distribution of the structural steel plates and of the reinforcement)

The value $\sigma_{s,0} = 141 \text{ MPa}$ is never exceeded along the bridge (see Figure 10.9). It would have been possible to keep the in-span reinforcement design (high bond bars with diameter of 16 mm) with regards to the crack width control. The increase in reinforcement area at support is justified by other checks: combination of global and local longitudinal bending at ULS (see chapter 12 of this Part II), or design check of the upper steel flange at ULS for instance.

The reinforcement design chosen in paragraph 3.5.3 of this Part II of the guide is therefore justified regarding the SLS longitudinal bending calculations.

11 - Shear connection

11.1 - General

To design the shear connection at SLS as well as at ULS EN1994-2 uses an elastic calculation based on the equilibrium of a slab segment between two clearly defined specific cross-sections which are assumed to have an uncracked behaviour even if the concrete is in tension. In the zones with class 1 or 2 cross-sections where at least one fibre yields for ULS combination of actions, an elasto-plastic calculation for the connection is also necessary. This non-linear calculation is performed by using an interaction diagram in the in-span cross-section (noted B) subjected to the maximum sagging bending moment. This diagram establishes a relationship between the design moment M_{Ed} and the resulting compression F in the slab.

EN1994-2 only deals with the shear stud connectors. The other types of shear connector traditionally used in France (angle connectors in particular) are dealt with in the National Annex to EN1994-2.

Apart from the traditional vertical shear studs used for the connection of a horizontal concrete top slab, Clause 6.6.4 of EN1994-2 also deals with shear studs horizontally arranged in the direction of the slab thickness, as for example the studs welded on the steel main webs of a bridge and used for the connection of a lower slab. Only vertical shear studs are addressed in the remainder of this chapter.

11.2 - Design resistance of headed stud connectors

Two collapse modes are distinguished for this type of shear connector:

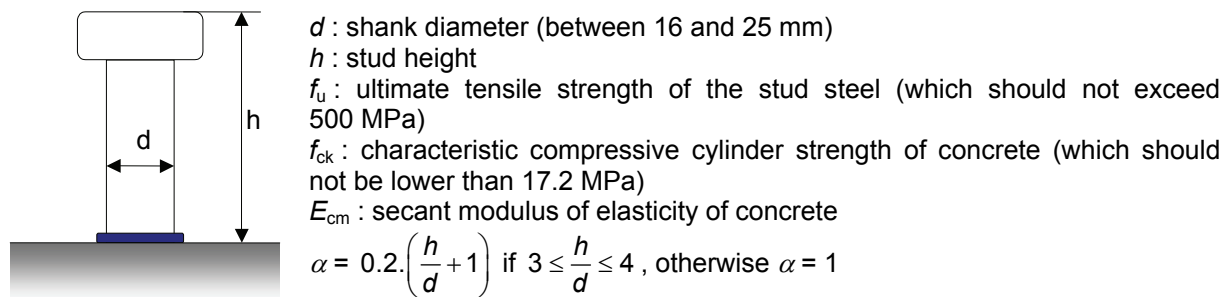
EN1994-2, 6.6.3.1(1)

- a collapse by steel shearing at the shank toe for which the characteristic resistance is given by:

$$P_{Rk}^{(1)} = 0.8.f_u \cdot \frac{\pi d^2}{4}$$

- a collapse by concrete crushing around the shank toe for which the characteristic resistance is given by:

$$P_{Rk}^{(2)} = 0.29\alpha d^2 \sqrt{f_{ck} E_{cm}}$$



The characteristic value of the shear resistance of a single stud connector is thus written:

$$P_{Rk} = \min (P_{Rk}^{(1)}; P_{Rk}^{(2)})$$

The design resistance P_{Rd} is obtained by dividing P_{Rk} by the partial factor $\gamma = 1.25$. This is the recommended value of this factor, also adopted by the French National Annex to EN1994-2. Finally the design resistance is:

- at ULS, $P_{Rd}^{EUL} = P_{Rd} = 0.8.P_{Rk}$
- at characteristic SLS, $P_{Rd}^{ELS} = k_s.P_{Rd}$

EN1994-2, 7.2.2 (6)
which refers to à 6.8.1(3)

The factor k_s is subjected to the choice of the National Annex and in France the recommended value of 0.75 has been changed for 0.6.

In the context of the example, the choice falls on shear connectors of diameter $d = 22$ mm and height $h = 200$ mm. It is assumed that the shear connectors are arranged by rows of 4 studs. For a single stud, this therefore gives:

- $P_{Rk}^{(1)} = 0.1368$ MN ; $P_{Rk}^{(2)} = 0.1533$ MN
- $P_{Rd}^{ELS} = 0.0657$ MN ; $P_{Rd}^{ELU} = 0.1095$ MN

11.3 - Design for characteristic SLS combination of actions

11.3.1 - Shear force per unit length

When the structure's behaviour remains elastic in a given cross-section, each load case from the global longitudinal bending analysis produces a longitudinal shear force per unit length $v_{L,Ed}$ at the interface between the concrete slab and the steel main girder. For a girder with uniform second moment of area subjected to a continuous bending moment (fastening the shrinkage action to the deck ends will be considered elsewhere in paragraph 11.8), this shear force per unit length is easily deduced from the cross-section properties and the internal forces and moments the girder is subjected to:

$$v_{L,Ed} = \frac{\mu_c V_{Ed}}{I_{mixte}}$$

where:

- μ_c is the moment of area of the concrete slab with respect to the centre of gravity of the composite cross-section;
- I_{mixte} is the second moment of area of the composite cross-section;
- V_{Ed} is the shear force for the considered load case and coming from the elastic global cracked analysis (see chapter 7 of this Part II).

To calculate normal stresses, when the composite cross-section is ultimately (characteristic SLS combination of actions in this paragraph) subjected to a negative bending moment $M_{c,Ed}$, the concrete is taken to be cracked and does not contribute to the cross-section strength. But to calculate the shear force per unit length at the interface, even if $M_{c,Ed}$ is negative, the characteristic cross-section properties μ_c and I_{mixte} are calculated by taking the concrete strength into account (uncracked composite behaviour of the cross-section).

[EN1994-2, 6.6.2.1\(2\)](#)

The final shear force per unit length is obtained by adding algebraically the contributions of each single load case and by respecting the construction phases. As for the normal stresses calculated with an uncracked composite behaviour of the cross-section, the modular ratio used in μ_c and I_{mixte} is the same as the one used to calculate the corresponding shear force contribution for each single load case.

For SLS combination of actions, the structure's behaviour remains entirely elastic and the longitudinal global bending calculation is performed as an envelope. Thus the value of the shear force per unit length is determined in each cross-section at abscissa x by:

$$v_{L,Ed}^{ELS}(x) = \max[v_{min}(x); v_{max}(x)]$$

Figure 11.1 below illustrates the variations in this longitudinal shear force per unit length for the characteristic SLS combination of actions, for the design example in this guide.

11.3.2 - Design rules

In each cross-section of the deck there should be enough studs to take up all the shear force per unit length. EN1994-2, 6.8.1 (3)

The following should be therefore verified at all abscissa x :

$$v_{L,Ed}^{ELS}(x) \leq \frac{N_i}{l_i} P_{Rd}^{ELS}$$

For construction reasons, it is not normally planned to change the number of studs per unit length continuously. The bridge total length is therefore divided into n segments of length l_i , $i \in [1, n]$. A number N_i , $i \in [1, n]$ of studs is then arranged in each one (constant density per segment). The segments are chosen by observing the variations of $v_{L,Ed}^{ELS}(x)$, with each segment typically being between 5 and 15 m long.

Design example

For the example in this guide, it is proposed to break down the bridge length into segments delimited by the following abscissa (in m) which correspond to nodes in the design model:

0.0	6.0	12.5	25.0	35.0	42.0	50.0	62.5
80.0	87.5	100.0	108.0	112.5	120.0	132.0	140.0
150.0	162.5	170.0	176.0	187.5	194.0	200.0	

For example, for the segment [50.0 m ; 62.5 m] around the support P1, the shear force per unit length obtained in absolute value for characteristic SLS combination of actions is successively (in MN/m):

x (m)	50^+	54^-	54^+	60^-	60^+	62.5^-
$v_{L,Ed}(x)$	0.736	0.785	0.785	0.860	0.795	0.765

The maximum SLS shear force per unit length to be taken up is therefore 0.86 MN/m, which is guaranteed providing the stud rows are placed at the maximum spacing of (4 studs per row):

$$\frac{4P_{Rd}^{ELS}}{\max(v_{L,Ed})} = 4 \times 0.0657 / 0.86 = 306 \text{ mm}$$

By arranging the integer of stud rows that is just necessary in each segment, the shear force per unit length taken up per segment can be calculated. Figure 11.1 illustrates this elastic design of the connection for characteristic SLS combination of actions. The curve representing the shear force per unit length that the shear connectors are able to take up thus encompasses fully the curve of the SLS design shear force per unit length. The corresponding values of row spacings are summarized in paragraph 11.7 of this chapter. They are compared with all the connection calculations to deduce the spacing ultimately to be applied.

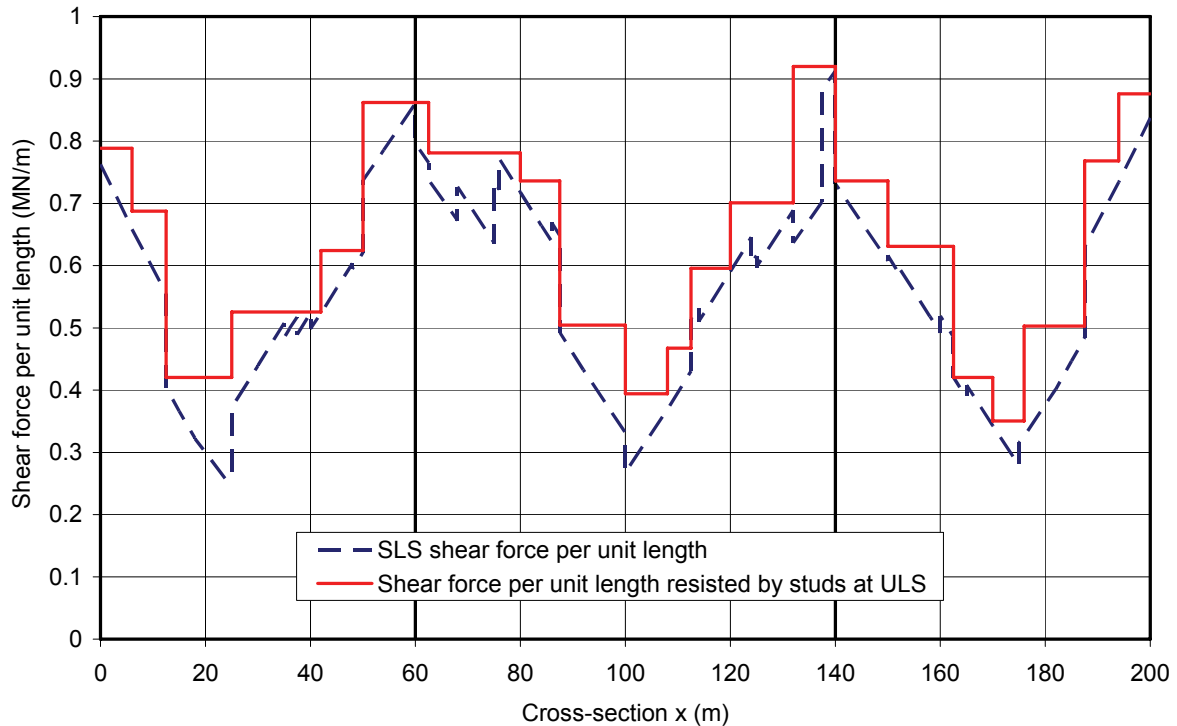


Figure 11.1: SLS shear force per unit length resisted by the studs (MN/m)

11.4 - Design for ULS combination of actions other than fatigue

11.4.1 - Elastic design

Whatever the behaviour of the bridge at ULS – elastic in all cross-sections or elasto-plastic in some cross-sections – the design of the connection starts by an elastic calculation of the shear force per unit length, with the same method as for the characteristic SLS design (see paragraph 11.3.1). In each cross-section, the shear force per unit length at ULS is therefore given by:

$$v_{L,Ed}^{ELU}(x) = \max[v_{\min}(x); v_{\max}(x)]$$

This value is calculated from shear forces at ULS and mechanical properties of the uncracked cross-sections, respecting the construction phases.

The number of shear connectors by unit length, constant per segment, should therefore verify the following two criteria:

- locally in each segment i , the shear force per unit length should not exceed by more than 10% what the number of shear connectors per unit length can take up:

$$v_{L,Ed}^{ELU}(x) \leq 1.1 \frac{N_i}{l_i} P_{Rd}^{ELU}$$

- the number of shear connectors should be sufficient per segment to transfer all the shear force of this segment:

$$\int_{x_i}^{x_{i+1}} v_{L,Ed}^{ELU}(x) dx \leq N_i P_{Rd}^{ELU}$$

where x_i and x_{i+1} designate the abscissa at the borders of the segment i .

EN1994-2, 6.6.2.2(4)

EN1994-2, 6.6.1.2(1)

To simplify, the breakdown into segments is the same as the one defined for SLS calculations. In the example in this guide, for the segment [50.0 m ; 62.5 m] around the support P1, the shear force per unit length obtained in absolute value for ULS combination of actions is successively (in MN/m):

EN1994-2, 6.6.2.2(4)

x (m)	50 ⁺	54 ⁻	54 ⁺	60 ⁻	60 ⁺	62.5 ⁻
$v_{L,Ed}(x)$	0.979	1.046	1.046	1.146	1.069	1.028

The maximum ULS shear force per unit length to be resisted is therefore 1,146 MN/m.

$$\int_{50}^{62.5} v_{L,Ed}^{ELU}(x) dx = 13.25 \text{ MN}$$

is also calculated.

Finally, the maximum longitudinal spacing between rows of four studs in the segment [50.0 m ; 62.5 m] to verify the design criteria at ULS is:

$$\min \left(1.1 \frac{4P_{Rd}^{ELU}}{v_{\max}^{ELU}[50;62.5]}, \frac{4P_{Rd}^{ELU}(62.5 - 50)}{\int_{50}^{62.5} v^{ELU}(x) dx} \right) = \min (420 \text{ mm} ; 413 \text{ mm}) = 413 \text{ mm}$$

In Figure 11.2, similar to Figure 11.1, the relative positions of the curves representing the shear force per unit length that the shear connectors are able to resist, and the ULS shear force per unit length, are different from those in the SLS calculation. See also the synopsis in paragraph 11.7.

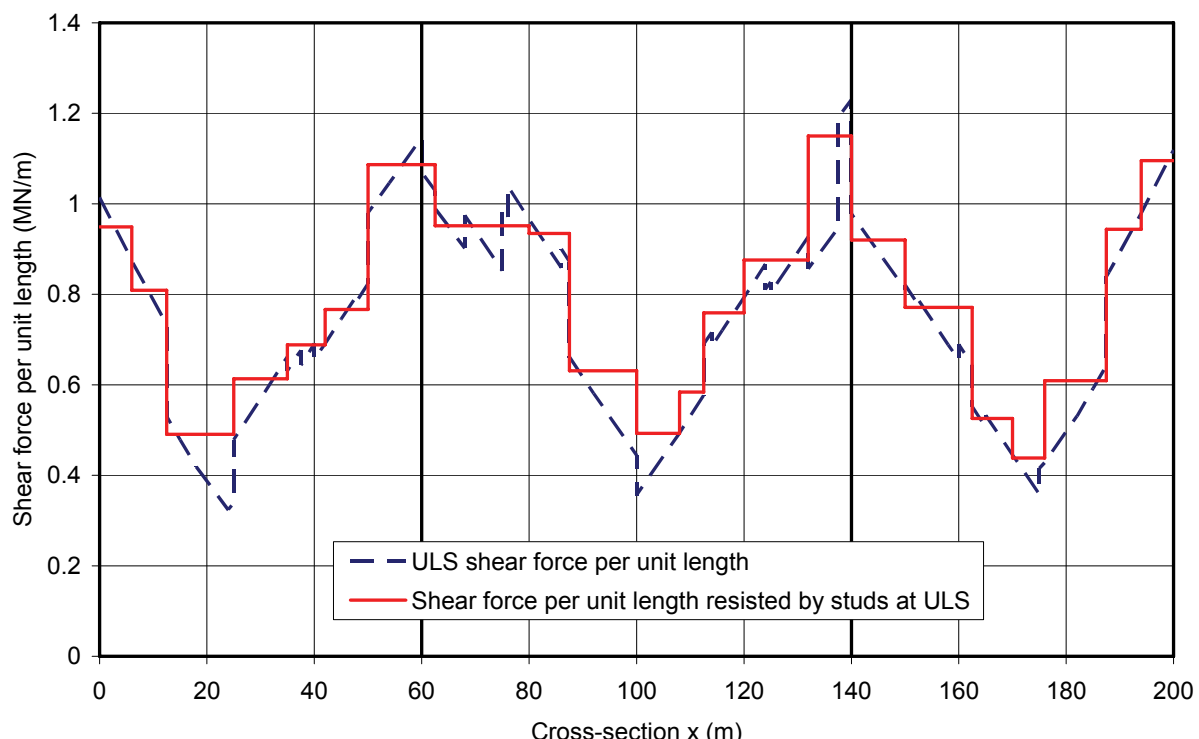


Figure 11.2: ULS shear force per unit length resisted by the studs (MN/m)

11.4.2 - Design with plastic zones in sagging bending

When a cross-section loaded by a positive bending moment at ULS is even partially yielded the previous calculation should be supplemented. As soon as the structure behaviour is no longer elastic, the relationship between the shear force per unit length and the global internal forces and moments is no longer linear. Therefore the previous calculation becomes inaccurate. In a plastic zone, the shear connection is normally heavily loaded and substantial bending moment redistribution occurs between neighboring cross-sections.

EN1994-2, 6.6.2.2 (1)

In the example in this guide, although the in-span cross-sections are class 1 sections, no yielding occurs (see paragraph 8.4 of this Part II). There is therefore no need to perform the calculations presented below.

a) Boundaries of the plastic zone

The initial phase consists in identifying zones where this non-linear connection calculation should be performed.

The in-span cross-section, noted B by EN1994-2, is first identified and defined as the one where the maximum yielding occurs. In general, and without abrupt variation in section properties, section B is the one where the maximum bending moment M_{Ed} occurs at ULS.

EN1994-2, 6.6.2.2 (2)

The sections located at the boundaries of the plastic zone (noted A and C) correspond to the sections where at ULS the bending moment M_{Ed} is equal to the design value of the elastic resistance moment (see Figure 11.3):

$$M_{Ed} = M_{a,Ed} + M_{c,Ed} = M_{el,Rd}$$

Given the elastic resistance moment definition (see point c below), A and C are the sections framing B where the normal stress distribution at ULS reaches for the first time one of its elastic limits for one of the section fibres (concrete or structural steel).

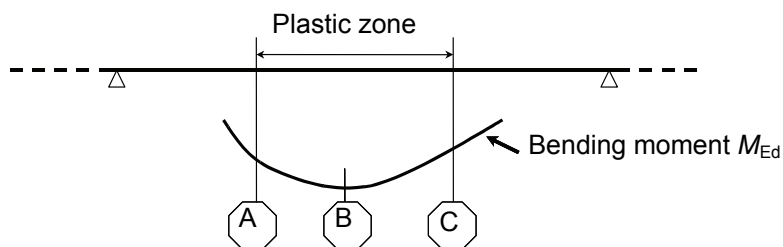


Figure 11.3: Defining the plastic zone for the connection calculation

b) Interaction diagram in section B

The elasto-plastic calculation for the connection is based on the construction of the interaction diagram $M-F$ in section B where M is the design bending moment loading the section and F is the resulting compression in the concrete slab. This diagram is defined from three noteworthy points (see Figure 11.4):

EN1994-2, 6.2.1.4 (6)

- point **G** which characterizes the state of section B for the bridge construction phase corresponding to the concreting of the slab segment comprising this section B. The section B resistance is therefore ensured by the structural steel part only and no compression is found in the slab, i.e. $M = M_{a,Ed}$ and $F = 0$;

- point **H** which corresponds to the state where section B reaches its

maximum design plastic resistance moment with a composite plastic behaviour. This therefore gives if the plastic neutral axis is located in the concrete slab:

$$M = M_{pl,Rd}$$

$$F = F_{pl,B} = \frac{0.85f_{ck}}{\gamma_c} b_{eff} h_c \text{ (noted } N_{c,f} \text{ in EN1994-2)}$$

where b_{eff} is the effective width of the slab in cross-section B and h_c is the height of the compressed part of the slab.

See also chapter 8 for further details on how to calculate $M_{pl,Rd}$.

- point J which corresponds to the first yielding in section B for which $M = M_{el,Rd}$. To this bending moment M corresponds a normal stress distribution that reaches a yield limit in one of the fibre of section B. The integration of this diagram within the slab height and the effective width gives the resulting compression $F_{el,B}$ in the slab (noted $N_{c,el}$ in EN1994-2).

The interaction diagram $M-F$ in section B then corresponds to two straight lines GJ and JH (see Figure 11.4). As a simplified alternative, the calculation of $M_{el,Rd}$ can be avoided by using the linear diagram GH.

EN1994-2, 6.2.2.2 (2)

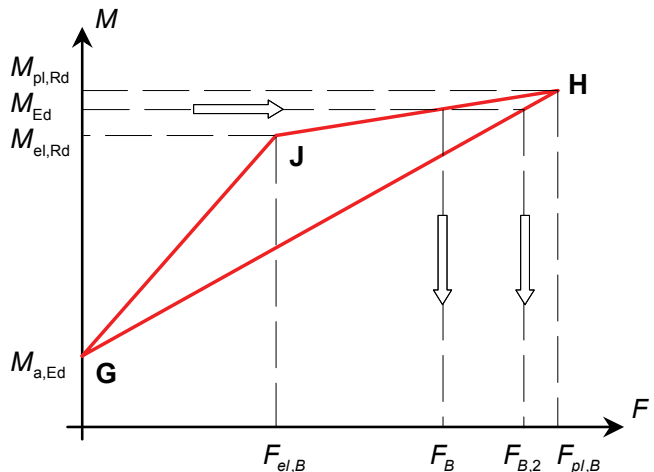


Figure 11.4: Interaction diagram $M-F$ in section B

c) Design value of the elastic resistance moment $M_{el,Rd}$

Figure 11.5 represents a possible stress state in section B as the result of the cracked elastic global analysis, respecting the construction phases. This Class 1 cross-section is justified under bending by $M_{Ed} \leq M_{pl,Rd}$. Note that the stress in the lower fibre has exceeded the yield strength of structural steel, meaning that $M_{Ed} > M_{el,Rd}$. The design value of the elastic resistance moment is obtained in this case by applying a factor $k < 1$ to the stress distribution induced by $M_{c,Ed}$ (composite behaviour of section B) so as to bring the final stress state under M_{Ed} back in its elastic limits. For the example in Figure 11.5, this gives:

$$k = \frac{f_{yd} - \sigma_{ai}^{(1)}}{\sigma_{ai}^{(2)}} \text{ then } M_{el,Rd} = M_{a,Ed} + k \cdot M_{c,Ed}$$

EN1994-2, 6.2.1.4 (6)

Note that the section B can also be yielded by excessive compression in the concrete, even if that is rarer than the situation in Figure 11.5.

Note: An interesting case is worth mentioning. $k = 1$ means that the section B reaches just the limit of its elastic behaviour and consequently the sections A, C and B are in the same location.

The resulting compression $F_{el,B}$ in the concrete slab – when $M = M_{el,Rd}$ – is calculated by integrating the elastic stress distribution under $k \cdot M_{c,Ed}$.

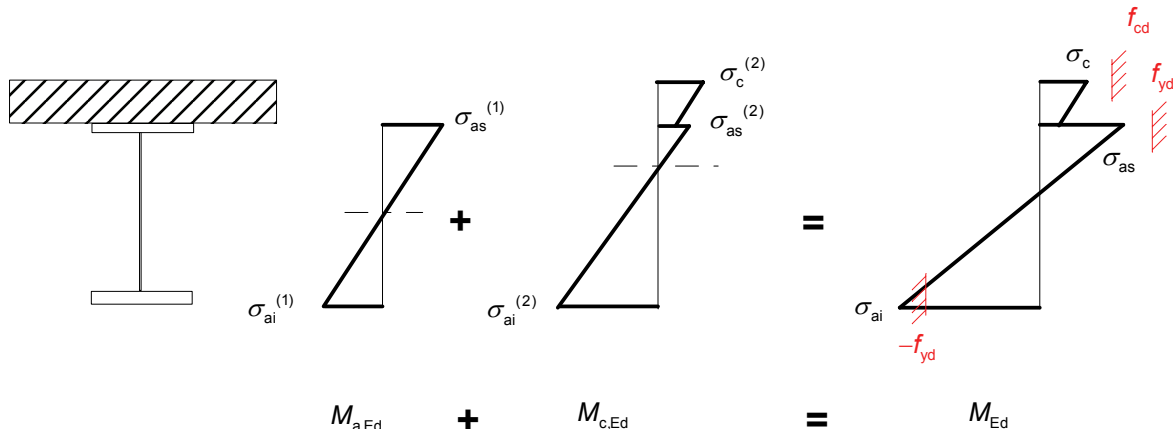


Figure 11.5: Calculation of $M_{el,Rd}$

d) Shear studs design in the plastic zone

Between the sections A and B (resp. B and C), the number of shear connectors N_{AB} (resp. N_{BC}) should be sufficient to resist the variation in compression in the slab:

$$N_{AB} \geq \frac{F_B - F_A}{P_{Rd}^{ELU}} \quad ; \quad N_{BC} \geq \frac{F_B - F_C}{P_{Rd}^{ELU}}$$

The shear connectors can be distributed with a constant density between the sections A and B (resp. B and C).

F_B is determined by reading the interaction diagram $M-F$ drawn in section B, either the diagram GJH or the simplified one GH (see Figure 11.4). This compression in the slab corresponds to the bending moment M_{Ed} which is applied to the section B at ULS and which comes from the cracked elastic global analysis of the bridge. Using the simplified diagram GH is normally very unfavourable and can result in over-designing the number of shear connectors.

In section A (resp. C), the compression F_A (resp. F_C) in the concrete slab is obtained by integrating the ULS elastic stress distribution over the slab area.

EN1994-2, 6.6.2.2 (2)

11.5 - Design for fatigue ULS combination of actions

Designing shear connectors under fatigue follows on from chapter 9 which deals with fatigue in general and the corresponding verifications for the structural steel part and the reinforcement of the bridge.

11.5.1 - Crossing of the fatigue load model

The crossing of the fatigue load model FLM3 (see paragraph 9.1.2 for the traffic conditions for this load model and paragraph 9.1.5 for the combination of actions to be considered) induces the following stress ranges:

- $\Delta\tau$, shear stress range in the stud shank, calculated at the level of its weld on the upper structural steel flange.

Unlike normal stress range (see paragraph 9.1.5), the shear stresses at the steel-concrete interface are calculated using the uncracked cross-section mechanical properties. The shear stress for the basic combination of non-cyclic loads (EN1992-1-1, 6.8.3) has therefore no influence. $\Delta\tau$ is thus deduced from variations in the shear force per unit length under the FLM3 crossing only – noted $\Delta V_{L,FLM3}$ – by taking account of its transverse location on the pavement and using the short-term modular ratio n_0 . $\Delta\tau$ also depends on the local shear connector density and the nominal value of the stud shank area:

$$\Delta\tau = \frac{\Delta V_{L,FLM3}}{\left(\frac{\pi d^2}{4}\right) \cdot \frac{N_i}{l_i}} \quad (N_i \text{ number of studs in the segment } l_i)$$

- $\Delta\sigma_p$, normal stress range in the upper steel flange to which the studs are welded (see paragraph 9.1.5 for its calculation).

EN1994-2, 6.8.5.5(1)
and (2)

11.5.2 - Equivalent constant amplitude stress range

As for the structural steel part and the reinforcement, the equivalent constant amplitude stress range simplified method at two millions cycles is used for the shear connectors:

$$\Delta\tau_{E,2} = \lambda_v \cdot \Delta\tau$$

where $\lambda_v = \lambda_{v,1} \lambda_{v,2} \lambda_{v,3} \lambda_{v,4}$ is similar to factors λ and λ_s defined in chapter 9 for the structural steel part and the reinforcement.

$$\lambda_{v,1} = 1.55 \text{ for road bridges.}$$

$\lambda_{v,2}$ to $\lambda_{v,4}$ are defined in the same way as for the structural steel part (see paragraph 9.1.3 of this Part II), but taking account of the slope $m = 8$ in the stud S-N curve instead of the slope $m = 5$ in the S-N curves for a structural steel detail under a shear stress range.

$$\lambda_{v,2} = \frac{Q_{m1}}{Q_0} \left(\frac{N_{obs}}{N_0} \right)^{\frac{1}{8}} = 0.927$$

$$\lambda_{v,3} = 1.0$$

$$\lambda_{v,4} = \left[1 + \frac{N_2}{N_1} \left(\frac{\eta_2 Q_{m2}}{\eta_1 Q_{m1}} \right)^8 \right]^{\frac{1}{8}} = 1.0$$

$\lambda_v = 1.437$ is deduced for the example in this guide.

Remember also the calculation $\Delta\sigma_{E,2} = \lambda\Phi\Delta\sigma_p$ in the upper steel flange (see chapter 9).

EN1994-2, 6.8.6.2 (1)

EN1994-2, 6.8.6.2(4)

EN1993-1-9, Fig. 7.2

11.5.3 - Fatigue verifications

Whatever the stresses in the upper steel flange – tension or compression – the fatigue verification of the shear connection starts with the criterion:

$$\gamma_{ff} \Delta\tau_{E,2} \leq \frac{\Delta\tau_c}{\gamma_{Mf,s}}$$

which corresponds to a crack propagation in the stud shank.

The partial factor for the fatigue loads is taken as equal to $\gamma_{ff} = 1.0$.

The recommended value of the partial factor for fatigue strength of studs in shear has been modified by the French National Annex to EN1994-2, $\gamma_{Mf,s} = 1.25$.

EN1994-2, 6.8.7.2

EN1994-2, 2.4.1.2 (6)
and National Annex

The reference value for the fatigue strength at 2 millions cycles is $\Delta\tau_c = 90$ MPa. EN1994-2, 6.8.3(3)

For the example in this guide, $\Delta\tau$ is calculated by using the number of shear studs coming from SLS and ULS previous design. Figure 11.6 illustrates the variation of this shear stress range along the bridge. The maximum observed value is equal to 48.7 MPa. The following criterion is thus verified:

$$\gamma_{\text{ff}} \lambda_v \Delta\tau = 70.0 \text{ MPa} \leq \frac{\Delta\tau_c}{\gamma_{\text{Mf,s}}} = 72 \text{ MPa}$$

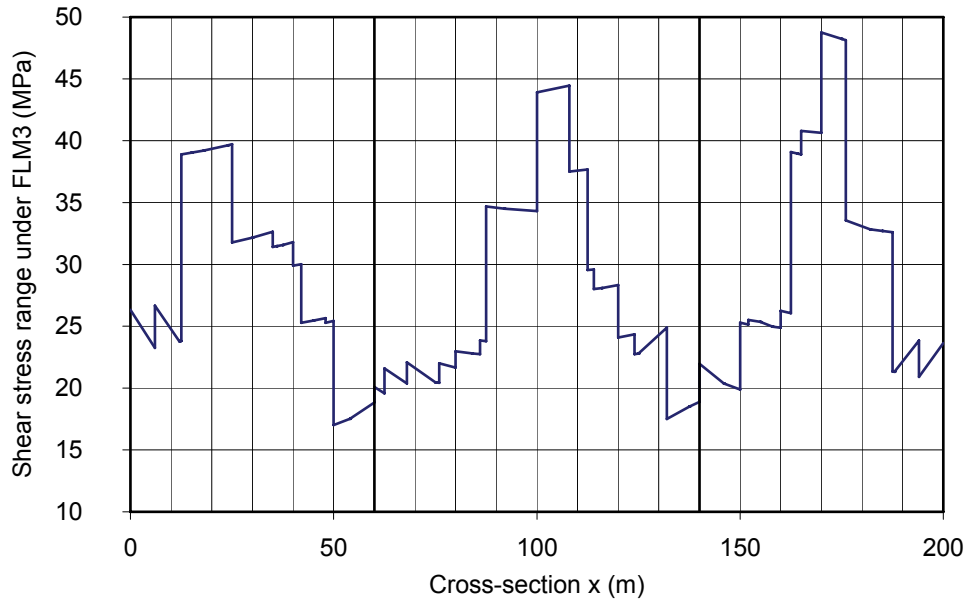


Figure 11.6: Shear stress range under the FLM3 crossing (MPa)

If the upper steel flange is in tension for fatigue ULS combination of actions (see paragraph 9.1.5 for its definition), fatigue cracks are likely to propagate under the variations in $\Delta\sigma_p$ through the structural detail of the stud weld on the upper face of this flange. This gives two additional verifications:

- a criterion in the steel flange:

$$\gamma_{\text{ff}} \Delta\sigma_{E,2} \leq \frac{\Delta\sigma_c}{\gamma_{\text{Mf}}} \text{ with } \Delta\sigma_c = 80 \text{ MPa for the detail category.}$$

The partial factor γ_{Mf} is taken as equal to 1.35 (safe life assessment method with high consequences of the upper steel flange failure for the bridge).

- an interaction criterion between $\Delta\sigma_{E,2}$ and $\Delta\tau_{E,2}$:

$$\frac{\gamma_{\text{ff}} \Delta\sigma_{E,2}}{\Delta\sigma_c / \gamma_{\text{Mf}}} + \frac{\gamma_{\text{ff}} \Delta\tau_{E,2}}{\Delta\tau_c / \gamma_{\text{Mf,s}}} \leq 1.3$$

Strictly speaking $\Delta\sigma_p$ and $\Delta\tau$ (the origin of $\Delta\sigma_{E,2}$ and $\Delta\tau_{E,2}$) should be concomitant values. To simplify, the maximum values can be used (that is on the safe side).

Figure 11.7 represents the maximum tensile stresses in the upper face of the upper flange along the bridge for the fatigue ULS combination of actions, in other words the basic combination of non-cyclic loads defined by EN1992-1-1, 6.8.3, to which is added the fatigue load model FLM3 multiplied by a transverse distribution factor ($k=0.75$ for the example). Two envelope calculations have been performed, with and without the concrete strength partaking to the cross-

EN1994-2, 6.8.7.2(2)

EN1993-1-9, Table 3.1

section resistance. For each envelope only the maximum tensile stress curve is drawn. In a given cross-section the choice between the two values is determined by the sign of the bending moment $M_{c,Ed}$ acting on the composite section for the fatigue ULS combination of actions.

Therefore the two previous criteria should be verified in a zone extending from the abscissa $x = 37.5$ m to the abscissa $x = 86$ m around P1, and in a zone extending from the abscissa $x = 116$ m to $x = 162.5$ m around P2. The $\Delta\sigma_p$ values already calculated in chapter 9 are used, see Figure 9.8. In the zone around P1 the maximum $\Delta\sigma_p$ value reaches 21.8 MPa (at $x = 37.5$ m where $\lambda = 1.9$ and $\phi = 1.0$), whereas in the zone around P2 it reaches 18.6 MPa (at $x = 116$ m where $\lambda = 1.715$ and $\phi = 1.0$). It is deduced:

$$\max(\gamma_{Ff} \cdot \Delta\sigma_{E,2}) = 1.0 \times 1.9 \times 1.0 \times 21.8 = 41.4 \text{ MPa} \leq \Delta\sigma_c / \gamma_{Mf} = 59.3 \text{ MPa}$$

In the zone around P1, in Figure 11.6, the maximum $\Delta\tau$ value is 31.8 MPa at the abscissa $x = 40$ m, whereas in the zone around P2 it is 26.2 MPa at $x = 160$ m. It is deduced:

$$\max(\gamma_{Ff} \cdot \Delta\tau_{E,2}) = 1.0 \times 1.437 \times 31.8 = 45.7 \text{ MPa} \leq \Delta\tau_c / \gamma_{Mf,s} = 72 \text{ MPa}$$

The interaction criterion is thus verified in the tensile zones of the upper flange for fatigue ULS without the need to take account of concomitances:

$$41.4 / 59.3 + 45.7 / 72 = 1.3 \leq 1.3$$

The shear connectors put in place according to SLS and ULS design – other than fatigue – are therefore sufficient for the fatigue ULS verifications.

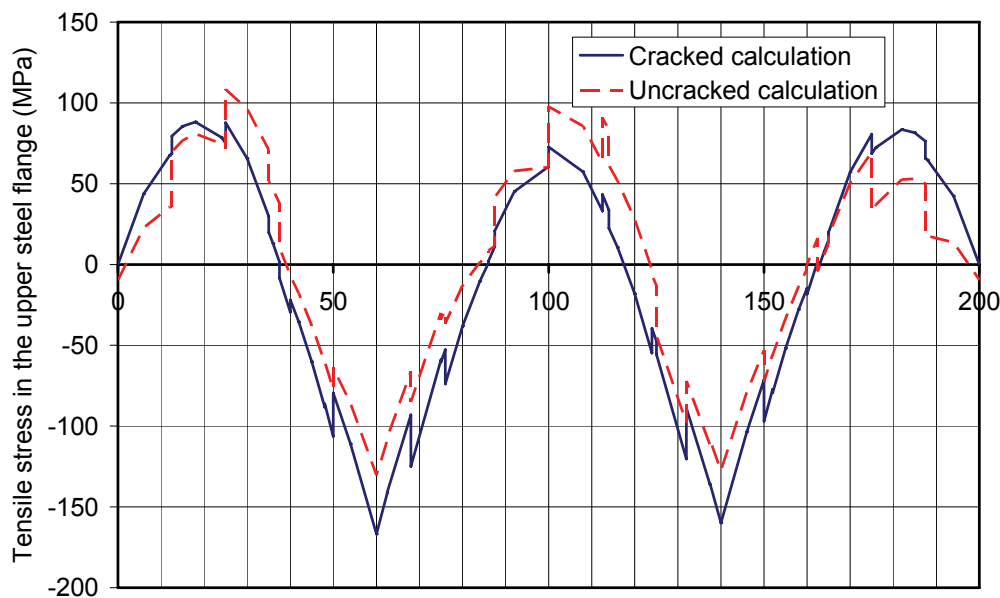


Figure 11.7: Maximum tensile stress in the upper steel flange for the ULS fatigue combination of actions

11.6 - Shear connection detailing

The following construction detailing applies for in-situ pouring concrete slabs. When the slab is precast, these provisions may be reviewed paying particular attention to the various instability problems (buckling in the composite upper flange between two groups of shear connectors, for example) and to the non-uniformity of the longitudinal shear flow at the steel-concrete interface.

EN1994-2, 6.6.5

EN1994-2, 6.6.5.5(4)

11.6.1 - Criteria related to the structural steel main girder

Generally speaking, to ensure a composite behaviour of the main girder, the maximum longitudinal spacing between two successive rows of connectors is fixed to $e_{\max} = \min(800 \text{ mm} ; 4e)$ where e is the slab thickness.

EN1994-2, 6.6.5.5(3)

When justifying the mid-span cross-section (see paragraph 8.4), it was considered that the upper structural steel flange in compression was a Class 1 element as it was connected to the concrete slab. However it verifies $c/t_f = 14.9 \varepsilon \geq 14 \varepsilon$ and then without the slab it would have been a Class 4 element. To classify it as a Class 1 element, the shear connector rows should be sufficiently close to each other to prevent buckling between two successive rows. This gives an additional criterion in e_{\max} :

$$\frac{e_{\max}}{t_f} \leq 22\varepsilon = 22\sqrt{\frac{235}{f_y}}$$

EN1994-2, 6.6.5.5(2)

where t_f is the thickness of the steel upper flange and f_y is the yield strength of the structural steel used in this flange.

This criterion is supplemented by defining a maximum distance between the longitudinal row of shear connectors closest to the free edge of the upper flange in compression – on which they are welded – and the free edge itself. Here again the aim is to prevent local buckling of the steel flange along its free edge:

$$\frac{e_D}{t_f} \leq 9\varepsilon$$

(see Figure 11.8 for the definition of e_D).

This plate buckling risk only concerns the zones where the connected steel flange is in compression and classified as a Class 3 (or 4) element. For the example of the guide where $b_f = 1000 \text{ mm}$, this involves zones in span where $t_f = 50$ or 55 mm . Thus is obtained:

- for $t_f = 40 \text{ mm}$, $e_{\max} = 726 \text{ mm}$ and $e_{D,\max} = 297 \text{ mm}$
- for $t_f = 55 \text{ mm}$, $e_{\max} = 800 \text{ mm}$ and $e_{D,\max} = 414 \text{ mm}$

This distance e_D should not be too small to ensure correct stud welding. $e_D \geq 25 \text{ mm}$ should therefore be verified. In the design example,

$$e_D = \frac{b_f - b_0}{2} - \frac{d}{2} = 114 \text{ mm} \geq 25 \text{ mm.}$$

EN1994-2, 6.6.5.6(2)

This value of 25 mm should be considered as a lower limit. It could be necessary for each individual case to increase this distance to ensure correct stud welding.

11.6.2 - Criteria related to the studs anchorage in the slab

Where a concrete haunch is used between the upper structural steel flange and the soffit of the concrete slab, the clear distance between the lower face of the stud head and the lower reinforcement layer should be not less than 40 mm. This value is decreased to 30 mm if no concrete haunch is used. The design of the lower transverse reinforcement for the longitudinal shear flow at the steel/concrete interface is explained in paragraphs 12.1.7 and 12.1.8.

There are two additional requirements where a concrete haunch is used (see Figure 11.8):

- the clear distance e_v between the side of the haunch and the outside of the closest shear connector to the upper flange free edge should be not less than 50 mm; EN1994-2, 6.6.5.4(2)
- the haunch should lie outside a straight line drawn at 45° from the outside of the closest shear connector to the upper flange free edge. EN1994-2, 6.6.5.4(1)

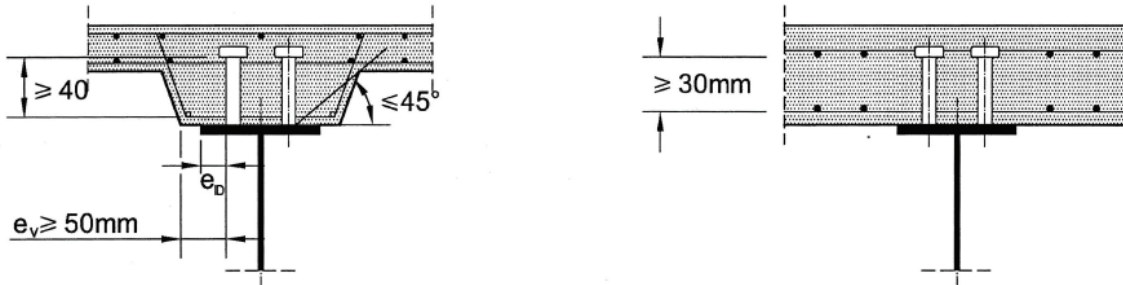


Figure 11.8: Transverse studs detailing

11.6.3 - Criteria related to the type of shear connectors

As EN1994-2 only deals with the studs, only their related criteria are defined by the standard:

- $h \geq 3d$ (in the example, $200 > 3 \times 22 = 66$ mm)
- design of the stud head: $h_{\text{head}} \geq 0.4 d$ and $d_{\text{head}} \geq 1.5.d$
- $d \leq 1.5.t_f$ if the thickness t_f of the flange to which the stud – with a diameter d – is welded, is in tension for the fatigue ULS combination of actions. Figure 11.7 demonstrates that t_f is equal to 55, 80 or 120 mm in the tensile zones of the flange, which verifies this criterion comprehensively. This verification allows the use of the detail category $\Delta\tau_c = 90$ MPa established under this assumption.

EN1994-2, 6.6.5.7 (1) to (3)

The criteria relating to the structural steel part of the bridge give maximum longitudinal spacings to be respected (see paragraph 11.6.1). There are also minimum spacings to be respected where studs are used:

- in the longitudinal direction: $e_{\text{min}} \geq 5.d$
- in the transverse direction: $e_{\text{min}} \geq 2.5.d$

EN1994-2, 6.6.5.7(4)

In the example, $e = b_0/3 = 250 \text{ mm} \geq 2.5.d = 55 \text{ mm}$.

11.7 - Synopsis for the design example

The various maximum longitudinal spacings between stud rows resulting from the previous calculations (SLS design, ULS design, fatigue design and construction detailing) are summarised in Figure 11.9. The fatigue design (for which only the interaction criterion is drawn) does not govern the shear connectors spacing for the design example. The spacing to be finally used in the bridge design is deduced from this figure.

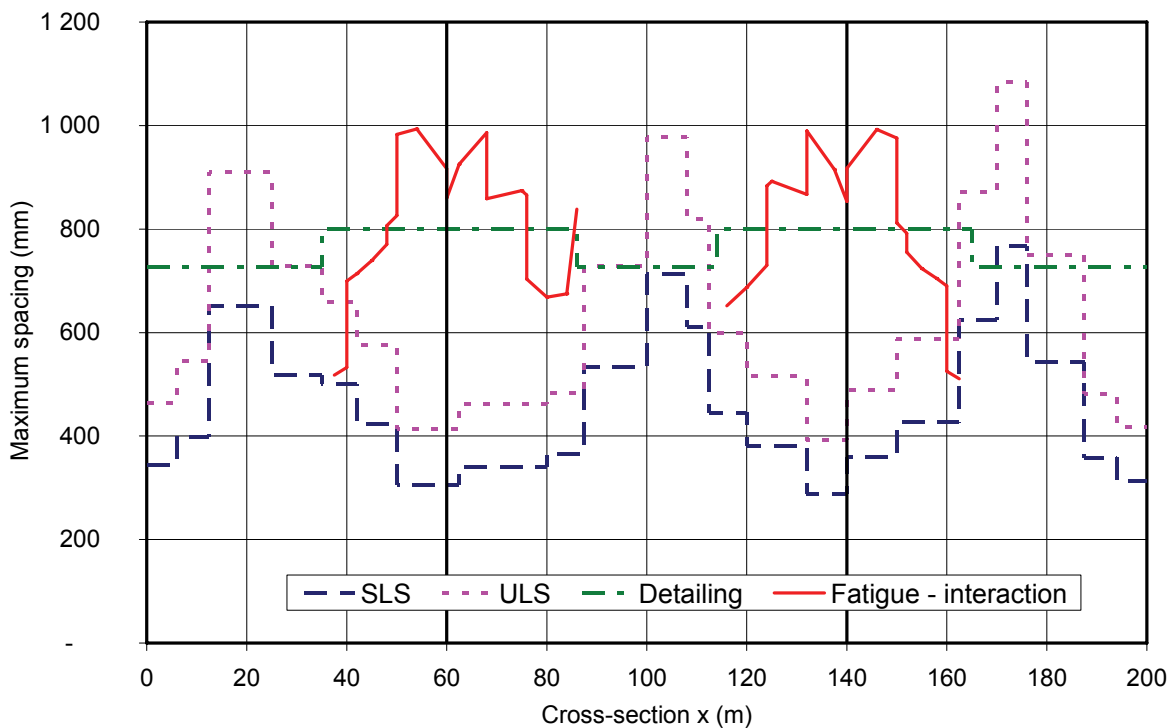


Figure 11.9: Maximum longitudinal spacing between stud rows (mm)

Note that the SLS criteria nearly always govern the design, except for the sections around the mid-span. In these zones, the spacing just necessary to resist the SLS shear flow becomes too large to avoid buckling in the steel flange between two successive stud rows. And then the governing criterion becomes the construction detailing.

11.8 - Influence of shrinkage and thermal action on the studs design at both deck ends

The shear force per unit length at the steel/concrete interface, used in the previous calculations, only takes account of hyperstatic (or secondary) effects of shrinkage and thermal actions. It is therefore necessary to also verify that sufficient shear connectors have been put in place at both free deck ends, to anchor the shear force per unit length coming from the isostatic (or primary) effects of shrinkage and thermal actions.

EN1994-2, 6.6.2.4(1)

The first step consists in calculating – in the cross-section at a distance L_v from the free deck end (called anchorage length) – the normal stresses due to the isostatic effects of the shrinkage (envelope of short-term and long-term calculations) and thermal actions. Integrating these stresses over the slab area gives the longitudinal shear force at the steel/concrete interface for the two considered load cases.

The second step consists in determining the maximum longitudinal spacing between stud rows over the length L_v which is necessary to resist the corresponding shear force per unit length. The calculation is performed for ULS combination of actions only. In this case, EN1994-2 considers that the studs are enough ductile for the shear force per unit length $v_{L,Ed}$ to be assumed constant over the anchorage length L_v . This length is taken as equal to b_{eff} , in other words the effective slab width in the global analysis at mid-end span, i.e. 6 m for the example in this guide (see chapter 7 of this Part II).

EN1994-2, 6.6.2.4(3)

All calculations performed for the design example, a maximum longitudinal shear force of 2.15 MN is obtained at the steel/concrete interface under shrinkage action (obtained with the long-term calculation) and 1.14 MN under thermal actions.

This therefore gives $V_{L,Ed} = 2.15 + 1.5 \cdot 1.14 = 3.86$ MN for ULS combination of actions. The design value of the shear flow $v_{L,Ed}^{ELU}$ and then the maximum spacing e_{max} over the anchorage length $L_v = b_{eff}$ between the stud rows are deduced:

$$v_{L,Ed}^{ELU} = \frac{V_{L,Ed}}{b_{eff}} = 0.64 \text{ MN/m (rectangular shear stress block)}$$

$$e_{max} = \frac{4P_{Rd}^{ELU}}{V_{L,Ed}^{ELU}} = 681 \text{ mm}$$

This spacing is considerably higher than the one already obtained through previous justifications (see Figure 11.9). As it is generally the case, the anchorage of the shrinkage and thermal actions at the free deck ends does not govern the connection design.

Notes:

- To simplify the design example, the favourable effects of the permanent loads are not taken into account (self-weight and non-structural bridge equipments). Anyway they cause a shear flow which is in the opposite direction to the shear flow caused by shrinkage and thermal actions. So the suggested calculation is on the safe side.

Note that it is not always true. For instance, for a cross-girder in cantilever outside the main steel girder and connected to the concrete slab, the shear flow coming from external load cases should be added to the shear flow coming from shrinkage and thermal actions. Finally the shear flow for ULS combination of these actions should be anchored at the free end of the cross-girder.

- Reading EN1994-2, 6.6.2.4(3) suggests that the same verification could be performed by using the shear flow for SLS combination of actions and a triangular variation between the end cross-section and the one at the distance L_v . However, this will never govern the connection design and it is not explicitly required by section 7 of EN1994-2 dealing with the SLS justifications.

Note:

Other situations where shear forces may have to be anchored:

EN1994-2, 6.6.2.4(5)

EN1994-2, 6.6.2.3

- Shrinkage and thermal action should be anchored at the ends of the slab concreting segments, for each construction phase.

- Shrinkage and thermal action are not the only actions to cause local effects of concentration in the longitudinal shear flow. They can also be result of external load cases as for instance, an internal prestressing cable anchored in the concrete slab or the anchorage of the cables in a cable-stay bridge with composite deck. EN1994-2 also suggests a method to calculate the local concentration effects in the shear flow resulting from these external load cases.

12 - Local justifications in the concrete slab

The concrete slab should undergo the following verifications:

- minimum reinforcement ratio to be put in place,
- limitations of the stresses for the characteristic SLS combination of actions,
- limitations of the crack widths for the frequent SLS combination of actions,
- bending resistance for the ULS combination of actions,
- punching shear,
- vertical shear resistance for the ULS combination of actions,
- longitudinal shear resistance for the ULS combination of actions,
- shear resistance of the joints between adjacent slab concreting segments,
- rules for combining global and local reinforcement layers.

The verifications in this chapter are presented for two specific longitudinal sections of the concrete slab – above the main steel girder and at mid-span between the main steel girders – under transverse bending moment. The emphasis is on the peculiar topics for a composite bridge concrete slab, particularly the fact that it is in tension longitudinally around the internal supports. The reinforced concrete calculations are not detailed; further information may be found in the SETRA guidance book on concrete bridges designed under Eurocode 2.

12.1 - Transverse reinforcement verifications

12.1.1 - Internal forces and moments from transverse global analysis

a) Permanent loads

The internal forces and moments under permanent loads are pure bending and may be calculated from a truss element model. A transverse slab strip – which is 1-m-wide in the bridge longitudinal direction – is modelled as an isostatic girder lying on two vertical point supports representing the boundaries with the main steel girders. This hypothesis is unfavourable regarding the partially blocked boundary conditions that are applied to the concrete slab in relation with the width b_f of the upper steel flange. This isostatic model is subjected to the variable distributed loads – concrete selfweight and non-structural bridge equipments – according to Figure 12.1.

After performing all calculations, the transverse bending moments in Figure 12.2 are obtained.

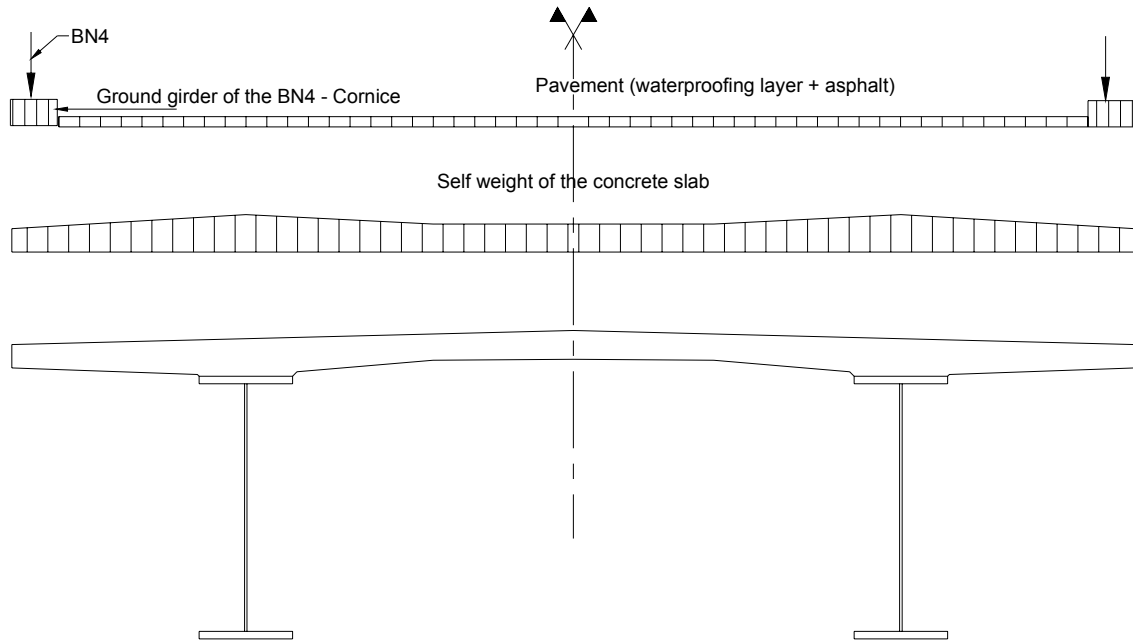


Figure 12.1: Transverse distribution of permanent loads

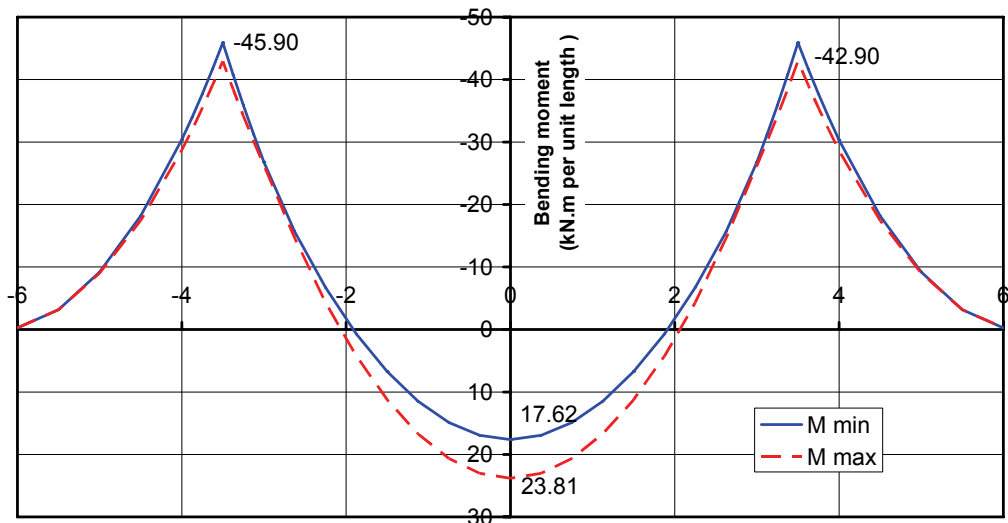


Figure 12.2: Transverse bending moment envelope due to permanent loads

b) Traffic loads

The internal forces and moments are obtained reading charts which have been established by SETRA for the local bending of the slab in two-girder bridge with transverse girders [42]. The traffic load model LM1 is always governing the design.

For the studied slab section located above the steel main girder, the characteristic value of the transverse bending moment is equal to $M_{LM1} = 135 \text{ kN.m}$ and the frequent value is equal to $M_{LM1} = 95 \text{ kN.m}$.

For the studied slab section at mid-span between the steel main girders, the characteristic value of the transverse bending moment is equal to $M_{LM1} = 134 \text{ kN.m}$ and the frequent value is equal to $M_{LM1} = 91 \text{ kN.m}$.

c) Combinations of actions

Using the combinations of actions defined in chapter 6 of this Part II finally gives the bending moment values in the table below (for a 1-m-wide slab strip):

M (kN.m)	Quasi-permanent SLS	Frequent SLS	Characteristic SLS	ULS
Section above the main girder	46	141	181	244
Section at mid-span	24	115	158	213

12.1.2 - Minimum reinforcement area

EN1992-1-1 gives a minimum bending reinforcement area to be set in the concrete slab. The recommended value (which can be modified by the National Annex of each European country) is:

$$A_{s,min} = 0.26 \cdot \frac{f_{ctm}}{f_{sk}} b_t d \geq 0.0013 \cdot b_t d$$

where b_t is the slab width (reasoning here is based on a 1-m-wide slab strip therefore $b_t = 1$ m) and d is the effective depth of the cross-section (i.e. the distance between the centre of gravity of the considered reinforcement layer and the extrem compressed fibre of the concrete).

For the design example, the reinforcement area which has been used in the design is clearly greater than the minimum reinforcement area.

*EN1992-1-1, 9.3.1
which refers to 9.2.1.1(1)*

12.1.3 - Stress limitation for characteristic SLS combination of actions

The following limitations should be checked:

$$\sigma_s \leq k_3 f_{sk} = 0.8 \cdot 500 = 400 \text{ MPa}$$

$$\sigma_c \leq k_1 f_{ck} = 0.6 \cdot 35 = 21 \text{ MPa}$$

*EN1992-1-1, 7.2(5)
and 7.2(2)*

where k_1 and k_3 are defined by the National Annex to EN1992-1-1.

These stress calculations are performed neglecting the tensile concrete contribution. The most unfavourable tensile stresses σ_s in the reinforcement are generally provided by the long-term calculations, performed with a modular ratio n (reinforcement/concrete) equal to 15. The most unfavourable compressive stresses σ_c in the concrete are generally provided by the short-term calculations, performed with a modular ratio $n = E_s / E_{cm} = 5.9$. The structure behaves as a reinforced concrete structure under transverse bending moment, therefore $E_s = 200000 \text{ MPa}$ has been adopted (see also paragraph 4.3 of this Part II).

The design example in the section above the steel main girder gives $d = 0.36 \text{ m}$, $A_s = 18.48 \text{ cm}^2$ and $M = 0.181 \text{ MN.m}$.

Using $n = 15$, $\sigma_s = 305 \text{ MPa} < 400 \text{ MPa}$ is obtained.

Using $n = 5.9$, $\sigma_c = 13.8 \text{ MPa} < 21 \text{ MPa}$ is obtained.

The design example in the section at mid-span between the steel main girders gives $d = 0.26 \text{ m}$, $A_s = 28.87 \text{ cm}^2$ and $M = 0.158 \text{ MN.m}$.

Using $n = 15$, $\sigma_s = 250 \text{ MPa} < 400 \text{ MPa}$ is obtained.

Using $n = 5.9$, $\sigma_c = 17.5 \text{ MPa} < 21 \text{ MPa}$ is obtained.

Note: The stresses calculations have not be detailed above because they are related to reinforced concrete rules which are explained in the SETRA guidance book on concrete bridges under Eurocode 2.

12.1.4 - Limitation of crack widths for frequent SLS combination of actions

The direct method (see paragraph 3.5.2 of this Part II) has been chosen for controlling the crack width. EN1992-1-1, 7.3.4

The calculations are not detailed here and further information can be found in the SETRA guidance book on concrete bridges under Eurocode 2.

After doing the calculations for the design example in this guide, the following crack widths are obtained:

- section above the steel main girder: $w_k = 0.20 \text{ mm} < 0.30 \text{ mm}$
- section at mid-span between the steel main girders: $w_k = 0.13 \text{ mm} < 0.30 \text{ mm}$

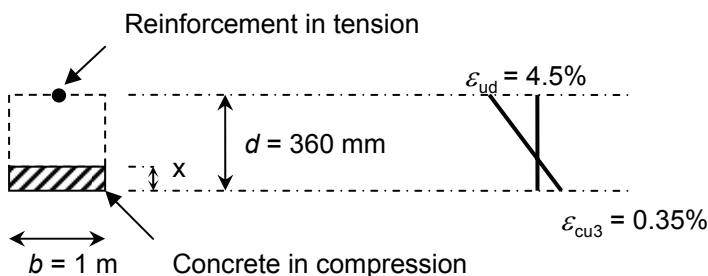
12.1.5 - ULS bending resistance

The design value of the bending moment M_{Ed} at ULS should be less than the design value of the resistance bending moment M_{Rd} which is calculated according to the following stress-strain relationships: EN1992-1-1, 6.1

- for the **concrete**, a simplified rectangular stress distribution: EN1992-1-1, 3.1.7(3), 3.1.6(1), Table 3.1
 $\lambda = 0.80$ and $\eta = 1.00$ as $f_{ck} = 35 \text{ MPa} \leq 50 \text{ MPa}$
 $f_{cd} = 23.3 \text{ MPa}$ (with $\alpha_{cc} = 1$ chosen by the National Annex)
 $\varepsilon_{cu3} = 3.5 \text{ mm/m}$
- for the **reinforcement**, a bi-linear stress-strain relationship with strain hardening (Class B steel bars according to Annex C to EN1992-1-1): EN1992-1-1, 3.2.7(2)a and Annex C
 $f_{sd} = 435 \text{ MPa}$
 $k = 1.08$
 $\varepsilon_{ud} = 0.9, \varepsilon_{uk} = 45 \text{ mm/m}$ (chosen by the National Annex)

Reinforcement in compression is neglected.

The calculation of M_{Rd} in the section example above the steel main girder gives:



$$M_{Rd} = \lambda x b \eta f_{cd} \left(x - \frac{\lambda x}{2} \right) + f_{sd} A_s (d - x) \quad \text{with} \quad x = \frac{d \varepsilon_{cu3}}{\varepsilon_{ud} + \varepsilon_{cu3}}$$

Therefore $M_{Rd} = 0.285 \text{ MN.m} > M_{Ed} = 0.244 \text{ MN.m}$. In the same way for the section example at mid-span between the two main girders, $M_{Rd} = 0.292 \text{ MN.m}$ which is greater than $M_{Ed} = 0.213 \text{ MN.m}$.

The transverse reinforcement in Figure 3.6 is well designed regarding the local transverse bending at ULS. $M_{Rd} = M_{ELU}$ would be reached in the section above the steel main girder for $A_s = 15.6 \text{ cm}^2/\text{m}$ only. It is useful to know this value to justify the interaction between the transverse bending moment and the longitudinal shear stress (see paragraph 12.1.8).

12.1.6 - Resistance to vertical shear force

The shear force calculations are not detailed. The maximum shear force at ULS is obtained in the section located above the steel main girder by applying the traffic load model LM1 between the two steel main girders. This gives $V_{\text{ELU}} = 210 \text{ kN}$ to be resisted by a 1-m-wide slab strip.

The concrete slab is not in tension in the transverse direction of the bridge. It behaves as a reinforced concrete element and its resistance to vertical shear – without specific shear reinforcement – is thus obtained directly by using the formula (6.2a) in EN1992-2, with the modifications made by the French National Annex to EN1992-2:

$$V_{\text{Rd,c}} = b_w d \left\{ k_1 \sigma_{\text{cp}} + \max \left[C_{\text{Rd,c}} k (100 \rho_i f_{\text{ck}})^{1/3}; V_{\text{min}} \right] \right\}$$

where:

- f_{ck} is given in MPa
- $k = 1 + \sqrt{\frac{200}{d}} \leq 2.0$ with d in mm
- $\rho_i = \frac{A_{\text{sl}}}{b_w d} \leq 0.02$

A_{sl} is the area of reinforcement in tension (see Figure 6.3 in EN1992-2 for the provisions that have to be fulfilled by this reinforcement). For the example in this guide, A_{sl} represents the transverse reinforcing steel bars of the upper layer in the studied section above the steel main girder. b_w is the smallest width of the studied section in the tensile area. In the studied slab $b_w = 1000 \text{ mm}$ in order to obtain a resistance $V_{\text{Rd,c}}$ to vertical shear for a 1-m-wide slab strip.

- $\sigma_{\text{cp}} = \frac{N_{\text{Ed}}}{A_c} \leq 0.2 f_{\text{cd}}$ in MPa. This stress is equal to zero where there is no normal force (which is the case in the transverse slab direction in the example).

• The values of $C_{\text{Rd,c}}$ and k_1 can be given by the National Annex to EN1992-2. The recommended ones are used:

$$C_{\text{Rd,c}} = \frac{0.18}{\gamma_c} = 0.12$$

$$k_1 = 0.15$$

- V_{min} has been modified by the French National Annex to EN1992-2:

$$V_{\text{min}} = 0.035 \cdot k^{3/2} \cdot \sqrt{f_{\text{ck}}} \text{ for beam elements}$$

$$V_{\text{min}} = (0.34 / \gamma_c) \cdot \sqrt{f_{\text{ck}}} \text{ for slab elements}$$

EN1992-2, 6.2.2

EN1992-2, Figure 6.3

Design example

The design example in the studied slab section above the steel main girder gives successively:

$$f_{\text{ck}} = 35 \text{ MPa}$$

$$C_{\text{Rd,c}} = 0.12$$

$$d = 360 \text{ mm}$$

$$k = 1 + \sqrt{\frac{200}{360}} = 1.75$$

$A_{\text{sl}} = 1848 \text{ mm}^2$ (high bond bars with diameter of 20 mm and spacing of 170 mm).

$$b_w = 1000 \text{ mm}$$

$$\rho_i = \frac{1848}{1000 \cdot 360} = 0.51 \%$$

$$C_{\text{Rd,c}} k (100 \rho_i f_{\text{ck}})^{1/3} = 0.55 \text{ MPa}$$

$$\sigma_{cp} = 0$$

$$v_{min} = (0.34/1.5) \cdot 35^{1/2} = 1.34 \text{ MPa} > 0.55 \text{ MPa}$$

The criterion is thus clearly verified:

$$V_{Rd,c} = v_{min} b_w d = 483 \text{ kN / ml} > V_{Ed} = 210 \text{ kN / ml.}$$

There is no need to add shear reinforcement in the slab, except those resulting from construction detailing (overlap, vacuum compression, etc.). A minimum of three or four reinforcement frames per m^2 is necessary to maintain the reinforcing steel bars during concreting.

12.1.7 - Resistance to longitudinal shear stress

The longitudinal shear force per unit length at the steel/concrete interface was determined in chapter 11 of this Part II by an elastic analysis at characteristic SLS and at ULS. The number of shear connectors was designed thereof, to resist to this shear force per unit length and thus to ensure the longitudinal composite behaviour of the deck.

At ULS this longitudinal shear stress should also be resisted to for any potential surface of longitudinal shear failure within the slab. This means that the reinforcing steel bars holing such kind of surface should be designed to prevent any shear failure of the concrete or any longitudinal splitting within the slab.

EN1994-2, 6.6.6.1(2)

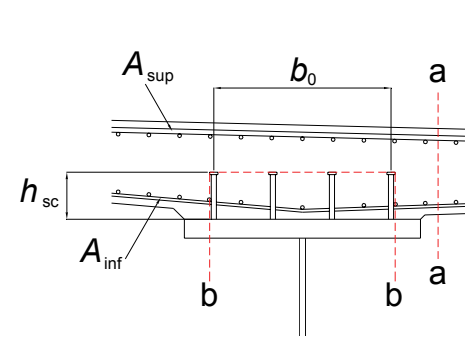
Two potential surfaces of shear failure are defined in EN1994-2 (see Figure 12.3(a)) :

- surface a-a holing only once by the two transverse reinforcement layers, $A_s = A_{sup} + A_{inf}$
- surface b-b holing twice by the lower transverse reinforcement layer, $A_s = 2 \cdot A_{inf}$

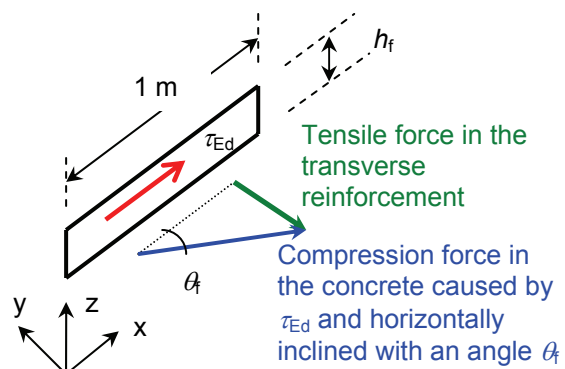
EN1994-2, Figure 6.15

According to Figure 11.2 the maximum longitudinal shear force per unit length V_{Ed} resisted to by the shear connectors is equal to 1.15 MN/m. This value is used here for verifying shear failure within the slab.

EN1994-2, 6.6.6.1(4)



(a) potential surfaces of shear failure



(b) shear resistance for the shear plane a-a

Figure 12.3: Potential surfaces of shear failure in the concrete slab

Failure in shear plane a-a

The longitudinal shear force per unit length applied in the shear plane a-a is equal to $v_{Ed,a} = 1.15/2 = 0.57 \text{ MN/m}$ (as there is a shear plane on each side of the main girder). The resulting shear stress is calculated by $\tau_{Ed} = v_{Ed,a}/h_f$ where

EN1992-1-1, Figure 6.7

h_f is the height of the surface of shear failure. This shear stress causes horizontal compressive struts in the concrete slab. They are inclined with an angle θ_f with regards to the longitudinal axis of the deck (see Figure 12.3(b)).

Two different verifications should be carried out:

- the transverse reinforcement should be designed to resist to the tensile force:

$$\tau_{Ed} h_f \tan \theta_f \leq \frac{A_s}{s} f_{sd}$$

where s is the spacing between the transverse reinforcing steel bars and A_s is the corresponding area within the 1-m-wide slab strip.

- the crushing should be prevented in the concrete compressive struts:

$$\tau_{Ed} \leq v \cdot f_{cd} \sin \theta_f \cos \theta_f$$

with $v = 0.6 \left(1 - \frac{f_{ck}}{250}\right)$ and f_{ck} in MPa (strength reduction factor for the concrete cracked in shear).

As the concrete slab is in tension in the longitudinal direction of the deck, the angle θ_f for the concrete compressive strut should be limited to $\cotan \theta_f = 1.25$ i.e. $\theta_f = 38.65^\circ$.

For the design example in this guide, above the steel main girder, the transverse reinforcement is made of high bond bars with a 20 mm diameter for the upper layer, and of high bond bars with a 16 mm diameter for the lower layer (see Figure 3.6) with a spacing $s = 170$ mm, i.e. $A_s/s = 30.3 \text{ cm}^2/\text{m}$. The previous criterion is thus verified:

$$\frac{A_s}{s} \geq \frac{\tau_{Ed} h_f}{f_{sd} \cdot \cotan(\theta_f)} = 0.57/(435 \cdot 1.25) = 10.5 \text{ cm}^2/\text{m}$$

$$v = 0.516$$

A slab thickness $h_f = 0.4$ m has been considered for the shear plane a-a.

$$\tau_{Ed} = 0.57/0.4 = 1.425 \text{ MPa} \leq v \cdot f_{cd} \sin \theta_f \cos \theta_f = 6.02 \text{ MPa}$$

A minimum reinforcement area of $10.8 \text{ cm}^2/\text{m}$ should be put in the concrete slab in order to prevent the longitudinal shear failure for the surface a-a.

Failure in shear plane b-b

The longitudinal shear force per unit length applied in the shear plane b-b is equal to $v_{Ed,b} = 1.15 \text{ MN/m}$. The length of this shear surface is calculated by encompassing the studs as closely as possible within 3 straight lines (see Figure 12.3(a)):

$$h_f = 2h_{sc} + b_0 + \phi_{head} = 2 \cdot 0.200 + 0.75 + 0.035 = 1.185 \text{ m.}$$

The shear stress for the surface b-b of shear failure is equal to:

$$\tau_{Ed} = 1.15/1.185 = 0.97 \text{ MPa}$$

For the design example in this guide, the two previous criteria are justified:

$A_s/s = 23.65 \text{ cm}^2/\text{m}$ (two layers of high bond bars with a 16 mm diameter and a spacing $s = 170$ mm)

$$\frac{A_s}{s} \geq \frac{\tau_{Ed} h_f}{f_{sd} \cdot \cotan(\theta_f)} = 1.15/(435 \cdot 1.25) = 21.15 \text{ cm}^2/\text{m}$$

$$\tau_{Ed} = 0.97 \text{ MPa} \leq v \cdot f_{cd} \sin \theta_f \cos \theta_f = 6.02 \text{ MPa}$$

*EN1994-2, 6.6.6.2(2)
which refers to
EN1992-1-1, 6.2.4(4)*

*EN1992-1-1, 6.2.2(6) +
National Annex*

*EN1992-1-1, 6.2.4(4) +
National Annex*

12.1.8 - Interaction between longitudinal shear stress and transverse bending moment

The traffic load models are such that they can be arranged on the pavement to provide a maximum longitudinal shear flow and a maximum transverse bending moment simultaneously. EN1992-2 sets the following rules to take account of this concomitance:

- the criterion for preventing the crushing in the compressive struts (see paragraph 12.1.7) is verified with a height h_f reduced by the depth of the compressive zone considered in the transverse bending assessment (as this concrete is worn out under compression, it cannot simultaneously take up the shear stress);
- the total reinforcement area should be not less than $A_{\text{flex}} + A_{\text{cis}}/2$ where A_{flex} is the reinforcement area needed for the pure bending assessment and A_{cis} is the reinforcement area needed for the pure longitudinal shear flow.

EN1992-2, 6.2.4(105)

Crushing in the compressive struts

Paragraph 12.1.7 above notes that the compression in the struts is much lower than the limit. The reduction in h_f is not a problem therefore.

- shear plane a-a:

$$h_{f,\text{red}} = h_f - x_{\text{ELU}} = 0.40 - 0.05 = 0.35 \text{ m}$$

$$\tau_{\text{Ed,red}} = \tau_{\text{Ed}} \cdot \frac{h_f}{h_{f,\text{red}}} = 0.57/0.35 = 1.63 \text{ MPa} \leq 6.02 \text{ MPa}$$

- shear plane b-b:

$$h_{f,\text{red}} = h_f - 2x_{\text{ELU}} = 1.185 - 2 \cdot 0.05 = 1.085 \text{ m}$$

$$\tau_{\text{Ed,red}} = \tau_{\text{Ed}} \cdot \frac{h_f}{h_{f,\text{red}}} = 1.15/1.085 = 1.06 \text{ MPa} \leq 6.02 \text{ MPa}$$

Total reinforcement area

The question of adding reinforcement areas is only raised for the shear plane a-a where the upper transverse reinforcement layer is provided for both the transverse bending moment and the longitudinal shear flow.

For the longitudinal slab section above the steel main girder, the minimum reinforcement area $A_{\text{flex,up}}$ required by the transverse bending assessment at ULS is equal to $15.6 \text{ cm}^2/\text{m}$ (see paragraph 12.1.5). The minimum reinforcement area A_{cis} required by the longitudinal shear flow is equal to $10.8 \text{ cm}^2/\text{m}$.

In general terms, it should be verify that:

$$A_{\text{sup}} \geq A_{\text{flex,up}}$$

$$A_{\text{inf}} \geq A_{\text{flex,inf}}$$

$$A_{\text{inf}} + A_{\text{sup}} \geq \max \left\{ A_{\text{cis}}, \frac{A_{\text{cis}}}{2} + A_{\text{flex,up}}, \frac{A_{\text{cis}}}{2} + A_{\text{flex,inf}} \right\}$$

The Eurocode does not specify how to distribute the final total reinforcement area between the two layers. It is recommended to adopt the distribution rules suggested in the SETRA guidance book on concrete bridges designed under Eurocode 2:

$$A_{\text{sup}} \geq \frac{A_{\text{cis}}}{4} + A_{\text{flex,sup}}$$

$$A_{\text{inf}} \geq \frac{A_{\text{cis}}}{4} + A_{\text{flex,inf}}$$

$$A_{\text{sup}} + A_{\text{inf}} \geq A_{\text{cis}}$$

Design example

$$A_{\text{flex,sup}} = 15.6 \text{ cm}^2/\text{m} ; A_{\text{flex,inf}} = 0 ; A_{\text{cis}} = 10.8 \text{ cm}^2/\text{m}$$

$$\frac{A_{\text{cis}}}{4} + A_{\text{flex,sup}} = \frac{10.8}{4} + 15.6 = 18.3 \leq A_{\text{sup}} = 18.5 \text{ cm}^2/\text{m}$$

$$\frac{A_{\text{cis}}}{4} + A_{\text{flex,inf}} = \frac{10.8}{4} = 2.7 \leq A_{\text{inf}} = 11.8 \text{ cm}^2/\text{m}$$

$$A_{\text{cis}} = 10.8 \leq A_{\text{inf}} + A_{\text{sup}} = 30.3 \text{ cm}^2/\text{m}$$

The rules for adding reinforcement areas govern the design in the upper layer of reinforcement.

12.2 - Longitudinal reinforcement verifications

12.2.1 - Resistance for local bending – Adding local and global bending effect

The local longitudinal bending moment at ULS in the middle of the concrete slab – halfway between the structural steel main girders – is estimated to be as equal to $M_{\text{loc}} = 90 \text{ kN.m}$ per longitudinal unit length. It causes compression in the upper reinforcement layer (just below the contact surface of a wheel, for example).

The internal forces and moments from the longitudinal global analysis at ULS cause tensile stresses in the reinforcement for the composite cross-section at support P1 which are equal to 171 MPa in the upper layer and to 149 MPa in the lower layer (see Figure 8.5 of this Part II). The corresponding values for the internal forces and moments in the concrete slab are:

$$\begin{aligned} N_{\text{glob}} &= A_{\text{s,sup}} \sigma_{\text{s,sup}} + A_{\text{s,inf}} \sigma_{\text{s,inf}} \\ &= 24.2 \text{ cm}^2/\text{m} * 171 \text{ MPa} + 15.5 \text{ cm}^2/\text{m} * 149 \text{ MPa} \\ &= 645 \text{ kN/ml} \end{aligned}$$

$$\begin{aligned} M_{\text{glob}} &= -A_{\text{s,sup}} \sigma_{\text{s,sup}} \left(\frac{h}{2} - d_{\text{sup}} \right) + A_{\text{s,inf}} \sigma_{\text{s,inf}} \left(d_{\text{inf}} - \frac{h}{2} \right) \\ &= -24.2 \text{ cm}^2/\text{m} * 171 \text{ MPa} * (308/2 - 60) \text{ mm} + \\ &15.5 \text{ cm}^2/\text{m} * 149 \text{ MPa} * (240 - 308/2) \text{ mm} \\ &= -19.0 \text{ kN.m/ml} \end{aligned}$$

The longitudinal reinforcement around support P1 should be designed for these local and global effects. The local (M_{loc}) and global ($N_{\text{glob}} + M_{\text{glob}}$) effects should be combined according to Annex E to EN1993-2. The following combinations should be taken into account:

EN1994-2, 5.4.4 +
National Annex

$$(N_{\text{glob}} + M_{\text{glob}}) + \psi \cdot M_{\text{loc}} \text{ and } M_{\text{loc}} + \psi (N_{\text{glob}} + M_{\text{glob}})$$

where ψ is a combination factor equal to 0.7 for spans longer than 40 m.

First combination: $(N_{\text{glob}} + M_{\text{glob}}) + \psi \cdot M_{\text{loc}}$

$N = N_{\text{glob}} = 645$ kN per longitudinal unit length

$M = M_{\text{glob}} + \psi M_{\text{loc}} = -19 + 0.7 \cdot 90 = 44$ kN.m per longitudinal unit length

The slab is fully in tension for this first combination and the tensile stresses in the upper and lower reinforcement layers (resp. -171.2 MPa and -149.2 MPa for N_{glob} alone) become:

$$\sigma_{s,\text{sup}} = -26 \text{ MPa}$$

$$\sigma_{s,\text{inf}} = -375 \text{ MPa}$$

which remain less than $f_{\text{sd}} = 435$ MPa.

Second combination: $M_{\text{loc}} + \psi (N_{\text{glob}} + M_{\text{glob}})$

$N = \psi N_{\text{glob}} = 0.7 \cdot 645 = 452$ kN per longitudinal unit length

$M = M_{\text{loc}} + \psi M_{\text{glob}} = 90 + 0.7 \cdot (-19) = 77$ kN.m per longitudinal unit length

The upper reinforcement layer is in compression for this second combination and the tensile stress in the lower reinforcement layer is equal to:

$$\sigma_{s,\text{inf}} = -401 \text{ MPa}$$

which remains less than $f_{\text{sd}} = 435$ MPa.

Note that this verification governs the design of the longitudinal reinforcement at internal support. There are also advantages in designing a strong longitudinal reinforcement lower layer at support (nearly half the total area) in case of a two-girder bridge with cross-girders.

12.2.2 - Shear stress for the transverse joint surfaces between slab concreting segments

As the slab is concreted in several steps, it should be verified that the shear stress can be transferred through the joint interface between the slab concreting segments:

$$\tau_{\text{Ed},i} \leq \tau_{\text{Rd},i} = \min\{cf_{\text{ctd}} + \mu\sigma_n + \mu\rho f_{\text{sd}}, 0,5v f_{\text{cd}}\}$$

where

- $\tau_{\text{Ed},i}$ is the design value of the shear stress at the joint interface,
- σ_n is the normal stress at the interface (negative for tension),
- ρ is the reinforcement ratio of longitudinal high bond bars holding the interface (assumed to be perpendicular to the interface plane),
- μ, c are parameters depending on the roughness quality for the interface. In case of interface in tension $c = 0$.
- $v = 0.6 \left(1 - \frac{f_{\text{ck}}}{250}\right)$ with f_{ck} in MPa (strength reduction factor for the concrete cracked in shear).

EN1992-1-1, 6.2.5(1)

The shear stresses at the interface are small (in the order of 0.2 MPa). But applying the formula directly can cause problems as it gives $\tau_{\text{Rd},i} < 0$ as soon as $\sigma_n + \rho f_{\text{sd}} < 0$, i.e. $\sigma_n < -1.19\% \cdot 435$ MPa = -5.18 MPa in the design example in this guide. The ULS stress calculation assuming an uncracked behaviour of the composite cross-sections shows that this tensile stress is exceeded at internal support.

In fact, as the slab is cracked at ULS, $A_c \sigma_n$ should be taken as equal to the

tensile force in the longitudinal reinforcement of the cracked cross-section, i.e.:

$$\sigma_n = \frac{A_{s,sup}\sigma_{s,sup} + A_{s,inf}\sigma_{s,inf}}{A_c}$$

(as this involves ULS calculations, the tension stiffening effects are not taken into account)

In the design example in this guide, the following is obtained for the joint interface closest to the cross-section at support P1:

$$\sigma_n = 0.73\% * (-171.2 \text{ MPa}) + 0.46\% * (-149.2 \text{ MPa}) = -1.94 \text{ MPa}$$

(see Figure 8.5 for the values of stresses in the reinforcement)

The shear resistance $\tau_{Rd,i}$ is deduced:

$$\tau_{Rd,i} = \mu(\sigma_n + \rho f_{sd}) = \mu(-1.94 + 5.18) = \mu \cdot 3.24 \text{ MPa}$$

$\mu = 0.7$ if a good roughness quality is assumed at the interface. Hence $\tau_{Rd,i} = 2.27 \text{ MPa}$. The resistance to shear at the joint interface is thus verified.

EN1992-1-1, 6.2.5(2)

12.3 - Punching shear (ULS)

12.3.1 - Rules for a composite bridge slab

The punching shear verification is carried out at ULS. It involves verifying that the shear stress caused by a concentrated vertical load applied on the deck remains acceptable for the concrete slab. If appropriate, it could be necessary to add shear reinforcement in the concrete slab.

EN1992-1-1, 6.4

EN1992-1-1, 6.4.5

This verification is carried out by using the single wheel of the traffic load model LM2 which represents a much localized vertical load.

Control perimeter around loaded areas

The diffusion of the vertical load through the concrete slab depth induces a distribution of the load on a larger surface. To take account of this favorable effect, EN1992-1-1 defines reference control perimeters. It is thus assumed that the load is uniformly distributed in the area within this perimeter u_1 (see Figure 12.4).

EN1992-1-1, 6.4.2

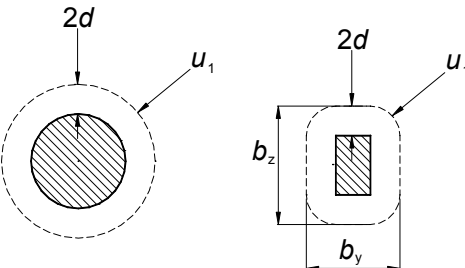


Figure 12.4: Reference control perimeters

d is the mean value of the effective depths of the reinforcement in longitudinal and transverse directions of the slab – vertical distance between the lower reinforcement layer in tension and the contact surface of the wheel – noted respectively d_y and d_z :

$$d = \frac{d_y + d_z}{2}$$

Note that the load diffusion is considered not only over the whole depth of the concrete slab, but also at 45° through the thickness of the asphalt and the waterproofing layers. Thus, the reference control perimeter should take account of these additional depths (i.e. 8+3 = 11 cm).

Design value of the shear stress τ_{Ed} around the control perimeter

The vertical load is applied on a shear surface $u_1 h$ in the concrete slab. The shear stress is then given by:

$$\tau_{Ed} = \beta \frac{V_{Ed}}{u_1 d} \text{ where:}$$

- V_{Ed} is the punching shear force
- β is a factor representing the influence of an eventual load eccentricity on the pavement (boundary effects); $\beta = 1$ is taken in case of a centered load.

EN1992-1-1, 6.4.3(3)

Shear resistance $\tau_{Rd,c}$ of the concrete

$$\tau_{Rd,c} = \beta \frac{V_{Rd,c}}{u_1 d} \text{ where } V_{Rd,c} \text{ is the design value of the resistance of the concrete section to vertical shear at ULS and is given by:}$$

$$V_{Rd,c} = \max \left\{ \left(C_{Rd,c} k (100 \rho_1 f_{ck})^{1/3} + k_1 \sigma_{cp} \right) u_1 d; (v_{min} + k_1 \sigma_{cp}) u_1 d \right\}$$

where:

- f_{ck} is in MPa
- $k = 1 + \sqrt{\frac{200}{d}} \leq 2.0$ with d in mm
- $\rho_1 = \sqrt{\rho_{ly} \rho_{lz}} \leq 0.02$ is the ratio of reinforcement in tension (lower layer) in the two orthogonal directions y and z
- $\sigma_{cp} = \frac{\sigma_{cy} + \sigma_{cz}}{2}$ (MPa) with a minimum value of -1.85 MPa

EN1992-1-1, 6.4.4(1)

EN1994-2, 6.2.2.5(3)

In the concrete slab of a composite bridge, around an internal support, there is no tension in the transverse direction but the tensile stress is very high in the longitudinal direction (about -9 MPa for the design example). This gives thus:

$$\sigma_{cp} = \max \left(\frac{\sigma_{c,long}}{2}; -1.85 \right) = -1.85 \text{ MPa.}$$

- The values for $C_{Rd,c}$ and k_1 can be provided by the National Annex to EN1994-2:

$$C_{Rd,c} = \frac{0.15}{\gamma_c} = 0.15/1.5 = 0.10$$

$$k_1 = 0.12$$

It will be seen that the note in EN1994-2, 6.2.2.5(3), only relates to concrete flanges in tension ($\sigma_{cp} < 0$) as part of a steel/concrete composite structural beam, which is the case here in the longitudinal direction. In case of a concrete slab under bending moment or compression, the values for $C_{Rd,c}$ and k_1 would have been provided by the National Annex to EN1992-1-1. See also paragraph 12.1.5 in this chapter.

EN1994-2, 6.2.2.5(3),
note

- $v_{min} = 0.035 \cdot k^{3/2} \cdot \sqrt{f_{ck}}$

12.3.2 - Design example

The vertical load induced by the single wheel of the traffic load model LM2 is equal to:

$$V_{Ed} = \frac{\beta_Q \cdot Q_{ak}}{2} = 0.9 \cdot 400/2 = 180 \text{ kN}$$

Its contact surface is a rectangular area of $0.35 \times 0.6 \text{ m}^2$.

EN1991-2, 4.3.3 + National Annex

Note: Whilst waiting for the French National Annex to EN1991-2, not available when this guidance book was written, the adjustment factor β_Q of the French National Application Document (NAD) to ENV1991-3 is used.

To calculate the depth d , the wheel of LM2 is put along the outside edge of the pavement on the cantilever part of the slab. The centre of gravity of the load surface is therefore at $0.5 + 0.6/2 = 0.8 \text{ m}$ from the free edge of the slab. At this location, the slab thickness to consider is equal to 0.30 m. It is deduced:

$$d = 0.5 \cdot [(0.30 - 0.035 - 0.016/2) + (0.30 - 0.035 - 0.016 - 0.016/2)] = 0.249 \text{ m}$$

The reference control perimeter is defined following the contact surface dimensions. $u_1 = 2 \cdot (0.35 + 0.6 + 4 \cdot 0.11) + 4\pi d = 5.91 \text{ m}$ is obtained.

EN1992-1-1, Figure 6.13

The shear stress along this control perimeter is then equal to:

$$\tau_{Ed} = \beta \frac{V_{Ed}}{u_1 d} = 0.12 \text{ MPa} \text{ (with } \beta = 1)$$

The design value of the resistance to punching shear is as follows:

$$\rho_i = \sqrt{\rho_{ly} \rho_{lz}} = \sqrt{0.394\% \cdot 0.52\%} = 0.45\%$$

$$k = 1 + \sqrt{\frac{200}{249}} = 1.90 \leq 2.0$$

$$\sigma_{cp} = -1.85 \text{ MPa}$$

$$C_{Rd,c} = 0.10$$

$$k_1 = 0.12$$

$$C_{Rd,c} k (100 \rho_i f_{ck})^{1/3} = 0.48 \text{ MPa}$$

$$V_{min} = 0.035 \cdot 1.90^{3/2} \cdot 35^{1/2} = 0.54 \text{ MPa} > 0.48 \text{ MPa}$$

$$\tau_{Rd,c} = V_{min} + k_1 \sigma_{cp} = 0.32 \text{ MPa}$$

The punching shear is thus verified:

$$\tau_{Ed} = 0.13 \text{ MPa} \leq \tau_{Rd,c} = 0.32 \text{ MPa.}$$

There is no need to add shear reinforcement in the concrete slab.

Part III

Special features of composite box-girder bridge



The aim of this Part III is not to repeat all the calculations performed for the composite two-girder bridge by transposing them into a box section but rather to address its special design features. The emphasis is therefore on the shear lag in the steel bottom flange (according to EN1993-1-5), the justification of stiffened plates, etc. The justification of the box section for torsion is not addressed in this guide.

1 - Description of the composite box section

1.1 - Main characteristics

The bridge dealt with in this Part III of the guide is a symmetrical composite open box-girder bridge connected to a concrete slab. The general data (span lengths, cross-section, loading hypotheses and construction phases of the concrete top slab) are identical to those of the two-girder bridge discussed in Part II (see chapters 2 to 5). Only the steel structure is modified: the two I-girders are replaced by an inclined web box section.

The concrete slab is connected to an open box section with the following features (see Figure 1.1):

- total depth of the steel box section: 2.60 m
- centre-to-centre distance between webs in the upper part (identical to the two-girder bridge): 7.00 m
- centre-to-centre distance between webs in the lower part: 5.60 m
- width of upper flanges: 1.10 m
- width of lower flange: 5.80 m

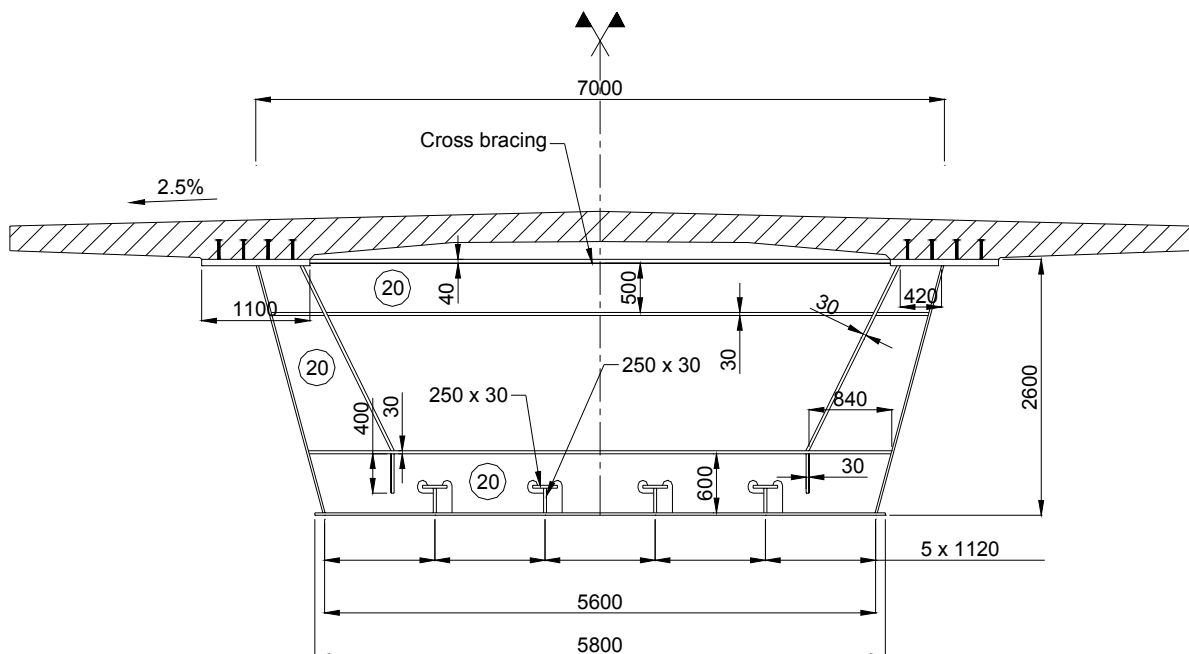


Figure 1.1: Cross-section of the composite box-girder bridge

As the upper flange is wider for the box section ($b_{fs} = 1100$ mm) than for the two-girder bridge ($b_{fs} = 1000$ mm), the geometry of the slab should be slightly reworked. The box section calculations are therefore performed with the following equivalent thicknesses for the slab:

$$e_1 = 31.3 \text{ cm} \text{ (to model the main slab)}$$

$$e_2 = 10.2 \text{ cm} \text{ (to model the concrete haunch)}$$

Figure 1.2 illustrates the modeled concrete slab.

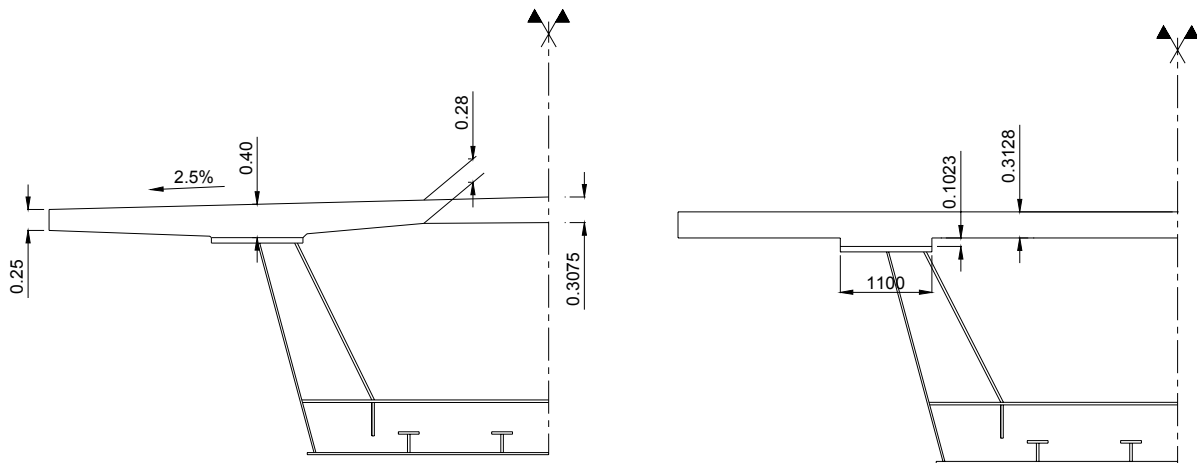


Figure 1.2: Modeling the concrete slab for the longitudinal global analysis

The longitudinal and transverse reinforcement described in Part II, Figures 3.6 and 3.7, is maintained for the box section calculations presented in this Part III.

For the longitudinal bending calculations, a reinforcement layer is modeled by concentrating all its high bond bars at the same location, just above the junction point of the steel main web with the upper box section flange. As for the two-girder bridge (see Part II, paragraph 3.5.4), the reinforcement areas are introduced into the design model as ratios of the total area of the concrete slab:

- upper layer in mid-span sections: $\rho_s = 0.46\%$ located at a distance $y = 0.061$ m
- lower layer in mid-span sections: $\rho_s = 0.46\%$ located at a distance $y = 0.021$ m
- upper layer in support sections: $\rho_s = 0.73\%$ located at a distance $y = 0.063$ m
- lower layer in support sections: $\rho_s = 0.46\%$ located at a distance $y = 0.021$ m

For the total reinforcement in a transverse section, this corresponds to a ratio of 0.92% in mid-span sections and of 1.19% in support sections (see Figure 3.7 of Part II for classifying the sections between mid-span and support zones).

1.2 - Structural steel distribution

The structural steel distribution (upper flange, bottom flange and main web) is illustrated in Figure 1.4. Only the design of the cross-section at internal support is justified for ULS combination of actions (see paragraph 5 of this Part III). In this cross-section the upper flange is 125 mm thick against 40 mm thick for the bottom flange. The web is 23 mm thick.

The main stiffening of the structural steel part of the bridge is formed of transverse frames every 4.0 m. These frames are made up of T-shaped transverse stiffeners in the bottom flange and the webs. The bottom flange is also stiffened by four T-shaped longitudinal stiffeners as shown in Figure 1.3 below. The web and flange plate of each T-shaped longitudinal stiffener is a 250 x 30 mm² section.

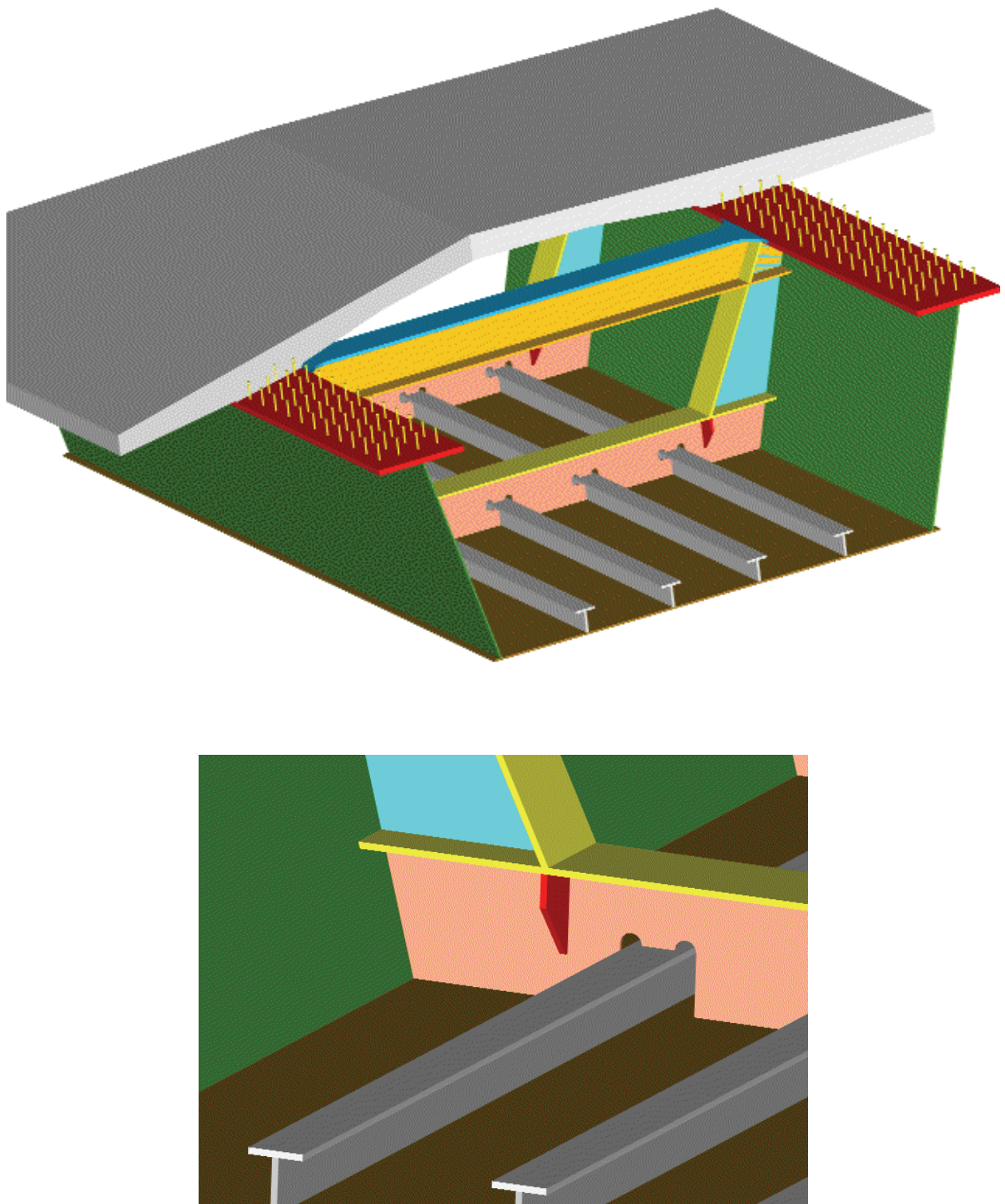


Figure 1.3: Longitudinal stiffeners and transverse cross-bracing in the box-girder bridge

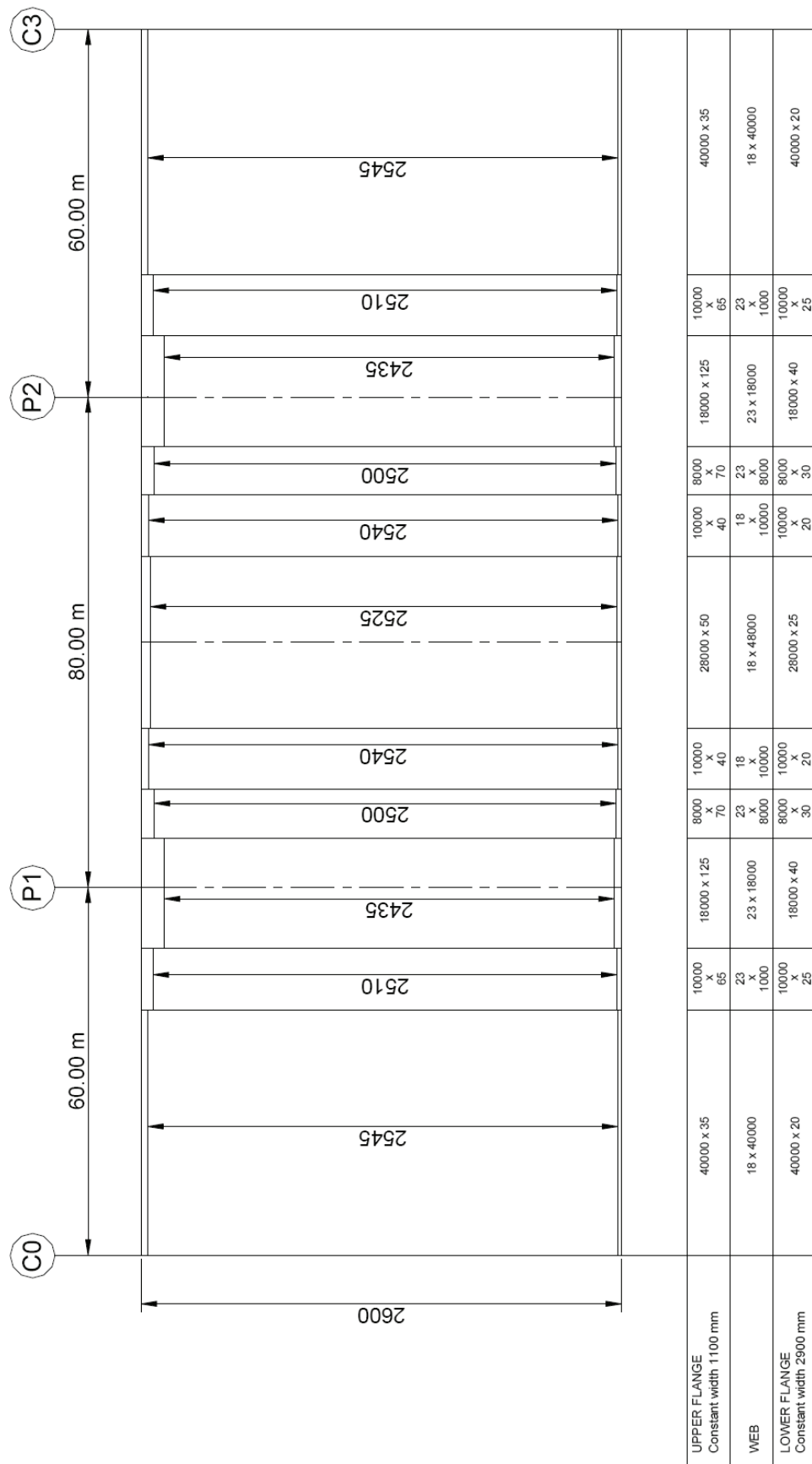


Figure 1.4: Structural steel distribution for the half box-girder

2 - Actions and combinations of actions

The actions used for the box-girder bridge design are the same as described for the two-girder bridge in Part II, chapter 5. All the combinations of actions in Part II, chapter 6 can also be used here.

2.1 - Permanent loads

2.1.1 - Selfweight

Based on the structural steel distribution in Figure 1.4, the weight of the main steel part for a half box section (over the 200 m long deck) is 2946 kN.

To calculate internal forces and moments as well as stresses in the main girders, it is assumed that the weight of transverse frames and longitudinal stiffeners in the bottom flange is uniformly distributed. It is estimated by using the dimensions proposed in Figure 1.1. This gives a uniform load of 4.5 kN per unit length for a half box section. For the design example, the stiffening therefore represents 23.4% of the total weight of the box section (main structural steel part + stiffening) or 30.5% of the weight of the main structural steel part alone.

The modeled slab section is illustrated in Figure 1.2. Its density is $\gamma_b = 25 \text{ kN/m}^3$ (reinforced concrete).

2.1.2 - Non-structural bridge equipments

The non-structural bridge equipments (parapet, surfacing,...) of the composite box-girder bridge are the same as for the two-girder bridge (see Part II, paragraph 5.1.2).

2.2 - Concrete shrinkage

The shrinkage at early age and at infinite time is calculated using the same rules as developed in Part II, paragraph 5.2 of this guide.

The only modification lies in the value of the notional size $h_0 = 703 \text{ mm}$ due to the new dimensions of the concrete slab section. The coefficient k_h is not changed and only the value of $\beta_{ds}(t, t_s)$ moves from 0.10 to 0.095. The influence is really small ($\varepsilon_{cs} = 6.9 \cdot 10^{-5}$ instead of $7 \cdot 10^{-5}$) on the shrinkage at early age and this has not been considered in the global analysis of the composite box-girder bridge.

Remember therefore that the shrinkage strain considered is $1.7 \cdot 10^{-4}$ at traffic opening and $2.4 \cdot 10^{-4}$ at infinite time.

2.3 - Concrete creep – Modular ratio

The modular ratio for the calculations at traffic opening – determined in Part II, paragraph 5.3 for the two-girder bridge – is still valid for the box-girder bridge: $n_0 = 6.1625$.

At infinite time, the modification of the notional size $h_0 = 703 \text{ mm}$ (instead of 674 mm) changes the modular ratio values very slightly. This modification has no impact on the results of the global analysis and the modular ratios already calculated for the two-girder bridge have therefore been retained for the box-girder bridge.

2.4 - Variable actions

The climatic actions (wind and temperature) are identical to those already defined for the two-girder bridge in Part II, paragraphs 5.4.6 and 5.4.7. For the traffic loads, the lanes are positioned exactly as described in Part II, paragraph 5.4.2. On the assumption that there is sufficient stiffening to prevent the deformation of the cross-sections, the eccentric traffic loads Q and q are dealt with by modeling them using centered loads with the same values Q and q , and torque loads (M_Q for the concentrated one and m_q for the distributed one). See Figure 2.1. Point C is the shear centre of the cross-section.

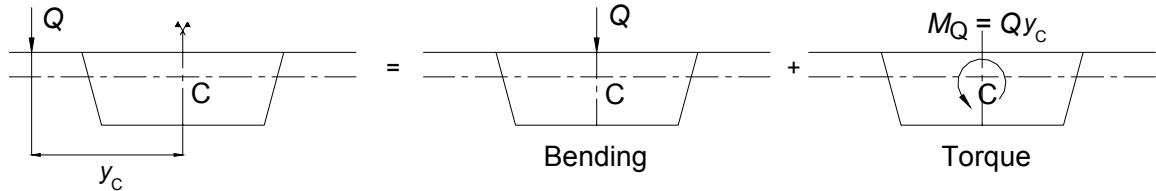


Figure 2.1: Calculation of the box-girder for eccentric concentrated load

The eccentric horizontal actions (like transverse wind, for example) should be dealt with in the same way. No provision has been made for them in the calculations performed for this Part III, however. Remember also that the torque verifications in the box section at support P1 are not addressed in this guide.

2.4.1 - Tandem System TS

Two unfavourable load cases should be considered depending on whether the bending behaviour or torque behaviour is studied:

- case 1: loading on the three traffic lanes (the least favourable vertical load for bending);
- case 2: loading on lanes no. 1 and no. 2 (the least favourable for torque).

For case 1, by taking up the positions and loads of tandem systems in Part II, Figure 5.3, it is deduced that the concentrated vertical load due to TS traffic loads and centered in the box section axis is $Q = 270+160+80 = 510$ kN and that the concentrated torque moment due to TS traffic loads is $M_Q = 270 \times 4 + 160 \times 1 - 80 \times 2 = 1080$ kN.m.

For case 2, the values becomes $270+160 = 430$ kN for the concentrated vertical load and 1240 kN.m for the concentrated torque moment.

2.4.2 - Uniformly Distributed Load UDL

As for the tandem systems, two unfavourable load cases can be envisaged:

- case 1: loading on the three traffic lanes and the remaining area (the least favourable vertical load for bending), see Figure 2.2;
- case 2: loading on whole traffic lane no. 1 and partially on traffic lane no. 2 up to the box section axis of symmetry (the least favourable for torque).

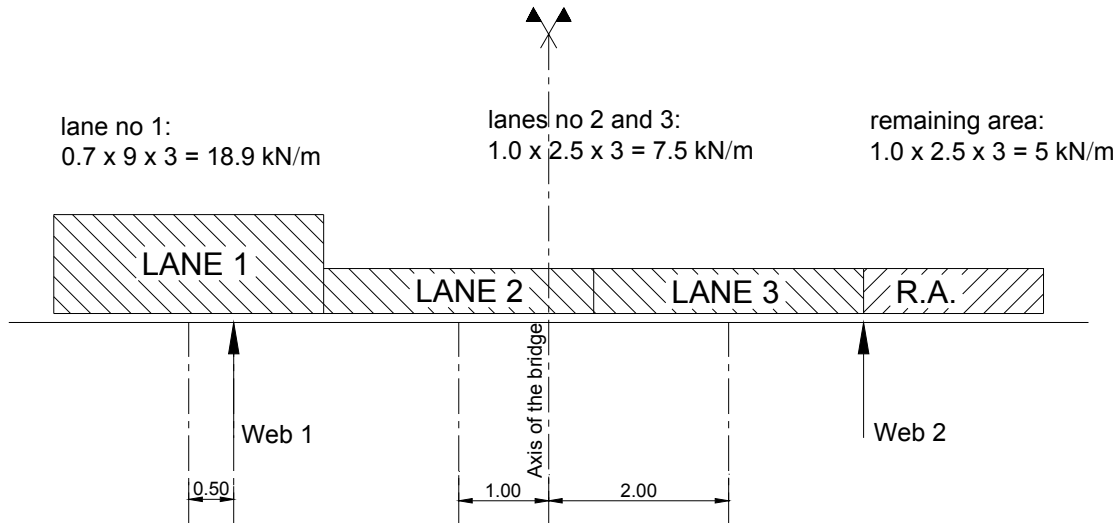


Figure 2.2: UDL transverse distribution on the bridge deck for unfavourable case no. 1

For case 1, it is deduced that the distributed vertical load centered in the box section axis is $q = 18.9 + 7.5 \times 2 + 5 = 38.9 \text{ kN}$ per unit length and that the distributed torque moment is $m_q = 18.9 \times 4 + 7.5 \times 1 - 7.5 \times 2 - 5 \times 4.5 = 45.6 \text{ kN.m}$ per unit length.

For case 2, the values become $18.9 + 1.0 \times 2.5 \times 2.5 = 25.15 \text{ kN}$ for the distributed vertical load per unit length and $m_q = 18.9 \times 4 + 6.25 \times (2.5/2) = 83.4 \text{ kN.m}$ for the distributed torque moment per unit length.

2.4.3 - Climatic loads

As for the two-girder bridge, the temperature effects are considered with a thermal stress block corresponding to $\pm 10^\circ\text{C}$ in the concrete slab compared with the structural steel part.

The wind action is not taken into account in the global analysis.

3 - Global analysis

3.1 - General

The global analysis methods outlined in Part II, paragraph 7.1 are also valid for the composite box-girder bridge. Like the concrete slab in the two-girder bridge, the steel bottom flange has a significant width in comparison with the span lengths. Its shear lag should therefore be taken into account in the global analysis. The effective width concept is used as for the concrete slab.

EN1993-1-5, 2.2(1)

However, unlike for the slab, distinction will be made here between:

- the effective width resulting from the shear lag and designated by « effective^s width » (s for shear lag);
- the effective width resulting from local and/or global plate buckling of the stiffened plate and designated by « effective^p width » (p for plate buckling).

The effective^s width is taken into account in the global analysis. The effective^p width should be considered in the global analysis only in the rare cases when the corresponding effective^p cross-sectional area of the stiffened bottom flange becomes less than half the gross cross-sectional area of this same flange. Note that this will then imply an iterative global analysis, as the ULS internal forces and moments need to be known in order to determine the effective^p cross-sectional area.

EN1993-1-5, 2.2(5)

3.2 - Shear lag

For the box-girder bridge global analysis, the shear lag is taken into account by:

- an effective width of the concrete slab which is the same as the one determined for the two-girder bridge (see Part II, paragraph 7.2.2);
- an effective^s width of the steel bottom flange which is equal to the smallest of the values between the actual total width and $L/8$ on each side of the web where L is the span length or twice the distance between the support and the free end for a cantilever element.

EN1993-1-5, 2.2(3)

In this design example, given the fairly large span lengths, the shear lag effect does not reduce the width at all for the concrete slab as well as for the bottom plate.

A bottom flange with a half-width $b_0 = 2800$ mm gives:

- for the end spans, $b_{\text{eff}} = \min(b_0; L/8) = b_0$ with $L_1 = 60$ m;
- for the central span, $b_{\text{eff}} = \min(b_0; L_2/8) = b_0$ with $L_2 = 80$ m.

3.3 - Internal forces and moments

The internal forces and moments in the composite box-girder bridge have been calculated using a beam model and respecting the construction phases defined in Part II, paragraph 3.4. The model is simply supported at the abutments and piers.

As for the two-girder bridge, a cracked global analysis is performed and the concrete strength is neglected in the cracked zones surrounding the intermediate supports P1 and P2. Compared with the two-girder bridge where the eccentric position of the conventional traffic lane no 1 results in higher loads in the closest main girder, the traffic loads are now equally resisted by the two webs of the box section. Their influence in the stress calculations is thus reduced. Following the uncracked global analysis, the tensile stresses in the concrete slab for characteristic SLS combination of actions (see Figure 3.1) are therefore lower in absolute value (compared with Part II, Figure 7.2). The cracked zones for the composite box-girder bridge are thus smaller than for the two-girder bridge:

- around internal support P1, the cracked zone extends from the abscissa 54.8 m to 67.1 m, i.e. 8.6% of the end span length and 8.9% of the central span length;
- around internal support P2, the cracked zone extends from the abscissa 135.0 m to 145.4 m, i.e. 9.1% of the end span length and 6.2% of the central span length.

The lack of symmetry in the cracked zones between the two supports is related to the concreting steps. The observed cracked lengths are clearly smaller than the ones obtained by using the simplified calculation method (15% of span lengths either side of each support).

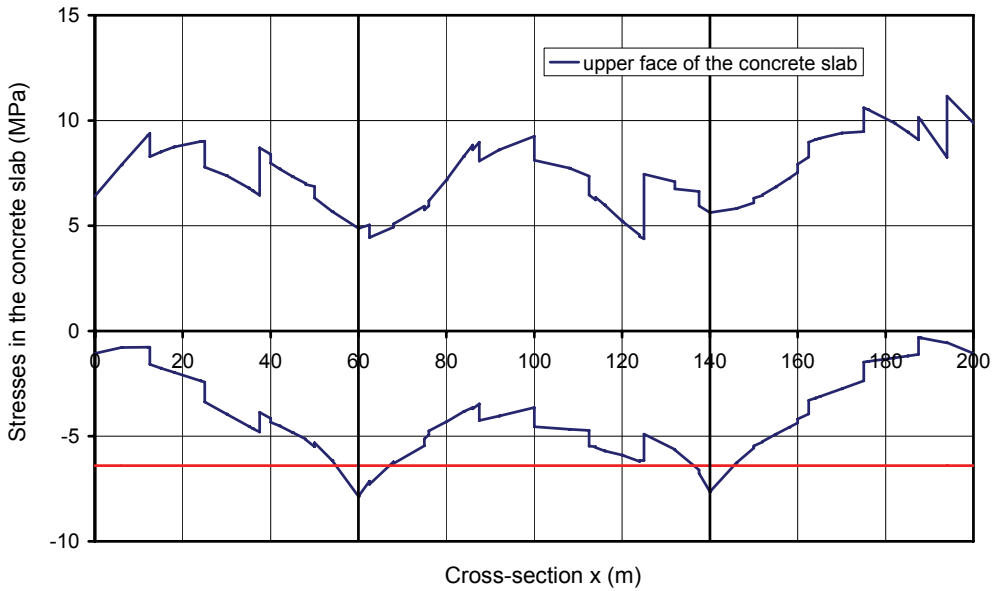


Figure 3.1: Cracked zones for the global analysis

The stresses (for characteristic SLS combination of actions) in Figure 3.1 have been calculated by multiplying the internal forces and moments from the uncracked global analysis (obtained by taking account of effective^s widths for the global analysis, see paragraph 3.2 above) with the mechanical properties of cross-sections (taking account of effective^s widths for the section analysis, explained in paragraph 4.1 of this Part III).

Figures 3.2 and 3.3 illustrate the envelope of bending moments and shear forces obtained for the characteristic SLS combination of actions and the ULS combination of actions after the cracked analysis.

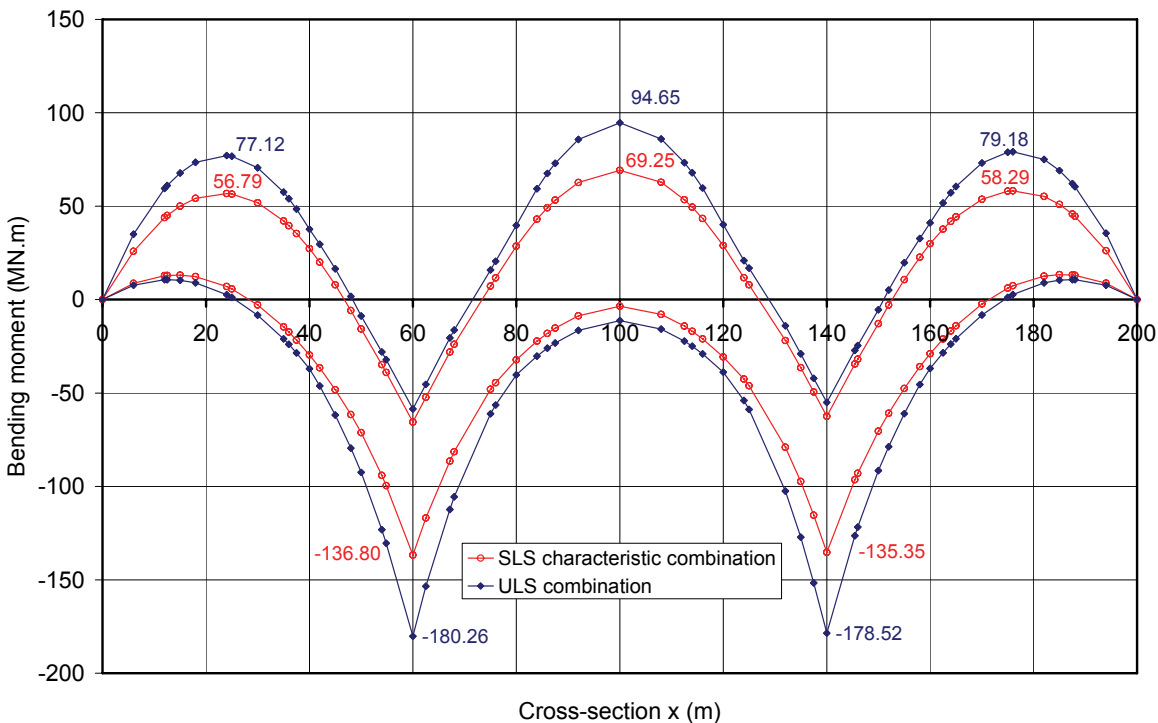


Figure 3.2: Bending moments for the final combinations of actions (ULS and characteristic SLS)

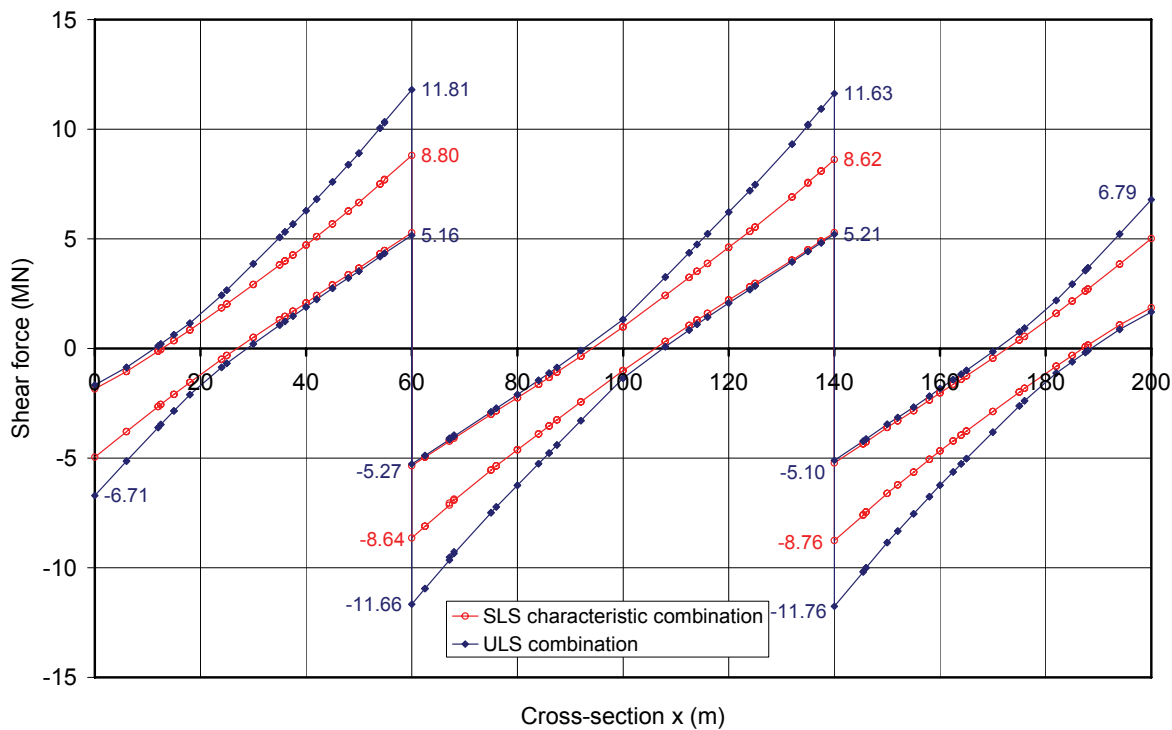


Figure 3.3: Shear force for the final combinations of actions (ULS and characteristic SLS)

4 - Section analysis

The normal and shear stresses are calculated in the structural steel part, in the concrete slab and the reinforcement by using the internal forces and moments determined in the previous paragraph for each load case.

The only difference in comparison with the two-girder bridge lies in the use of the effective cross-sectional area of the bottom flange. Distinction is made between the shear lag effects for calculating stresses at SLS and at fatigue ULS on one hand, and the shear lag effects for calculating stresses at ULS on the other hand.

EN1993-1-5, 3.1(2)

4.1 - Shear lag (SLS and fatigue ULS)

The effective^s width is determined by applying a reduction factor $\beta \leq 1.0$ to the actual width b_0 of the bottom flange: $b_{\text{eff}} = \beta \cdot b_0$

EN1993-1-5, 3.2.1(1)

The factor β is given in function of κ in Table 3.1 of EN1993-1-5. The coefficient κ is calculated using the following equation:

$$\kappa = \frac{\alpha_0 b_0}{L_e} \text{ where } \alpha_0 = \sqrt{1 + \frac{A_{\text{sl}}}{b_0 t}} \text{ and } L_e \text{ is the equivalent length for each span.}$$

EN1993-1-5, Table 3.1

A_{sl} represents the area of all the longitudinal stiffeners within the actual width b_0 (see Figure 4.1) and t is the flange thickness.

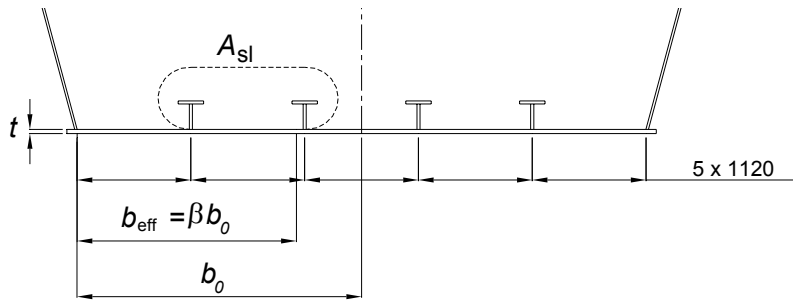


Figure 4.1: Defining A_{sl} , b_0 , t and b_{eff}

In the design example $A_{sl} = 2x[2x(250x30)] = 30000 \text{ mm}^2$ and $b_0 = 2800 \text{ mm}$.

The bottom flange thickness t varies along the bridge length (see Figure 1.4). The coefficients α_0 are therefore calculated with the thickness in the considered cross-section, i.e. at mid-span for the in-span calculations (factor β_1) and at support for the calculations around internal support (factors β_0 and β_2). For the design example, this gives:

- at mid-end span and at end support: $t = 20 \text{ mm}$ therefore $\alpha_0 = 1.239$
- at mid-central span: $t = 25 \text{ mm}$ therefore $\alpha_0 = 1.195$
- at internal support: $t = 40 \text{ mm}$ therefore $\alpha_0 = 1.126$

EN1993-1-5, Table 3.1

EN1993-1-5, Figure 3.1

The equivalent spans L_e are:

- at mid-end span and at end support: $L_e = 0.85 \cdot L_1 = 51 \text{ m}$
- at mid-central span: $L_e = 0.7 \cdot L_2 = 56 \text{ m}$
- at internal support: $L_e = 0.25 \cdot (L_1 + L_2) = 35 \text{ m}$

EN1993-1-5, 3.2.1(2)

The following values of κ are obtained:

- at mid-end span and at end support: $\kappa = 0.068$
- at mid-central span: $\kappa = 0.060$
- at internal support: $\kappa = 0.090$

EN1993-1-5, Table 3.1

This finally gives the values for the reduction factor β :

- in end span (sagging bending moment zone $M>0$):

$$0.02 \leq \kappa = 0.068 \leq 0.70$$

$$\beta = \beta_1 = \frac{1}{1 + 6.4\kappa^2} = 0.971$$

- in central span (sagging bending moment zone $M>0$):

$$0.02 \leq \kappa = 0.060 \leq 0.70$$

$$\beta = \beta_1 = \frac{1}{1 + 6.4\kappa^2} = 0.977$$

- at internal support (hogging bending moment zone $M<0$):

$$0.02 \leq \kappa = 0.090 \leq 0.70$$

$$\beta = \beta_2 = \frac{1}{1 + 6.0 \left(\kappa - \frac{1}{2500\kappa} \right) + 1.6\kappa^2} = 0.655$$

- at end support:

$$\kappa = 0.068$$

$$\beta = \beta_0 = \left(0.55 + \frac{0.025}{\kappa} \right) \beta_1 \leq \beta_1 \text{ with } \beta_1 = 0.971 \text{ (end span)}$$

hence $\beta_0 = 0.891$

EN1993-1-5, Table 3.1

The following effective widths are finally obtained:

- in end span: $b_{\text{eff}} = \beta_1 \cdot b_0 = 2719 \text{ mm}$;
- in central span: $b_{\text{eff}} = \beta_1 \cdot b_0 = 2736 \text{ mm}$;
- at internal support: $b_{\text{eff}} = \beta_2 \cdot b_0 = 1834 \text{ mm}$; at end support: $b_{\text{eff}} = \beta_0 \cdot b_0 = 2495 \text{ mm}$.

Figure 4.2 illustrates the part of the box-girder bottom flange that would have to be taken into account to calculate the stresses at SLS and at fatigue ULS. As for the effective width of the concrete slab, the effective^s width of the steel bottom flange varies by quarter of a span based on the values calculated above.

EN1993-1-5, Figure 3.1

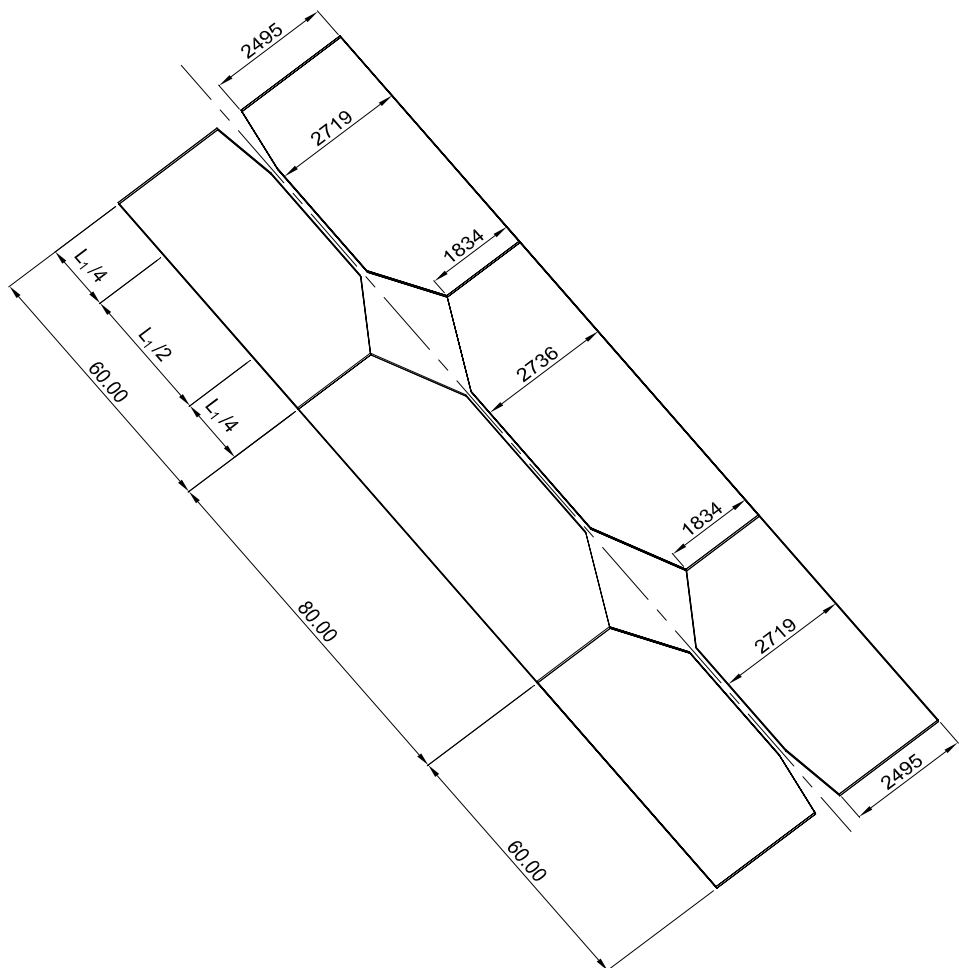


Figure 4.2: Effective^s width for the cross-section analysis at SLS or at fatigue ULS

For a longitudinally stiffened plate, in order to avoid discontinuous longitudinal changes in the mechanical properties of the cross-sections (a stiffener is not taken into account if its location is outside the effective^s width), the method suggested here is to multiply the thickness of the bottom plate, the thickness of stiffener webs and the thickness of stiffener flanges by β , rather than to reduce only the width b_0 (as in Figure 4.2). The mechanical properties obtained with

these reduced dimensions maintain the initial location of the neutral plane of each plate element. They are used to calculate the stresses at SLS and at fatigue ULS in conjunction with the internal forces and moments from the global analysis.

4.2 - Shear lag (ULS)

At ULS three methods of calculating the effective^s width for shear lag are proposed in EN1993-1-5, 3.3, to be chosen by the National Annex. The method recommended in note 3 of EN1993-1-5, paragraph 3.3(1) is adopted here. The shear lag effects are therefore elastic-plastic allowing limited plastic strains.

EN1993-1-5, 3.3(1)
note 3 + National Annex

The shear lag is taken into account at ULS via the reduction factor β^s where β is the elastic factor determined in the previous paragraph. The coefficient κ is also determined according to the previous paragraph.

For example, for the cross-section at internal support, this gives:
 $\beta^s = 0.655^{0.09}$ i.e. $0.9626 \geq \beta = 0.655$

This coefficient is then applied to the effective^p cross-sectional area $A_{c,eff}$ obtained by reducing the gross area A_c of the **compressed** bottom flange to take account of its buckling (see the design example in paragraph 5 of this Part III for further detail). The bottom flange effective cross-sectional area A_{eff} which is used to calculate the stresses at ULS, is therefore equal to $\beta^s A_{c,eff}$.

Where the bottom flange is **in tension** (in span), the factor β^s is applied directly to the gross area A_c of the stiffened bottom flange (no risk of buckling) to obtain the effective cross-sectional area A_{eff} .

As explained further on in the case of the **compressed** bottom flange (around internal support), see Figure 5.5, the method suggested here is to apply the factor β^s to all the thicknesses of plate elements rather than to reduce only the width of the bottom flange.

5 - Verification of the box section at support P1 for ULS combination of actions

5.1 - Mechanical properties of the gross cross-section

The steel box section is 2600 mm deep. It is made up of the following elements (see Figure 5.1):

- upper flanges 1100 mm wide and 125 mm thick,
- web 2522 mm deep (following the inclination) and 23 mm thick,
- bottom flange 5800 mm wide and 40 mm thick.

The steel bottom flange is stiffened by 4 longitudinal T-shaped stiffeners:

- stiffener web 250 mm deep and 30 mm thick,
- stiffener flange 250 mm wide and 30 mm thick.

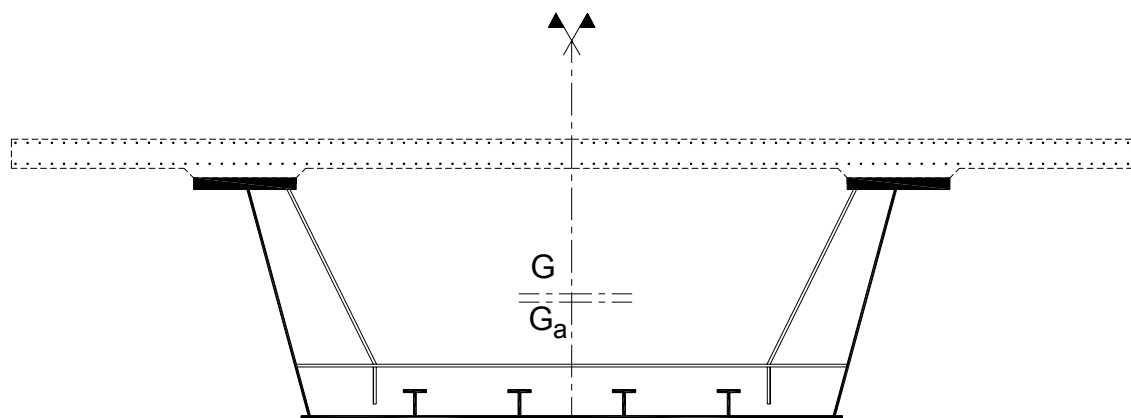


Figure 5.1: Gross cross-section at support P1

As the concrete slab is in tension around internal support P1, its strength is not taken into account for checking the cross-section. Only the longitudinal slab reinforcement is considered.

The mechanical properties of the box section structural steel part alone (including the four longitudinal stiffeners) are therefore:

- area : $A_a = 0.6830 \text{ m}^2$
- second moment of area : $I_a = 0.9267 \text{ m}^4$
- distance between the centre of gravity G_a and the upper face of the upper flange: $v_{s,a} = 1337 \text{ mm}$
- distance between the centre of gravity G_a and the lower face of the bottom flange: $v_{i,a} = 1263 \text{ mm}$

The mechanical properties of the composite box section (structural steel part and reinforcement) are therefore:

- area : $A = 0.7298 \text{ m}^2$
- second moment of area : $I = 1.0394 \text{ m}^4$
- distance between the centre of gravity G and the upper face of the upper flange: $v_s = 1235 \text{ mm}$
- distance between G and the lower face of the bottom flange: $v_i = 1365 \text{ mm}$
- distance between G and the upper reinforcement layer: $v_{arma} = 1587 \text{ mm}$

5.2 - Internal forces and moments

The internal forces and moments obtained by the design model at ULS after the cracked global analysis and respecting the construction steps are as follows for the whole box section (see Figures 3.2 and 3.3):

$$M_{Ed} = -180.26 \text{ MN.m}$$

$$V_{Ed} = 11.81 \text{ MN i.e. } 6.11 \text{ MN in each steel web by taking its inclination into account}$$

The bending moment M_{Ed} is the sum of the moment $M_a = -102.12 \text{ MN.m}$ applied to the box section as long as it behaves as a pure structural steel structure (before the concreting step of the slab segment which includes the studied box section) and of the moment $M_c = -78.14 \text{ MN.m}$ applied to the composite box section (structural steel part + reinforcement).

5.3 - Effective area of the bottom flange

The bottom flange is a stiffened plate illustrated in Figure 5.2. It is stiffened by the four longitudinal T-shaped stiffeners previously described and by transverse stiffeners which are regularly spaced every 4 m. As it is in compression at ULS for the studied box section at internal support P1, attention should be paid to its potential plate buckling.

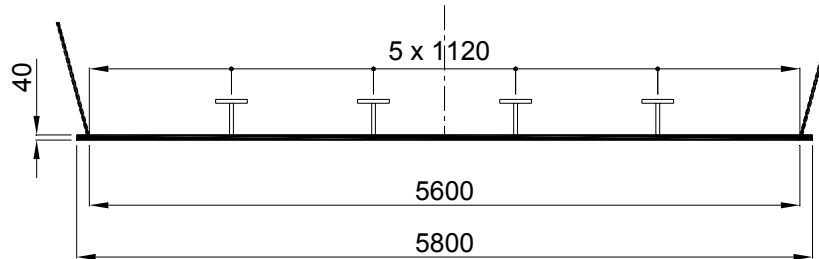


Figure 5.2: Steel bottom flange with longitudinal stiffeners

5.3.1 - Plate buckling of elementary sub-panels

The first task is to verify that the elementary sub-panels do not buckle. In the section at support P1, these sub-panels are all uniformly in compression ($\gamma = 1$):

- bottom flange sub-panel: $1090 \times 40 \text{ mm}^2$
 $c/t = 27.25 = 33.02 \cdot \varepsilon \leq 38 \cdot \varepsilon$ therefore class 2 element
- stiffener web: $250 \times 30 \text{ mm}^2$
 $c/t = 8.33 = 10.1 \cdot \varepsilon \leq 33 \cdot \varepsilon$ therefore class 1 element
- outstand cantilever flange of the stiffener: $110 \times 30 \text{ mm}^2$
 $c/t = 3.66 = 4.44 \cdot \varepsilon \leq 9 \cdot \varepsilon$ therefore class 1 element

EN1993-1-1, Table 5.2
(sheet 1/3)

EN1993-1-1, Table 5.2
(sheet 2/3)

None of these sub-panels therefore show any risk of plate buckling and are fully effective: $\rho = 1$ where ρ is the reduction factor applied to the gross area to obtain the effective^p area.

If one of them had been a class 4 element, it would have been necessary to determine its effective^p area using EN1993-1-5, 4.4 (see Annex II at the end of the guide for a design example in this case).

5.3.2 - Global buckling of the stiffened panel

The second task is to verify that the stiffened bottom plate does not buckle as a whole.

The corresponding effective^p area $A_{c,eff}$ is calculated using the following equation:

$$A_{c,eff} = \rho_c A_{c,eff,loc} + A_{c,eff,edges}$$

where:

- $A_{c,eff,loc}$ is the effective^p area of the central part of the stiffened plate taking account of the buckling in the sub-panels (see Figure 5.3);
- $A_{c,eff,edges}$ is the effective^p area of the edges of the stiffened plate taking account of the buckling in the lateral sub-panels (see Figure 5.3);
- ρ_c is the reduction factor of the stiffened plate determined by examining its overall behaviour. This factor only affects the central part of the stiffened plate.

Figure 5.3 illustrates these effective^p areas in the case of the studied geometry by assuming that there would have been a reduction in area for buckling of the elementary sub-panels uniformly in compression.

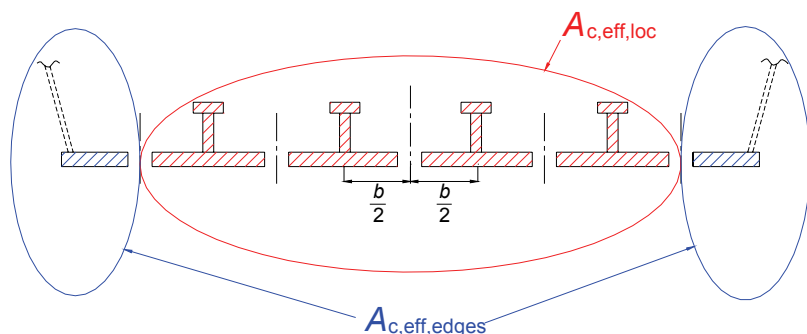


Figure 5.3: Distinguishing central and edge parts in the longitudinally stiffened steel bottom flange

The effective^p area $A_{c,eff}$ thus determined is then reduced by the coefficient for the shear lag effect (see paragraph 4.2 of this Part III).

EN1993-1-5, 3.3(1)
note 3

The reduction factor ρ_c is determined by interpolation between the reduction factors determined for the column buckling of a stiffener associated with a partaking width of the bottom plate (column type behaviour χ_c) and for the plate buckling of the global stiffened flange (plate type behaviour ρ):

$$\rho_c = (\rho - \chi_c) \xi (2 - \xi) + \chi_c$$

The coefficient ξ is defined further on.

EN1993-1-5, 4.5.4(1)

a) Column type behaviour (factor χ_c)

The column cross-section to be considered is made up of the effective cross-section of a longitudinal stiffener and the effective cross-section of the partaking bottom plate surrounding the stiffener. All these effective areas are calculated with respect to the buckling of elementary sub-panels (see Figure 5.4). For the design example, this cross-section is fully in compression ($\psi = 1$).

EN1993-1-5, Figure A-1

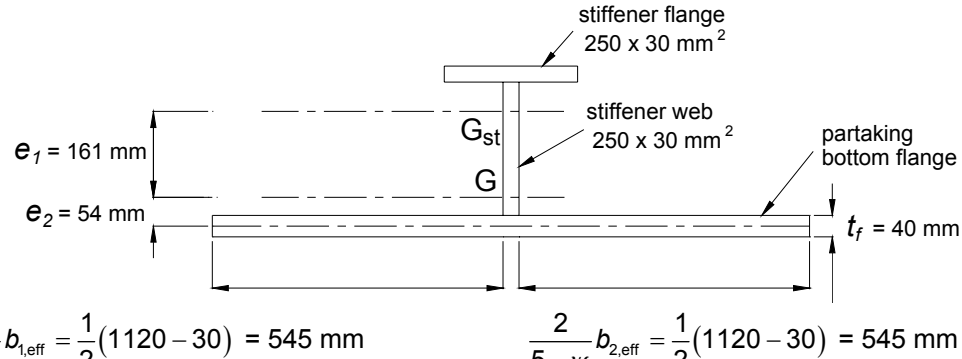


Figure 5.4: Column cross-section

The mechanical properties of this column are as follows:

- $e_1 = 161 \text{ mm}$ (distance between the centre of gravity of the column and the centre of gravity of the stiffener alone);
- $e_2 = 54 \text{ mm}$ (distance between the centre of gravity of the column and the centre of gravity of the partaking bottom plate)
- $A_{sl,1} = 59800 \text{ mm}^2$
- $I_{sl,1} = 6.385 \cdot 10^8 \text{ mm}^4$

The elastic critical column buckling stress is:

$$\sigma_{cr,c} = \frac{\pi^2 E_a I_{sl,1}}{A_{sl,1} a^2} = 1383 \text{ MPa}$$

(with $a = 4 \text{ m}$, length of the column between transverse frames of the box-girder).

The efficiency coefficient of the column with respect to local plate buckling (see paragraph 5.3.1) is:

$$\beta_{A,c} = \frac{A_{sl,1,eff}}{A_{sl,1}} = 1.0$$

The reduced slenderness of the column is deduced:

$$\bar{\lambda}_c = \sqrt{\frac{\beta_{A,c} f_y}{\sigma_{cr,c}}} = 0.5$$

The reduction factor χ_c is calculated by using the column buckling curve c for open stiffeners. In case of closed stiffeners, the column buckling curve b should be adopted. The usual imperfection factor $\alpha = 0.49$ of the curve c is replaced by:

$$\alpha_e = \alpha + \frac{0.09}{i/e} = 0.63$$

where $i = \sqrt{\frac{I_{sl,1}}{A_{sl,1}}} = 103.3 \text{ mm}$ and $e = \max(e_1; e_2) = 161 \text{ mm}$

This therefore gives:

$$\Phi = 0.5 \cdot \left[1 + \alpha_e (\bar{\lambda}_c - 0.2) + \bar{\lambda}_c^2 \right] = 0.72$$

$$\chi_c = \frac{1}{\Phi + \sqrt{\Phi^2 - \bar{\lambda}_c^2}} = 0.808$$

EN1993-1-5, 4.5.3(3)

EN1993-1-5, 4.5.3(4)

EN1993-1-5, 4.5.3(5)

EN1993-1-1, 6.3.1.2

b) Plate type behaviour (factor ρ)

The elastic critical plate buckling stress of the stiffened plate is:

$$\sigma_{\text{cr,p}} = k_{\sigma,p} \cdot \sigma_E \text{ with } \sigma_E = \frac{\pi^2 E_a t^2}{12(1-\nu^2)b^2} = 9.68 \text{ MPa}$$

The plate buckling coefficient $k_{\sigma,p}$ is obtained using specific software or appropriate charts. Annex A1 to EN1993-1-5 gives an approximate formulation where the plate is fitted with at least three longitudinal stiffeners equally spaced:

$$\psi = 1$$

$$\alpha = a/b = 0.714 \geq 0.5$$

$$\delta = \frac{\sum A_{\text{sl}}}{bt_f} = 0.268$$

$$\gamma = I_{\text{sl}} \frac{12(1-\nu^2)}{bt_f^3} \text{ where } I_{\text{sl}} = 2.67 \cdot 10^9 \text{ mm}^4 \text{ is the second moment of area of the stiffened plate.}$$

Hence $\gamma = 81.35$

As $\alpha \leq \sqrt[4]{\gamma} = 3.003$, this gives:

$$k_{\sigma,p} = \frac{2 \left[(1+\alpha^2)^2 + \gamma - 1 \right]}{\alpha^2 (\psi + 1)(1+\delta)} = 127.83$$

$\sigma_{\text{cr,p}} = 1237.4 \text{ MPa}$ is deduced.

The efficiency coefficient of the plate with respect to local plate buckling (see paragraph 5.3.1) is $\beta_{A,c} = \frac{A_{c,\text{eff,loc}}}{A_c} = 1.0$.

$$\bar{\lambda}_p = \sqrt{\frac{\beta_{A,c} f_y}{\sigma_{\text{cr,p}}}} = 0.528$$

As $\bar{\lambda}_p \leq 0.673$ the reduction factor for the plate type behaviour is $\rho = 1$.

EN1993-1-5, Annex A

EN1993-1-5, Annex A1, note 4

c) Reduction factor ρ_c

The interpolation between plate type behaviour and column type behaviour is given by:

$$\rho_c = (\rho - \chi_c) \xi (2 - \xi) + \chi_c \text{ where } 0 \leq \xi = \frac{\sigma_{\text{cr,p}}}{\sigma_{\text{cr,c}}} - 1 \leq 1$$

$\frac{\sigma_{\text{cr,p}}}{\sigma_{\text{cr,c}}} - 1 = -0.105$ therefore $\xi = 0$ i.e. that the bottom flange behaves as a pure column: $\rho_c = \chi_c = 0.808$.

EN1993-1-5, 4.5.2(1)

EN1993-1-5, 4.4(2)

EN1993-1-5, 4.5.4(1)

d) Effective area of the stiffened plate

The effective^{s+p} area (noted effective in EN1993-1-5 without any subscript) of the stiffened plate taking account of plate buckling and shear lag is obtained by:

EN1993-1-5, 4.5.1(3)

$$A_{c,eff}^* = \beta^* A_{c,eff} = \beta^* [\rho_c A_{c,eff,loc} + A_{c,eff,edges}]$$

$\beta^* = 0.9626$ according to paragraph 4.2 of this Part III

$\rho_c = 0.808$ according to the previous paragraph

In the design example there is no reduction for local plate buckling therefore $A_{c,eff,loc}$ and $A_{c,eff,edges}$ correspond to the gross cross-sectional areas of the "middle" and "edge" parts defined in Figure 5.3:

$$A_{c,eff,loc} = 239200 \text{ mm}^2$$

$$A_{c,eff,edges} = (5800-4 \times 1120) \times 40 = 52800 \text{ mm}^2$$

$A_{c,eff}^* = 236870.45 \text{ mm}^2$ is deduced. It may be compared to the initial gross area in compression of the stiffened bottom flange $A_c = 292000 \text{ mm}^2$. This corresponds to a reduction of 19% in the area of the bottom flange.

Figure 5.5 illustrates the geometry of the effective area of the bottom flange when calculating the mechanical properties:

EN1993-1-5, 4.5.1(7)

$$\begin{aligned} t_{st,f} &= 0.78 \times 30 \text{ mm} ; t_{st,w} = 0.78 \times 30 \text{ mm} \\ t_{f,loc} &= 0.78 \times 40 \text{ mm} ; t_{f,edges} = 0.96 \times 40 \text{ mm} \end{aligned}$$

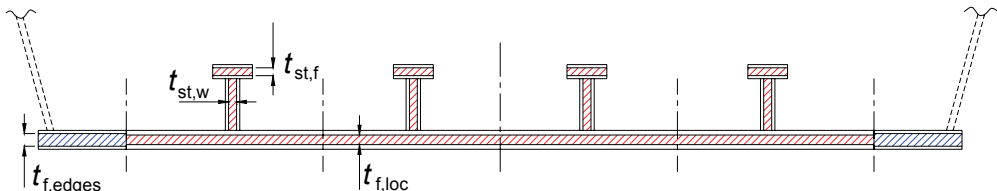


Figure 5.5: Effective cross-section of the stiffened bottom flange

The new mechanical properties of the cross-section are then calculated by replacing the gross area of the bottom flange by its effective area, following the principle in Figure 5.5.

The shape of the bottom flange is thus preserved. The thicknesses of various elements in the "middle" part are multiplied by a coefficient $k_1 = \rho_c \beta^*$ whereas the thicknesses of elements in the "edge" part are multiplied by a coefficient $k_2 = \beta^*$.

The new mechanical properties of the steel part of the box section are therefore:

- area: $A_a = 0.626 \text{ m}^2$
- second moment of area: $I_a = 0.840 \text{ m}^4$
- distance between the centre of gravity G_a and the upper face of the steel top flange: $v_{s,a} = 1230 \text{ mm}$
- distance between the centre of gravity G_a and the lower face of the bottom flange: $v_{i,a} = 1370 \text{ mm}$

The new mechanical properties of the composite box section are therefore (structural steel part + reinforcement):

- area: $A = 0.666 \text{ m}^2$
- second moment of area: $I = 0.927 \text{ m}^4$
- distance between the centre of gravity G and the upper face of the

steel top flange: $v_s = 1138$ mm

- distance between the centre of gravity G and the lower face of the bottom flange: $v_i = 1462$ mm

5.4 - Effective area of the web

From the values of the bending moments M_a and M_c (see paragraph 5.2) and of the mechanical properties in previous paragraph 5.3, the normal extreme stresses in the web at ULS are as follows:

$$\sigma_{\text{inf}} = M_a \cdot \frac{v_{i,a} - t_{\text{fi}}}{I_a} + M_c \cdot \frac{v_i - t_{\text{fi}}}{I} = 280.26 \text{ MPa}$$

$$\sigma_{\text{sup}} = M_a \cdot \frac{v_{s,a} - t_{\text{fs}}}{I_a} + M_c \cdot \frac{v_s - t_{\text{fs}}}{I} = -218.40 \text{ MPa}$$

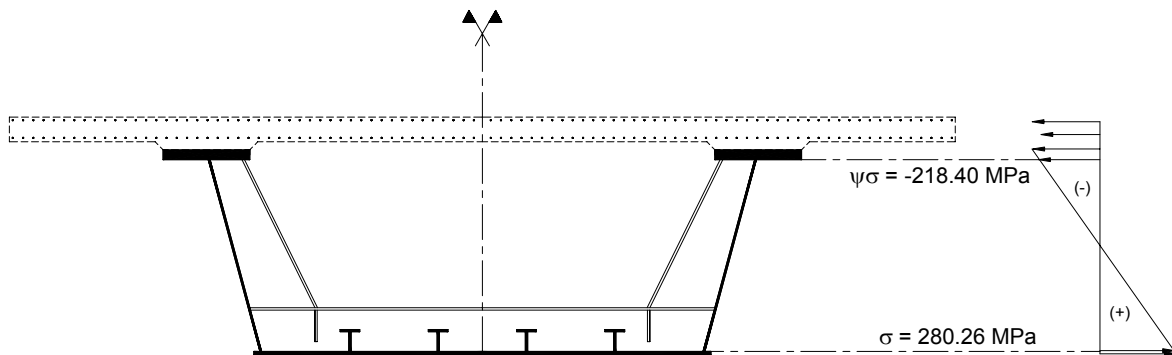


Figure 5.6: Stresses in the web for studying its buckling

$$\psi = \sigma_{\text{sup}} / \sigma_{\text{inf}} = -0.78 > -1$$

$$h_w / t_w = 2521 / 23 = 109.6 \geq \frac{42\epsilon}{0.67 + 0.33\psi} = 84.0$$

The web is therefore a class 4 element and its effective area should be determined.

As $0 > \psi > -1$ the elastic critical plate buckling stress of the web is obtained by:

$$k_\sigma = 7.81 - 6.29\psi + 9.78\psi^2 = 18.67$$

$$\sigma_{\text{cr}} = k_\sigma \cdot \sigma_E = k_\sigma \cdot \frac{\pi^2 E_a}{12 [1 - \nu^2]} \left[\frac{t_w}{h_w} \right]^2 = 295.02 \text{ MPa}$$

The reduced web slenderness is then given by:

$$\bar{\lambda}_p = \sqrt{\frac{f_{yw}}{\sigma_{\text{cr}}}} = 1.081 \geq 0.673$$

The reduction coefficient for web buckling is then given by:

$$\rho = \frac{\bar{\lambda}_p - 0.055[3 + \psi]}{\bar{\lambda}_p^2} = 0.821$$

Using this coefficient ρ and the web depth in compression $h_{w,c} = h_w / (1 - \psi) = 1416$ mm, the effective web depth in compression is deduced $h_{w,\text{eff}} = \rho h_{w,c} = 1163$ mm. This is made up of two web portions:

EN 1993-1-1, Table 5.2

EN 1993-1-5, Table 4.1

EN 1993-1-5, 4.4 (2)

- on the side of the bottom flange over a depth of:
 $h_{w,eff,1} = 0.4 \cdot h_{w,eff} = 465 \text{ mm}$
- above the « plate buckling hole » over a depth of:
 $h_{w,eff,2} = 0.6 \cdot h_{w,eff} = 698 \text{ mm}$

EN 1993-1-5, Table 4.1

Figure 5.7 illustrates the location of the « plate buckling hole » in the web depth.

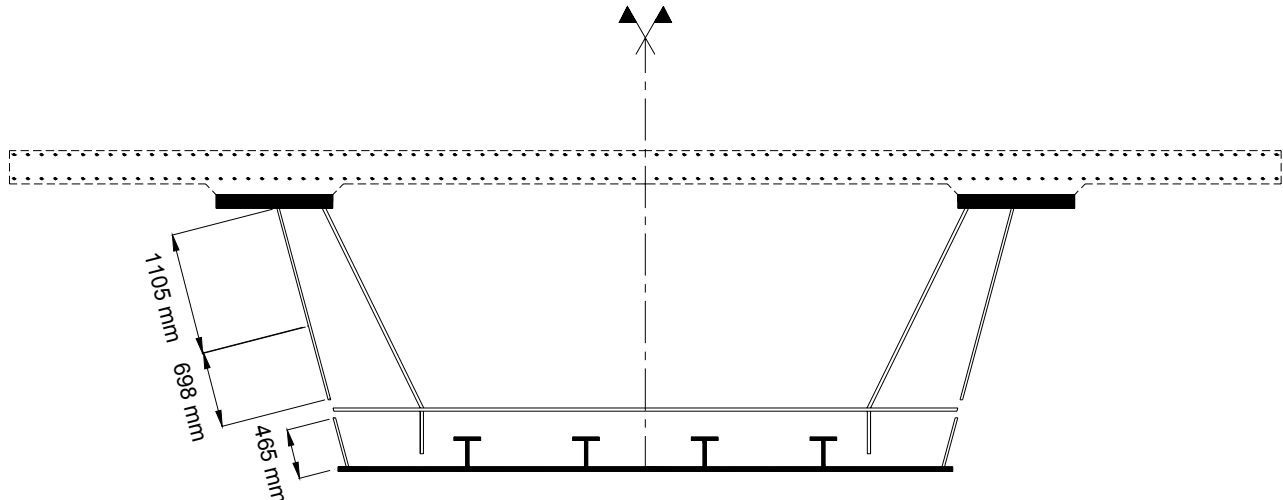


Figure 5.7: Effective cross-section of the webs in the cross-section at P1

Note that the effective area of the box section webs is determined after that of its stiffened bottom flange. The reverse calculation would not lead to the same effective area of the cross-section at P1 and it would not comply with EN1993-1-5.

5.5 - Effective mechanical properties of the box section

The final mechanical properties of the effective structural steel box section (bottom flange and web) are therefore:

- area: $A_{a,eff} = 0.6162 \text{ m}^2$
- second moment of area: $I_{a,eff} = 0.8343 \text{ m}^4$
- distance between the centre of gravity G_a and the upper face of the steel top flange:
 $v_{s,a,eff} = 1218.5 \text{ mm}$
- distance between the centre of gravity G_a and the lower face of the bottom flange:
 $v_{i,a,eff} = 1381.5 \text{ mm}$

The final mechanical properties of the effective composite box section (structural steel and reinforcement) are therefore:

- area: $A_{eff} = 0.6621 \text{ m}^2$
- second moment of area: $I_{eff} = 0.9285 \text{ m}^4$
- distance between the centre of gravity G and the upper face of the steel top flange:
 $v_{s,eff} = 1116 \text{ mm}$
- distance between the centre of gravity G and the lower face of the bottom flange:
 $v_{i,eff} = 1484 \text{ mm}$
- distance between G and the upper reinforcement layer: $v_{reinf.,eff} = 1468 \text{ mm}$

5.6 - Bending resistance verification

From the values of the bending moments M_a and M_c (see paragraph 5.2) and of the mechanical properties in previous paragraph 5.5, the normal extreme stresses at ULS are as follows:

$$\sigma_{s,inf} = M_a \frac{V_{i,a,eff}}{I_{a,eff}} + M_c \frac{V_{i,eff}}{I_{eff}} = 294.0 \text{ MPa}$$

$$\sigma_{s,sup} = M_a \frac{V_{s,a,eff}}{I_{a,eff}} + M_c \frac{V_{s,eff}}{I_{eff}} = -243.1 \text{ MPa}$$

$$\sigma_{s,reinf.} = M_c \frac{V_{reinf.,eff}}{I_{eff}} = -123.5 \text{ MPa}$$

It is then clearly verified that:

$$\sigma_{s,inf} \leq \frac{f_y}{\gamma_{M0}} = 345 \text{ MPa, i.e. } \eta_{1,inf} = 0.852 \leq 1.0$$

$$\sigma_{s,sup} \geq \frac{f_y}{\gamma_{M0}} = -295 \text{ MPa, i.e. } \eta_{1,sup} = 0.824 \leq 1.0$$

$$\sigma_{s,reinf.} \geq \frac{f_{sk}}{\gamma_s} = -434.8 \text{ MPa}$$

EN 1993-1-5, 4.6(1)

The effective box section has been checked here with the calculated bending moment in the cross-section at support P1. This should normally be carried out with a lower value calculated in the cross-section located at the distance $\min [0.4.a; 0.5.h_w] = 1217.5 \text{ mm}$ from the support P1.

EN 1993-1-5, 4.6(3)

Lastly, remember that it is allowable to calculate the stresses in the neutral plan of flanges instead of in the extreme fibres.

EN 1993-1-1, 6.2.1(9)

5.7 - Shear resistance verification

5.7.1 - Shear in the box section webs

The box section web is transversally stiffened every 4 m:

$$\frac{h_w}{t_w} = 2521/23 = 109.6 > \frac{31\epsilon}{\eta} \sqrt{k_t} = 56.13 \text{ (with } \eta = 1.2)$$

EN 1993-1-5, 5.1(2) +
National Annex

The transverse stiffeners of the bracing frames bordering the web panel close to support P1 are assumed to be rigid (to be verified using section 9 of EN1993-1-5, see also Part II, 8.5.1 of this guide).

$$\alpha = \frac{a}{h_w} \geq 1 \text{ therefore } k_t = 5.34 + 4 \left(\frac{h_w}{a} \right)^2 = 6.93$$

EN1993-1-5, A.3(1)

It is deduced that the web should be checked against shear plate buckling.

The maximum design value of the shear resistance is given by $V_{Rd} = \min (V_{b,Rd}; V_{pl,a,Rd})$ with $V_{b,Rd} = V_{bw,Rd}$ neglecting the flange contribution to the resistance (see Part II, paragraph 8.3.4 of this guide).

The elastic critical shear buckling stress is given by $\tau_{cr} = k_t \sigma_E = 109.5 \text{ MPa}$ with $\sigma_E = \frac{\pi^2 E_a t_w^2}{12[1-\nu^2]h_w^2} = 15.80 \text{ MPa}$.

EN1993-1-5, 5.3(3)

The reduced slenderness $\bar{\lambda}_w = \sqrt{\frac{f_{yw}}{\tau_{cr} \sqrt{3}}} = 1.35 \geq 1.08$ is deduced, then the reduction factor $\chi_w = \frac{1.37}{0.7 + \bar{\lambda}_w} = 0.669$.

EN1993-1-5, Table 5.1

Hence $V_{bw,Rd} = \min \left[\frac{\chi_w f_{yw} h_w t_w}{\gamma_{M1} \sqrt{3}}, \frac{\eta f_{yw} h_w t_w}{\gamma_{M1} \sqrt{3}} \right] = 7.024 \text{ MN}$.

EN1993-1-5, 5.2(1)

In addition $V_{pl,a,Rd} = \eta \frac{h_w t_w}{\gamma_{M0}} \frac{f_{yw}}{\sqrt{3}} = 13.86 \text{ MN}$.

EN 1993-1-1, 6.2.6

Finally it is clearly verified that: $\eta_3 = V_{Ed}/V_{Rd} = 6.11/7.024 = 0.87 \leq 1.0$.

EN 1993-1-5, 5.5

5.7.2 - Shear in the stiffened bottom flange of the box section

a) Calculation of the shear stress in the bottom flange

The shear stress in the bottom flange varies from $\tau_{Ed,min} = 0$ in the vertical symmetry axis of the cross-section to $\tau_{Ed,max}$ at the junction of the bottom flange with the main web. $\tau_{Ed,max}$ is calculated respecting the construction phases and using the initial gross cross-section.

The shear force $V_{Ed} = 11.8 \text{ MN}$ at support P1 is broken down into:

- $V_{Ed,a} = 6.7 \text{ MN}$ applied to the structural steel box section only ($I_a = 0.9267 \text{ m}^4$; $v_{i,a} = 1243 \text{ mm}$) and which corresponds to a shear stress in the bottom flange equal to $\frac{V_{Ed,a}}{I_a} \frac{\mu_{f,a}}{t_f}$ where $\mu_{f,a} = \frac{b_f}{2} t_f v_{i,a}$ is the moment of area of the bottom flange with respect to the elastic neutral axis of the cross-section, i.e. $\tau_{Ed,a} = 25.2 \text{ MPa}$;
- $V_{Ed,c} = 5.1 \text{ MN}$ applied to the composite box section ($I = 1.0394 \text{ m}^4$; $v_i = 1345 \text{ mm}$) and which corresponds to a shear stress in the bottom flange equal to $\frac{V_{Ed,c}}{I} \frac{\mu_{f,c}}{t_f}$ where $\mu_{f,c} = \frac{b_f}{2} t_f v_i$, i.e. $\tau_{Ed,c} = 18.5 \text{ MPa}$.

$\tau_{Ed,max} = 43.7 \text{ MPa}$ is deduced. Note also that the shear stress due to torsion should be added to this value (but it is not considered in this guide).

b) Shear stress check in the global stiffened bottom flange

The bottom flange is stiffened every 4 m transversally and every 1120 mm longitudinally by 4 T-shaped stiffeners equally spaced:

EN 1993-1-5, 5.1 (2) + National Annex

$$\frac{b_f}{t_f} = 5600/40 = 140.0 < \frac{31\varepsilon}{\eta} \sqrt{k_t} = 202.5 \text{ (avec } \eta = 1.2 \text{)}$$

The shear buckling coefficient k_t of the stiffened bottom flange is given by $(\frac{a}{b_f} = \frac{4}{5.6} < 1)$:

EN1993-1-5, Annex A3 (1)

$$k_t = 4 + 5.34 \left(\frac{b_f}{a} \right)^2 + k_{t,sl} \text{ where } k_{t,sl} = 9 \left(\frac{b_f}{a} \right)^2 \sqrt[4]{\left(\frac{I_{sl}}{t_f^3 b_f} \right)^3} \geq \frac{2.1}{t_f} \sqrt[3]{b_f}$$

The second moment of area of a single longitudinal stiffener is equal to $I_{st} = 625.5 \cdot 10^6 \text{ mm}^4$ (with a partaking web area which has a cantilever width equal to $15 \cdot \varepsilon \cdot t_f = 495 \text{ mm} < (1120-30)/2 = 545 \text{ mm}$). $I_{sl} = 4 \cdot I_{st}$ is therefore adopted to calculate k_t . $k_{t,sl} = 75.76 \geq 4.01$ is deduced, then $k_t = 90.2$.

Note: The analytical formula used for the buckling coefficient assumes that an average uniform shear stress is applied to the edges of the stiffened panel. The vertical stiffeners of the bracing frames bordering the bottom flange are also assumed to be rigid (to be verified using section 9 of EN1993-1-5, see also Part II, 8.5.1 in this guide).

It is therefore deduced that no global plate buckling occurs due to shear stress in the bottom flange. The following is clearly verified:

$$\tau_{Ed,max} \leq \tau_{Rd} = \frac{\eta f_y}{\gamma_{M1} \sqrt{3}} = 217.3 \text{ MPa} \text{ (with } \eta = 1.2\text{),}$$

i.e. $\eta_3 = 0.20 < 1$.

EN1993-1-1, 6.2.6(4)

c) Shear stress check in each sub-panel of the bottom flange

The longitudinal stiffeners are assumed to be rigid. In the bottom flange they demarcate sub-panels of size $a = 4000 \text{ mm}$ and $b = 1090 \text{ mm}$. These sub-panels should be individually checked for shear resistance. The verification is only performed in the most loaded sub-panel, namely the one bordering the main steel web of the box section where the average shear stress reaches

$$\tau_{Ed} = \tau_{Ed,max} \frac{5600/2 - 1120/2}{5600/2} = 35.0 \text{ MPa.}$$

$$\alpha = \frac{a}{b_f} = 3.67 \geq 1 \text{ therefore } k_t = 5.34 + 4 \left(\frac{b_f}{a} \right)^2 = 5.64$$

$$\sigma_E = \frac{\pi^2 E_a t_f^2}{12 [1 - \nu^2] b_f^2} = 255.6 \text{ MPa}$$

$$\tau_{cr} = k_t \sigma_E = 1441.6 \text{ MPa}$$

EN1993-1-5, 7.1(5)

The reduced slenderness parameter is deduced:

$$\bar{\lambda} = \sqrt{\frac{f_y}{\tau_{cr} \sqrt{3}}} = 0.37 \leq \frac{0.83}{\eta} = 0.69$$

And then $\chi = \eta = 1.2$. Thus the shear buckling does not occur in the sub-panels and it is clearly verified:

$$\tau_{Ed} = 35 \text{ MPa} \leq \tau_{Rd} = \tau_{b,Rd} = \chi \frac{f_y}{\sqrt{3} \gamma_{M1}} = 217.3 \text{ MPa.}$$

5.8 - Interaction between moment and shear force

5.8.1 - Interaction M-V in the box section webs

The section to be verified is at a distance $h_w/2$ from support P1, i.e. 1.261 m. In this section $M_{Ed} = -166.73 \text{ MN.m}$ and $V_{Ed} = 5.853 \text{ MN}$ (with inclination of the web).

EN1993-1-5, 7.1(2)

$$\bar{\eta}_3 = \frac{V_{Ed}}{V_{bw,Rd}} = 0.833 \geq 0.5$$

The M-V interaction should be considered by justifying the following criterion in the box section webs:

EN 1993-1-5, 7.1(1)

$$\bar{\eta}_1 + \left(1 - \frac{M_{f,Rd}}{M_{pl,Rd}}\right) (2\bar{\eta}_3 - 1)^2 \leq 1,0 \text{ if } M_{Ed} \geq M_{f,Rd}$$

The plastic resistance moment of the section, as well as the plastic resistance moment of the flanges only, are calculated based on the rules of Part II, Figures 8.6 and 8.7 of this guide. The effective cross-sections of the flanges (by considering the shear lag effect and the possibly plate buckling) and the gross area of the web (irrespective to its section class) are used. This gives:

$$M_{f,Rd} = 212.47 \text{ MN.m} \text{ and } M_{pl,Rd} = 262.03 \text{ MN.m}$$

$$\text{Then } \bar{\eta}_1 = \frac{M_{Ed}}{M_{pl,Rd}} = 166.73/262.03 = 0.6363$$

As $M_{Ed} \leq M_{f,Rd}$ (in absolute value), there is finally no need to verify the interaction criterion. The design example dealt with would give:

$$\bar{\eta}_1 + \left(1 - \frac{M_{f,Rd}}{M_{pl,Rd}}\right) (2\bar{\eta}_3 - 1)^2 = 0.72 \leq 1.0$$

5.8.2 - Interaction M-V in the bottom flange of the box section

The criterion in paragraph 5.8.1 should also be checked in the steel bottom flange of the box section by imposing the value of the plastic resistance moment of the flanges only $M_{f,Rd} = 0$, by using $\bar{\eta}_1 = \eta_1$ calculated in paragraph 5.6 above, and by considering the average shear stress τ_{Ed} in the bottom flange.

EN 1993-1-5, 7.1(5)

For the symmetrical box section in the design example the average shear stress is equal to zero in the bottom flange, but the criterion should nevertheless be checked for a shear stress not less than $\tau_{Ed,max}/2 = 43.7/2 = 21.8 \text{ MPa}$.

Note: Strictly speaking, the value of $\tau_{Ed,max}$ should be recalculated from the shear force in the cross-section at a distance $h_w/2$ from support P1.

The value $\eta_3 = 0.20$ has already been calculated in paragraph 5.7.2. Thus $\eta_3 \leq 0.5$ and there is no need to verify the interaction criterion in the bottom flange.

5.9 - Conclusion

The box section at internal support P1 is justified at ULS for bending moment, for shear force and for the interaction between bending moment and shear force.

6 - Verification of the box section at support P1 for SLS combination of actions

As the shear lag in the bottom flange is clearly less favorable to calculate stresses at the SLS than at ULS (see paragraphs 4.1 and 4.2 of this Part III), the structural steel cross-section could be designed by the stress limitations at SLS (see Part II, chapter 10 for further detail).

In the design example, the following criteria are checked:

$$\sigma_{Ed,ser} = -199.2 \text{ MPa} \geq \frac{f_{yf}}{\gamma_{M,ser}} = -295 \text{ MPa} \text{ in the upper steel flange,}$$

$$\sigma_{Ed,ser} = 283.2 \text{ MPa} \leq \frac{f_{yf}}{\gamma_{M,ser}} = 345 \text{ MPa} \text{ in the effective bottom flange,}$$

$$\tau_{Ed,ser} = 108.5 \text{ MPa} \leq \frac{f_{yw}}{\gamma_{M,ser} \sqrt{3}} = 199 \text{ MPa}$$

$$\sqrt{\sigma_{Ed,ser}^2 + 3\tau_{Ed,ser}^2} = 339.9 \text{ MPa} \leq \frac{f_y}{\gamma_{M,ser}} = 355 \text{ MPa} \text{ (without considering concomitant stresses)}$$

Appendices



Appendice I - References

Any EN standard published by AFNOR – the French Association for Standardisation – becomes an NF-EN standard. It keeps the same number as the European one and AFNOR adds a "classification index". The standards used in this guide belong to series P22, P18 or P06, for example. The National Annexes which have to be published after this guidance book – their content is however fixed from a technical point of view – are mentioned in italic characters.

Note: *The European standards adopted by the members of the European Committee for Standardisation (CEN) should be transposed into national standards. In France this publishing work has been performed by AFNOR. The following references (especially the standards numbers) correspond to the French set of Eurocodes.*

Eurocode 0

- [1] NF EN 1990 (P06-100-1): Basis of structural design. March 2003.
- [2] NF P06-100-2: French National Annex to the norm NF EN 1990. June 2004.
- [3] NF EN 1990/A1 (P06-100-1/A1): Basis of structural design. Annex A2, Application for bridges. July 2006.
- [4] *NF EN 1990/A1/NA (P06-100-1/A1/NA): French National Annex to the norm NF EN 1990/A1. To be published in August 2007.*

Eurocode 1

- [5] NF EN 1991-1-1 (P06-111-1): Eurocode 1, Actions on structures. Part 1-1, General actions – Densities, self weight, imposed loads for buildings. March 2003.
- [6] NF P06-111-2: French National Annex to the norm NF EN 1991-1-1. June 2004.
- [7] NF EN 1991-1-4 (P06-114-1): Eurocode 1, Actions on structures. Part 1-4, General actions – Wind actions. November 2005.
- [8] *NF EN 1991-1-4/NA (P06-114-1/NA): French National Annex to the norm NF EN 1991-1-4. To be published in September 2007.*
- [9] NF EN 1991-1-5 (P06-115-1): Eurocode 1, Actions on structures. Part 1-5, General actions – Thermal actions. Mai 2004.
- [10] NF EN 1991-2 (P06-120-1): Eurocode 1, Actions on structures. Part 2, Traffic loads on bridges. March 2004.
- [11] *NF EN 1991-2/NA (P06-120-1/NA): French National Annex to the norm NF EN 1991-2. To be published in August 2007.*

Eurocode 2

- [12] NF EN 1992-1-1 (P18-711-1): Eurocode 2, Design of concrete structures. Part 1-1, General rules and rules for buildings. October 2005.
- [13] NF EN 1992-1-1/NA (P18-711-1/NA): National Annex to the norm NF EN 1992-1-1. March 2007.
- [14] NF EN 1992-2 (P18-720-1): Eurocode 2, Design of concrete structures. Part 2, Concrete bridges, Design and detailing rules. May 2006.
- [15] NF EN 1992-2/NA (P18-720-1/NA): National Annex to the norm NF EN 1992-2. April 2007.

Eurocode 3

- [16] NF EN 1993-1-1 (P22-311-1): Eurocode 3, Design of steel structures. Part 1-1, General rules and rules for buildings. October 2005.

- [17] NF EN 1993-1-1/NA (P22-311-1/NA): National Annex to the norm NF EN 1993-1-1. May 2007.
- [18] NF EN 1993-1-5 (P22-315): Eurocode 3, Design of steel structures. Part 1-5: Plated structural elements. March 2007.
- [19] *NF EN 1993-1-5/NA (P22-315/NA): National Annex to the norm NF EN 1993-1-5. To be published in September 2007.*
- [20] NF EN 1993-1-9 (P22-319-1): Eurocode 3, Design of steel structures. Part 1-9: Fatigue. December 2005.
- [21] NF EN 1993-1-9/NA (P22-319-1/NA): National Annex to the norm NF EN 1993-1-9. April 2007.
- [22] NF EN 1993-1-10 (P22-380-1): Eurocode 3, Design of steel structures. Part 1-10: Material toughness and through-thickness properties. December 2005.
- [23] NF EN 1993-1-10/NA (P22-380-1/NA): National Annex to the norm NF EN 1993-1-10. April 2007.
- [24] NF EN 1993-2 (P22-320): Eurocode 3, Design of steel structures. Part 2: Steel bridges. March 2007.
- [25] *NF EN 1993-2/NA (P22-320/NA): National Annex to the norm NF EN 1993-2. To be published in September 2007.*

Eurocode 4

- [26] NF EN 1994-1-1 (P22-411-1): Eurocode 4, Design of composite steel and concrete structures. Part 1-1: General rules and rules for buildings. June 2005.
- [27] NF EN 1994-1-1/NA (P22-411-1/NA): National Annex to the norm NF EN 1994-1-1. April 2007.
- [28] NF EN 1994-2 (P22-420-1): Eurocode 4, Design of composite steel and concrete structures. Part 2: General rules and rules for bridges. February 2006.
- [29] NF EN 1994-2/NA (P22-420-1/NA): National Annex to the norm NF EN 1994-2. May 2007.

Others normative references

- [30] NF EN 206-1 (P18-325-1): Concrete. Part 1: Specification, performance, production and conformity. April 2004.
- [31] NF EN 206-1/A1 (P18-325-1/A1): Amendment A1 to the norm NF EN 206-1. April 2005.
- [32] NF EN 206-1/A2 (P18-325-1/A2): Amendment A2 to the norm NF EN 206-1. October 2005.
- [33] NF EN 10025-1 (A35-501-1): Hot rolled products of structural steels. Part 1: General technical delivery conditions. March 2005.
- [34] NF EN 10025-2 (A35-501-2): Hot rolled products of structural steels. Part 2: Technical delivery conditions for non-alloy structural steels. March 2005.
- [35] NF EN 10025-3 (A35-501-3): Hot rolled products of structural steels. Part 3: Technical delivery conditions for normalized/normalized rolled weldable fine grain structural steels. March 2005.
- [36] NF EN 10025-4 (A35-501-4): Hot rolled products of structural steels. Part 4: Technical delivery conditions for thermomechanical rolled weldable fine grain structural steels. March 2005.
- [37] NF EN 10025-5 (A35-501-5): Hot rolled products of structural steels. Part 5: Technical delivery conditions for structural steels with improved atmospheric corrosion resistance. March 2005.
- [38] NF EN 10025-5 (A35-501-6): Hot rolled products of structural steels. Part 6: Technical delivery conditions for flat products of high yield strength structural steel in the quenched and tempered conditions. March 2005.

Guides, Books, Papers

- [39] « Recommandations pour maîtriser la fissuration des dalles », Guide SETRA pour le calcul des ponts mixtes. September 1995.
- [40] « Ponts métalliques et mixtes ; Résistance à la fatigue », Guide SETRA/CTICM/SNCF de conception et de justifications. May 1996.
- [41] J. ROCHE & J. FOUCRIAT, « Conception et calcul des éléments transversaux dans les ponts-routes mixtes », Bulletin Ponts Métalliques n°11, OTUA, 1985.
- [42] S. BRISARD, « Abaqus pour la flexion locale de la dalle d'un bipoutre à entretoises », Bulletin Ouvrages d'Art n°54 du SETRA, March 2007.

Appendice II - Class 4 I-shaped cross-section

In this annex, the thickness of the two-girder bridge web is modified compared to the design example of the main part of the guide and has now a constant value equal to 18 mm along the whole length of the bridge (see Part II, Figure 3.2). After recalculating the longitudinal normal stresses, the justifications at ULS from paragraph 8.3 are repeated for this new geometry of the composite cross-section at internal support P1.

Note: This new design will not be justified, but the aim of this annex is to illustrate a design example of verification in a Class 4 cross-section.

1. Geometry and stresses

At internal support P1 at ULS the concrete slab is in tension over its whole height. Its contribution is therefore neglected in the cross-section resistance. The stresses in Figure II.1 are subsequently calculated and obtained by summing the various steps whilst respecting the construction phases.

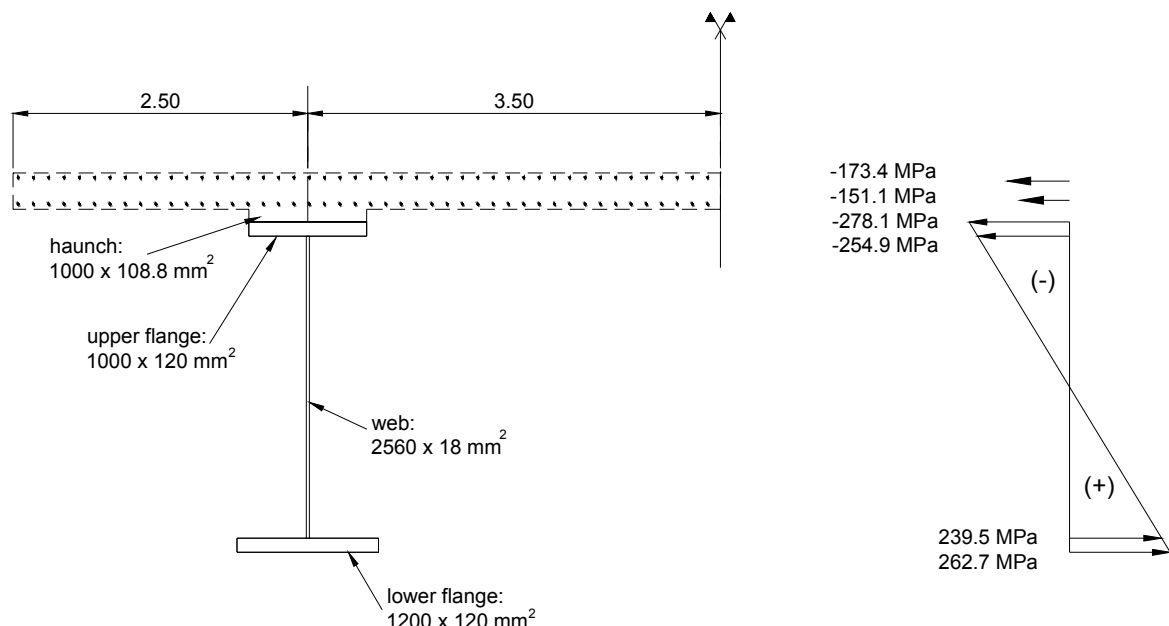


Figure II.1: Stresses at ULS in cross-section at internal support P1

The internal forces and moments in this cross-section are:

$$M_{Ed} = 102.6 \text{ MN.m}$$

$$V_{Ed} = 7.4 \text{ MN}$$

The mechanical properties of the composite cross-section (structural steel part and reinforcement) by taking the shear lag effects in the concrete slab into account – which has no influence for this example because the effective slab width is equal to the gross one – are equal to:

$$A = 333266 \text{ mm}^2$$

$$I = 5640.5 \cdot 10^8 \text{ mm}^4$$

$y_G = 1796 \text{ mm}$ (position of the centre of gravity in the composite section with regards to the upper fibre of the concrete slab)

2. Determining the cross-section Class

- Upper flange in tension therefore classified as a Class 1 element
- Lower flange in compression:

$$\frac{b_{fi} - t_w}{2t_{fi}} = 5.52\epsilon \leq 9\epsilon$$
 therefore classified as a Class 1 element
- The web is in tension in its upper part and in compression in its lower part. The position of the Plastic Neutral Axis (PNA) is determined as follows:

EN 1993-1-1, Table 5.2
(sheet 2/3)

Design plastic resistance of reinforcing steel bars: $F_{ap} = A_s f_{sk} / \gamma_s = 10.08 \text{ MN}$
 Design plastic resistance of the upper steel flange: $F_{fs} = A_{fs} f_{yf} / \gamma_{M0} = 35.40 \text{ MN}$
 Design plastic resistance of the lower steel flange: $F_{fi} = A_{fi} f_{yf} / \gamma_{M0} = 42.48 \text{ MN}$
 Design plastic resistance of the steel web assumed to be entirely in compression:
 $F_w = A_w f_{yw} / \gamma_{M0} = 15.90 \text{ MN}$

From $F_{ap} + F_{fs} \leq F_w + F_{fi}$ and $F_{ap} + F_{fs} + F_w \geq F_{fi}$ the PNA is deduced to be located in the steel web at a distance x from the web to upper flange weld. Writing the moment equilibrium with regards to the PNA deduces:

$$x = \frac{F_w + F_{fi} - (F_{ap} + F_{fs})}{2t_w f_{yw}} = 1039 \text{ mm}$$

Over half the web height is in compression:

$$\alpha = \frac{h_w - x}{h_w} = 0.594 > 0.5$$

Therefore the limiting slenderness between Class 2 and Class 3 is given by:

$$\frac{h_w}{t_w} = 142.22 \geq \frac{456\epsilon}{13\alpha - 1} = 55.98$$

The steel web is at least classified as a Class 3 element and reasoning is now based on the elastic stress distribution at ULS given in Figure II.1:

$$\psi = -254.9/239.5 = -1.064 \leq -1$$

Therefore the limiting slenderness between Class 3 and Class 4 is given by:

$$\frac{h_w}{t_w} = 142.22 \geq 62\epsilon(1 - \psi)\sqrt{-\psi} = 108.94$$

It is deduced that the steel web is a Class 3 element.

EN 1993-1-1, Table 5.2
(sheet 1/3)

Conclusion: The section at support P1 is a Class 4 section which is checked by an elastic section analysis using the effective reduced area for taking the web buckling into account.

3. Determining the effective cross-section

Reasoning is based on the stress distribution in Figure II.1 (initial gross cross-section taking account of the shear lag effect).

EN1994-2, 6.2.1.5(7)

$\psi = -1.064$ between -1 and -3, therefore the web buckling coefficient is given by $k_o = 5.98(1 - \psi)^2 = 25.475$.

EN1993-1-5, Table 4.1

The reduced plate slenderness parameter for web buckling is then equal to:

$$\bar{\lambda}_p = \sqrt{\frac{f_y}{\sigma_{cr}}} = \frac{h_w/t_w}{28.4\varepsilon\sqrt{k_\sigma}} = 1.202 > 0.673$$

EN1993-1-5, 4.4(2)

The reduction factor for the web area is deduced:

$$\rho = \frac{\bar{\lambda}_p - 0.055(3 + \psi)}{\bar{\lambda}_p^2} = 0.758 \leq 1.0$$

The effective^p widths in the compressed part of the gross web ($h_{w,c} = \frac{h_w}{1-\psi} = 1240.1 \text{ mm}$) are equal to:

- on the side of the lower compressed steel flange:

$$b_{e1} = 0.4b_{\text{eff}} = 0.4\rho \frac{h_w}{1-\psi} = 376.1 \text{ mm}$$

- on the side of the Elastic Neutral Axis (ENA):

$$b_{e2} = 0.6b_{\text{eff}} = 0.6\rho \frac{h_w}{1-\psi} = 564.1 \text{ mm}$$

EN1993-1-5, Table 4.1

Figure II.2 illustrates the effective^p cross-section and the location of the neglected web part.

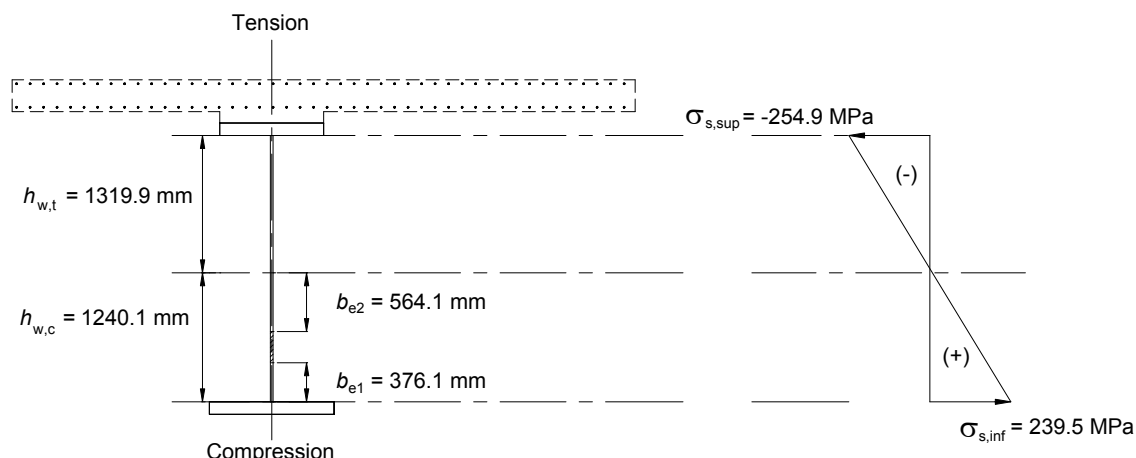


Figure II.2: Effective cross-section of the class 4 web

To recalculate normal stresses at ULS with the effective area in Figure II.2, the following is required:

- mechanical properties of the effective cracked composite section (effective^p structural steel part + reinforcement in the effective^s slab width):

$$A_{\text{eff}} = 327869 \text{ mm}^2$$

$$I_{\text{eff}} = 5607.10^8 \text{ mm}^4$$

$$y_{G,\text{eff}} = 1783 \text{ mm} \text{ (with regards to the upper fibre of the concrete slab)}$$

Note: The shift of the centre of gravity is equal to $e_N = 13 \text{ mm}$ upwards with regards to the initial Elastic Neutral Axis. No bending moment $N_{Ed}e_N$ is added as no normal force is applied to the section in the example.

- mechanical properties of the effective^p structural steel part only:

$$A_{a,\text{eff}} = 304682 \text{ mm}^2$$

$$I_{a,\text{eff}} = 4938.10^8 \text{ mm}^4$$

$$y_{G,a,\text{eff}} = 1908 \text{ mm} \text{ (with regards to the upper fibre of the concrete slab)}$$

4. Bending resistance verification

By following the construction phases in the studied cross-section, a part of M_{Ed} – noted M_a – is first resisted by the structural steel part alone. From the instant the slab segment including the cross-section is concreted, the behaviour of this section becomes composite and the remaining part of the design bending moment $M_{Ed} - M_a$ – noted M_c – is resisted by the composite section.

As the concrete is cracked at support P1, the mechanical properties of the cross-section are the same for all the load cases applied after its behaviour has become composite. The stress distribution due to M_c alone is therefore linear over the whole height of the composite cross-section (see Figure II.3). The final stresses in the reinforcement are directly proportional to the bending moment M_c . This means that the composition of M_{Ed} – as $M_a + M_c$ – may be easily determined from the final stress distribution at ULS.

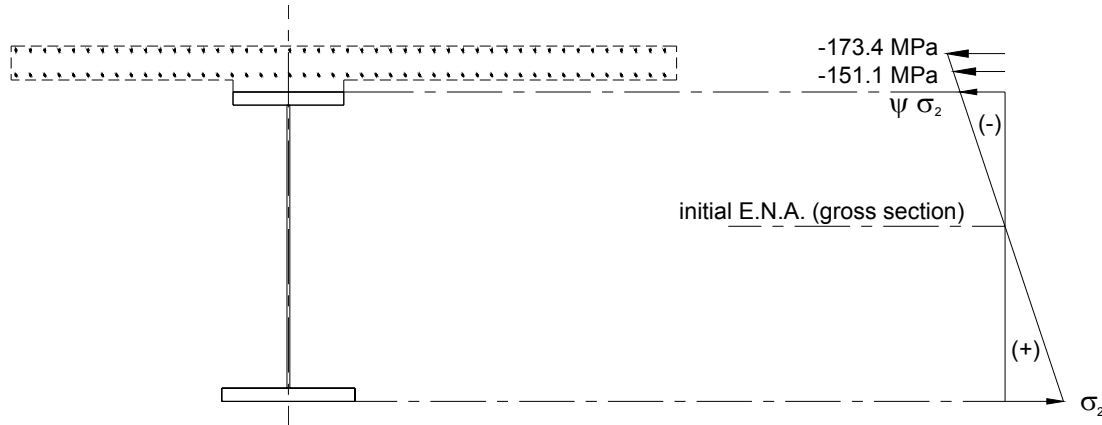


Figure II.3: Stress distribution due to M_c only

As $\frac{M_c v}{I} = -173.4 \text{ MPa}$ with $v = 1796 - 61 = 1735 \text{ mm}$ taking account of the reinforcing bars concrete cover, $M_c = -56.4 \text{ MN.m}$ is deduced. This then gives $M_a = M_{Ed} - M_c = -46.2 \text{ MN.m}$. The construction phases are then integrally repeated to calculate the stresses over the effective composite cross-section. Due to M_a and by using the mechanical properties of the effective structural steel part only, the following stresses are obtained:

$\sigma_{s,sup}^{eff(1)} = -139.6 \text{ MPa}$ in the upper fibre of the structural steel upper flange,

$\sigma_{s,inf}^{eff(1)} = 122.3 \text{ MPa}$ in the lower fibre of the structural steel lower flange.

Due to M_c and by using the mechanical properties of the effective cracked composite cross-section, the following stresses are obtained:

$\sigma_{s,sup}^{eff(2)} = -137.7 \text{ MPa}$ in the upper fibre of the structural steel part,

$\sigma_{s,inf}^{eff(2)} = 144.2 \text{ MPa}$ in the lower fibre of the structural steel part,

$\sigma_{arma,max}^{eff(2)} = -173.1 \text{ MPa}$ in the upper reinforcement layer.

The following is successively checked:

$$\sigma_{s,inf} = 266.5 \text{ MPa} \leq \frac{f_{yf}}{\gamma_{M0}} = 295 \text{ MPa}$$

$$\sigma_{s,sup} = -277.3 \text{ MPa} \geq -\frac{f_{yf}}{\gamma_{M0}} = -295 \text{ MPa}$$

$$\sigma_{arma,sup}^{eff} = -173.1 \text{ MPa} \geq -\frac{f_{sk}}{\gamma_s} = -434.8 \text{ MPa}$$

EN1994-2, 6.2.1.5(2)

The Class 4 cross-section at support P1 is justified for bending at ULS.

5. Shear resistance verification

The fact that a cross-section is classified as a class 4 section for bending has no affect whatsoever on the shear resistance check. These verifications are nevertheless carried out in this example. Refer to paragraph 8.3.4 of Part II for further detail on the following calculations.

$$\frac{h_w}{t_w} = 142.22 \geq \frac{31\epsilon}{\eta} \sqrt{k_t} = 51.1$$

EN1993-1-5, 5.1(2)

The vertical stiffeners bordering the web panel are assumed to be rigid:

$$\alpha = \frac{a}{h_w} \geq 1 \text{ then } k_t = 5.34 + 4 \left(\frac{h_w}{a} \right)^2 = 5.75$$

EN1993-1-5, Annex A3

The web should be checked in terms of shear buckling.

The maximum design shear resistance is given by $V_{Rd} = \min (V_{b,Rd}; V_{pl,a,Rd})$ where:

- $V_{b,Rd} = V_{bw,Rd} = \frac{\chi_w f_{yw} h_w t_w}{\gamma_{M1} \sqrt{3}} \leq \frac{\eta f_{yw} h_w t_w}{\gamma_{M1} \sqrt{3}} = 10.0 \text{ MN}$
- $V_{pl,a,Rd} = \frac{\eta h_w t_w f_{yw}}{\gamma_{M0} \sqrt{3}} = 11.0 \text{ MN}$

EN1993-1-1, 6.2.6

$$\sigma_E = \frac{\pi^2 E t_w^2}{12(1-\nu^2) h_w^2} = 9.4 \text{ MPa}$$

EN1993-1-5, 5.3(3)

$$\bar{\lambda}_w = \sqrt{\frac{f_{yw}}{k_t \sigma_E \sqrt{3}}} = 1.92 \geq 1.08$$

$$\chi_w = \frac{1.37}{0.7 + \bar{\lambda}_w} = 0.523 \leq \eta = 1.2$$

EN1993-1-5, Table 5.1

Therefore $V_{Rd} = V_{bw,Rd} = 4.4 \text{ MN}$.

$$\text{Note that } \eta_3 = \frac{V_{Ed}}{V_{Rd}} = \frac{7.4}{4.4} = 1.68 \geq 1.0$$

The cross-section at support P1 is therefore not justified for shear when the web thickness is reduced from 26 mm to 18 mm.

The solution is of course to make the web thicker (see paragraph 8.3.4). Nevertheless, as an example of applying EN1993-1-5 (even if this is neither very economical nor very effective), two longitudinal flat stiffeners with an area 300x30 mm², located at one third and two thirds the web clear height, have been welded to the web panel which is closest to support P1.

Adding longitudinal stiffeners

The buckling coefficient k_t for this new stiffened panel can be calculated by using the formulae in Annex A.3 to EN1993-1-5 (their use has to be set by the National Annex of each European country). These formulae already take account of the reduction to 1/3 of the actual second moment of area of the longitudinal stiffener:

EN1993-1-5, 5.3(3)

note 1

EN1993-1-5, 5.3(4)

$$\frac{a}{h_w} = 3.125 \geq 3 \text{ therefore } k_t \text{ can be calculated with the equation:}$$

EN1993-1-5, Annex A3 (2)

$$k_{\tau} = 5.34 + 4 \left(\frac{h_w}{a} \right)^2 + k_{\tau,sl} \text{ where } k_{\tau,sl} = 9 \left(\frac{h_w}{a} \right)^2 \sqrt[4]{\left(\frac{I_{sl}}{t_w^3 h_w} \right)^3} \geq \frac{2.1}{t_w} \sqrt[3]{\frac{I_{sl}}{h_w}}$$

EN1993-1-5, Annex A3(1)

The second moment of area of a single longitudinal stiffener acting with a web part is equal to $I_{sl} = 70.258 \cdot 10^6 \text{ mm}^4$.

Therefore $I_{sl} = 2 I_{st}$ is retained for calculating k_{τ} .

$k_{\tau,sl} = 4.95 \geq 4.43$ is deduced, then $k_{\tau} = 10.7$.

$$\frac{h_w}{t_w} = 142.2 \geq \frac{31}{\eta} \varepsilon \sqrt{k_{\tau}} = 69.7$$

EN1993-1-5, 5.1(2)

The web should therefore be checked in terms of shear buckling.

$$\bar{\lambda}_w = \sqrt{\frac{f_{yw}}{k_{\tau} \sigma_E \sqrt{3}}} = 1.41$$

$\bar{\lambda}_w$ should be not less than the largest slenderness parameter of all subpanels within the calculated stiffened web panel. All subpanels are identical in the example and have a slenderness of:

$$\frac{a}{h_{w,i}} = 3 \frac{a}{h_w} = 9.375 \geq 3$$

$$k_{\tau,i} = 5.34 + 4 \left(\frac{h_{w,i}}{a} \right)^2 = 5.386 \text{ and } \sigma_{E,i} = 9 \sigma_E = 84.6 \text{ MPa}$$

$$\bar{\lambda}_{w,i} = \sqrt{\frac{f_{yw}}{k_{\tau,i} \sigma_{E,i} \sqrt{3}}} = 0.66$$

$\bar{\lambda}_w \geq \bar{\lambda}_{w,i}$ is clearly verified. As $\bar{\lambda}_w \geq 1.08$ it is deduced:

$$\chi_w = \frac{1.37}{0.7 + \bar{\lambda}_w} = 0.65$$

$V_{bw,Rd} = 5.42 \text{ MN}$ (which is greater than the previously calculated value without longitudinal stiffeners).

$V_{pl,a,Rd} = 11.0 \text{ MN}$ is still applicable.

EN1993-1-5, 5.3(5)

EN1993-1-5, Table 5.1

EN1993-1-5, 5.5(1)

Therefore the web, even stiffened, is not verified for shear:

$V_{Ed} = 7.4 \text{ MN} \geq V_{Rd} = 5.42 \text{ MN}$.

Note: The longitudinal stiffening use would induce a new web partitioning into subpanels for determining the cross-section Class. The check for bending would then have to be carried out over.

6. M-V interaction verification

Even if the web panel is not justified for shear, the M-V interaction verification is still carried out.

$$V_{Ed} = 7.4 \text{ MN} \geq 0.5 \cdot V_{Rd}$$

EN1994-2, 6.2.2.4(1)

Therefore the bending/shear force interaction should be checked. The cross-section at support P1 is classified as a Class 4 section. The interaction is then verified according to the criterion in EN1993-1-5, 7.1:

$$\bar{\eta}_1 + \left(1 - \frac{M_{f,Rd}}{M_{pl,Rd}}\right) \left(2\bar{\eta}_3 - 1\right)^2 \leq 1.0$$

EN1993-1-5, 7.1(1)

The design values for the internal forces and moments have to be calculated in the cross-section at a distance $h_w/2$ from the support P1. This gives $V_{Ed} = 7.2$ MN and $M_{Ed} = 94.1$ MN.m to be used within the criterion.

The design value of the plastic resistance moment is calculated without considering the web Class and by using its initial gross cross-section. Remember that the Plastic Neutral Axis is located at a distance $x = 1039$ mm from the web to upper flange weld (see paragraph 2 in this annex). $M_{pl,Rd} = 131.0$ MN.m is then deduced (see Figure II.4).

By neglecting the web contribution when calculating the plastic resistance moment, the PNA is shifted upwards in the upper steel flange at a distance $x = 114.9$ mm from the upper fibre of this flange (see Figure II.5). $M_{f,Rd} = 117.3$ MN.m is then deduced.

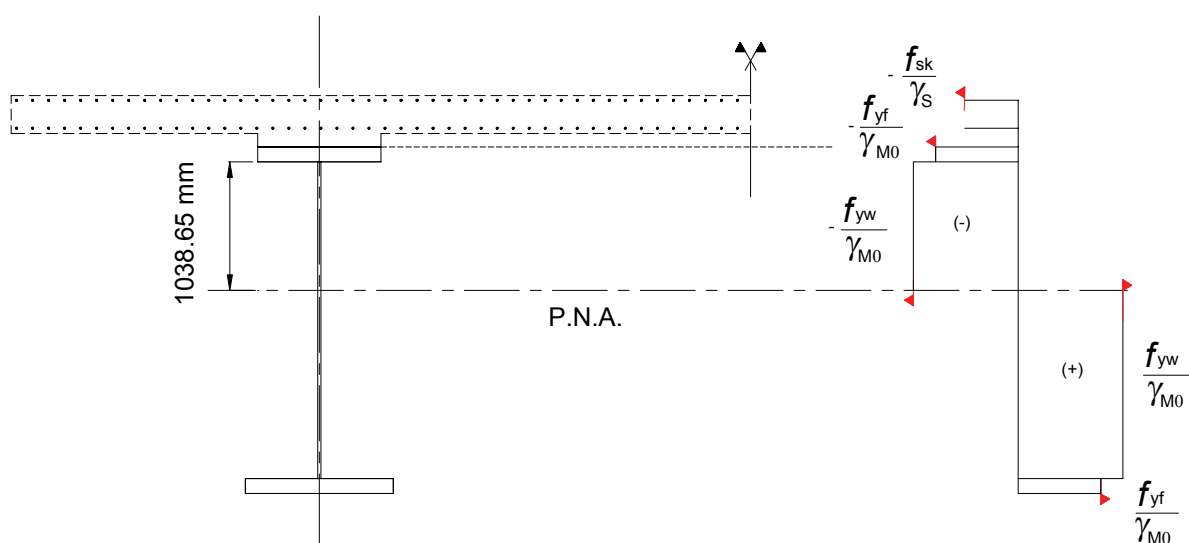


Figure II.4: Calculation of the plastic resistance moment $M_{pl,Rd}$

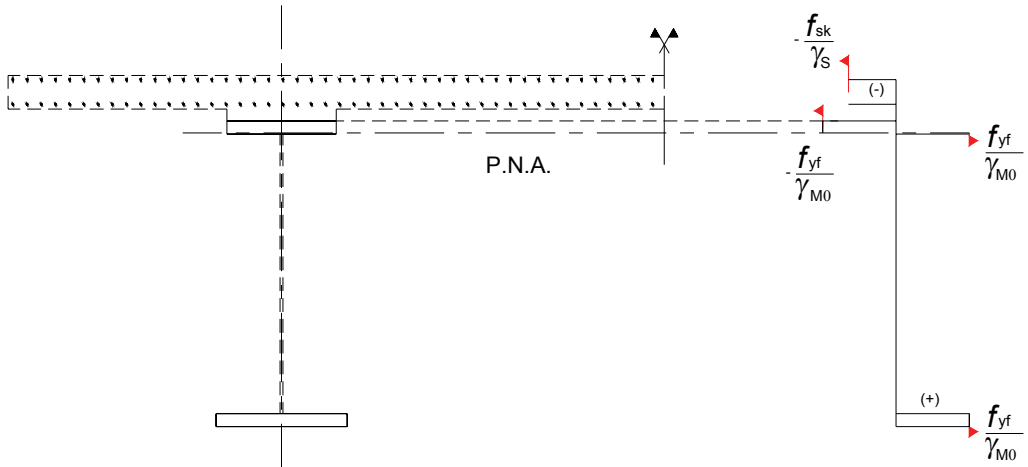


Figure II.5: Plastic resistance moment of the cross-section consisting of the flanges only $M_{f,Rd}$

$$\bar{\eta}_3 = \frac{V_{Ed} \text{ (at } h_w/2)}{V_{Rd}} = 1.636 \geq 1 \text{ (not verified)}$$

$$\bar{\eta}_1 = \frac{M_{Ed} \text{ (at } h_w/2)}{M_{pl,Rd}} = 0.718$$

As $\bar{\eta}_1 \leq \frac{M_{f,Rd}}{M_{pl,Rd}} = 0.896$ the bending moment can be entirely resisted by the flanges only. Considering that the shear force is resisted by the web only, the interaction criterion is no longer to be verified.

EN1993-1-5, 7.1(1)

46 avenue
Aristide Briand
BP 100
92225 Bagneux Cedex
France
phone :
33 (0)1 46 11 31 31
fax :
33 (0)1 46 11 31 69
internet : www.setra.equipement.gouv.fr

This guidance book explains two numerical examples for the design of bridges with steel-concrete composite structure under the Eurocodes (a two-girder bridge with transverse cross-girders and an open box-girder bridge). All the main justifications are addressed with precise references to the new set of applied standards. Emphasis is placed on the differences or new features of these standards compared to the usual French practice.

This document is intended to support the application of Eurocodes in European countries and particularly in France. It is intended especially for design engineers, design offices and contractors in charge of building steel-concrete composite bridges.



This document is available and can be downloaded on Sétra website:
<http://www.setra.equipement.gouv.fr>

Cover - Photographers: Gérard Forquet (Sétra) - Design: Eric Rillardon (Sétra)
The Sétra authorization is required for reproduction of this document (all or even part)
© 2007 Sétra - Reference: 0720A - ISRN: EQ-SETRA-07-ED31-FR+ENG

Sétra is part of the
scientific and technical
network of the French
Ministry of Transport and
Infrastructure (RST)

**Le Sétra appartient
au Réseau Scientifique
et Technique
de l'Équipement**

